U.PORTO

FACULDADE DE CIÊNCIAS
UNIVERSIDADE DO PORTO

PhD

PhD

3º CICLO

FCUP
2024

U.PORTO

Steps toward the reconstruction of the mass assembly history of Active Galactic Nuclei with FADO

Abhishek Rajesh Chougule

FC

Steps toward the reconstruction of the mass assembly history of Active Galactic Nuclei with FADO

Abhishek Rajesh Chougule

Doctoral dissertation in Astronomy presented to
the Faculty of Sciences of the University of Porto

2024

U.PORTO

FACULDADE DE CIÊNCIAS
UNIVERSIDADE DO PORTO

PhD

Steps toward the reconstruction of the mass assembly history of Active Galactic Nuclei with FADO

Abhishek Rajesh Chougule
Thesis carried out as part of the Doctoral Program in Astronomy
Department of Physics and Astronomy
2024

Supervisor
Dr Jean Michel Gomes, Researcher, Instituto de Astrofísica e Ciências do Espaço
Co-supervisor
PD Dr Polychronis Papaderos, Researcher, Instituto de Astrofísica e Ciências do Espaço

Acknowledgements

Firstly, I would like to thank my PhD advisors, Dr. J. M. Gomes and PD Dr. Polychronis Papaderos for their guidance, support and immense help with the PhD thesis. I want to thank them for going out of their way at times to help me. They have made me feel as a co-worker rather than a student.

I want to thank Maria João de Araújo Martins Sousa e Vasconcelos for her immense support, love, care and encouragement. I want to thank my parents and my brother who have always been there for me, encouraged me and have been just a phone call away even though we are miles away. I dedicate my thesis to Maria, mom, dad and my brother.

I extend my gratitude to Paula Marques from the post graduation office for her help and quick response to my queries. I want to thank André Silva from IA/CAUP for his assistance throughout the PhD course, especially for the last minute assistance with the thesis template.

I, Abhishek Rajesh Chougule, acknowledge funding by Fundação para a Ciência e a Tecnologia through the grants: PD/BD/150439/2019 in the context of the PhD::SPACE and COVID/BD/153484 /2022 in the context of "Prorrogação de bolsas de investigação com fundamento na crise pandémica provocada pela doença da COVID-19". I also acknowledge funding by Fundação para a Ciência e a Tecnologia for FCT-CAPES Transnational Cooperation Project: "Parceria Estratégica em Astrofísica Portugal-Brasil: conexão entre buracos negros e galáxias usando uma nova e poderosa instrumentação e visão teórica"

Dr. J. M. Gomes thanks Fundação para a Ciência e a Tecnologia (FCT), which supported this work via Fundo Europeu de Desenvolvimento Regional (FEDER) through COMPETE2020–Programa Operacional Competitividade e Internacionalização (POCI) through the research grants UID/-FIS/04434/2019, UIDB/04434/2020, and UIDP/04434/2020 and an FCT-CAPES Transnational Cooperation Project: "Parceria Estratégica em Astrofísica Portugal-Brasil: conexão entre buracos negros e galáxias usando uma nova e poderosa instrumentação e visão teórica". The Departamento de Astronomia do Instituto de Física da UFRGS is acknowledged for its cordial reception and support under the FCT-CAPES project. JMG is supported by the DL 57/2016/CP1364/CT0003 contract and acknowledges the previous support by the fellowships CIAAUP- 04/2016-BPD in the context of the FCT project UID/FIS/04434/2013 and POCI-01-0145-FEDER-007672, and SFRH/-BPD/66958/2009 funded by FCT and POPH/FSE (EC).

PD Dr. Polychronis Papaderos acknowledges support by Fundação para a Ciência e a Tecnologia (FCT) through FCT grants UID/FIS/04434/2019, UIDB/04434/2020, UIDP/04434/2020 and

the Principal Investigator contract CIAAUP-092023-CTTI, as well as through the project "Identifying the Earliest Supermassive Black Holes with ALMA (IdEaS with ALMA)" (PTDC/FIS-AST/29245/2017). He also gratefully acknowledges support by the Wenner-Gren Foundation and the hospitality of the Astronomy Department at Stockholm University.

This research has made use of the NASA/IPAC Extragalactic Database (NED) which is operated by the Jet Propulsion Laboratory, California Institute of Technology, under contract with the National Aeronautics and Space Administration.

This research has made use of "Aladin sky atlas" (Bonnarel et al. 2000; Boch and Fernique 2014; Baumann et al. 2022) developed at CDS, Strasbourg Observatory, France.

This research also made use of Sloan Digital Sky Survey (SDSS) data release 7. Funding for the SDSS and SDSS-II has been provided by the Alfred P. Sloan Foundation, the Participating Institutions, the National Science Foundation, the U.S. Department of Energy, the National Aeronautics and Space Administration, the Japanese Monbukagakusho, the Max Planck Society, and the Higher Education Funding Council for England. The SDSS Web Site is http://www.sdss.org/.

The SDSS is managed by the Astrophysical Research Consortium for the Participating Institutions. The Participating Institutions are the American Museum of Natural History, Astrophysical Institute Potsdam, University of Basel, University of Cambridge, Case Western Reserve University, University of Chicago, Drexel University, Fermilab, the Institute for Advanced Study, the Japan Participation Group, Johns Hopkins University, the Joint Institute for Nuclear Astrophysics, the Kavli Institute for Particle Astrophysics and Cosmology, the Korean Scientist Group, the Chinese Academy of Sciences (LAMOST), Los Alamos National Laboratory, the Max-Planck-Institute for Astronomy (MPIA), the Max-Planck-Institute for Astrophysics (MPA), New Mexico State University, Ohio State University, University of Pittsburgh, University of Portsmouth, Princeton University, the United States Naval Observatory, and the University of Washington.

Abstract

Faculty of Science of the University of Porto
Department of Physics and Astronomy

PhD in Astronomy

Steps toward the reconstruction of the mass assembly history of Active Galactic Nuclei with FADO

by Abhishek Rajesh CHOUGULE

Understanding the formation and evolution of galaxies, except for the few systems in our close vicinity, depends to a large degree on deciphering the galactic spectra using spectral synthesis techniques, e.g., Population Spectral Synthesis (PSS). Even though spectral synthesis techniques have undergone significant development in the past for studying normal galaxies, their application to Active Galactic Nuclei (AGNs) is a work in progress. This work focuses on the PSS of AGNs using Fitting Analysis using differential evolution Optimisation (FADO). The study aims to benchmark FADO by assessing its performance and accuracy on synthetic data, followed by its application to the Sloan Digital Sky Survey (SDSS) observations.

We have produced about 14,000 single power-law models with continuum and emission lines for a range of spectral index, ionisation parameters, hydrogen number density and gas-phase metallicity. Besides, using SKIRTOR models as the base, we have produced 1920 AGN Spectral Energy Distributions (SEDs) with emission lines for a more realistic ionisation continuum field. These models account for polar dust and anisotropic radiation emission by the accretion disc. It has been subject to extensive work for nearly eight months and primarily built from scratch in Python3. This development has permitted us to have a standalone AGN module for the continuum incident radiation field of AGNs, dependent on their viewing angle. We also create 1432 Composite Stellar Populations (CSPs) of ages ranging from 6 Myr to 15 Gyr with an instantaneous burst and constant star formation history (SFH). Finally, we create a grid of 128 536 32 Seyfert 2 synthetic models by combining single power-law models and CSPs for ten different AGN fractions in the range 0.0-1.0, SN = 5, 15, and ∞, and V-band extinction with Av values of 0.0, 1.0, 2.0.

As the data set is humongous, after the initial tests with FADO on single power-law models, we use 145200 Seyfert 2 synthetic models to investigate the accuracy and limitations of FADO in recovering the properties of the synthetic spectrum. We selected Seyfert 2 models composed of

single PL models with α_ν = -1.2, -1.4, -1.6, -1.8 and CSPs with instantaneous burst and constant SFHs of eleven ages in the range of 1 Myr to 10 Gyr, solar metallicity, X_{AGN} = 0.2 to 0.8, SN = 5, 15, ∞ and Av in the range of 0.0 to 2.0.

We use mean absolute error (MAE) to quantify the accuracy of FADO's performance. MAE indicates how far off the predictions are from the actual values on average. The recovery of stellar properties strongly depends on the X_{AGN} of the input model. In contrast, the recovery of AGN properties is comparatively less sensitive to the X_{AGN} of the input model. The recovery of stellar properties also depends on the age of the system and the SFH. We refer to systems with ages 1 Myr to 6.3 Myr as young systems, 15.86 Myr to 251 Myr as intermediate systems, and 630 Myr to 10 Gyr as old systems. The MAE for stellar properties are the highest for intermediate systems, followed by young and old systems for models with instantaneous burst and constant SFH. Overall, for models with constant SFH, the mean absolute errors are higher than the models with instantaneous burst SFH. The uncertainties in estimating the mass-weighted quantities are higher than in estimating the light-weighted quantities due to the non-linear nature of the mass-to-light ratio. As many factors introduce degeneracy concerning stellar properties, including age-metallicity degeneracy, their recovery is worse than that of AGN properties. The recovery of X_{AGN} is best followed by the recovery of α_ν with mean absolute errors of less than 0.10% and 0.16%, respectively. Hence, we apply FADO to the SDSS Seyfert spectra to gain insights into the characteristics of the featureless AGN continuum in this galaxy class.

Applying the benchmarked version of FADO to 17000 SDSS Seyfert galaxies gives a broad distribution of the average power-law indices. FADO finds a range of PL spectral index values for the Seyfert 2 galaxies instead of the usually adopted 'canonical' spectral index value of $\alpha_\nu \sim -1.5$. So, there is no canonical or standard value of PL spectral index applicable for all Seyfert 2 galaxies. We find the prominence of high excitation lines with increasing X_{AGN} and the equivalent width of HeII λ4686 Å increasing with X_{AGN}, indicating that FADO traces the strength of the non-thermal ionising radiation well. We further investigated the FADO results for the Seyfert 2 galaxy SDSS J023301.24+002515.0 from our sample. FADO gives an X_{AGN} of $\sim$ 11% and α_ν of $\sim$ -1.4 for this galaxy. This galaxy has also been detected in other wavelengths: in 1.4 GHz radio continuum by NVSS - The NRAO VLA Sky Survey, in IR by the Wide-field Infrared Survey Explorer (WISE), and in X-ray (0.5-1 Kev, 1-2 Kev and 2-4.5 Kev) by XMM-Newton. The galaxy also falls in the AGN region of the WISE MIR Color diagram used for AGN diagnostics. In light of all these evidences, we can be certain that the FADO concept for application to AGNs is sound and worth exploring further.

Resumo

Faculdade de Ciências da Universidade do Porto
Departamento de Física e Astronomia

Doutoramento em Astronomia

Passos para a reconstrução da história da montagem em massa de Núcleos Galácticos Ativos com FADO

por Abhishek Rajesh CHOUGULE

Compreender a formação e evolução das galáxias, exceto para os poucos sistemas nas nossas proximidades, depende em grande medida da decifração dos espectros galácticos utilizando técnicas de síntese espectral, como, por exemplo, a Síntese Espectral de Populações (PSS). Embora as técnicas de síntese espectral tenham passado por um desenvolvimento significativo no passado para o estudo de galáxias normais, a sua aplicação aos Núcleos Ativos de Galáxias (AGNs) ainda está em progresso. Este trabalho foca-se na PSS de AGNs utilizando a Análise de Ajuste através da Otimização por Evolução Diferencial (FADO). O estudo visa avaliar o FADO ao analisar o seu desempenho e precisão em dados sintéticos, seguido da sua aplicação às observações do Sloan Digital Sky Survey (SDSS).

Produzimos cerca de 14.000 modelos de lei de potência única com linhas de emissão e contínuo para uma gama de índices espectrais, parâmetros de ionização, densidade numérica de hidrogénio e metalicidade da fase gasosa. Além disso, utilizando modelos SKIRTOR como base, produzimos 1920 Distribuições de Energia Espectral (SEDs) de AGNs com linhas de emissão para um campo de ionização contínuo mais realista. Estes modelos consideram poeira polar e emissão de radiação anisotrópica pelo disco de acreção. Este trabalho foi realizado ao longo de quase oito meses e foi desenvolvido principalmente do zero em Python3. Este desenvolvimento permitiu-nos ter um módulo independente de AGN para o campo de radiação contínua incidente dos AGNs, dependente do seu ângulo de visão. Também criámos 1432 Populações Estelares Compostas (CSPs) com idades variando de 6 Myr a 15 Gyr com uma explosão instantânea e um histórico de formação estelar (SFH) constante. Finalmente, criámos uma grelha de 128 536 32 modelos sintéticos de Seyfert 2 combinando modelos de lei de potência única e CSPs para dez diferentes frações de AGN na gama de 0,0-1,0, SN = 5, 15 e ∞, e extinção na banda V com valores de Av de 0,0, 1,0, 2,0.

Como o conjunto de dados é enorme, após os testes iniciais com o FADO em modelos de lei de potência única, usamos 145200 modelos sintéticos de Seyfert 2 para investigar a precisão e

limitações do FADO na recuperação das propriedades do espectro sintético. Selecionámos modelos de Seyfert 2 compostos por modelos PL únicos com α_ν = -1,2, -1,4, -1,6, -1,8 e CSPs com explosão instantânea e SFHs constantes de onze idades na gama de 1 Myr a 10 Gyr, metalicidade solar, X_{AGN} = 0,2 a 0,8, SN = 5, 15, ∞ e Av na gama de 0,0 a 2,0.

Utilizamos o erro absoluto médio (MAE) para quantificar a precisão do desempenho do FADO. O MAE indica quão distantes estão as previsões dos valores reais, em média. A recuperação das propriedades estelares depende fortemente do X_{AGN} do modelo de entrada. Em contraste, a recuperação das propriedades do AGN é comparativamente menos sensível ao X_{AGN} do modelo de entrada. A recuperação das propriedades estelares também depende da idade do sistema e do SFH. Referimo-nos a sistemas com idades de 1 Myr a 6,3 Myr como sistemas jovens, de 15,86 Myr a 251 Myr como sistemas intermédios, e de 630 Myr a 10 Gyr como sistemas antigos. O MAE para propriedades estelares é mais elevado para sistemas intermédios, seguido de sistemas jovens e antigos para modelos com explosão instantânea e SFH constante. No geral, para modelos com SFH constante, os erros absolutos médios são maiores do que para modelos com SFH de explosão instantânea. As incertezas na estimativa das quantidades ponderadas por massa são maiores do que na estimativa das quantidades ponderadas por luz, devido à natureza não-linear da razão massa/luz. Como muitos fatores introduzem degeneração em relação às propriedades estelares, incluindo a degeneração idade-metalicidade, a sua recuperação é pior do que a das propriedades do AGN. A recuperação do X_{AGN} é a melhor, seguida da recuperação do α_ν com erros absolutos médios inferiores a 0,10% e 0,16%, respetivamente. Assim, aplicamos o FADO aos espectros Seyfert do SDSS para obter insights sobre as características do contínuo AGN sem características nesta classe de galáxias.

A aplicação da versão avaliada do FADO a 17000 galáxias Seyfert do SDSS dá uma ampla distribuição dos índices médios de lei de potência. O FADO encontra uma gama de valores de índice espectral de PL para as galáxias Seyfert 2 em vez do valor de índice espectral 'canónico' geralmente adotado de $\alpha_\nu \sim -1,5$. Portanto, não há um valor canónico ou padrão de índice espectral de PL aplicável a todas as galáxias Seyfert 2. Observamos a proeminência de linhas de alta excitação com o aumento do X_{AGN} e a largura equivalente de HeII λ4686 Å aumentando com X_{AGN}, indicando que o FADO rastreia bem a força da radiação ionizante não térmica. Investigámos ainda os resultados do FADO para a galáxia Seyfert 2 SDSS J023301.24+002515.0 da nossa amostra. O FADO dá um X_{AGN} de $\sim$ 11% e α_ν de $\sim$ -1,4 para esta galáxia. Esta galáxia também foi detetada em outros comprimentos de onda: em 1,4 GHz em contínuo de rádio pela NVSS - The NRAO VLA Sky Survey, em IR pelo Wide-field Infrared Survey Explorer (WISE), e em raios-X (0,5-1 Kev,

1-2 Kev e 2-4,5 Kev) pelo XMM-Newton. A galáxia também se enquadra na região de AGN do diagrama de Cor MIR do WISE usado para diagnóstico de AGN. À luz de todas estas evidências, podemos ter a certeza de que o conceito do FADO para aplicação a AGNs é sólido e merece ser explorado mais a fundo.

Contents

Acknowledgements **v**

Abstract **vii**

Resumo **ix**

Contents **xiii**

1 Introduction **1**
1.1 Accretion-powered nuclear activity in galaxies . . . 1
1.1.1 The central engine: an accreting SMBH . . . 3
1.1.1.1 A simplified theoretical calculation . . . 3
1.1.1.2 Observational evidence for SMBH . . . 4
1.1.2 Orientation-based unification of AGNs . . . 5
1.1.3 The straw person model of AGN : A rough sketch of the unified model . . . 6
1.1.4 Emerging Evidence of the Central Engine's Role in AGN Classification . . . 8
1.2 Influence of AGNs on Galaxy Evolution . . . 10
1.3 Spectral synthesis technique . . . 11
1.3.1 Spectral modelling of Active Galaxies . . . 13
1.3.1.1 Contribution of the featureless continuum . . . 13
1.3.1.2 Inclusion of featureless continuum is a necessity . . . 15

2 Synthetic models of AGNs **19**
2.1 Challenges in modelling photoionisation of AGN narrow-Line regions . . . 19
2.1.1 Uncertainty surrounding ionising spectral energy distributions of AGNs . . . 20
2.1.2 The ionising spectral energy distributions lack physical justification . . . 21
2.1.3 The anisotropy of ionising spectral energy distributions of AGNs . . . 24
2.2 Developing Photoionisation Models for the Narrow-Line Region in AGNs . . . 25
2.2.1 Towards the production of more realistic Active Galactic Nuclei Spectral Energy Distributions . . . 25
2.2.2 Single power-law continuum as the ionising source . . . 29
2.3 Stellar Population Synthesis . . . 33
2.4 Grid of stellar population models . . . 34
2.5 Grid of galaxy models with AGN emission . . . 38

3 FADO benchmark tests for AGN Galaxies: assessing performance and accuracy **43**

3.1 FADO Analysis . . . 44
3.1.1 Updating the base of templates . . . 44
3.1.2 Construction of a new spectral base library of single power-law models . . . 45
3.1.3 Inclusion of stellar population templates in the base . . . 46
3.2 Benchmark tests: applying FADO to mock data . . . 46
3.2.1 Application of FADO to models using a single power-law models . . . 47
3.2.1.1 Full-Consistency Mode versus Nebular Continuum Mode . . . 47
3.2.1.2 Masking regions . . . 48
3.2.1.3 Power-law with energy cutoff vs power-law without cutoff . . . 49
3.2.1.4 Recovery of PL index for models with different velocity line broadening. . . . 50
3.2.1.5 Application of FADO to single PL index models with noise . . . 50
3.3 Application of FADO to synthetic Seyfert 2 spectra . . . 50
3.3.1 Application of FADO to Seyfert 2 mock spectra . . . 51
3.3.1.1 Tables: Burst SFH, Av=0.0, SN = 15, base: BaseA . . . 51
3.3.1.2 Tables: Constant SFH, Av=0.0, SN = 15, base: BaseA . . . 52
3.3.1.3 Figures: Instantaneous burst SFH, Av=0.0, SN = 15.0, base: BaseA . 53
3.3.1.4 Figures: Constant SFH, Av=0.0, SN = 15, base: BaseA . . . 54
3.4 Summary of results . . . 55
$\Delta X_{\rm AGN}$ and $\Delta\langle\alpha_\nu\rangle_L$: . . . 56
$\Delta\langle\log(t_\star)\rangle_L$ and $\Delta\langle\log(t_\star)\rangle_M$: . . . 56
$\Delta\log(\langle Z_\star\rangle_L)$ and $\Delta\log(\langle Z_\star\rangle_M)$: . . . 56
$\Delta M_\star$: . . . 57

4 Applying FADO to Seyfert 2 galaxies from the Sloan Digital Sky Survey 59
4.1 Modelling Seyfert 2 Galaxies Using FADO: Insights from the SDSS sample . . . 60
4.2 Recovery of AGN fraction and power-law index . . . 60
4.3 Soundness of the FADO concept on AGN . . . 65
4.3.1 Prominence of high-excitation emission lines . . . 65
4.4 An example: SDSS J023301.24+002515.0 . . . 67
4.4.1 Detection in other wavelengths . . . 69
4.4.2 WISE MIR Colours . . . 70

5 Discussion and Conclusions 73
5.1 Conclusion . . . 76
5.2 Future prospects . . . 77

A Chapter 3 appendix: tables and figures 79
A.1 Tables: . . . 79
A.1.1 Tables: Burst SFH, Av=0.0, SN = 15, base: BaseA . . . 80
A.1.2 Tables: Constant SFH, Av=0.0, SN = 15, base: BaseA . . . 90
A.1.3 Tables: Burst SFH, Av=1.0, SN = 15, base: BaseA . . . 100
A.1.4 Tables: Constant SFH, Av=1.0, SN = 15, base: BaseA . . . 111
A.1.5 Tables: Burst SFH, Av=2.0, SN = 15, base: BaseA . . . 122
A.1.6 Tables: Constant SFH, Av=2.0, SN = 15, base: BaseA . . . 133
A.1.7 Tables: Instantaneous burst SFH, SN=5, Av=0.0, base: BaseA . . . 144
A.1.8 Tables: Instantaneous burst SFH, SN=5, Av=1.0, base: BaseA . . . 155

A.1.9 Tables: Instantaneous burst SFH, SN=5, Av=2.0, base: BaseA 166
A.1.10 Tables: Constant SFH, SN=5, Av=0.0, base: BaseA 177
A.1.11 Tables: Constant SFH, SN=5, Av=1.0, base: BaseA 188
A.1.12 Tables: Constant SFH, SN=5, Av=2.0, base: BaseA 199
A.1.13 Tables: Burst SFH, SN=15, Av=0.0, base: BaseD (just one PL in the base) . . . 210
A.2 Figures: 221
A.2.1 Figures: Instantaneous burst SFH, Av=0.0, SN = 15.0, base: BaseA 221
A.2.2 Figures: Constant SFH, Av=0.0, SN = 15.0, base: BaseA 229
A.2.3 Figures: Instantaneous burst SFH, Av=1.0, SN = 15.0, base: BaseA 237
A.2.4 Figures: Constant SFH, Av=1.0, SN = 15, base: BaseA 246
A.2.5 Figures: Instantaneous burst SFH, Av=2.0, SN = 15.0, base: BaseA 255
A.2.6 Figures: Constant SFH, Av=2.0, SN = 15, base: BaseA 264

Bibliography **273**

Chapter 1

Introduction

Galaxies are sprawling systems of dust, gas, dark matter, and a million to a trillion stars that are held together by gravity. Except for dark matter, all the other components contribute in different proportions to the overall radiation emitted by a normal galaxy. These galaxies radiate significantly over a narrow wavelength range.

However, there are galaxies which emit radiation over an enormous wavelength range–most of these objects show significant emission from radio to the X-rays, and often in the gamma rays–suggesting that the radiation is not a superposition of (approximately) thermally black-body radiating stellar sources. These galaxies are known as Active Galaxies (AG), and they emit this panchromatic radiation mainly from a very small central region which is called the Active Galactic Nucleus (AGN). At times, these sources are bright enough to outshine their host galaxies and have been detected far away within the observable Universe.

1.1 Accretion-powered nuclear activity in galaxies

AGNs exhibit a wide variety of features over the entire range of the electromagnetic spectrum and are classified into different types based on their spectral properties (e.g., Fig. 1.1). The wide variety of features discerned in different classes of AGNs is believed to be a result of the orientation of a thick, obscuring structure of gas and dust encompassing the central region that hosts a Super Massive Black Hole (SMBH), with respect to an observer's line of sight. This is known as orientation-based unification of AGNs. In the subsequent sections, I will discuss more about this unification, its success, limitation and modifications with respect to recent literature.

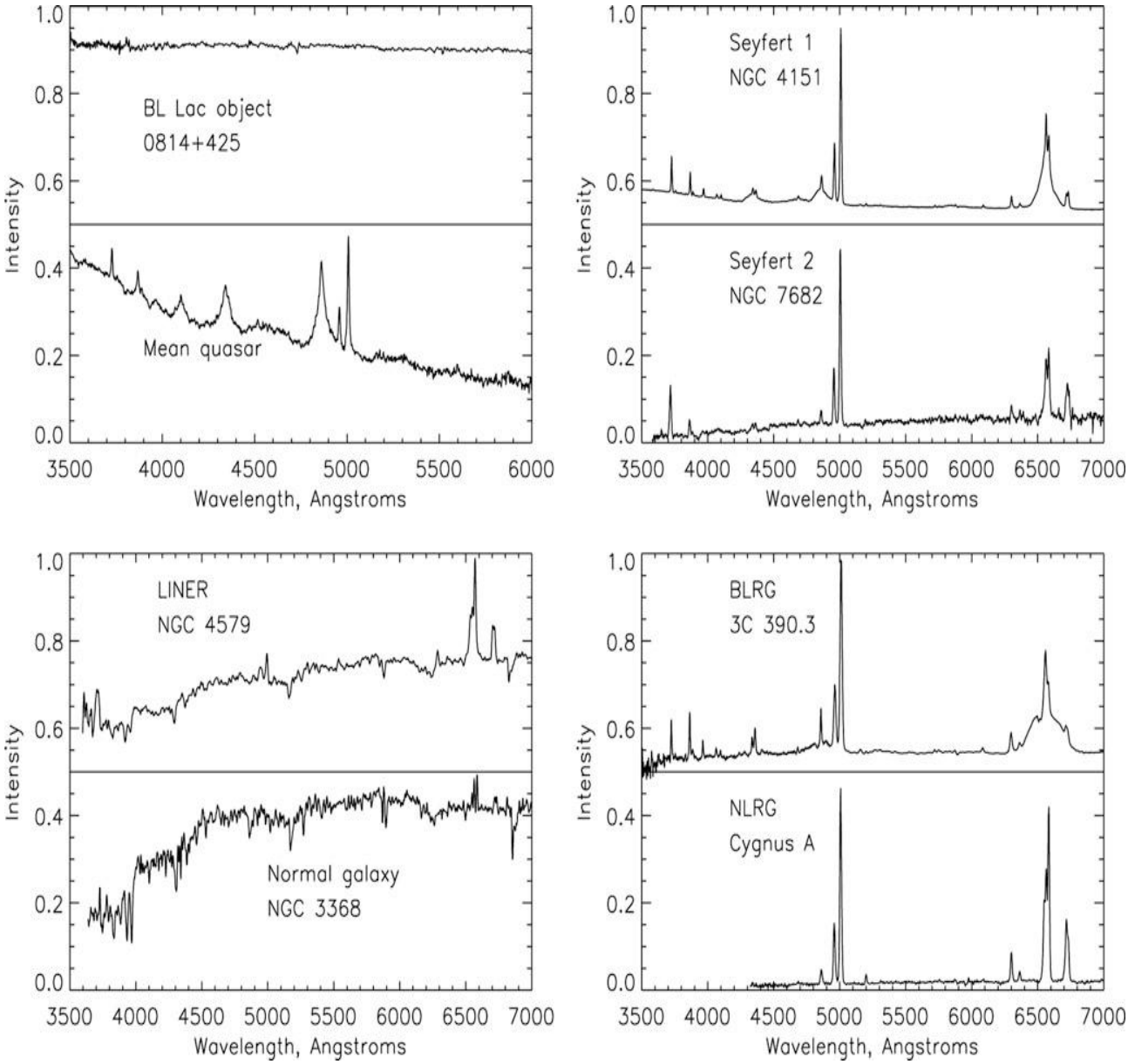

FIGURE 1.1: Comparison of distinct AGN galaxies. In the top left panels we have a BL Lac object and a mean quasar spectrum. We can see that the BL Lac has almost no features and emission-lines in the spectrum, while the quasar shows broad optical permitted emission-lines. On the other hand, LINER shows weak emission lines whereas a normal galaxy shows mostly absorption lines (bottom left panel). In case of Seyfert 1 and Seyfert 2 galaxy (top right panel), strong emission-lines are present: broad and narrow in former, while only narrow in case of latter. The bottom right panel shows a Broad and a Narrow Line Radio Galaxy (BLRG and NLRG, respectively). The optical spectral features of BRLG and NLRG closely resemble to those of Seyfert 1 and Seyfert 2, respectively. Source: Schneider (2015) (originally from Bill Keel's WWW Gallery; reproduced with his permission).

1.1.1 The central engine: an accreting SMBH

As mentioned in the previous section, AGNs are believed to be powered by a SMBH. In this section we will present arguments for this conclusion.

1.1.1.1 A simplified theoretical calculation

The conversion of mass (m) into energy (E), depends on the efficiency (η) of the process responsible for it. Therefore, using the mass–energy equivalence yields:

$$E = \eta mc^2 \tag{1.1}$$

The classical gravitational potential energy of a system of two masses (m and M), separated by a distance (r), is given by

$$E_{grav} = \frac{GMm}{r} \tag{1.2}$$

Ignoring relativistic effects, the energy available from a particle of mass m, falling within 5 times the
Schwarzschild radius R_S*, which is the region expected to have most of the optical/UV continuum radiation from an AGN, will, after substituting it in the formula 1.2, lead to:

$$E_{grav} = \frac{GMm}{5R_s} = \frac{GMm}{5(\frac{2GM}{c^2})} = \frac{mc^2}{10} = 0.1mc^2 \tag{1.3}$$

After a comparison of equations 1.1 and 1.3, we can clearly see that the AGN efficiency η_{AGN} is 0.1, i.e. $\sim$ 10%. On the other hand, even by burning hydrogen into iron—the nucleus with the highest binding energy per nucleon—8 MeV/nucleon are released, or $0.008m_pc^2$ per nucleon. The maximum efficiency of nuclear fusion (η_{TN}) is therefore $\lesssim$ 0.8%, which is about 12 times lower than the AGN estimate of efficiency in equation 1.3. Luminous QSOs have a bolometric luminosity of up to $L_{bol} \sim 10^{47} erg/sec$. As a comparison, the Milky Way has a total luminosity of the order of 10^{10} $L_\odot \sim 10^{43}$ erg/sec. This huge amount of energy released per second requires a process with high efficiency and hence, the possibility of the thermonuclear process as a prime energy source has been discarded. In contrast, the potential energy of matter can be converted into kinetic energy with high efficiency through the infall of matter onto a central black hole. Part of this inward-directed kinetic energy can then be converted into internal energy (heat) and subsequently emit

*The formula for the Schwarzschild radius R_s can be found using the escape velocity equal to the speed of light c. R_s is equal to $\frac{2GM}{c^2}$.

this in the form of radiation. In fact, as per the theory of accretion onto black holes, a maximum efficiency of $\sim$ 6% for accretion onto a non-rotating black hole, while $\sim$ 29% for a rotating black hole (with the maximum allowed angular momentum) is obtained Schneider (2015).

1.1.1.2 Observational evidence for SMBH

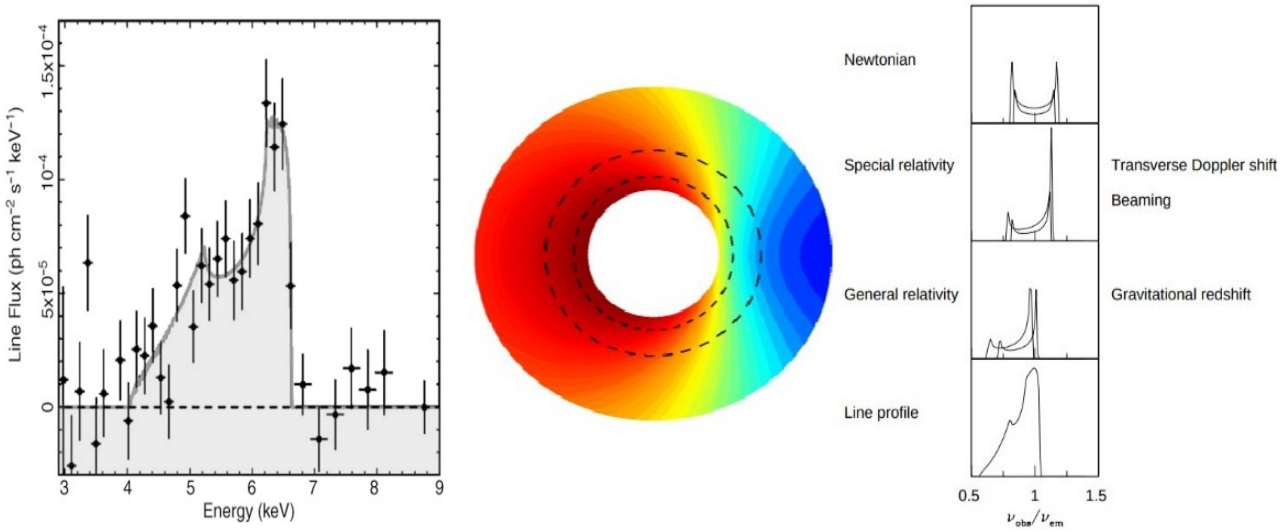

FIGURE 1.2: *Left*: ASCA satellite observation of Seyfert 1 galaxy MCG-6-30-15 showing the asymmetric iron K_α line. *Center*: rotating accretion disk; the symmetric double-peaked line shown in the right panel (topmost) originates from the two narrow annuli (dashed ellipses). *Right*: The profile of the broad iron K_α line. Processes like Doppler and transverse Doppler shifts, relativistic beaming, and gravitational redshift are responsible for the resulting line shape. a) Topmost: the shape of the line we would obtain if no relativistic effects occurred besides the non-relativistic Doppler effect. b) Second from the top: the shape of the line we would obtain taking the relativistic Doppler effect and beaming into account as well. c) Third from the top: this line profile is shifted towards smaller energies by gravitational redshift. d) Bottom: the line profile obtained considering all the previously mentioned effects. Source: Schneider (2015).

AGNs are observed to be copious X-ray emitters. X-ray observations of Seyfert galaxies reveal the intrinsically narrow iron K_α line of rest energy $h_p\nu = 6.35\,keV$ ($\sim$ 1.95 Å) to be broadened and asymmetric. This modified line profile shows the signature of high rotational velocity, resulting in strong Doppler effect (shift as well as relativistic beaming) and of the strong gravitational field of the black hole, resulting in gravitational redshift. These signatures indicate that the emission must be produced in the inner region of an accretion disk, within only a few Schwarzschild radii of a SMBH. Figure 1.2 shows a model for the line profile of iron K_α resulting from the emission of the disk in the radius range $R_S \leq r \leq 20R_S$ around a black hole. Figure 1.2 also shows the spectral form of the broad iron line in the Seyfert 1 galaxy MCG-6-30-15 as observed with the *Advanced Satellite for Cosmology and Astrophysics (ASCA)*. Stacked X-ray spectra of an ensemble of

AGNs have permitted to confirm the asymmetric 6.4 keV emission line with a high signal-to-noise ratio.

1.1.2 Orientation-based unification of AGNs

The identification of high anisotropy in the AGN continuum emission was the motivation for the development of the orientation-based unified schemes. In the context of this model, two types of anisotropy are considered: the beaming of the non-thermal synchrotron emission (radio jet) and the blocking effect of dust and gas in the circum-nuclear dust structures. The detection of apparently superluminal velocities in VLBI observations of the radio cores of blazar like objects (Cohen et al., 1977), serves as a direct evidence for beaming. One of the well known supporting evidence for the blocking effect comes from spectropolarimetry of NGC 1068 Seyfert galaxy. Seyfert galax-

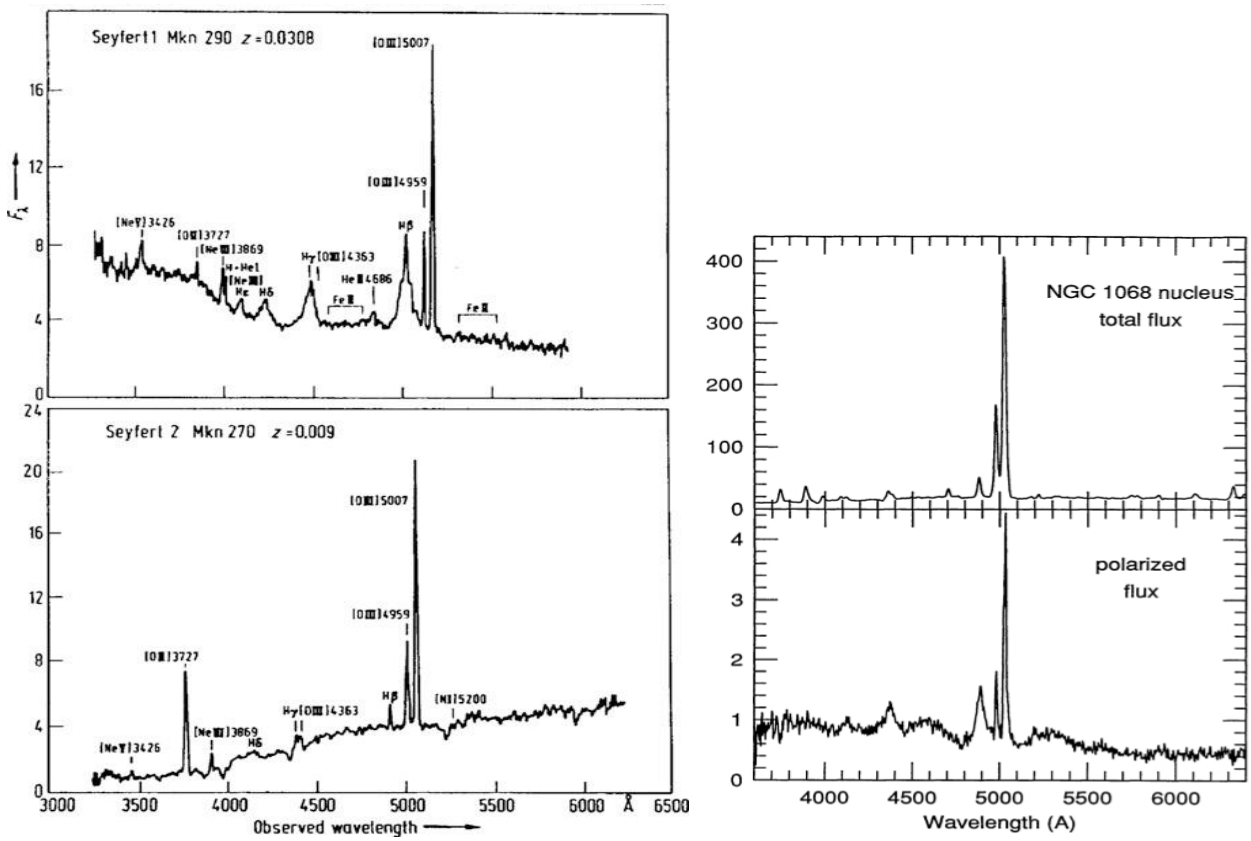

FIGURE 1.3: *Left*: The spectrum of the nearby Type 1 Seyfert galaxy Mkn 290. Here both very broad emission lines and narrow lines, in particular of double ionised oxygen, are visible. In contrast, the spectrum in the bottom panel, of a Seyfert galaxy of Type 2, shows only relatively narrow emission lines. *Right*: Spectrum of the Seyfert 2 galaxy NGC 1068. The top panel: displays the total flux spectrum which, besides the continuum, also shows narrow emission lines (e.g., [O III] at $\lambda = 5007$Å and $\lambda = 4959$Å). However, in JGpolarised light (bottom panel), broad emission lines (like $H_\beta\,\lambda = 4861$Å and $H_\gamma\,\lambda = 4340$Å) which are expected to be only seen in a Seyfert 1 galaxy are visible. Hence, it is concluded that the BLR, otherwise hidden in Seyfert 2 becomes visible in light polarised via scattering. Source: Schneider (2015).

ies, a class of AGNs, are traditionally divided into two classes according to the presence or absence of the broad permitted optical lines (e.g., Fig. 1.3): in Seyfert 1 the broad permitted optical lines are present and in Seyfert 2 they are absent. However, Antonucci and Miller (1985) found that the polarised flux spectrum of a prototypical Seyfert 2 galaxy NGC 1068 closely resembled the flux spectrum of Seyfert type 1 nuclei (Fig. 1.3). The polarised spectra of NGC 1068 showed broad Balmer lines and FeII emission, with polarisation $\gtrsim$ 15% at approximately the same position angle as that of the continuum. The non-stellar continuum exhibited polarisation of approximately $\sim$ 16%, regardless of wavelength. Their conclusion was as follows:

> "We favor an interpretation in which the continuum source and broad line clouds are located inside a thick disk, with electrons above and below the disk scattering continuum and broad line photons in to the line of sight."

Some other studies support the anisotropy due to the blocking effect of the circum-nuclear dust structures: detection of significant optical polarisation that is aligned perpendicular to the radio axes in nearby radio galaxies (Antonucci, 1982, 1984) and the detection of "ionisation cones" in narrow-band emission-line images of Seyfert galaxies (e.g. Pogge, 1988; Tadhunter and Tsvetanov, 1989) and radio galaxies (Jackson et al., 1998). If the viewing angle is high with respect to the axis of the radio jet and torus, i.e. almost perpendicular to it, then dust in the circum-nuclear region will have a prominent role in the attenuation of the UV/optical continuum and the broad line region emission. As per the orientation-based unification, all different classes of AGNs have the same central engine and the difference in their "appearance" can be explained in terms of anisotropy and orientation (Fig. 1.4).

1.1.3 The straw person model of AGN : A rough sketch of the unified model

In 1993, Antonucci proposed the straw person model (SPM) of AGN according to which, there are two basic types of AGNs: radio-quiet and radio-loud objects. For each class, there is a range in intrinsic luminosity and some properties are luminosity dependent. However, at a given intrinsic luminosity, the spectroscopic classification is dependent upon the orientation (Antonucci, 1993). Among the radio quiets, all have broad line regions and optical featureless continua, which are surrounded by optically thick tori, and the tori are oriented perpendicular to the weak radio jets. Face-on objects are called Type 1 spectroscopically, and the edge-on objects are called Type 2. The radio-loud sources have, in addition, twin synchrotron-emitting jets. Observed close to the jet direction, beamed synchrotron radiation from the base of the jet contributes heavily to or dominates the optical flux, leading to a blazar classification (Antonucci, 1993).

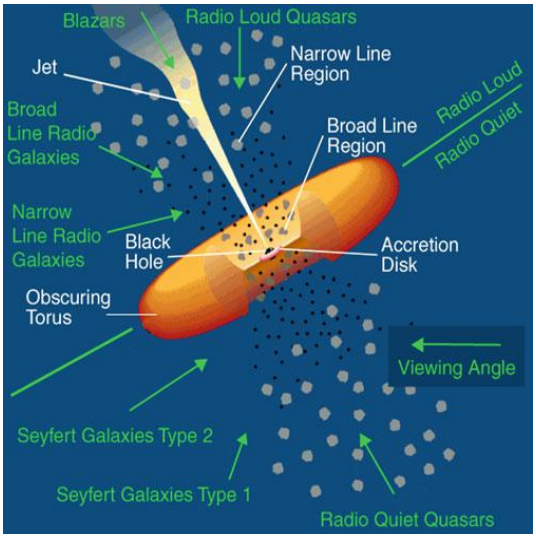

FIGURE 1.4: Schematic view of the AGN unification model. The central engine contains an accretion disk of matter and a donut shape dusty torus around this disk structure. Depending on the viewing angle, with respect to the line of sight, the torus may obscure the central parts of the AGN, leaving only visible the narrow line regions (NLRs) located far apart from the nucleus. On the other hand, a direct view to the nucleus will allow us to see the Broad line region (BLR) and the central engine. This is the main explanation for the Seyfert unification scheme. For instance, Seyfert 1s are Type 1 AGNs were we can observe the central regions, i.e. the BLR and power-law from the continuous source, while Seyfert 2s are type 2 AGNs were an obscuring torus prevent us from seen the BLRs, therefore, only NLRs are present and almost no featureless continuum. Source: Schneider (2015)

Radio-loud and Radio-quiet AGNs can be divided based on their radio-to-optical luminosity ratio ($R \equiv \frac{L_\nu(6\,cm)}{L_\nu(B)}$) , with the boundary set between the two classes at $R = 10$ (Kellermann et al., 1994). The spectroscopic classification of AGNs is based on the characteristics of the optical and ultraviolet spectra of AGNs: Type 1 has both very broad and also narrower emission lines and Type 2 shows only the narrower lines*(e.g., Fig. 1.3). With this convention, a radio-loud Type 1 AGN will have $R \gtrsim 10$ and show broad as well as narrow emission lines in the optical and ultraviolet spectra. On the other hand, a radio-loud Type 2 AGN will have $R \gtrsim 10$, but will only show narrow lines in the optical and ultraviolet spectra. The same convention applies to radio-quiet AGNs, characterised by $R < 10$.

Recent advancements in our understanding of AGN underscore that orientation alone cannot comprehensively account for the diversity observed in AGN properties and that central engine also plays a role in AGN classification.

*Narrow still means several hundred km/s and thus a significantly larger width than characteristic velocities (like rotational velocities) found in normal galaxies.

1.1.4 Emerging Evidence of the Central Engine's Role in AGN Classification

The discovery of changing-look AGNs has challenged the traditional static view of AGN classification. LaMassa et al. 2015 describe instances where AGNs exhibit dramatic transitions between Type 1 and Type 2 classifications over relatively short timescales, attributed to fluctuations in the accretion rate and alterations in the structure of the obscuring material. These transitions highlight the dynamic nature of the central engine and its direct influence on the AGN's spectral properties (LaMassa et al., 2015).

MacLeod et al. (2016) further explore this phenomenon, noting that variations in the ionizing flux from the central engine can lead to the rapid appearance and disappearance of broad emission lines. This variability directly impacts the observed spectral features of AGNs, reinforcing the concept that changing-look AGNs are critical to understanding the broader mechanisms at play in AGN classification.

Studies by Hickox et al. 2014 have illuminated how fluctuations in the accretion rate can lead to significant variability in the observed properties of AGNs. They show that variations in the accretion rate significantly impact the luminosity and spectral properties of AGNs. Periods of high accretion can enhance the brightness and emission lines, making the AGN appear more active. Such intrinsic variability indicates that the central engine plays a crucial role in AGN classification.

The role of low accretion rates in influencing AGN observables has been significantly documented by Heckman and Best (2014). Their research indicates that when the accretion disk becomes radiatively inefficient due to low accretion rates, broad emission lines may disappear, diminishing the need for an obscuring torus. Results of both Best and Heckman (2012) for SDSS-selected radio AGN and Mingo et al. (2014) for the 2Jy and 3CR samples, show a clear division between the Eddington ratios of low- and high-excitation objects at $L_{bol}/L_{edd} \sim 0.01$.

Heckman and Best (2014) introduced a framework categorizing AGNs into two primary modes: radiative-mode and jet-mode, each associated with distinct accretion dynamics and environmental impacts (see Fig. 1.5).

Radiative-mode AGNs efficiently convert the potential energy of the gas accreted by SMBH into electromagnetic radiation which is their main energy output. On the other hand, jet-mode AGNs mainly release energy in the form of the bulk kinetic energy transported in two-sided collimated outflows (jets) while producing relatively less radiation. Seyfert galaxies and quasi-stellar objects (QSOs) refer to the former group, while (low-excitation) radio galaxies refer to the latter group. Radiative-mode and jet-mode AGNs not only differ in terms of their primary energy output but also in the properties of their SMBHs and host galaxies (Heckman and Best, 2014). In

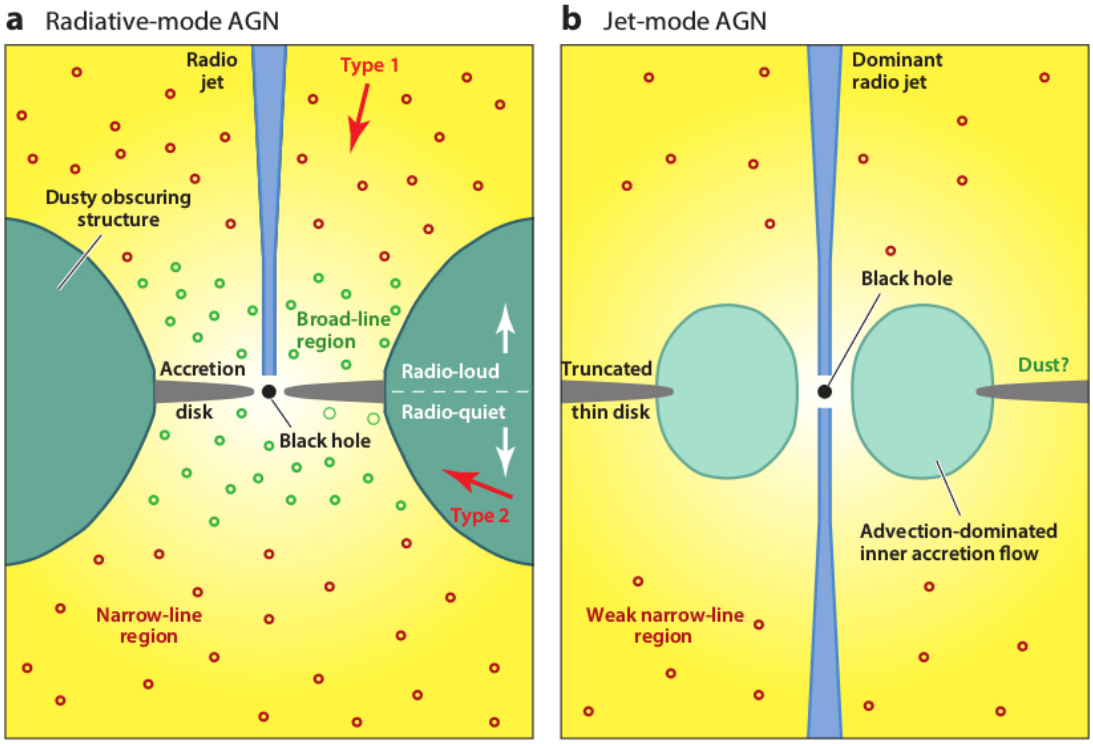

FIGURE 1.5: Various components of radiative-mode and jet-mode AGN are shown. (a) Radiative-mode AGNs contain a geometrically thin and optically thick accretion disk. The broad-line and narrow-line emission regions are irradiated by the luminous UV radiation from the accretion disk. An obscuring torus of dusty molecular gas obstructs the direct view of the central engine and the broad-line region from certain line of sights. Radiative-mode AGNs, predominantly toward the high end of the range of black hole masses, can also produce powerful radio jets. (b) Jet-mode AGNs contain a geometrically thick advection-dominated accretion flow in the inner regions. At larger radii, there maybe a transition to an outer (truncated) thin disk. Even though the radiative emission is less powerful in jet-mode Active Galactic Nuclei (AGN), it can still ionize weak, low-ionisation narrow-line regions, especially where the truncation radius of the thin disk is relatively low. Source: Heckman and Best, 2014.

the context of this framework, radiative mode AGNs are inherently axisymmetric and contain a blackhole, an accretion disk, which produces optical/UV and soft X-ray radiation, fast moving clouds giving rise to the broad lines observed in AGN spectra, gas, a torus, and slower moving clouds beyond the obscuring material emitting narrower lines, and possible outflows of energetic particles along the poles of the disk or torus, escaping and forming collimated jets (e.g., Fig. 1.5). A clear direct view of the SMBH, the disk/corona, and broad-line region (BLR) is obtained when a radiative mode AGN is observed from a sight line nearer the polar axis of the obscuring torus. These will be referred to as Type 1 (or unobscured) AGNs. On the other hand, this central region is hidden when a radiative mode AGN is observed from a sight line nearer to the equatorial plane of the obscuring torus. These will be referred to as Type 2 (or obscured) AGNs.

1.2 Influence of AGNs on Galaxy Evolution

Based on observations, it has been found that there are direct connections between the mass of the central black hole and the characteristic features of the host galaxy. Among these relationships, one of the most significant is the $M_{\rm BH}$-σ relation, which is an empirical correlation between the black hole mass and the bulge stellar velocity dispersion of the form $M_{\rm BH} \approx \sigma^4$ (Ferrarese and Merritt, 2000, Gebhardt et al., 2000). Another correlation exists between the black hole mass and the bulge stellar mass, which leads to $M_{\rm BH} \approx 10^{-3} M_{\rm bulge}$ (Häring and Rix, 2004, Marconi and Hunt, 2003). These correlations indicate a strong link between the growth of a central black hole and its host galaxy.

This connection is established through the interaction of the energy released by the AGN with the surrounding gaseous medium, a process known as AGN feedback. Negative AGN feedback occurs when the energy from the AGN displaces and heats up the matter surrounding the galaxy bulge and removes gas from the host galaxy. This gas is essential in fueling the central black hole and the gas reservoir supporting star formation. Clearing the gas halts further accretion and star formation (Di Matteo et al., 2005, Springel et al., 2005). However, AGN activity can also positively influence the star formation rate (Norman, 2009, Silk, 2013). There is evidence that AGN triggers star formation, suggesting a phase of positive feedback (Feain et al., 2007, Zinn et al., 2013). AGNs are thought to trigger SF in the extragalactic gas component through gas compression (Cresci and Maiolino, 2018, Maiolino et al., 2017).

Radiative-mode AGNs, often found in spiral and irregular galaxies rich in cold gas, primarily exert influence through intense radiation from the accretion disk. This radiative feedback heats and ionizes the ISM, driving powerful winds that can quench SF by ejecting gas from the galaxy's central regions. Conversely, these winds might also compress surrounding gas, potentially triggering new SF under certain conditions (Fabian, 2012, Gan et al., 2014). Jet-mode AGNs, typically located in massive elliptical galaxies and often at the centers of galaxy clusters, impact their environments through kinetic energy carried by relativistic particle jets. These jets extend far beyond the galaxy itself, heating the intracluster medium (ICM) and creating large cavities that inhibit gas cooling and subsequent SF over extensive areas. This "maintenance mode" feedback is pivotal in regulating the thermal state of galaxy clusters and preventing the formation of new stars, thus maintaining the quiescence of large elliptical galaxies (Fabian, 2012, Gaspari et al., 2012).

The phase of SF in a galaxy can significantly impact AGN activity. In the post-starburst phase, the cessation of SF due to the depletion of cold gas can lead to reduced fueling of the central black hole, potentially lowering AGN activity. However, the remnants of the starburst phase, such as

the dense stellar core and associated gravitational influences, may still support intermittent AGN activity. This complex interaction suggests a cyclical relationship where periods of intense SF and AGN activity are followed by quiescent phases (Chowdhury et al., 2022, Smith et al., 2020).

Investigating the star-formation history, which chronicles the rate of star formation over a galaxy's lifetime, plays a key role in understanding the interplay between star formation and AGN activity. Spectral synthesis techniques are used to recover the star-formation history of galaxies.

1.3 Spectral synthesis technique

Understanding the formation and evolution of galaxies, except for the few systems in our close vicinity, depends to a large degree on deciphering the galactic spectra using spectral synthesis techniques. There are two complementary techniques in spectral synthesis: evolutionary synthesis and population synthesis. These techniques were inspired by the works of Struck-Marcell and Tinsley (1978) and Faber (1972), respectively. Evolutionary Spectral Synthesis (ESS) aims to compute the time evolution of a galaxy's Spectral Energy Distribution (SED) based on assumed Star Formation History (SFH) and Chemical Enrichment History (CEH). On the other hand, Population Spectral Synthesis (PSS) aims to break down a galaxy's observed spectrum into its constituents, which are spectra of individual stars or spectral snapshots of instantaneously formed Simple Stellar Populations (SSPs). The PSS code selects these constituents (which are fully characterised by their age, chemical composition, and initial mass function) from a spectral base library.

Spectral synthesis methods have greatly enhanced our comprehension of the formation and evolution of galaxies. Among the significant revelations is the occurrence of galaxy downsizing (e.g., Cowie et al., 1996; Brinchmann et al., 2004; Heavens et al., 2004): low-mass galaxies are the primary sites of star formation during low redshifts, while massive galaxies underwent their major phase of mass assembly in earlier cosmic history. Spectral synthesis has also played a pivotal role in discovering the mass-metallicity relationship in galaxies. The groundbreaking study by Lequeux et al. (1979) on gas-phase metallicity in nearby star-forming galaxies and subsequent investigations by Trager et al. (2000) utilizing SDSS data, as well as spatially resolved data from the CALIFA survey (such as Sánchez et al., 2017, 2012 and González Delgado et al., 2014) further elucidated this correlation. Recent studies using Integral Field Spectroscopy (IFS) have provided evidence supporting the inside-out growth scenario of galaxies, like the works of Breda and Papaderos, 2018, Pérez et al., 2013, Gonzáez-Delgado et al., 2016, and Gomes et al., 2016b. Additionally, various studies have demonstrated a correlation between the SFH and gas-phase metallicity in star-forming galaxies. These studies have revealed that while all star-forming galaxies have

amassed most of their stellar mass over a billion years ago, systems with low-nebular metallicity evolve at a more gradual pace and currently exhibit a notably higher specific SFR (sSFR) in comparison to metal-rich galaxies (Asari et al., 2007, Lara-López et al., 2010).

Wilkinson et al. (2015) utilized full spectral fitting of galaxy data from P-MaNGA, a prototype of the MaNGA (Mapping Nearby Galaxies at Apache Point Observatory) instrument, to map the distribution of stellar populations across galaxies, highlighting how different regions within galaxies have distinct star formation histories and chemical compositions. They found that the gradients for galaxies identified as early type are on average flat in age, and negative (-0.15 dex$/R_e$) in metallicity, whereas the gradients for late-type galaxies are on average negative in age (-0.39 dex$/R_e$) and flat in metallicity. Zhou et al. (2020) applied a Bayesian full spectral fitting technique to a sample of low-mass galaxies from the MaNGA survey. Their study provided detailed measurements of stellar population properties, including the finding that more than half of the stellar mass in these galaxies formed over 8 billion years ago, with significant contributions from both old and young stellar populations.

Scott et al. (2017) utilized spectral synthesis to investigate the global stellar populations of galaxies in the SAMI survey. They find a general picture consistent with previous work in which high-mass galaxies are old, more metal-rich, and alpha-enhanced compared to low-mass galaxies, which are young, metal-poor, and alpha-deficient, albeit with significant scatter. Ferreras et al. (2019) focused on the internal radial gradients of stellar populations in early-type galaxies from SAMI survey, using spectral synthesis techniques to demonstrate that velocity dispersion is the primary driver of chemical composition gradients within these galaxies.

Over the past decade, various PSS codes were developed, each with a different priority. These codes include FIREFLY (Wilkinson et al., 2017), MOPED (Heavens et al., 2000), pPXF (Cappellari and Emsellem, 2004), STARLIGHT (Cid Fernandes et al., 2005, López Fernández et al., 2016), STECKMAP (Ocvirk et al., 2006), and ULySS (Koleva et al., 2009). The latter's mathematical concept complies with PSS, but it imposes assumptions on the best-fitting SFH and CEH. ULySS and STECKMAP are primarily intended for spectral fitting and kinematical analyses. MOPED aims to collapse a galaxy spectrum into its most robust and characteristic spectroscopic features. violet FIREFLY focuses on stellar populations, mapping out intrinsic spectral energy distribution degeneracies such as age, metallicity, and dust reddening. STARLIGHT has been the go-to PSS code for studying the SFH of galaxies with single-fibre large spectroscopic data sets, such as SDSS (York et al., 2000). On the other hand, Sánchez et al. (2016) developed PIPE3D for the analysis of the spectroscopic properties of the stellar populations and the ionized gas in the spatially resolved

data from optical IFU surveys. Even though spectral synthesis techniques have undergone significant development in the past for studying normal galaxies, their application to AGN is a work in progress.

1.3.1 Spectral modelling of Active Galaxies

The very early approach to spectral modelling of AGNs was the "template subtraction" technique, which was used to recover AGN emission from its spectra. In this technique, a template spectrum devoid of emission lines is suitably scaled to and subtracted from the spectrum of interest to yield a continuum-subtracted, pure emission-line spectrum. Several approaches have been adopted to construct the template. For instance, it was a common practice to assume that an AGN-hosting galaxy was composed solely of old and metal-rich stellar populations and to remove the underlying SED, which is, in general, represented by an elliptical galaxy spectral template, to study the recovery of the AGN emission (e.g., Koski, 1978). However, the absorption-line galaxy chosen as the template may not accurately reflect the stellar content and velocity dispersion of the object under study, as demonstrated by Schmitt et al., 1999. By examining the flux continuum ratios and absorption-line EWs, the researchers analysed the role of AGN Power Law (PL) in the optical spectra of 20 nearby Seyfert 2 galaxies. Their findings indicate that AGN PL typically accounted for no more than 5% of the spectrum, which differs significantly from the high Featureless Continuum contribution (up to approximately 70%) identified by Koski in 1978. Another method used to create a template to remove the starlight is to use the spectrum of an off-nuclear position within the same galaxy (e.g., Storchi-Bergmann et al., 1993). However, the off-nuclear spectrum may not be completely free of line emission, and the off-nuclear light may be a poor representation of the nuclear position if there are radial gradients in the stellar population (Ho, 2008). Some other approaches to constructing the template and their limitations have been discussed by Ho, 2008. These approaches, however, could not explore the reconstruction of active galaxies' stellar mass assembly history or did not have it as the prime objective.

1.3.1.1 Contribution of the featureless continuum

A featureless continuum, typically represented by a power-law of the form $F_\nu \propto \nu^{-\alpha_\nu *}$ (e.g., Koski, 1978; Veilleux and Osterbrock, 1987; Mathews and Ferland, 1987; Heckman, 1980; Kauffmann et al., 2003; Cid Fernandes et al., 2004), dominates the UV-optical spectra of type 1 AGNs. However, its

*α_ν is referred to as the PL index, defining the slope of the featureless continuum power-law. A featureless continuum can also be expressed as $F_\lambda \propto \lambda^{-\alpha_\lambda}$, where $\alpha_\lambda = 2 - \alpha_\nu$.

significance in the UV-optical spectra of type 2 AGNs, such as Seyfert 2 galaxies, has been subject to debate. Various studies have aimed to assess the contribution of the featureless continuum to optical spectra and whether it should be considered in AGN modelling.

Malkan and Filippenko (1983) studied the nuclei of 9 Seyfert galaxies with notably faint stellar absorption lines. Their findings suggested that stars might account for between 17% and 60% of the visual continuum. A PL with an alpha value of 1.1-1.2 from the optical range to 10 micrometres could roughly represent the remaining non-stellar continuum. Later on, Schmitt et al. (1999) investigated the contributions of AGN and stellar populations to absorption-line equivalent widths (EWs) and continuum ratios in the 3500–7000 Å range of 20 Seyfert 2 galaxies. They concluded that the contributions of stars younger than 10 Myr and an AGN featureless continuum should rarely exceed ∼5%.

Goerdt and Kollatschny (1998) developed a modified simplex optimisation algorithm to model AGN spectra through population and evolutionary analysis. To model the Seyfert 1 galaxy NGC 1365, they applied this algorithm to spatially resolved optical spectra. Their findings revealed that the non-thermal continuum component, represented by $F_\nu \propto \nu^{-\alpha_\nu}$, accounts for 60% of the flux at 5050 $\mathring{A}$. The FeII quasi-continuum contribution to the nuclear spectrum is only 0.2%.

According to Eracleous and Halpern (2001) findings, NGC 3065 exhibits characteristics of a LINER (low-ionisation nuclear emission-line region) and broad Balmer emission lines originating from an accretion disk. The authors used a combination of non-stellar components and starlight spectra from S0 galaxies to model the continuum. Interestingly, when the authors compared NGC 4339 to NGC 3065 as a template, the spectrum matched without requiring a non-stellar component. Nevertheless, other galaxy templates showcase a non-stellar continuum that has the potential to contribute up to 10% to the continuum flux at $H\alpha$ and $H\beta$ and up to roughly 15% at [OII]λ3727.

Cid Fernandes et al. (2004) studied the stellar population properties of a sample of 79 mostly Seyfert 2 galaxies by applying full-spectrum (pixel-by-pixel spectral synthesis) modelling with an early version of STARLIGHT. They applied STARLIGHT in the spectral region 3500–5200 Å while allowing for variations of a PL spectral component in the base library. This work found stellar populations of all ages and a fetureless continuum PL component with a mean contribution of ∼20–30% and a maximum contribution of ∼63% to the monochromatic flux at 4020 Å. The authors discuss that the featureless continuum PL component could describe the scattered starlight of a hidden AGN or a young and dusty starburst. Regardless of the origin of this featureless continuum, this work demonstrates a significant contribution of a featureless continuum in Seyfert 2 galaxies. Vega et al. (2009) analysed a sample of 64 Seyfert, 9 normal and 5 starburst galaxies with

STARLIGHT. They estimated the fractional contribution of multiple PLs with α_ν = 1-2 and found that the PL at 3933$\AA$ can be as high as $\sim$90% in Seyfert 1 and $\sim$50% in Seyfert 2.

Riffel et al. (2010) used IRTF SpeX NIR (0.8–2.4μm) spectra to investigate the stellar population, AGN, featureless continuum and hot dust properties in 9 Seyfert 1 and 15 Seyfert 2 galaxies. They found that about 50% of the Seyfert 2 galaxies require a featureless component contribution in excess of 20%, while this fraction increases to about 60% in Seyfert 1 galaxies.

1.3.1.2 Inclusion of featureless continuum is a necessity

Very few studies have evaluated the capability of spectral energy density (SED) fitting codes to retrieve AGN emission and stellar population properties in the presence of an PL continuum. Moultaka (2005) studied the retrieval of the luminosity contribution of stars, stellar velocity dispersion and reddening when a featureless continuum is present in a galactic spectrum. By summing 11 stellar spectra of different stellar classes taken from Boisson et al. (2000), the author constructed 3 types of galactic spectra: I) dominated by intermediate and late-type stars (G- and M-type), II) dominated by young and early-type stars and (O- and A-type) III) dominated by intermediate stars (G- and K-type). A PL with index α_ν = -1.5, -0.5, 0.5, 1.5 was added to the galactic spectra for 10% and 50% contribution to the V-band luminosity coming from the featureless continuum. The models were constructed without any attenuation (reddening) or kinematics (velocity dispersion). On modelling the spectra without a PL, the retrieved luminosity contribution from hot (O- and A-type) stars is significantly higher, and the reddening was significantly higher than the model, regardless of the index α_ν of PL. This discrepancy is because these stars have a quasi-featureless continuum in the optical band, mimicking the featureless continuum. However, a higher reddening is needed to straighten the spectra as the continuum of the hot stars decreases with increasing wavelength. So, the presence of a featureless continuum affects the estimation of stellar properties if this continuum is not modelled in the synthesis.

Bon et al. (2014) simulated over 7000 integrated spectra of Seyfert 2 galaxies with α_ν = -1.5, -0.5, 0.5, 1.5, 2; AGN power-law continuum contribution to the total continuum at 5100 Å in the range 10–90%; emission lines; single stellar population spectra of age 5 Gyr and solar metallicity; various SN emission line properties. Using ULySS code, they modelled the integrated spectrum as a combination of stellar template spectrum convolved with a line-of-sight velocity broadening function, featureless continuum with α_ν = -1.5, and AGN emission lines, represented by a sum of Gaussian/Gauss–Hermit functions. The study's goal was under which conditions an aged stellar population can still be recovered in the presence of an overlapped AGN continuum. They find that

if the spectra have SN>20 and the stellar population fraction is higher than 10%, the ULySS code can estimate the parameters of the gas and stars well. Also, they find that with increasing AGN power-law continuum contribution to the total continuum at 5100 Å, the degeneracies between AGN and stellar population parameters increase.

Cardoso et al. (2016) utilised STARLIGHT to fit synthetic SEDs with stellar emission and PL featureless continuum. This study aimed to examine whether the AGN component can be identified using current SPS methods in the optical spectrum, explicitly determining whether these techniques can effectively establish an AGN detection threshold in Lyman-continuum-leaking galaxies*. The authors used STARLIGHT to fit a grid of SEDs composed of a 10 Gyr early-type galaxies (ETGs) and a PL component that contributes a fraction $0 \leq xAGN < 1$ of the monochromatic luminosity at $\lambda_0 = 4020\AA$ for a signal-to-noise ratio of 5 to 1000. The authors found that the effective AGN detection threshold is when 26% of the monochromatic luminosity at $\lambda_0 = 4020\AA$ comes from the PL component, suggesting that a considerable fraction of ETGs hosting significant accretion-powered nuclear activity may be missing in the AGN demographics.

A recent study by Cardoso et al. (2017), investigated the impact of an AGN featureless continuum on estimating stellar population properties using the STARLIGHT code. The authors developed two synthetic spectra, one consisting solely of stellar models and the other with an additional featureless continuum contribution. The purely stellar model was generated by linearly combining the fluxes of SSPs of varying ages and metallicities based on a predetermined SFR. The resulting Composite Stellar Population (CSP) flux represents the emission of a galaxy at a specific age with a purely stellar output. The other set of models was produced by adding a simple AGN continuum of the form $F_\nu \propto \nu^{-\alpha_\nu}$ (α_ν = 0.5, 1, 1.5 and 2) to the purely stellar models with 20%, 40%, 60% and 80% contributions to the monochromatic fluxes at λ = 4020 Å (denoted by x_{AGN}). The spectral fitting was done for the wavelength range, 3400 to 8900 Å, assuming no stellar kinematics and V-band extinction Av to facilitate a more straightforward comparison between fits to purely stellar and active galaxy SEDs. According to this study, failing to factor in the PL component when fitting galaxies with a PL may result in significant uncertainties in estimating stellar mass, with a potential discrepancy of up to $\sim$3.5 dex. Additionally, the average age and metallicity of the stars, calculated based on both light and mass weightings, could be off by up to $\sim$2.0, $\sim$4.0, and $\sim$0.7 dex, respectively.

However, incorporating a PL component during the fitting process with STARLIGHT may result in uncertainties that cause an overestimation of the stellar mass by approximately one order

*In practice, without the presence of nebular emission in these galaxies.

of magnitude. Similarly, the light- and mass-weighted mean stellar age may be affected, with uncertainties of approximately 1.5 and 3 orders of magnitude, respectively. Additionally, the light- and mass-weighted mean stellar metallicity may be impacted by uncertainties of approximately 0.2 and 0.4 orders of magnitude, respectively (Cardoso et al., 2017).

Aside from the issue of omitting a featureless continuum contribution when modelling AGNs, most of the current PSS codes do not account for Nebular Emission (lines and continuum). Neglecting Nebular Emission (NE) in modelling galaxies introduces significant biases in estimating their properties (e.g., Izotov et al., 2011; Cardoso et al., 2019; Gomes and Papaderos, 2017). Hence, there is a need to develop a PSS code that takes featureless continuum and nebular emission for modelling AGNs, which is required to reconstruct the mass assembly history of AGNs accurately.

Hereafter in this thesis, we will employ the term 'power-law' interchangeably with 'featureless continuum' unless explicitly stated otherwise. This approach aims to streamline the terminology and avoid redundancy throughout the text.

This work aims to extensively test and benchmark the PSS code Fitting Analysis using Differential evolution Optimisation (FADO, Gomes and Papaderos, 2017) for application to AGNs, particularly Seyfert 2 galaxies. FADO not only includes NE but also ensures consistency between the best-fit population vector (i.e., SFH, intrinsic extinction and kinematics) and the observed nebular characteristics of a star-forming galaxy (e.g. Hydrogen Balmer-line luminosities and EWs, continuum shape around the Balmer and Paschen jumps).

Chapter 2

Synthetic models of AGNs

The primary objective of this thesis is to evaluate the applicability of the current FADO release to real observations of Seyfert 2 galaxies for property extraction. Nonetheless, before applying it to actual data, rigorous testing on synthetic spectra is imperative. This study endeavors to address several key questions: How accurately can FADO retrieve the properties of Seyfert 2 galaxies from their spectra? Is it proficient in effectively decomposing these spectra into their constituent parts? And under what conditions does it perform optimally?

Unlike in the case of observed spectra, we know the properties of the galaxy producing a synthetic spectrum apriori, and we can use the synthetic spectrum to evaluate the code's performance. A simple example: we can create a galaxy spectrum dominated by light from stars of a particular age and metallicity, apply FADO, and compare inputs (corresponding to the synthetic spectra) and outputs FADO gives. We created three classes of synthetic spectra, spanning a vast set of parameter space: Seyfert 2 NLR, CSPs, and composite of Seyfert 2 NLR and CSP. The latter attempts to mimic realistic spectra composed of NLR and stellar emission. In this chapter, we will explain the construction of each of them. But first, let us briefly review about photoionisation models of AGNs and the challenges in creating their self-consistent model.

2.1 Challenges in modelling photoionisation of AGN narrow-Line regions

In astrophysical research, photoionisation codes are utilised to calculate synthetic spectra of plasmas found in planetary nebulae, HIIRs, NLRs, and BLRs. These codes solve equations for ionisation and thermal equilibrium of a gas cloud, considering various processes such as photoionisation, recombination, free-free radiation, and collisional excitation when the gas cloud is exposed to

a radiation field.

The study of NLR involves comparing observed emission-line strengths to the ones predicted by photoionisation models on diagnostic diagrams. Diagnostic diagrams differentiate between objects based on their emission-line intensity ratios. For example, in the Baldwin, Phillips & Terlevich (BPT; Baldwin et al. 1981) diagnostic diagram (e.g., Fig. 2.1), emission line galaxies occupy four different regions of the diagram due to the difference in their emission-line intensity ratios. The same figure shows stacked spectra of the four types of emission line galaxies where difference in the emission line strengths can be clearly seen.

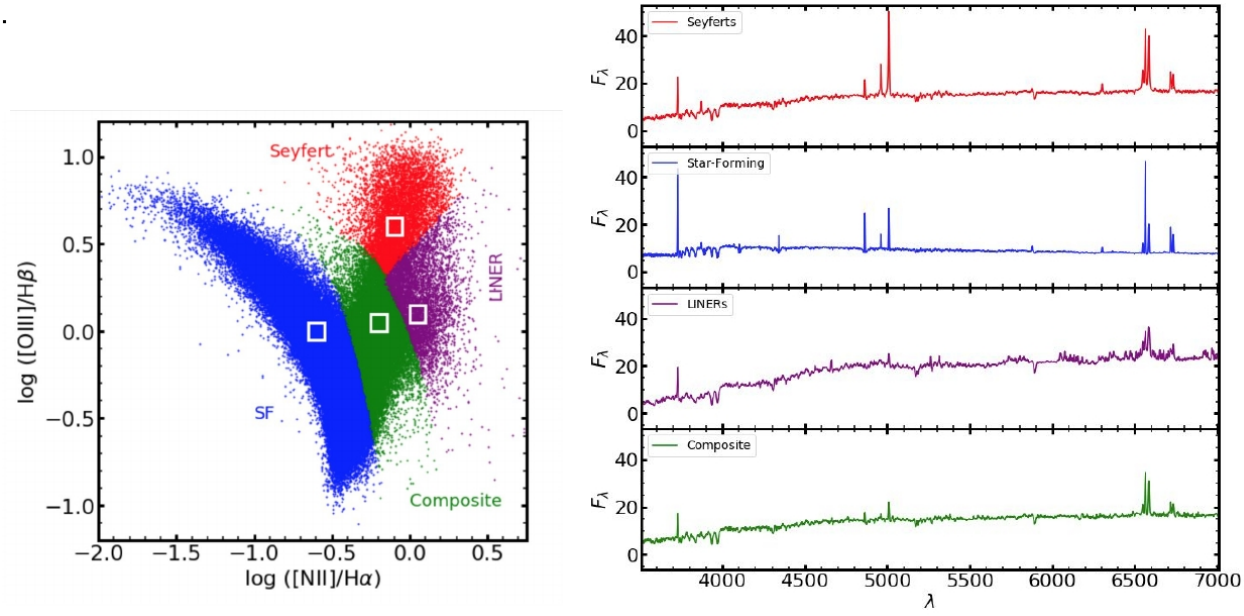

FIGURE 2.1: BPT-[NII] classical diagnostic diagram without the division lines (left; plotted without the demarcation lines for clarity) and stacked spectra representative of each object class (right). SF, Seyferts, Composites, and low-ionisation nuclear emission-line region (LINERS) occupy different regions of the diagram (left). Source: Pucha (2021), modified by Abhishek Rajesh Chougule.

2.1.1 Uncertainty surrounding ionising spectral energy distributions of AGNs

For modelling AGNs, various forms of the incident radiation field have been assumed in the literature: simple PL $f_\nu \propto \nu^{-\alpha\nu}$ (Binette et al. 1996; Groves et al. 2004;Feltre et al. 2016; Eq. 2.1), a combination of PL and blackbody continua (Komossa and Schulz 1997) and multi-component distributions (Richardson et al. 2014; Ferguson et al. 1997). And each of these fields have been successful in reproducing AGN like emission-line intensity ratios, at least qualitatively. *

*Models of photoionization encompass grids in emission-line ratio diagnostics, but it's important to note that they are not fits to the lines themselves, i.e., they do not self-consistently derive the exact relative emission-line strengths for all spectra. Nonetheless, each of these fields has been successful in broadly reproducing the region of AGN-like emission-line intensity ratios qualitatively.

For instance, Feltre et al. (2016) used a set of broken PLs to represent the incident ionising radiation field to produce photoionisation models:

$$S_\nu \propto \begin{cases} \alpha^\nu & 0.001 \leq \lambda/\mu m \leq 0.25 \\ \alpha^{-0.5} & 0.25 < \lambda/\mu m \leq 10.0 \\ \alpha^2 & 10.0 < \lambda/\mu m \end{cases} \tag{2.1}$$

The models span the following set of parameters: $-2.0 \leq \alpha_\nu \leq -1.2$ for $0.001 \leq \lambda/\mu m \leq 0.25$; hydrogen gas density ($n_H$) = 10^2, 10^3 and 10^4 $[cm^{-3}]$; metallicity (Z) = 0.0001, 0.001, 0.01774 and 0.03. Figure 2.2 is a BPT diagram for these models plotted over emission line galaxies observations from Sloan Digital Sky Survey Data Release 7 (SDSS DR7; Abazajian et al. 2009). Different combinations of incident radiation field and gas parameter are able to produce AGN like emission-line intensity ratios for the aforementioned models. The emission-line intensity ratios depend upon the incident radiation field as well as the chemical composition of the gas. However, even in the cases where the gas properties have been restricted to the local Universe (e.g., the middle panel of the last column in Fig. 2.2), different ionising continuum radiation field produce emission-line intensity ratios such that the models occupy the AGN region of the BPT diagram. Hence, ionising continuum radiation field for AGNs is degenerate in this sense.

2.1.2 The ionising spectral energy distributions lack physical justification

Only recently, Thomas et al. (2016) have attempted to link the shape of the incident radiation field (OXAF models) to the fundamental AGN parameters in order to produce emission lines ratios. The OXAF model draws from the OXAFAGNF (Done et al., 2012) and utilises three main parameters to characterise the spectral shape: E_{peak}, the energy of the accretion disk emission peak; Γ, the photon power-law index for the non-thermal Comptonized component; and p_{NT}, the proportion of the total flux attributed to the non-thermal component. The authors also computed photoionisation models using MAPPINGS (Sutherland et al., 2018) for default CLOUDY (Ferland et al., 2013) SED and two OXAF spectra, equivalent to the former (see Fig. 2.3). The default SED in CLOUDY is modelled as a single blackbody curve combined with a power law. The authors conclude that OXAF spectra have the potential to yield anticipated diagnostic line ratios that closely resemble those obtained from analytic ionising spectra (CLOUDY) which are not derived from physical models. However, this is contingent upon the degree of similarity in spectral shapes, particularly in the critical region of the spectrum, i.e., the hydrogen-ionising EUV.

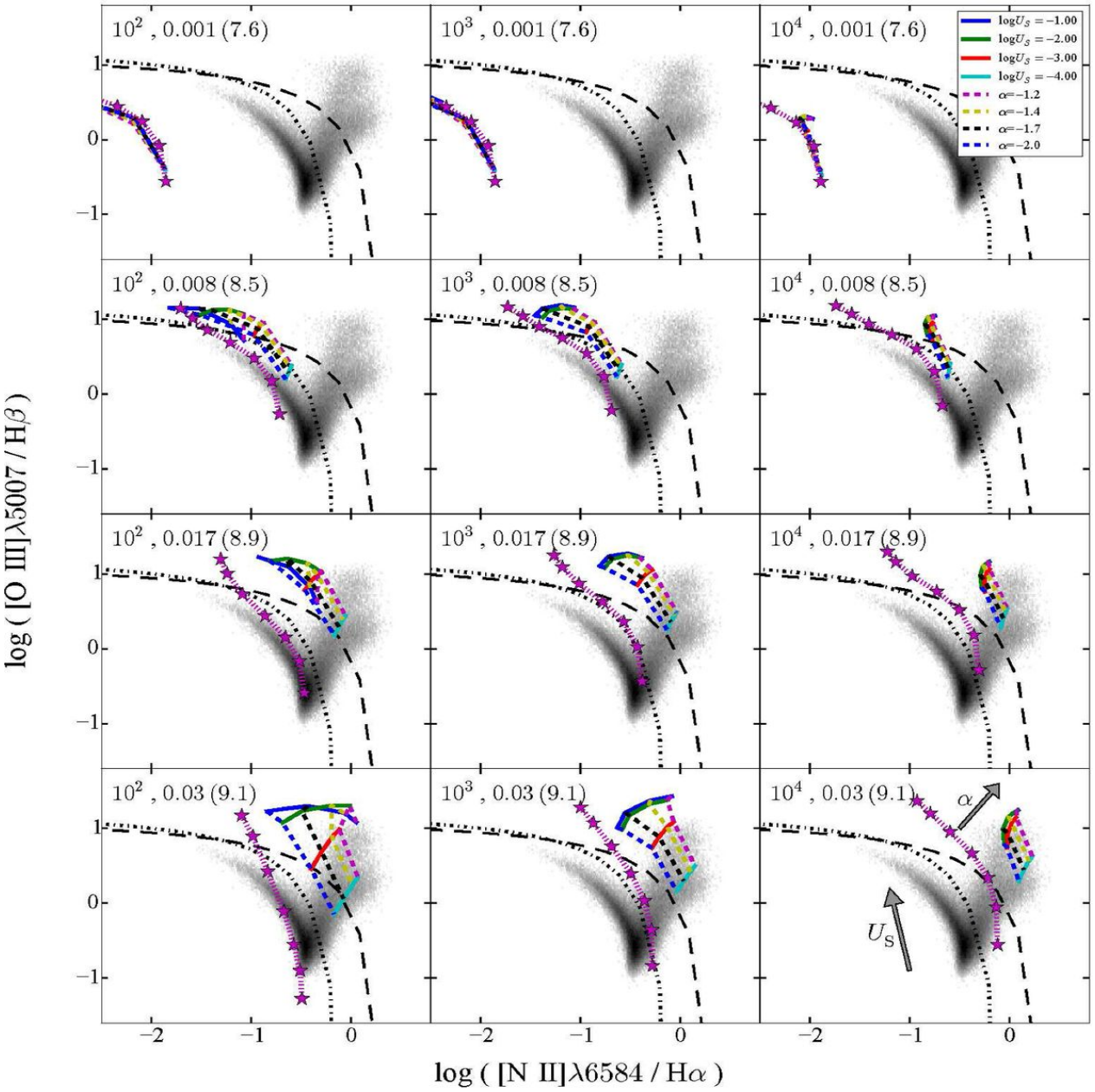

FIGURE 2.2: Standard BPT diagram (Baldwin et al., 1981) containing AGNs and SF models of Feltre et al. (2016) having different values of gas density, ionisation parameter, gas metallicity, and ionising continuum power-law index, plotted on top of SDSS DR7 observations. The long-dashed and dot–dashed black lines indicate, respectively, the criteria of (Kewley et al., 2001) and (Kauffmann et al., 2003) to distinguish AGN from star-forming galaxies. n_H and Z increase from left to right and top to bottom, respectively. Source: Feltre et al. (2016)

It is a common practice in photoionisation modelling to assume that there is no significant photon interaction between the central engine and the modelled clouds, i.e., the ionising spectrum will be intrinsic when it reaches the modelled clouds and the authors have done the same.

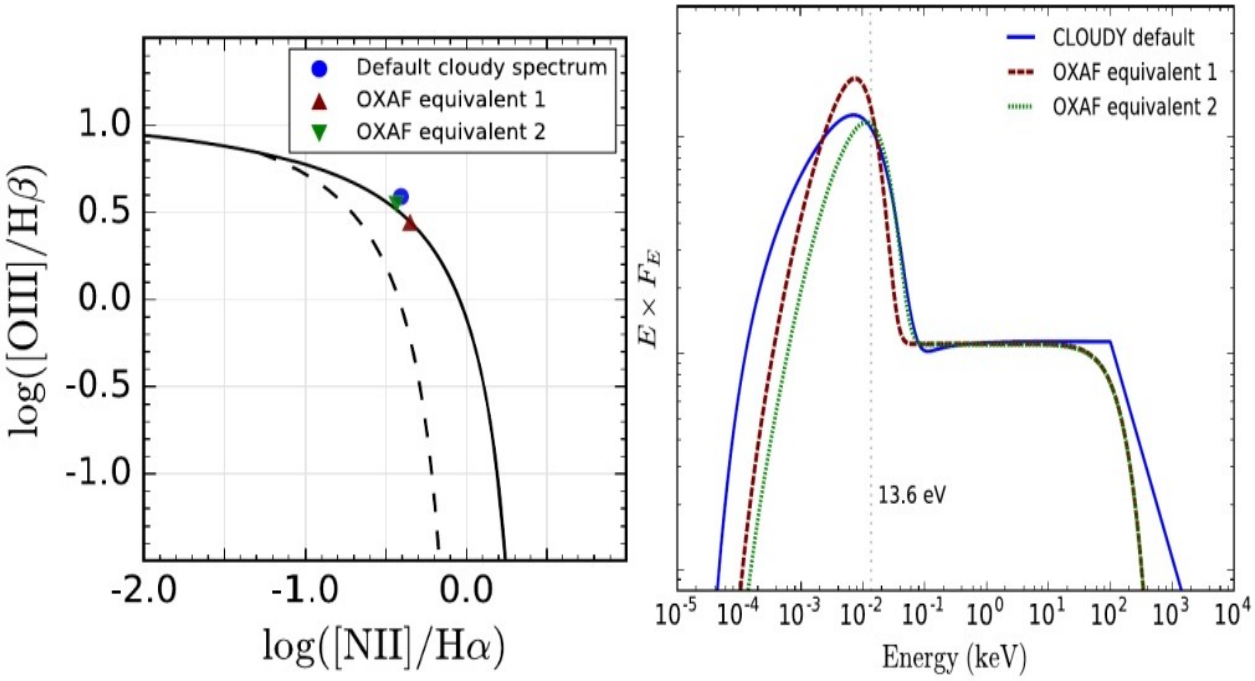

FIGURE 2.3: Comparison between physically motivated ionising OXAF SEDs and default CLOUDY SED (right panel) and the emission line ratios produced by each of them (left panel). All three of the SEDs are capable of producing AGN emission line ratios on the BPT diagram. Source: Thomas et al. (2016), modified by Abhishek Rajesh Chougule.

2.1.3 The anisotropy of ionising spectral energy distributions of AGNs

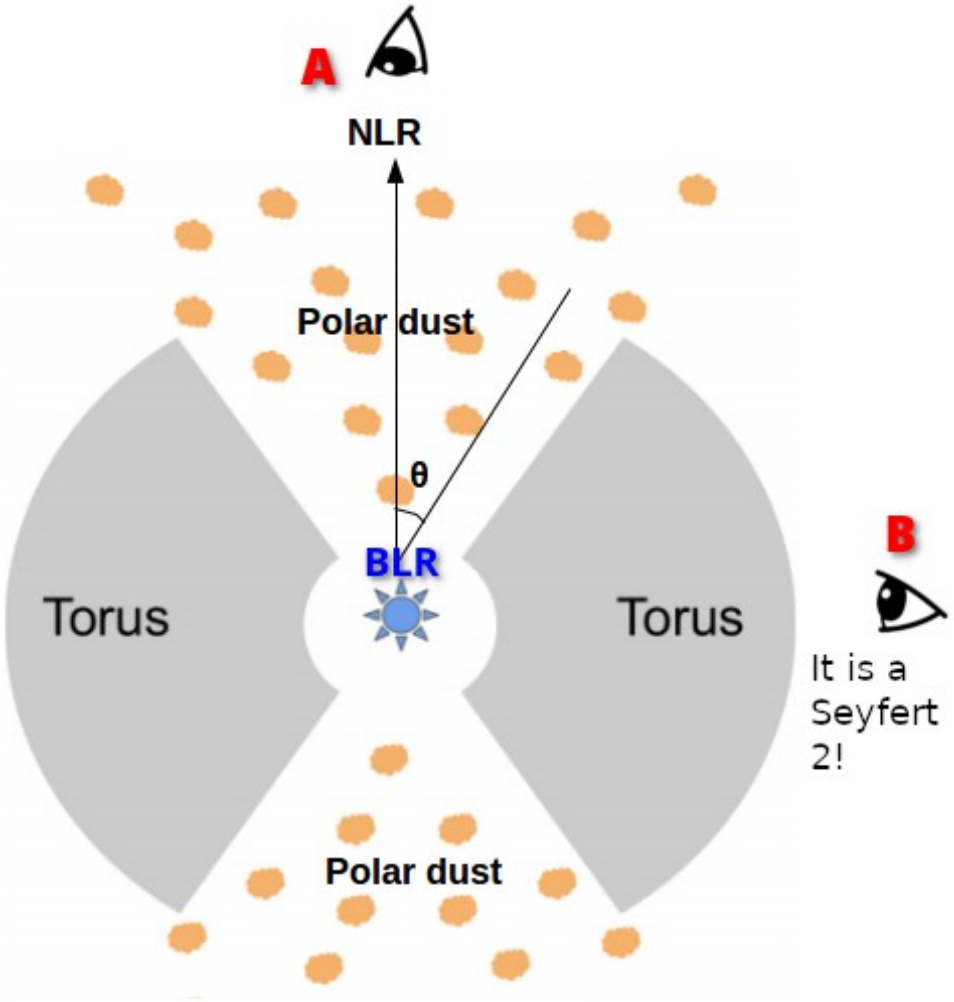

FIGURE 2.4: Cross-section of an AGN central engine. The NLR directly sees the central engine and receives the ionising continuum from the accretion disk. The radiation emitted by the central source interacts with the polar dust before reaching the NLR. For an observer viewing a Seyfert 2, the direct view of the central engine is blocked by the dusty torus. Hence, he cannot observe the ionising AGN continuum directly but the processed radiation field. The components are not scaled properly and the figure is only for an illustrative purpose. Source: Yang et al. (2020), modified by Abhishek Chougule.

The radiation field incident on emission-line gas clouds in case of Seyfert 2 galaxies is difficult to constrain due to anisotropic emission in AGNs. Studies by Antonucci and Miller (1985) and Tran (1995a,b)* suggest that Seyfert 2 exhibits anisotropic emission, with Seyfert 1 emission detected in the scattered light that enters our line of sight (LOS). As a result, it may not be accurate to use direct continuum measurements of Seyfert 2 nuclei to estimate the radiation field incident on emission-line clouds. Hence, the emission-line gas sees a different continuum than is observed

*we can see the hidden BLR from polarised light within the typical Seyfert 2 spectrum.

along our line of sight (LOS). Figure 2.4 explains this phenomenon. The observer located in the NLR (observer A) perceives a different ionising continuum radiation field compared to observer B as the ionising continuum radiation interacts with the BLR and polar dust before reaching the NLR (observer A). Therefore, observer B, who observes the same galaxy as Seyfert 2, does not see the ionising continuum radiation that strikes the NLR or the one emitted by the accretion disk. Instead, observer B sees the emission reprocessed by the NLR gas, potentially combined with reflection and scattering of the accretion disk emission. So, the observed FC in Seyfert 2 spectra may have nothing to do with the radiation field striking the NLR.

2.2 Developing Photoionisation Models for the Narrow-Line Region in AGNs

2.2.1 Towards the production of more realistic Active Galactic Nuclei Spectral Energy Distributions

We created Seyfert 2 NLR models that takes into account the anisotropic nature of the incident radiation field. This computation has been the subject of extensive work for nearly eight months and is primarily built from scratch in Python 3 by us. This development has permitted us to have a standalone AGN module for AGNs' continuum incident radiation field, depending on their viewing angle. Using SKIRTOR models* (Stalevski et al., 2012, 2016) as the base, we have produced AGN SEDs with emission lines, which are calculated self-consistently. The SKIRTOR models have been calculated for a clumpy two-phase torus model for an anisotropic radiation emission by the central source, the accretion disc. The projected area of the accretion disk and limb darkening affect the angular distribution of the radiative energy. As a result, the accretion disk luminosity is not isotropic but dependent on the polar angle. The accretion disk luminosity can be approximated as $L(\theta) \propto cos(\theta)[1 + 2cos(\theta)]$ (Netzer, 1987), where θ is measured from the AGN axis (see Fig. 2.4). Recent studies suggest that the AGN torus is not smooth but mainly made of dusty clumps–a large number of high-density clumps embedded in a smooth dusty component of low density (e.g., Nikutta et al. 2009; Ichikawa et al. 2012; Stalevski et al. 2012; Tanimoto et al. 2019). As our SED calculations use SKIRTOR models, these two aspects are taken care of. However, SKIRTOR models do not account for polar dust (see Fig. 2.4) emission and extinction, neither do they have emission lines, but our models do. The polar dust causes the extinction of UV and optical radiation and

*SKIRTOR is a library of emission models of the AGN dusty torus, calculated with SKIRT, a state-of-the-art radiative transfer code based on Monte Carlo technique. The models are publicly available on https://sites.google.com/site/skirtorus/sed-library

re-emits the radiation in IR. So, the polar dust extinction affects the number of ionising photons emitted from the polar region and reaching the NLR. This affects the strength of the lines produced by the NLR for a fixed gas phase metallicity. Depending on the relative orientation between an observer and an AGN, the polar dust emission also contributes to the overall IR emission.

In order to calculate realistic AGN SEDs, we use an AGN SED module which is composed of two branches, one Python script and a simple photoionisation code. The Python script was developed from scratch by me and Dr J.M. Gomes, in which I have been mainly involved in its coding and interpretation of the results. The Python script deals with the incident continuum radiation field. This script uses the SKIRTOR models that have been calculated assuming a particular set of multiple power laws. However, the Python code can take any set of power laws, modify a SKIRTOR model accordingly and produce two SEDs–one as seen by the NLR and the other as seen by an outside observer. The continuum SED seen by NLR is a sum of the accretion disk radiation extincted by polar dust, part of the emitted polar dust radiation (isotropic emission), accretion disk radiation scattered by the torus towards the NLR, and the radiation emitted by the torus towards the NLR (Fig. 2.5). This SED is then used to calculate the NLR emission lines using a photoionisation code. Hence, the photon distribution used for the line computation is very realistic.

The Seyfert 2 SED (Fig. 2.5) is obtained by normalising and re-scaling, according to the PLs, the various components of the original SKIRTOR model as well as the polar dust extinction and emission (the Python code can perform this and the aforementioned procedures for any AGN luminosity). Finally, the emission lines and continuum, computed self-consistently with the photoionisation code, are added to it (Fig. 2.6). Figure 2.7 is a flow chart explaining the working of Python AGN script-photoionisaton code module.

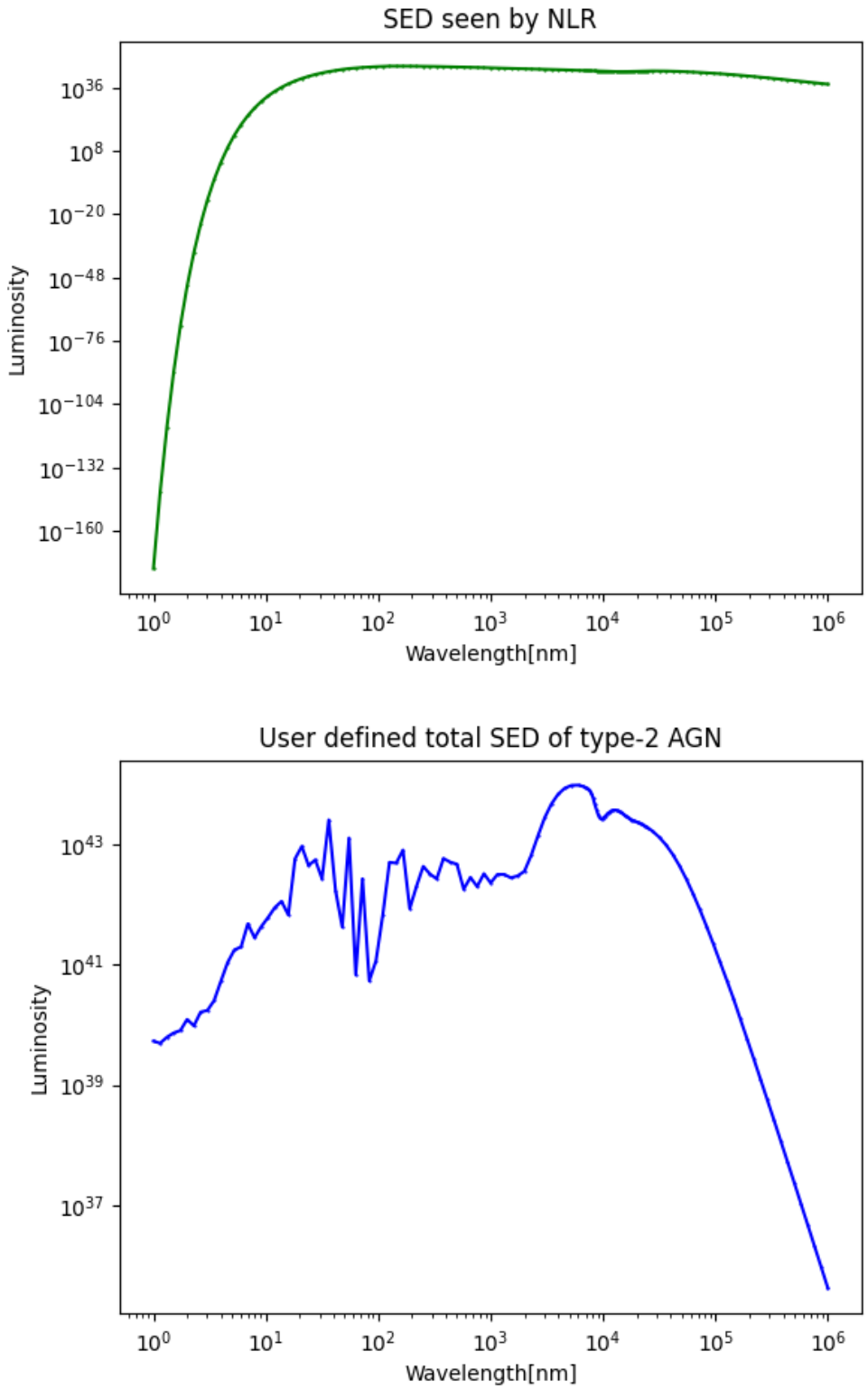

FIGURE 2.5: SEDs produced by our Python code. *Top*: The SED seen by the NLR and used to calculated the emission lines. *Bottom*: The continuum SED as seen by the observer. The calculated emission lines are combined with this SED in order to generate the final SED with emission lines.

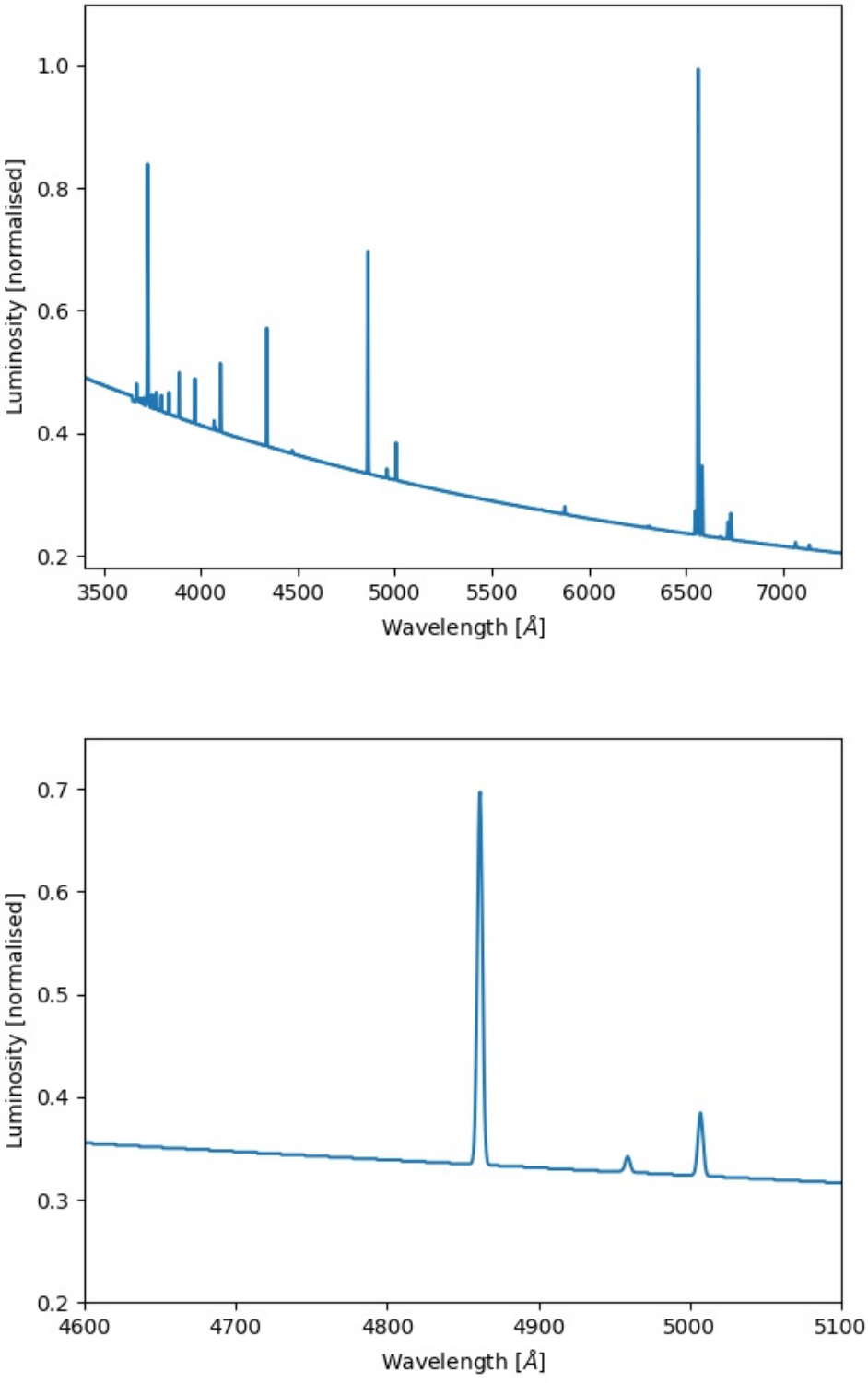

FIGURE 2.6: An example of our attempted construction of a physically grounded realistic AGN model. The SED was calculated using the SKIRTOR model with average edge-on optical depth at 9.7 micron = 5, opening angle equal to 10 degrees, and the ratio of outer to inner torus radius equal to 10. The detailed primary source is as given in Feltre et al. (2012). *Top*: A section of the SED with emission lines and continuum. *Bottom*: A zoomed-in section of the left SED.

Each SKIRTOR model depends upon: **t**: average edge-on optical depth at 9.7 micron ; **p**: power-law exponent that sets radial gradient of dust density; **q**: index that sets dust density gradient with polar angle; **oa**: angle measured between the equatorial plan and edge of the torus (see Fig. 2.4); **R**: ratio of outer to inner radius, R_{out}/R_{in}; **Mcl**: fraction of total dust mass inside clumps; **i**: viewing angle. i=0 for face-on, type 1 view and i=90 for edge-on, type 2 view.

For a fixed angle of inclination, following are the possible values of the parameters: **t**: [3, 5, 7, 9, 11]; **p**: [0.0, 0.5, 1., 1.5]; **q**: [0.0, 0.5, 1., 1.5]; **oa**: [10, 20, 30, 40, 50, 60, 70, 80]; R: [10, 20, 30]; **Mcl**: [0.97]. This leads to a total of 1920 models for a fixed angle of inclination and a set of power-law continuum. So, the total number of models produced are 1920 $\times$ 2 = 3840: 1920 ionising SED as seen by the NLR and 1920 SED as seen by an observer.

2.2.2 Single power-law continuum as the ionising source

We also produced a large set of simpler NLR models of AGNs, representing the ionising continuum radiation emitted by the accretion disk as a PL, $F_\nu \propto \nu^{-\alpha_\nu}$. We assume that the observed continuum in the spectrum of a Seyfert 2 galaxy, and the ionising continuum radiation emitted by the accretion disk are identical. Photoionisation calculations with this assumption have been extensively used in the literature and they yield reasonable consistency between predicted and observed emission-line strengths of AGNs for simple models (e.g., Ferland and Netzer 1983, Ferland and Osterbrock 1986, Halpern and Steiner 1983, Koski 1978, Stasińska 1984a,b, Terlevich and Melnick 1985), and also for models with dust and radiation pressure domination (Dopita et al., 2002, Groves et al., 2004). Having a single power law for the entire radiation field can lead to unrealistic predictions, such as unrealistic total luminosities towards lower wavelengths and unrealistic emission-line ratios of Seyfert 2 galaxies. Therefore, by imposing constraints on the minimum and maximum energy cutoffs, we can bypass these problems and have an equivalent single-power law characterised by one index when using $f_\nu \propto \nu^{-\alpha}$ as the ionising radiation field. In our models, the minimum and maximum energy cutoffs are at 10^4 and 10^{-4} Rydbergs, respectively, corresponding to wavelengths of around 0.0912 Å and 9112662 Å, respectively.

In order to generate our NLR models, version c13.03 of the photoionisation code CLOUDY (Ferland et al., 2013) was used assuming ionisation-bounded geometry so that the nebula absorbs all the ionising photons. The open geometry model was adopted as it is best suited for gas with a small covering factor, which is ideal for modelling AGN NLR. AGN NLRs typically have a covering factor of less than 10% (Maiolino et al. 2001; Baskin and Laor 2005).

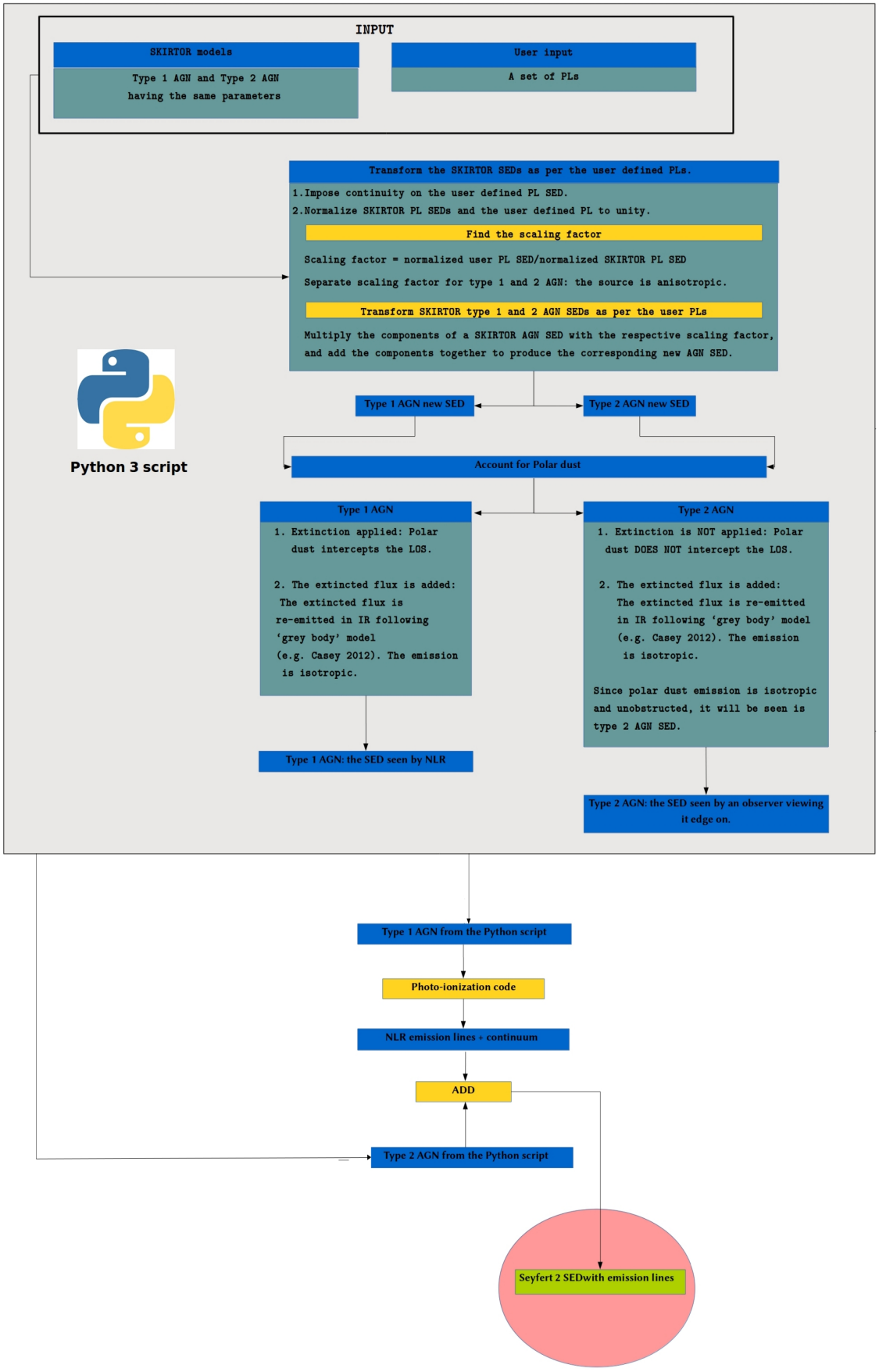

FIGURE 2.7: A flow chart explaining the working of our AGN python module.

For a given luminosity per unit frequency of the accretion disc (S_ν), the effective rate of ionising photons seen (in s^{-1}) by gas irradiated by an accretion disc of luminosity L_{AGN} is given by

$$Q = L_{AGN} \int_{\nu_0}^{\infty} d\nu \frac{S_\nu}{h\nu}, \tag{2.2}$$

where h and c are the Planck constant and the speed of light, respectively, and ν_0 is the frequency at the Lyman limit, $h\nu$ = 13.6 eV. We adopted $L_{AGN} = 10^{45}\, erg\, s^{-1} cm^{-2}$ and an inner radius of the NLR (r_{in}) $\approx$ 300 pc, corresponding to an incident flux of $L_{AGN}/4\pi r_{in}^2 \approx 10^2\, erg\, s^{-1} cm^{-2}$.

We created the grid of NLR models for a wide range of parameters:

- Ionising radiation field: we adopt here the form $f_\nu \propto \nu^{-\alpha}$ (or, $S_\nu \propto \nu^{-\alpha}$, interms of Eq. 2.2). We explored an extensive range of index values from $-2.0 \leq \alpha \leq +1.0$ using 0.1 steps in the index. A stricter range of values from $-2.0 \leq \alpha \leq -1.2$ is often assumed in the literature (e.g. Groves et al. 2004), consistent with observations (e.g., emission-line ratios in BPT - Baldwin et al. 1981 diagnostic diagram). We have confirmed the latter range of values are the ones consistent with observations. The original expansion of these values is because we wanted to certify the limits of validity of these simple models.

- Ionisation parameter U_S at the Strömgren radius: we use 9 values in the range $-4.0 \leq log(U_S) \leq 0.0$; however, we get realistic emission line ratios consistent with the local universe for $-4.0 \leq log(U_S) \leq -1.0$ (also, see Feltre et al. 2016). The ionisation parameter at a distance r from the ionising source, U(r), is defined as the dimensionless ratio of the number density of H-ionising photons to that of hydrogen (n_H): $Q/(c4\pi r^2 n_H)$.

- Hydrogen number density (n_H): we consider 13 values of this parameter in the range $10^0 \leq n_H[cm^{-3}] \leq 10^6$. We have computed this range for tests. However, values between 10^2 to 10^4 are safer and produce more realistic emission-line ratios.

- Gas-phase metallicity Z_{gas}: we adopt the same relative abundances of heavy elements as in Grevesse and Anders (1989). We have tested six distinct metallicities: 0.005, 0.02, 0.2, 0.4, 1.0, 2.5 $Z_\odot$, but only around solar we get matching results with the local universe.

A total of about 14,000 power-law models were created, spanning a huge range of physical values. Several of these models show incoherent results with local universe observations but are kept for checking purposes because they might be interesting for intermediate-to-higher redshift universe. 4446 models are consistent with local Seyfert 2 observations from SDSS using the classical BPT diagram; a total of 31.6% of the power-law models. The top panel of Fig. 2.8 is a BPT diagram

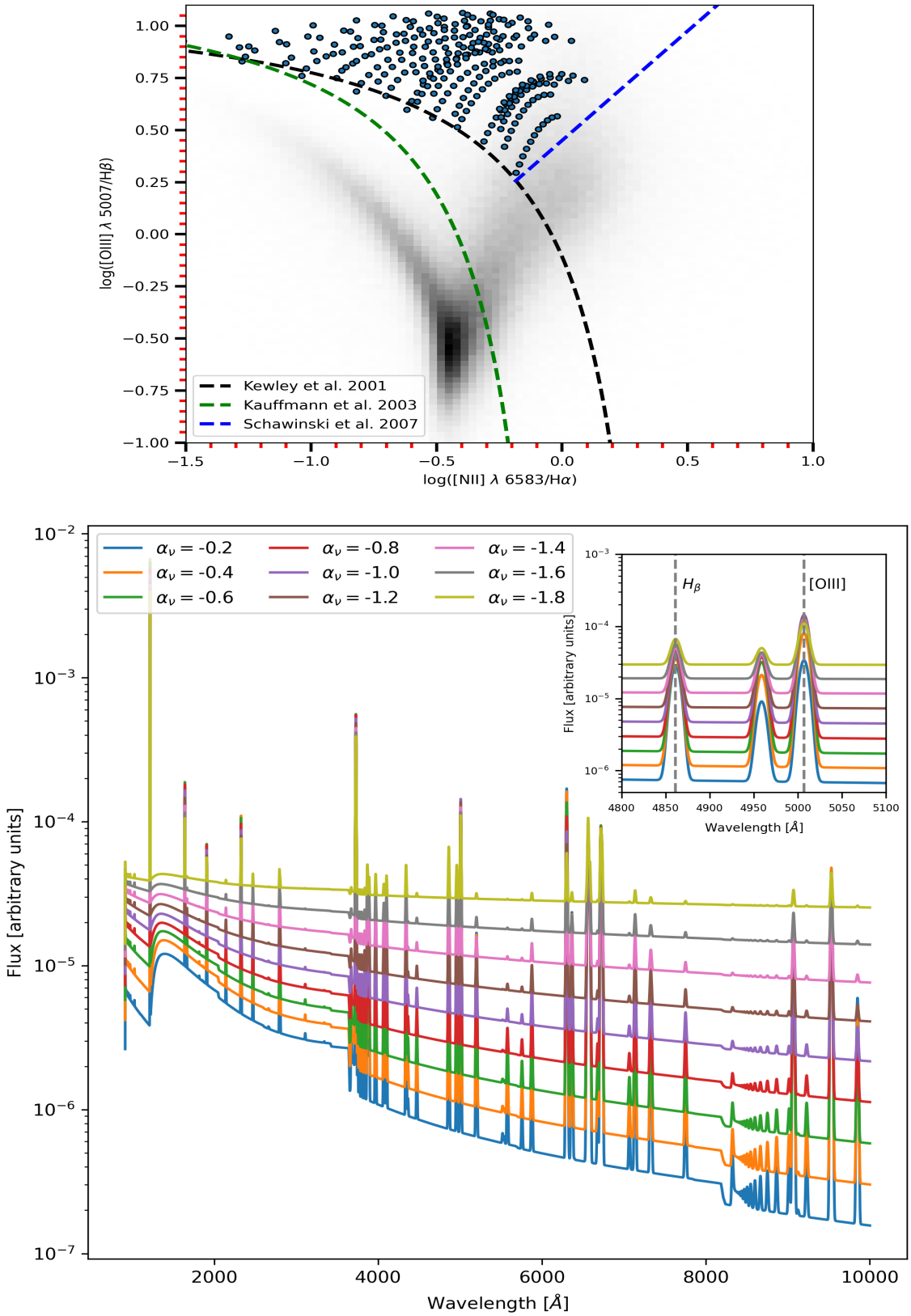

FIGURE 2.8: Single power-law AGN models with solar metallicity and different power-law indices. Top panel is a BPT diagram containing our single PL models (blue dots) with solar metallicity and emission line galaxies taken from MPA-JHU catalogue, SDSS DR 7 (grey points). Our single PL models are able to reproduce AGN-like emission line ratios for solar metallicity. The bottom shows a single PL model with gas-density, $n_H\,[cm^{-3}]$ = 100, and the emission line broadening = 300 km/sec. The top right figure in the bottom panel is a zoomed-in section showing the region around [OIII] and H_β. The effect of spectral index on the line strengths and the overall spectral shape can be clearly seen.

showing the single PL models with solar metallicity, plotted on top of emission line galaxies taken from the MPA-JHU catalog of SDSS DR 7*. The single PL models lie in the AGN region of the BPT diagram. We will use these models to construct our mock set of Seyfert 2 synthetic spectra (see sec. 2.5).

2.3 Stellar Population Synthesis

The emission from stars primarily dominates the SED of normal galaxies. Using SSPs as building blocks, we can create synthetic spectra for normal galaxies. An SSP is a group of stars born simultaneously and with the same initial chemical composition. The initial mass function (IMF) determines the number of stars at each mass within the SSP.

The SSP occupies a track (isochrone †) in the colour-magnitude diagram (CMD), where stars of different masses lie at different positions on the track. We can determine the track occupied by the SSP in the CMD through further calculations for any desired time based on a specific IMF, $\Phi(M)$. We can then deduce the effective temperatures (T_{eff}) and surface gravity (g) of the stars within the SSPs using the positions on the CMD. Finally, we can then determine the radiative contribution of the stars from libraries of stellar spectra (F_{star}) based on their spectral type and luminosity class. Integrating all the contributions yields the net spectra of the SSP, $F_{SSP}(t, Z)$, which depends on the initial metallicity (Z) of the stars and the time at which we observe it.

$$F_{SSP}(t, Z_\star) = \int_{m1}^{m2} F_{star}[T_{eff}(M), log\, g(M); t, Z]\Phi(M)dM, \tag{2.3}$$

So, the spectrum of an SSP is the sum of the spectra of individual stars, weighted by their respective contributions.

Representing a galaxy's SED using a SSP is inadequate, as it assumes all stars formed at the same time with the same metallicity. To accurately simulate a galaxy, we must consider its star formation history (SFH). Additionally, stars may form at different metallicities, which is often simplified in literature to a single value for all stars in the model galaxy. Therefore, to form a physically plausible galaxy model and generate an SED that reflects the expected measurement results, we need to perform integration over the formation ages and metallicities to create a CSP. Figure 2.9 summarises the aforementioned procedure.

*Available at https://wwwmpa.mpa-garching.mpg.de/SDSS/DR7/

†a curve that represents stars of different masses but the same age. Isochrones of SSPs are simpler and more accurate to estimate and interpret due to their uniformity in age and composition. In contrast, isochrones that account for stellar multiplicity are broader and more complex, requiring advanced techniques to correctly interpret the combined effects of multiple star systems. It is beyond the scope of the work to investigate the effects of stellar multiplicity on the SED.

2.4 Grid of stellar population models

In order to generate different spectral energy distributions using distinct star formation histories, we can use the general integral equation (as discussed in the PhD thesis, Cardoso 2017):

$$F_{CSP}(\lambda, t, Z_\star) = \int_0^t \Psi(t-t') F_{SSP}(\lambda, t', Z_\star) dt' + \frac{\gamma_{eff}(T_e)}{\alpha_B(T_e)} \int_0^t \Psi(t-t') q^{SSP}(t', Z_\star) dt' \tag{2.4}$$

where, the SFR is given by $\Psi(t) = \frac{dM_\star}{dt} - E(t)$, $M_\star$ is the mass of stars and $E(t)$ is the stellar mass ejected over time. In equation 2.4, $F_{SSP}(\lambda, t', Z_\star)$ represents the SSP spectrum as a function of the wavelength λ, age t', and, in mass fractions, the stellar metallicity $Z_\star$. The second integral signifies the nebular continuum that results from the multiplication of the stellar ionising photons, $\int_0^t q^{SSP}(t', Z_\star) dt'$, by the SFR, along with the ratio between the effective continuous emission coefficient γ_{eff} and the case B recombination coefficient α_B. For our first set of benchmark tests we have used $Z_\star = Z_{neb}$.

Equation 2.4 features the SFR function $\psi(t)$, which describes how gas mass is transformed into stars over a period of time. Its purpose is to provide an estimate of the SFH for different Hubble-type galaxies (Hubble 1926; de Vaucouleurs 1959). In environments with high-density, like galaxy clusters and their surrounding areas, it's expected that stochastic SFHs of galaxies can result from environmental effects such as galaxy harassment and mergers, combined with secular evolution processes of star formation. Semi-analytic (e.g., Quillen and Bland-Hawthorn 2008) and hydrodynamical simulations (e.g., Boquien et al. 2014) suggest the stochastic nature of SFHs. As the true SFHs of these galaxies can be highly complex, simple analytical formulas for their SFR evolution with time (e.g., Fioc and Rocca-Volmerange 1997; Gavazzi et al. 2002; Kotulla et al. 2009) are commonly assumed.

Figure 2.10 below shows CSPs that span a wide age range of 6 million years to 10 billion years for two SFHs. Notably, there are differences in the SED evolution between the two cases. For an instantaneous burst SFH, all CSP stars form at once and undergo stellar evolution without any new stars being added. Consequently, over time, the CSP SED is increasingly dominated by intermediate and older stellar populations, resulting in a redder SED continuum with strong absorption lines. Conversely, constant addition of young stars (which are the brightest) to the CSP with constant SFH keeps the SED bluer even at later times than the CSP with instantaneous SFH, with weaker absorption lines. It is vital to differentiate the age of a CSP and its luminosity-weighted mean stellar age. The former refers to the system's age, while the latter corresponds

to the age of the dominant stellar populations that contribute most to the CSP SED. The spectral features of a CSP are dictated by the dominant stellar populations at any age.

However, we have adopted a slighly different approach in our benchmark tests. We used the GALAXEV evolutionary synthesis code* (Bruzual and Charlot, 2003) to compute the SSPs and used them as building blocks of our mock synthetic database, i.e. $F_{SSP}(\lambda, t_j, Z_j)$.

A discretised version of the integral mentioned below has been used in Gomes and Papaderos (2017) and we follow the same approach. The integral,

$$F_{CSP}(\lambda, t, Z_\star) = \int_0^t \frac{dM(t-t')}{dt'} F_{SSP}(\lambda, t', Z_\star) dt' + \frac{\gamma_{eff}(T_e)}{\alpha_B(T_e)} \int_0^t \frac{dM(t-t')}{dt'} q^{SSP}(t', Z_\star) dt' \quad (2.5)$$

transformed into a discretised sum, taking sufficiently small steps in time, becomes:

$$F_{CSP}(\lambda, t, Z_\star) = \sum_{j=1}^{N_\star} F_{SSP}(\lambda, t_j, Z_\star) \times M_j + \frac{\gamma_{eff}(T_e)}{\alpha_B(T_e)} \sum_{j=1}^{N_\star} q^{SSP}(t_j, Z_\star) \times M_j \quad (2.6)$$

In our case we have two different extremes, one burst, i.e. the SSPs themselves and one constant star formation rate. But in both cases it is just a sum of the SSP from GALAXEV models. These are the building blocks without the need to recompute the SSPs and it is just a linear combination sum of elements.

We use instantenous burst and continuous SFH to represent the spectral evolution of galaxies of different Hubble types in a simple parametric form. The SFH of most Hubble types could be in principle described using the $\psi(t) = \psi_0 e^{-t/\tau}$ formula. ψ_0 represents the initial SFR value, while τ (e-folding timescale) regulates the sharpness of the decline. This analytical form is commonly used in the scientific community (e.g., Fioc and Rocca-Volmerange 1997; Bruzual and Charlot 2003 ; Kotulla et al. 2009; Serra et al. 2011) and can represent continuous star formation when $\tau \to \infty$ or an instantaneous burst when $\tau \to 0$. These limits are useful for understanding the formation history of stellar populations in galactic disks and bulges. The Kennicutt-Schmidt law (Schmidt 1959; Kennicutt 1989) motivates this formula and assumes that the SFR per unit area is proportional to the power of the local H gas surface density. We have produced, following equaiton 2.6, 1432 CSPs with instantaneous burst and constant SFH of ages in the range of 6 Myr to 15 Gyr (716 models for each SFH) by summing up the individual SSP contributions computed from GALAXEV models.

We added the nebular emission under the assumption of case B recombination in typical HI-IRs physical conditions, including low electron density ($n_e \leq 100\, cm^{-3}$) and an average electron

*https://www.bruzual.org/bc03/

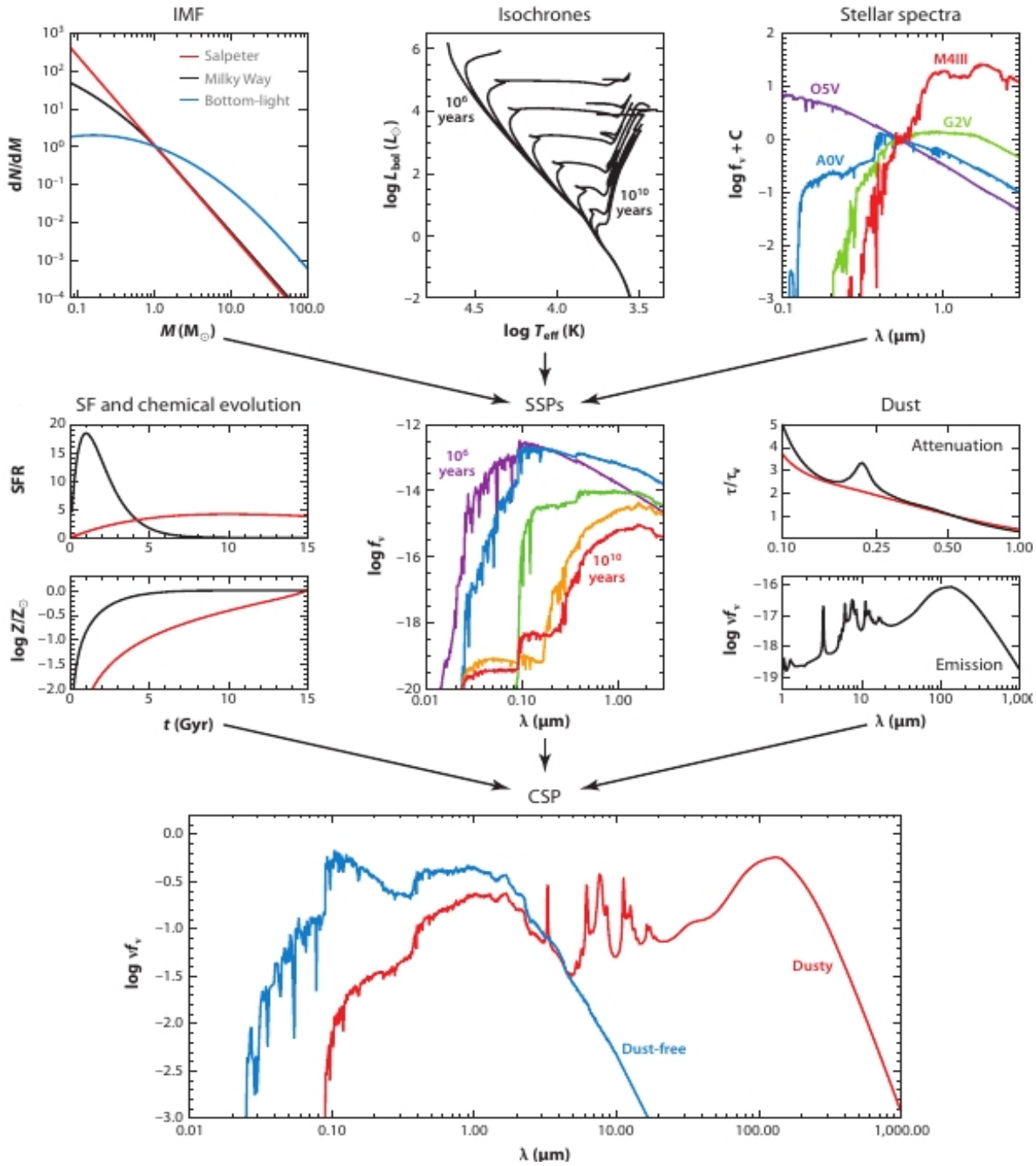

FIGURE 2.9: Overview of the construction process for Composite Stellar Populations (CSPs). This figure illustrates the step-by-step process involved in constructing CSPs. The figure is divided into three rows, each depicting different stages of the construction process. The first row (from left to right) presents the key components used in constructing CSPs, including the Initial Mass Function (IMF), isochrones, and stellar library of atmospheres, respectively. The second row highlights the incorporation of star formation rates over time (left panel) and the effects of dust attenuation and reemission in the UV/optical and IR bands (right panel). The middle panel shows the new final Simple Stellar Population spectra (stellar population of the same ages and metallicities).The final row demonstrates the combination of Simple Stellar Populations (SSPs) into a Composite Stellar Population model. Notably, nebular lines are not added or shown in this example. It's important to note that in this example, nebular lines coming from warm ionised gas are not added to the models. Source: Conroy (2013), modified by Abhishek Rajesh Chougule.

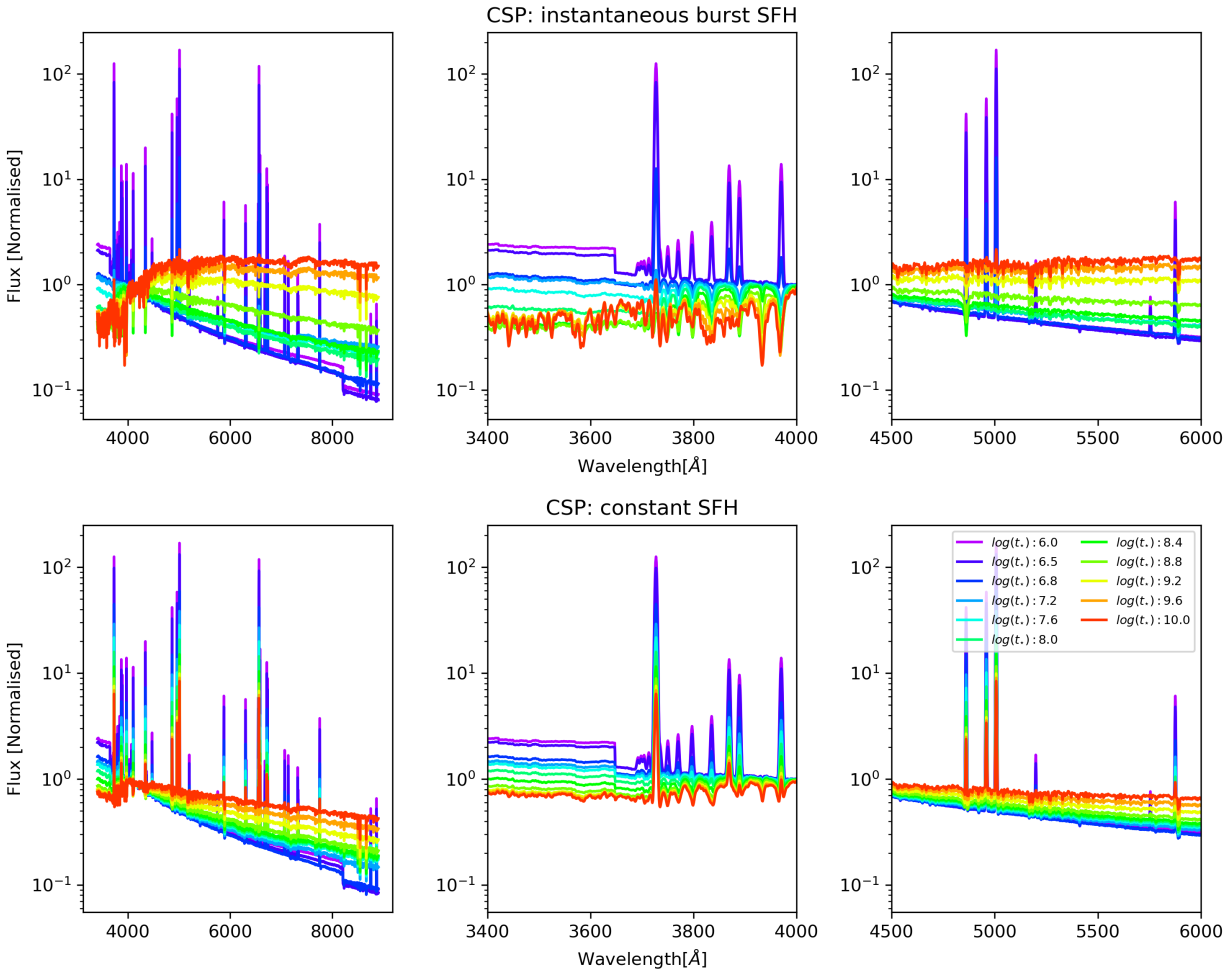

FIGURE 2.10: SED evolution of CSPs with instantaneous burst (top panels) and constant (bottom panels) SFHs. The changes in the spectral features with CSP evolution can be clearly for each SFH. In general, CSPs with constant SFH are bluer compared to CSPs with burst SFH and show weaker emission lines.

temperature of $T_e = 10^4 K$ (Osterbrock 1989; Osterbrock and Ferland 2006) for the H atom. Additionally, we determined γ_{eff} by combining contributions from hydrogen H and helium He atoms, which depend on 2-photon (Nussbaumer and Schmutz, 1984), free-free, and free-bound (Brown and Mathews, 1970) emission, which is the standard procedure. It's important to note that other species' contributions to the continuum emission are insignificant and can be ignored (Brown and Mathews 1970 for a complete discussion). The γ_{eff} coefficient can be expressed as,

$$\gamma_{eff} = \gamma(HI) + \gamma(2q) + \frac{n(He^+)}{n(H^+)}\gamma(HeI) + \frac{n(He^{++})}{n(H^+)}\gamma(HeII) \tag{2.7}$$

The emission coefficients for HI, HeI, and HeII, denoted by $\gamma(HI)$, $\gamma(HeI)$, and $\gamma(HeII)$ respectively, consider both free-free and free-bound emission processes. The 2-photon emission coefficient, $\gamma(2q)$, and the densities of once ionised Hydrogen and Helium, as well as twice ionised

Helium, are represented by $n(H^+)$, $n(He^+)$, and $n(He^{++})$. According to Osterbrock and Ferland (2006), the total recombination coefficient α_B ($T_e = 10000\,K$) = $2.59 \times 10^{-13}\,cm^3\,s^{-1}$. Finally, to calculate the fluxes of H emission lines, various electron temperatures and densities, as well as the UV ionising output from the stellar populations for radiation-bounded HIIRs, are taken into account, in accordance with Hummer and Storey (1987) and Zanstra (1961), respectively. Line fluxes for heavier elements are calculated using Anders and Fritze-v. Alvensleben (2003) semi-empirical calibration, which is a function of the nebular metallicity normalised to H_β. Several groups have used this approach, with varying degrees of complexity, and with some including only nebular continuum, others only line emission, and others both (e.g., Leitherer et al. 1999;Charlot and Longhetti 2001; Panuzzo et al. 2003; Groves et al. 2008; Mollá et al. 2009; Schaerer and de Barros 2010).

2.5 Grid of galaxy models with AGN emission

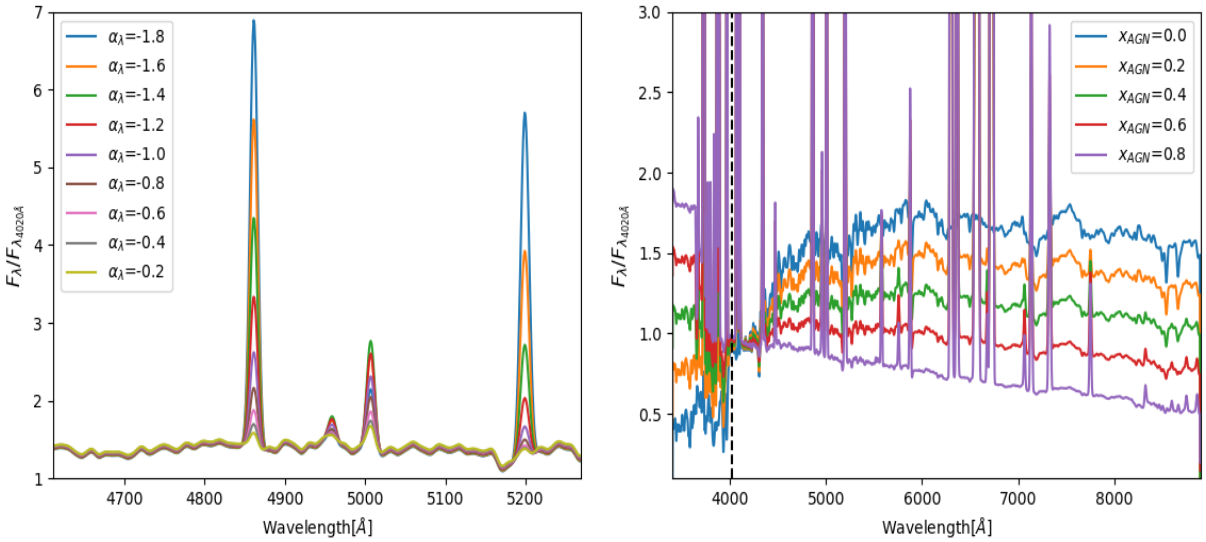

FIGURE 2.11: Examples of synthetic Seyfert 2 models generated by combining single PL models with a purely stellar galaxy model. *Left*: Models produced by combining a purely stellar galaxy model with a set of PL templates. In each model, the PL has 20% light contribution at 4020$Å$ to the combined spectra. The host galaxy model was produced with solar-metallicity simple stellar population of age 10 Gyr. *Right*: Models produced by combining a purely stellar galaxy model with a PL template of index -0.5 for distinct light contributions. The galaxy model was produced with solar-metallicity stellar population of age 10 Gyr following a burst SFH.

Following a similar approach in what concerns the relative contribution of AGN in comparison to stellar populations from Cardoso et al. (2019), we have created a grid of Seyfert 2 models. The difference here is that the mock dataset is constructed in such a way that they contain the nebular emission (continuum plus lines) computed self-consistently according to the stellar population

and power-law contribution. For each of these synthetic spectra, we combined one mock single PL model representing an AGN spectrum (with a specific PL index) with composite stellar populations. The continuum flux of the resulting combined spectrum, $F_\lambda^{\rm total}$, normalised at $\lambda_0 = 4020$Å, is given by

$$F_\lambda^{\rm total} = x_{\lambda 0}^\star \frac{F_\lambda^\star}{F_{\lambda_0}^\star} + x_{\lambda 0}^{AGN} \frac{F_\lambda^{AGN}}{F_{\lambda_0}^{AGN}}, \tag{2.8}$$

which is a combination of the purely stellar model computed with a given SFR (sec. 2.4), $F_\lambda^\star$, and single power-law model, F_λ^{AGN} (sec. 2.2.2). The light fractions $x_{\lambda_0}^\star$ and $x_{\lambda 0}^{AGN}$ (AGN fraction) are the fractional contributions of stellar and single PL model monochromatic fluxes at $\lambda_0 = 4020$Å. Equation 2.8 is constrained by the normalisation condition at λ_0: $x_{\lambda_0}^\star + x_{\lambda_0}^{AGN} = 1$. Figure 2.11 demonstrates the effect of adding our PL model to burst SFH CSP of 10 Gyr. As the absolute value of the PL index increases, it becomes bluer and emits harder radiation and we see stronger emission lines for a fixed metallicity. In the right panel of the same figure we can see the dilution of stellar spectral features with increasing fractional contributions of single PL model monochromatic fluxes at $\lambda_0 = 4020$Å. We will refer to these models as mock Seyfert 2 galaxy spectra in this work.

Using equation 2.8, we created an enormous library of synthetic Seyfert 2 galaxies ($\sim$ 2.1 million, without noise), covering a large span of physical parameters. Figure 2.12 shows some of our mock Seyfert 2 galaxy spectra constructed with a PL model of $\alpha_\nu = -1.5$ and eleven CSP ages for instantaneous burst SFH. Each panel contains a CSP of a particular age combined with a single PL model with varying contribution to the monochromatic flux at 4020 $\mathring{A}$. Each panel also contains PL FC with $\alpha_\nu = -1.5$ and an SSP (without nebular emission) of the same age as the CSP. The grey plots are SSPs without nebular emission and a CSP with purely stellar emission but with nebular emission included (xAGN=0.0). Hence, for young CSPs we see a difference between these two spectra continuum and lines. It also demonstrates the importance of including nebular emission in spectral modelling. The plots also show the effect of adding a single PL FC with the corresponding emission lines to CSPs.

- **The effect on the continuum shape:** For young CSPs, as xAGN increases, the continuum slope increases, while for older CSPs, the continuum slope decreases with increasing xAGN. Hence, adding PL model makes the CSP spectrum bluer, the extent of which depends on its fractional contribution to the total spectra.

- **The effect on emission and absorption lines:** In case of young CSPs (their spectra is dominated by emission lines), PL model contribution increases the emission line strengths with increasing xAGN. On the other hand, in case of older CSPs (their spectra is dominated by

absorption lines), the PL model addition decreases the absorption line strengths. Hence, addition of single PL model to a CSP dilutes the stellar features.

As the goal of our work is to investigate the recovery of galaxy properties in the presence of an AGN using PSS code FADO, we stick to simple photoionisation models for our further investigations. We do not explore photoionisation models having a physically motivated ionising radiation field as it will elevate degeneracies; however, this can be done in the future for comparison. It is worth acknowledging that deriving AGN physical properties using a PSS code and observed integrated spectra is extremely challenging due to aperture effects. For instance, depending on the area of a galaxy captured by a fiber and the fiber position relative to the galaxy center, the AGN signatures will be diluted by stellar emission.

As discussed earlier, the exact functional form of the non-thermal ionising incident radiation hitting the emission line gas cloud in AGNs is difficult to constrain; however, we know that its energy injection to the gas is higher than that of a thermal radiation produced by OB type stars [*]. Using FADO, we investigate if we can accurately trace the high-energy incident radiation field (regardless of its exact functional form). We also attempt to recover the PL index of the incident radiation field represented by $F_\nu \propto \nu^{-\alpha_\nu}$ and its fractional contribution to the total spectra. In the next chapter, we describe the application of FADO to synthetic data to benchmark it and the phases of its development for the application to Seyfert 2 galaxies.

[*]That is why diagnostic diagrams can separate SF galaxies from AGNs

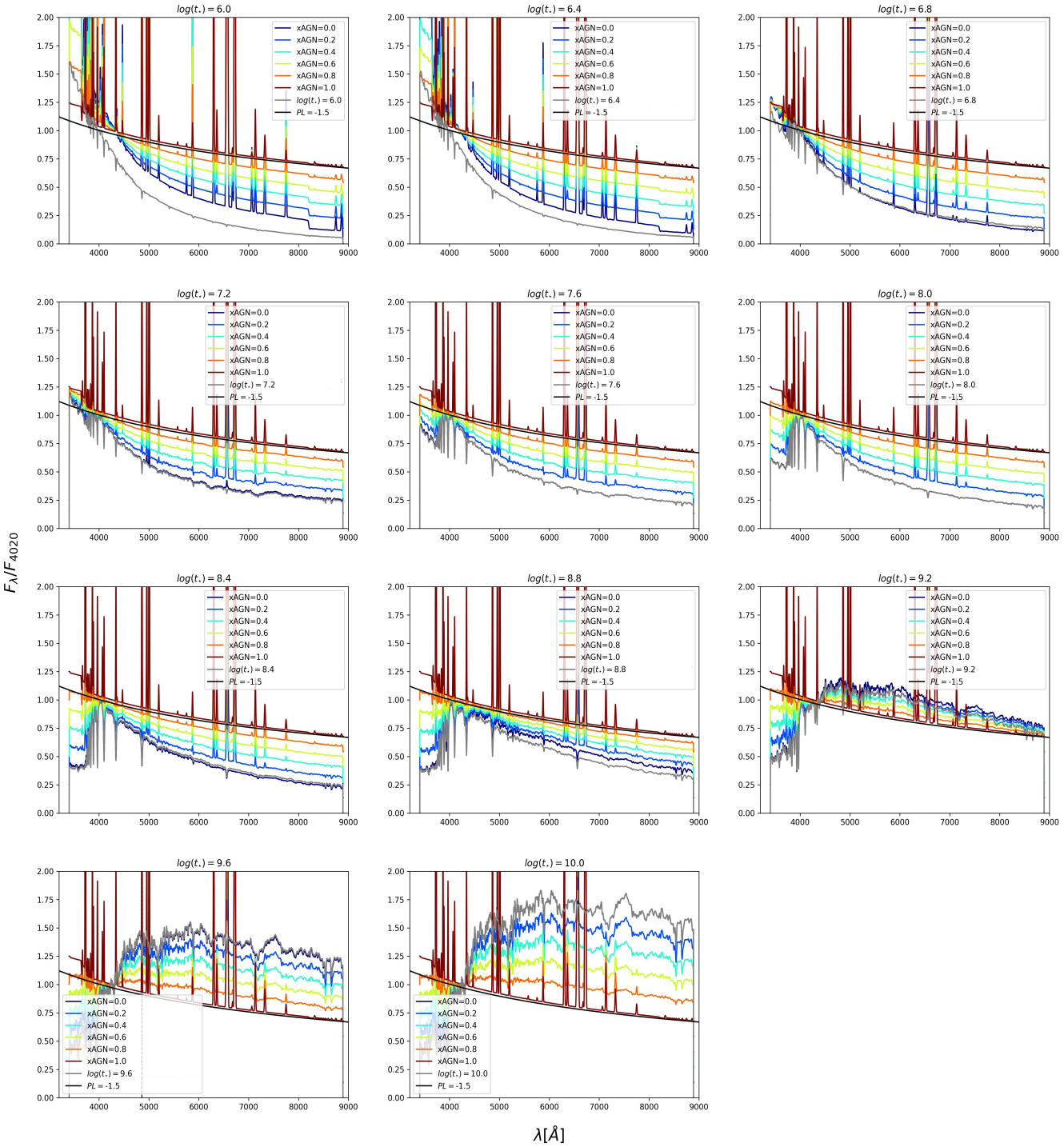

FIGURE 2.12: An example of our Seyfert 2 synthetic spectra produced by combining our single PL model with $\alpha_\nu = -1.5$ and CSPs with instantaneous burst SFH. Each panel contains a CSP of a particular age combined with single PL models for different fractional contribution to the total spectra. Each panel also contains PL FC of $\alpha_\nu = -1.5$ (black) and an SSP (grey) of the same age as the CSP. The SSPs do not have nebular emission and hence we see the difference between CSP with xAGN=0.0 (purely stellar emission) and the SSP. The difference in their continuum gets less pronounced with increasing CSP age.

Chapter 3

FADO benchmark tests for AGN Galaxies: assessing performance and accuracy

As FADO was initially fine-tuned for working self-consistently with SF galaxies, a slight modification of FADO was done by Dr. J. M. Gomes in order to change its input and output. The constraint limiting the operation of self-consistency mode exclusively to SF galaxies was removed.*

The development's first phase involved the creation and inclusion of single power-laws in the main base of templates. A single PL model means a PL model defined by a single spectral index (α_ν; $F_\nu \propto \nu^{-\alpha_\nu}$) for the entire wavelength range of interest. Firstly, we only included single PL models† (each model defined as $F_\nu \propto \nu^{-\alpha_\nu}$ with a spectral index, α_ν) in the base file and tested it on mock single PL models without stellar contribution. This test aimed to ensure that FADO recovers the PLs in the base and fits the mock PL models with the correct PL from the base. In the second stage of the development, we focused on selecting the correct type of PL for the base: power-law featureless continuum with cutoffs vs power-law without cutoffs. The results were practically the same when using PL with cutoffs and PL without cutoffs in the base file, at least for the wavelength range of our interest, 3400 Å to 8900 Å (nearly the optical region). Including PL in the base did not improve the result but increased the base file size and computation/spectral fitting time for the previously-mentioned wavelength 3400 Å to 8900 Å, and we decided to perform remaining tests using PL without cutoff. The next phase involved investigating the reason for bad fits (high χ^2 best-fit solutions) for fitting high velocity PL synthetic models with PL without cutoff in the base. Are bad fits due to the FADO fitting mode being used, or a result of FADO failing to mask some regions

*It's important to note that this change can be potentially hazardous. Users who apply this feature without the proper base template definition may encounter errors or unexpected results for non-SF galaxies.

†In this document, single PL models means the PL models present in the FADO base file; they are continuum. Mock single PL models means the set of synthetic single PL spectra (continuum plus emission lines), which have been used as inputs for FADO.

of the input spectra while fitting? As FADO was fine-tuned for narrow-line emission galaxies, the automatic masking procedure for certain regions (e.g., $H\alpha_{6563Å}$ and $[NII]_{6548,6584Å}$ lines) can be compromised for AGN galaxies as they may contain strong, broad emission lines ($\sigma \gtrsim 300$ km/s). Changing FADO fitting mode to 'soft' consistency mode (Nebular-Continuum mode, or NC mode for short) from Full Consistency mode (FC mode) did not improve the results, but masking, more precisely, masking the emission-line regions of the model a priori from fitting, did (as discussed previously using the STARLIGHT code in Asari et al. 2007). We used noiseless mock single PL models for the first phase tests.

The final phase involved applying FADO to synthetic spectra of Seyfert 2 galaxies. FADO reading module was changed because it required the same number of metallicities in the base. By combining mock single PL models with CSPs of different star SFHs of various ages, we produced a vast library of synthetic spectra of Seyfert 2 galaxies for ten different AGN fractions and three S/N values. The work was humongous, with a total number of **128 536 32** models. Just as a comparison, other studies like Gutkin et al. (2016) and Plat et al. (2019) have used a limited number of synthetic models to fit certain ultraviolet and optical emission-lines, and here we are attempting a full pixel-by-pixel fitting with a much larger set of models (a few orders of magnitude higher). We developed several Python codes to create the FADO base templates' file, combine mock single PL models with CSPs to produce synthetic Seyfert 2 spectra, add noise to the synthetic spectra, calculate luminosity weighted PL index ($< \alpha_\nu >_L$) and AGN fraction (X_{AGN}: the fractional contribution to the monochromatic luminosity at $\lambda_0 = 4020$ Å), and automatise FADO execution which is necessary considering the extensive set of models. In this chapter, we describe in detail each of the development made to use the PSS code FADO. We also discuss the application of FADO to **145200** synthetic Seyfert 2 models and the recovery of galaxy properties for various SN and Av using different bases.

3.1 FADO Analysis

3.1.1 Updating the base of templates

Since FADO is a population spectral synthesis code, its goal is to decompose the observed spectrum of a galaxy into its elementary and no further divisible constituents (e.g., SSPs, individual stars or even power laws). To do so, FADO selects, from a spectral base library, the linear combination of templates (e.g., spectra of SSPs) that best matches the observed spectrum. As the nebular emission (continuum plus lines) is self-consistently evaluated within the code, it is not included in the base.

The continuum from the base templates interacts with the nebula and produces the corresponding nebular features.

Spectral base library refers to a set of synthetic spectra that is accessible to FADO for fitting an input spectra. However, the spectra from the spectral base library that FADO will actually consider to construct a best fitting solution is governed by the base file*. On execution, FADO reads the base file given by the user, and uses the spectra mentioned therein to construct the best fitting solution. We have constructed three types of spectral base libraries: **a)** containing PLs (with cutoffs and without cutoffs) **b)** containing PLs and SSPs and **c)** one PL as well as SSPs. We have also generated the respective base files.

3.1.2 Construction of a new spectral base library of single power-law models

We included single PL continuum models in a newly created spectral base library devoted to Seyfert galaxies and generated the corresponding base files. In that manner, FADO can consider single PL continuum models while constructing the best-fitting self-consistent solution. It is essential to notice that FADO uses the number of ionising photons to add nebular emission to the final solution. The single PL continuum models have been normalised to the continuum monochromatic flux in the blue region at $4020\mathring{A}$. As an extra backup factor, we included to the base file the single PL continuum models by assigning them zero stellar masses, and negative ages, where the ages actually are the respective PL indices. FADO was slightly modified by Dr. J. Gomes to interpret the input components with negative or zero age as single PL continuum models, and use them to fit observations, but automatically exclude them from all mass-weighted calculations.

For testing this new approach, we created spectral base libraries and the corresponding base files spanning different single PL continuum models and ingredients:

- **BasePL:** PL defined as $F_\nu \propto \nu^{-\alpha_\nu}$, or $F_\lambda \propto \lambda^{\alpha_\lambda}$; $\alpha_\nu = -(\alpha_\lambda + 2)$. PL FC models with wavelength range of $91\mathring{A}$ to $160\mu m$. The spectral base library contains 21 single PL continuum models with PL index from 0.0 to -2.0, in steps of 0.1.

- **BasePLWC:** PL with cutoffs, defined as $F_\nu \propto \nu^{-\alpha_\nu} exp(-\frac{\nu}{\nu_{highcut}}) exp(-\frac{\nu_{lowcut}}{\nu})$. $\nu_{highcut}$ and ν_{lowcut} are frequencies corresponding to high-energy cutoff and low-energy cutoff that have value of 10^4 and 10^{-4} Rydbergs, respectively (A similar approach is adopted in the work by Dopita et al. 2002). We created a spectral base library containing 21 single PL continuum with PL index from 0.0 to -2.0, in steps of 0.1. The models have wavelength range $1.0\mathring{A}$ to $\sim 20,000\mathring{A}$,

*The base file is a list of spectra from the spectral base library and their properties (e.g., for SSPs: ages, metallicities, stellar mass, etc.)

and cutoffs at $\sim$ 0.0911$\mathring{A}$ and $\sim$ 9112667$\mathring{A}$, corresponding to high and low energy cutoff value, respectively.

3.1.3 Inclusion of stellar population templates in the base

We constructed four spectral base libraries (and the base files) composed of PL and SSPs (Bruzual and Charlot, 2003). The bases contain SSPs with Padova 1994 evolutionary tracks and a Chabrier (2003) IMF.

- **BaseA:** 111 elements; 11 single PL (α_ν = -1.0 to -2.0 in steps of 0.1) and 100 SSPs (4 metallicities, 25 ages and 100 stellar masses)
- **BaseB:** 167 elements; 11 single PL (α_ν = -1.0 to -2.0 in steps of 0.1) and 156 SSPs (6 metallicities, 26 ages and 156 stellar masses)
- **BaseC:** 177 elements; 21 single PL (α_ν = 0.0 to -2.0 in steps of 0.1) and 156 SSPs (6 metallicities, 26 ages and 156 stellar masses)
- **BaseD:** 157 elements; 1 single PL (α_ν = -1.6 in steps of 0.1) and 156 SSPs (6 metallicities, 26 ages and 156 stellar masses)

We also created **BaseL** which only contains SSPs: 100 SSPs (4 metallicities, 25 ages and 100 stellar masses).

To summarise, we created two types of bases, one composed only of PL (BasePL and BasePLWC), and another composed of PL and SSPs (BaseA, BaseB, BaseC, and BaseD). BasePL and BasePLWC contain PL with and without cutoff, respectively. BaseA, BaseB, BaseC, and BaseD contain SSPs and PL without cutoff, while BaseL contains only SSPs.

3.2 Benchmark tests: applying FADO to mock data

We used FADO to fit a wide range of synthetic models in the wavelength range 3400Å to 8900Å (SDSS-like), which is nearly the optical region. All these models include in their construction the reprocessing of ionising photons by the gas clouds into nebular emission (line plus continuum). We also developed a Python script that reads FADO ASCII outputs and calculates luminosity- and mass-weighted quantities. One difference is that we also compute the luminosity weighted PL

index (aka average PL index)*:

$$< \alpha_\nu >_L = \frac{\sum_{i=1}^{N_{PLs}} x_{i,\lambda_0}^{AGN} PL_i}{\sum_{i=1}^{N_{PLs}} x_{i,\lambda_0}^{AGN}} \tag{3.1}$$

where PLi represents the power-law index and N_{PLs} denotes the total number of power-law templates.

It is observed that a single power-law representation typically cannot encompass the linear combination of various PLs. Nevertheless, this study serves as the inaugural quantitative evaluation of FADO's ability to discern AGN properties in galaxies. Additionally, it stands as the sole examination in literature testing pixel-by-pixel spectral synthesis incorporating a wider range of PLs.

3.2.1 Application of FADO to models using a single power-law models

As a first step, we applied FADO to a diverse set of our mock single PL models without noise, using the base file composed of only single PL continuum models. The goal of this test was to check if FADO recognises the single PL continuum models in the base and uses the base element having the same PL index as the input spectra to fit the input spectra. We observed that FADO was unable to fit well the input spectra with high velocity broadening and strong emission lines (see Fig. 3.1), but performed well in case of lower velocity broadening and strong emission lines. We investigated the reason for bad fits.

3.2.1.1 Full-Consistency Mode versus Nebular Continuum Mode

FADO can operate in different modes like FC mode (Full-Consistency mode) and NC mode (Nebular-Continuum mode). In FC mode, to fit an input spectrum, FADO ensures consistency between observed and predicted SED continuum (stellar plus nebular) and Balmer emission-line luminosities and EWs. In NC mode, FADO fits the input spectra without the requirement for consistency between predicted and observed Balmer-line luminosities and EWs. We applied FADO to the same set of mock single PL models for FC and NC mode and compared the results. We hardly saw any difference between the results obtained from FC and NC mode.

*It is worth mentioning that AGN characterised by power-law spectra could theoretically have been weighted by mass quantities, such as black hole mass. However, the models are devoid of mass; they were constructed with simplicity in mind, utilizing only a functional form.

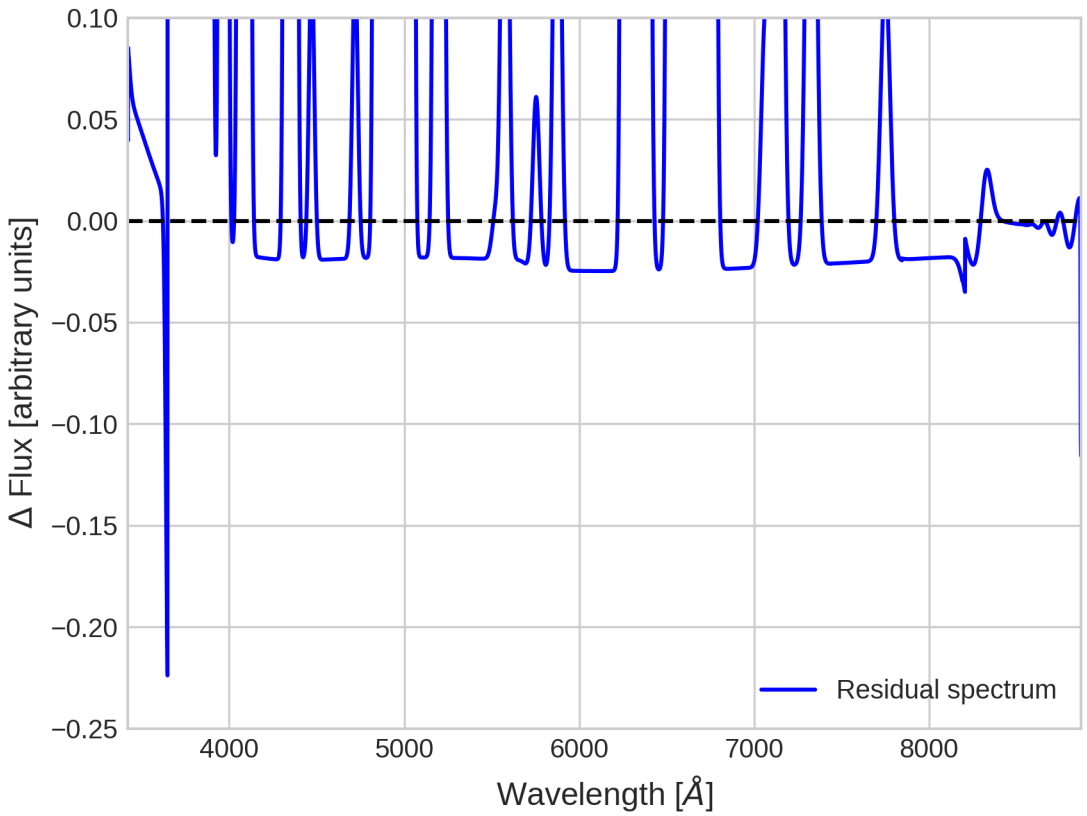

FIGURE 3.1: An example of a bad fit due to poor masking of broad emission lines. The PL model has a broadening velocity dispersion of σ = 300km/s. The plot shows best-fit minus input spectrum, i.e., the residual. The dashed black line is y = 0 line. An ideal fit means all points will be on the dashed black line.We can see that there is a clear offset in the residual. This is driven by a poor masking of the emission-line features. Due to the broadening effect, the wings and blending lines impact the fits, contributing to the observed discrepancy.

3.2.1.2 Masking regions

FADO although was developed for any sort of ionising spectrum, it was fine-tuned to SF galaxies. To avoid the errors by the user, the self-consistency FADO fitting option was locked for other types of sources, but now it is unlocked. No real modification was needed for this part.

FADO has an internal routine for masking regions of the input spectra. However, mock single PL models have stronger and broader emission lines than SF galaxies and hence may not be masked well by FADO.

Hence, we masked certain lines a priori from fitting, and applied FADO. We observed that FADO is now able to fit well the input spectra. This benchmark test will help to generate better masking of regions and obtaining of ameliorated fits (as pointed out in Asari et al. 2007) for earlier tests with the STARLIGHT code (Cid Fernandes et al., 2005).

3.2.1.3 Power-law with energy cutoff vs power-law without cutoff

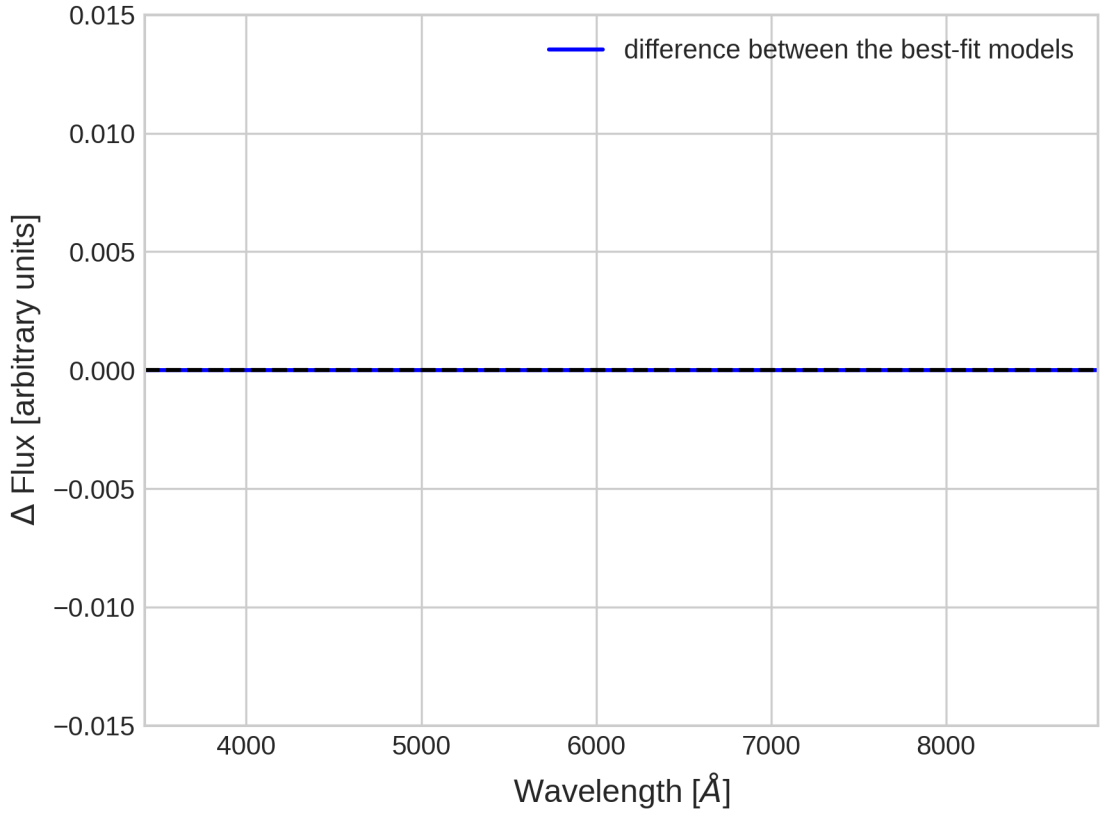

FIGURE 3.2: The difference between the best-fit models when using the base containing single PL with and without cut-off. The lack of discrepancy between the best-fit models when utilising the base containing a single power-law with and without a high-energy cut-off is negligible in the optical range. We can observe that there is no discernible distinction in the best-fit models. This lack of difference can be attributed to the similarity in Q (the number of ionising photons), which is responsible for generating the continuum and lines in the near UV/optical spectrum. Typically, deviations between these models begin to manifest in the UV and other wavelength ranges. In reality, the inclusion of a high-energy cut-off in the power-law model introduces additional parameters that can affect the shape and intensity of the modelled spectrum. These parameters, such as the cut-off energy and the steepness of the cut-off, can have significant impacts on the predicted emission spectrum, particularly in regions where high-energy photons dominate the emission process (Ferland et al., 2013)

We applied FADO to mock single PL with a base file containing single PL continuum models with cutoff and a base file containing single PL without cutoff. In the wavelength range of our interest, 3400 Å to 8900 Å, the results obtained using different bases are hardly dissimilar (see Fig. 3.2). A single PL model without cut-off means a PL model defined by a single spectral index for the entire wavelength range of interest. As it is defined as $F_\nu \propto \nu^{-\alpha_\nu}$, the luminosity at high energy increases indefinitely, which is non realistic. To avoid this issue, energy cut-offs are placed

on the single PL model, and we call them single PL models with cut-off. This approach to spectral modelling has also been adopted in other works (see Dopita et al. 2002).

3.2.1.4 Recovery of PL index for models with different velocity line broadening.

We applied FADO to the mock single PL models having velocity line broadening of 50, 100, 150, 200, 250, and 300 km/s and studied the recovery of the luminosity weighted PL index. We observe that the recovery of the luminosity weighted PL index decreases with increasing velocity broadening. We concluded that to fit a spectrum for the wavelength range of our interest (3400 to 8900$\mathring{A}$), the base containing single PL continuum models without cutoff is sufficient.

3.2.1.5 Application of FADO to single PL index models with noise

We created a large set of mock single PL models with noise such that S/N (at $\lambda = 4020\mathring{A}$) is constant and error varies randomly. Although the fits are good for majority of the models, the recovery of luminosity weighted PL index is the best for high S/N models.

3.3 Application of FADO to synthetic Seyfert 2 spectra

After extensively testing FADO on single PL models, we applied FADO to synthetic Seyfert 2 spectra. As discussed earlier, the created dataset is huge (12853632) and FADO takes 3 minutes on an average to fit one spectrum in an Intel®Core™i9-9900KF CPU @ 3.60GHz workstation desktop. Hence, due to time constraints, we selected a subset of the models spanning a large space of parameters to benchmark FADO.

We selected Seyfert 2 models composed of single PL models with $\alpha_\nu = -1.2, -1.4, -1.6, -1.8$ and CSPs with Burst and Constant SFHs of eleven ages in the range of 1Myr to 10 Gyr, $Z_\star = Z_\odot$, X_{AGN}=0.2 to 0.8, SN = 5 and 15, and Av in the range of 0.0 to 2.0. The α_ν values are in the range generally adopted in the literature as discussed in the previous chapter. In total we have **145200** models and we do a pixel-by-pixel fitting.

We also investigate the effect of the choice of base elements on the recovery of the galaxy properties. We tested a base (BaseD) composed of a single PL of $\alpha_\nu = -1.5$ and SSPs on Seyfert 2 mock data (see Tab. A.1.13) which has been widely done in the literature.

As the goal of this study is to evaluate how well does FADO recover the properties of a Seyfert 2 galaxy from its spectrum, we present the results in terms of Δ (output$-$input): mean, standard deviation (SD), Mean Absolute Error (MAE), Mean Square Error (MSE) for each case. The best case

scenario would be when the Δ values are zero, i.e., the values of galaxy properties computed by FADO matches exactly the properties of the input spectrum.

3.3.1 Application of FADO to Seyfert 2 mock spectra

3.3.1.1 Tables: Burst SFH, Av=0.0, SN = 15, base: BaseA

	SFH=Burst; SN=15.0; Av=0.0; Age of the system = 6.0															
	ΔX_{AGN}				$\Delta < \alpha_v >_L$				$\Delta < \log(t_\star) >_L$				$\Delta < \log(t_\star) >_M$			
X^i_{AGN}	0.2	0.4	0.6	0.8	0.2	0.4	0.6	0.8	0.2	0.4	0.6	0.8	0.2	0.4	0.6	0.8
Mean	-0.01	-0.02	-0.03	-0.03	-0.0	-0.01	-0.01	0.01	0.13	0.15	0.23	0.26	1.64	1.56	2.09	1.73
SD	0.02	0.02	0.03	0.02	0.07	0.04	0.03	0.04	0.12	0.12	0.14	0.15	1.44	1.46	1.49	1.66
MAE	0.01	0.02	0.03	0.03	0.06	0.04	0.03	0.03	0.13	0.15	0.23	0.26	1.64	1.56	2.09	1.73
MSE	0.0	0.0	0.0	0.0	0.01	0.0	0.0	0.0	0.03	0.04	0.07	0.09	4.75	4.56	6.6	5.72

	SFH=Burst; SN=15.0; Av=0.0; Age of the system = 6.0															
	$\Delta \log < Z_\star >_L$				$\Delta \log < Z_\star >_M$				$\Delta M_\star$				ΔA_v			
X^i_{AGN}	0.2	0.4	0.6	0.8	0.2	0.4	0.6	0.8	0.2	0.4	0.6	0.8	0.2	0.4	0.6	0.8
Mean	-0.03	-0.01	0.01	0.04	-0.07	-0.12	-0.13	-0.12	-0.48	-0.48	-0.73	-0.68	-0.0	-0.0	-0.0	-0.01
SD	0.04	0.05	0.09	0.11	0.12	0.18	0.21	0.23	0.47	0.52	0.64	0.75	0.0	0.0	0.02	0.03
MAE	0.04	0.04	0.06	0.08	0.08	0.14	0.18	0.18	0.48	0.48	0.73	0.68	0.0	0.0	0.0	0.01
MSE	0.0	0.0	0.01	0.01	0.02	0.05	0.06	0.07	0.45	0.5	0.95	1.01	0.0	0.0	0.0	0.0

TABLE 3.2: A table showing mean, standard deviation (SD), mean absolute error (MAE) and mean square error (MSE) of Δ (output-input) of stellar and AGN properties. The top panel displays the SFH, SN, V band extinction and system age, respectively. X^i_{AGN} is the AGN fraction of the input spectrum, and spans 0.2-0.8 for each galaxy property. All the other tables follow the same format.

3.3.1.2 Tables: Constant SFH, Av=0.0, SN = 15, base: BaseA

	SFH=Constant; SN=15.0; Av=0.0; Age of the system = 6.0															
	ΔX_{AGN}				$\Delta < \alpha_v >_L$				$\Delta < \log(t_\star) >_L$				$\Delta < \log(t_\star) >_M$			
X^i_{AGN}	0.2	0.4	0.6	0.8	0.2	0.4	0.6	0.8	0.2	0.4	0.6	0.8	0.2	0.4	0.6	0.8
Mean	-0.01	-0.02	-0.03	-0.03	-0.02	-0.01	-0.01	0.02	0.13	0.2	0.22	0.26	1.59	2.23	1.53	1.5
SD	0.02	0.02	0.03	0.02	0.06	0.04	0.03	0.04	0.11	0.12	0.12	0.13	1.36	1.45	1.59	1.6
MAE	0.02	0.02	0.03	0.03	0.05	0.03	0.03	0.03	0.13	0.2	0.22	0.26	1.59	2.23	1.53	1.5
MSE	0.0	0.0	0.0	0.0	0.0	0.0	0.0	0.0	0.03	0.05	0.07	0.08	4.38	7.07	4.85	4.8

	SFH=Constant; SN=15.0; Av=0.0; Age of the system = 6.0															
	$\Delta \log < Z_\star >_L$				$\Delta \log < Z_\star >_M$				$\Delta M_\star$				ΔA_v			
X^i_{AGN}	0.2	0.4	0.6	0.8	0.2	0.4	0.6	0.8	0.2	0.4	0.6	0.8	0.2	0.4	0.6	0.8
Mean	-0.02	-0.02	-0.02	0.05	-0.07	-0.13	-0.1	-0.1	-0.47	-0.72	-0.56	-0.58	-0.0	-0.0	-0.0	-0.01
SD	0.05	0.06	0.07	0.09	0.13	0.22	0.18	0.2	0.45	0.53	0.67	0.72	0.0	0.0	0.01	0.03
MAE	0.04	0.05	0.06	0.08	0.1	0.18	0.14	0.14	0.47	0.72	0.56	0.58	0.0	0.0	0.0	0.01
MSE	0.0	0.0	0.01	0.01	0.02	0.07	0.04	0.05	0.42	0.8	0.76	0.85	0.0	0.0	0.0	0.0

TABLE 3.4

3.3.1.3 Figures: Instantaneous burst SFH, Av=0.0, SN = 15.0, base: BaseA

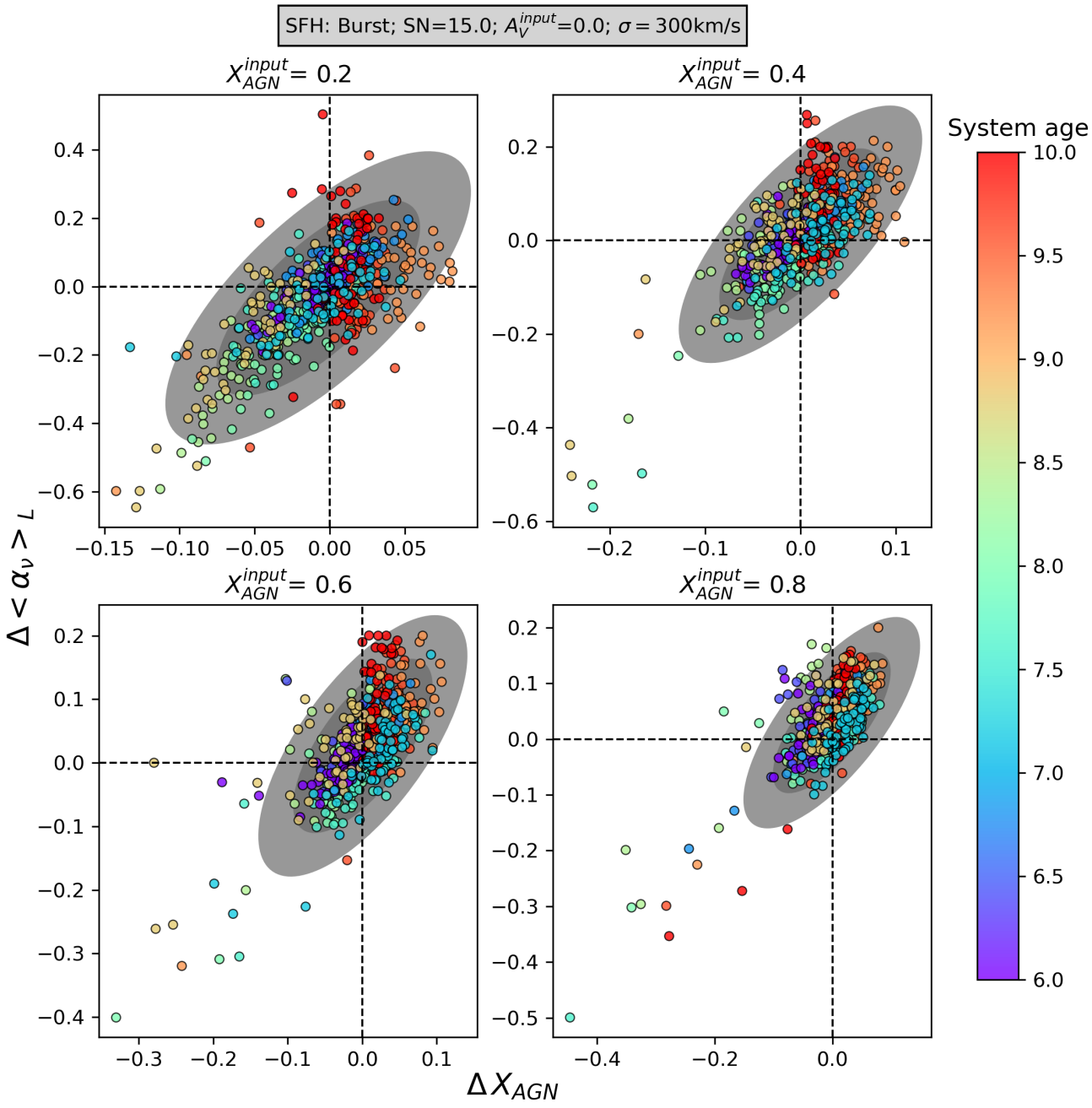

FIGURE 3.3: $\Delta < \alpha_\nu >_L$ vs ΔX_{AGN}; SFH: Burst, SN = 15.0, base: BaseA. The top left, top right, bottom left and bottom right panels correspond to models with AGN fraction of 0.2, 0.4, 0.6, and 0.8, respectively. The intersection of the dashed lines, x = 0 and y = 0, enables one to visualise how far from (0,0) are the data points. The ellipses show 1σ, 2σ and 3σ regions (darker to lighter) with their eccentricity being defined by the covariance of the variables. The colour bar shows the age of the system. All the other scatter plots follow the same format.

3.3.1.4 Figures: Constant SFH, Av=0.0, SN = 15, base: BaseA

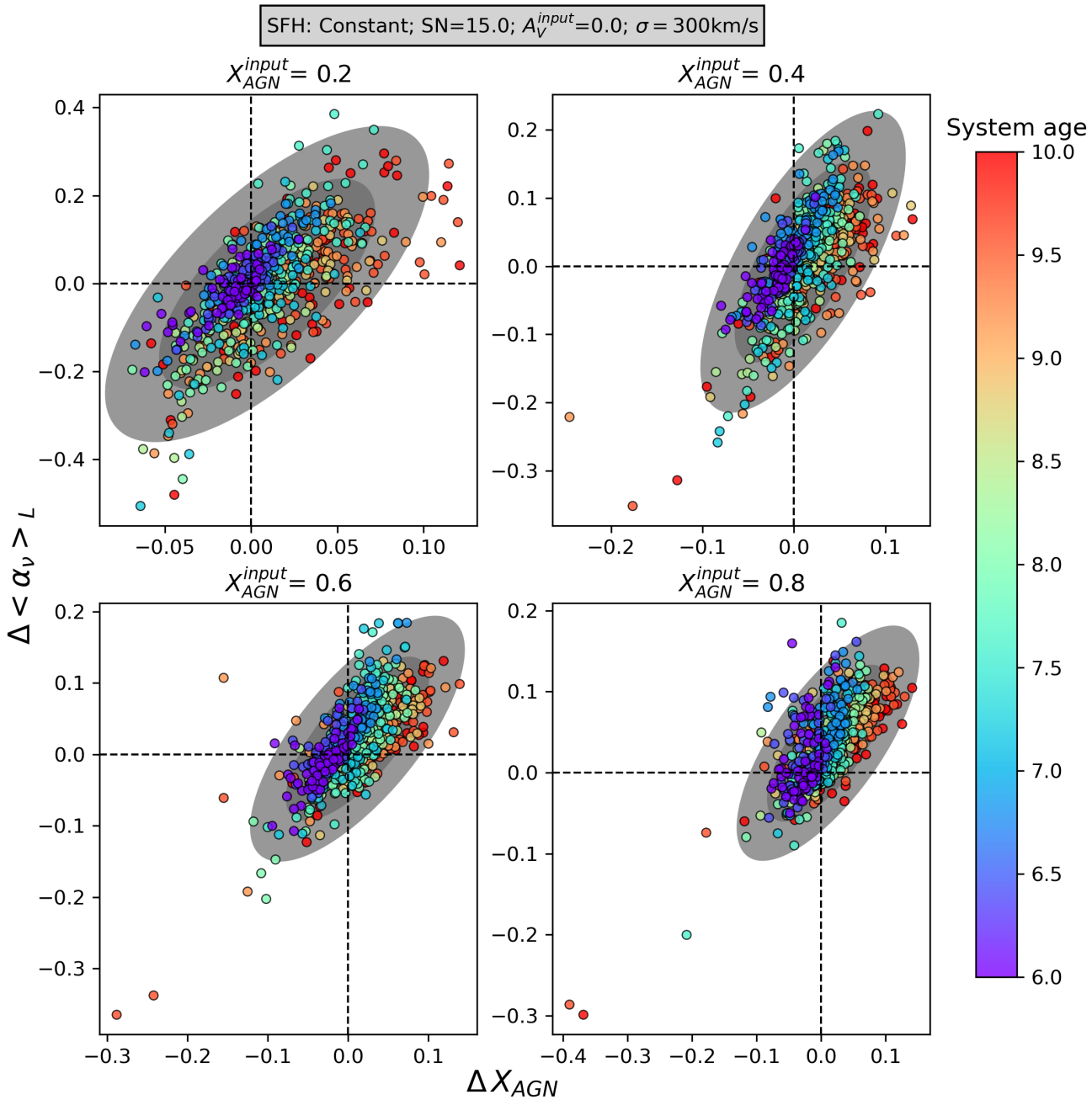

FIGURE 3.4: $\Delta < \alpha_\nu >_L$ vs ΔX_{AGN}; SFH: Constant, SN = 15.0, base: BaseA

As the parameter space is large for our tests, we have obtained around 143 and 54 aforementioned tables and scatter plots, respectively. To improve the readability of the text, we put 141 tables and 52 scatter plots in the Appendix A.1.6. The tables in the the Appendix A.1.6 correspond to FADO modelling with:

- Instantaneous burst SFH, SN = 15, Av = 0.0 using Base A
- Instantaneous burst SFH, SN = 15, Av = 1.0 using Base A
- Instantaneous burst SFH, SN = 15, Av = 2.0 using Base A
- Constant SFH, SN = 15, Av=0.0 using Base A
- Constant SFH, SN = 15, Av=1.0 using Base A
- Constant SFH, SN = 15, Av=2.0 using Base A
- Instantaneous burst SFH, SN = 5, Av = 0.0 using Base A
- Instantaneous burst SFH, SN = 5, Av = 1.0 using Base A
- Instantaneous burst SFH, SN = 5, Av = 2.0 using Base A
- Constant SFH, SN = 5, Av = 0.0 using Base A
- Constant SFH, SN = 5, Av = 1.0 using Base A
- Constant SFH, SN = 5, Av = 2.0 using Base A
- Instantaneous burst SFH, SN = 15, Av = 0.0 using Base D (see Sec. 3.1.3)

3.4 Summary of results

In this section, stellar properties mean $< log(t_\star) >_L$, $< log(t_\star) >_M$, $log < Z_\star >_L$ and $log < Z_\star >_M$, and AGN properties mean X_{AGN} and $< \alpha_\nu >_L$. We refer to systems with age 6.0, 6.4 and 6.8 dex (1 Myr, 2.5 Myr and 6.3 Myr) as young, with age 7.2, 7.6, 8.0 and 8.4 dex (16 Myr, 40 Myr, 0.1 Gyr and 0.25 Gyr) as intermediate, and with age 8.8, 9.2, 9.6 and 10.0 dex (0.63 Gyr, 1.5 Gyr, 4 Gyr and 10 Gyr) as old.

The term, 'recovery', is related to MAE of the quantities. MAE gives an indication of how far off the FADO calculated values are from the actual values on average. So, when we say the recovery of a parameter increases/gets better, we mean that on an average, the FADO calculated value of

the parameter gets closer to the input value of that parameter. When we say the recovery of a parameter decreases/gets worse, we mean that on an average, the FADO calculated value of the parameter gets farther from the input value of that parameter. We summarise the results using this terminology.

AGN Properties

ΔX_{AGN} and $\Delta\langle\alpha_\nu\rangle_L$:

- The MAEs for AGN properties varied with different input AGN fractions. For both burst and constant star formation histories, the AGN properties generally exhibited lower MAEs compared to stellar properties, indicating a better recovery performance.
- Specifically, ΔX_{AGN} had lower variability across different AGN fractions, suggesting a robust recovery of the AGN fraction itself.
- $\Delta\langle\alpha_\nu\rangle_L$ showed a similar trend, though with slightly higher MAEs, implying that the spectral slope of AGN components is reasonably well-recovered by FADO.

Stellar Properties

$\Delta\langle\log(t_\star)\rangle_L$ and $\Delta\langle\log(t_\star)\rangle_M$:

- The MAEs for stellar age, $\Delta\langle\log(t_\star)\rangle_L$ and $\Delta\langle\log(t_\star)\rangle_M$, were higher than those for AGN properties.
- For burst star formation histories, old systems exhibited the lowest MAEs, followed by young systems, with intermediate systems having the highest MAEs. This suggests that older stellar populations are better recovered than younger ones under burst conditions.
- For constant star formation histories, a similar trend was observed where old systems had the lowest MAEs, followed by young systems, and intermediate systems had the highest MAEs.

$\Delta\log(\langle Z_\star\rangle_L)$ and $\Delta\log(\langle Z_\star\rangle_M)$:

- The metallicity, $\Delta\log(\langle Z_\star\rangle_L$and $\Delta\log(\langle Z_\star\rangle_M$, also exhibited higher MAEs compared to AGN properties.

- In burst star formation histories, old systems showed the lowest MAEs, followed by young systems, with intermediate systems having the highest MAEs. This implies that the metallicity of older stellar populations is more accurately recovered.
- For constant star formation histories, old systems again had the lowest MAEs, followed by young and intermediate systems. This consistency across star formation histories highlights the challenges in recovering metallicity for intermediate-age systems.

$\Delta M_\star$**:**

- The MAEs for stellar mass ($\Delta M_\star$) were higher in general, with intermediate systems showing the highest errors, followed by young and old systems. This trend was consistent across both burst and constant star formation histories.

The recovery of stellar and AGN properties using FADO demonstrated several key trends:

- **Dependency on AGN Fraction:** The recovery performance for both AGN and stellar properties showed some dependency on the input AGN fraction. While AGN properties were less affected, stellar properties exhibited more significant variations.
- **Age Dependency:** The recovery of stellar properties improved with the age of the system. Older systems consistently showed lower MAEs across all parameters, indicating that FADO performs better for more evolved stellar populations. Young systems, while exhibiting higher MAEs compared to old systems, still performed better than intermediate systems. Intermediate systems showed the highest MAEs, suggesting that these systems pose the greatest challenge for FADO, likely due to their more complex star formation histories and dynamic stellar populations.
- **Star Formation History:** Overall, the recovery of stellar properties for Burst SFH is better than that for Constant SFH. Burst histories generally led to higher MAEs for intermediate systems, highlighting the complexities in modeling younger, more dynamically active systems. For constant star formation histories, intermediate systems still showed the highest MAEs, indicating that the challenges in recovering properties for these systems persist regardless of the star formation history.
- The MAE for mass-weighted quantities is higher than luminosity-weighted quantities. This is because the mass-to-light ratio is non-linear; small uncertainties in light estimations can result in large uncertainties in mass-weighted quantities.

- A single PL refers to a PL defined by one spectral index α_ν, i.e., $F_\nu \propto \nu^{-\alpha_\nu}$ for the entire wavelength range of interest. Modelling spectra with a base containing a single PL and SSPs results in higher MAE values (see Tab. A.1.13) than for modelling with a base composed of multiple single PLs, i.e., when single PLs of different α_ν values are present in the base along with the SSPs. Modelling AGNs with a base containing just one single PL of $\alpha_\nu \sim -1.5$ and SSPs has been widely done in the literature.

- MAE values of stellar and AGN properties increase with increasing V-band extinction, Av, of the input spectra. Adding extinction to the input spectra changes its shape and introduces an additional degeneracy.

- MAE values of stellar and AGN properties depend upon the SN of the input spectra.

- Out of all the parameters, the recovery of X_{AGN} is the best, followed by $< \alpha_\nu >_L$. Hence, we can be certain that FADO traces the contribution of high energy non-stellar radiation field.

The application of FADO to synthetic spectra of Seyfert 2 galaxies has shown that there are significant and systematic biases corresponding to the recovery of mean stellar ages and metallicity, in particular for intermediate age systems. But FADO performs well in retrieving X_{AGN} and the spectral index, $< \alpha_\nu >_L$ which justifies an initial application of FADO also to observed spectra of Seyfert 2 galaxies, with the goal of getting insights into the characteristic of the featureless AGN continuum in this galaxy class. Of special interest in this regard is the shape of the best-fitting AGN continuum (which is governed by the number of power law components selected from the base to fit the spectrum, and their spectral indices, α_ν) and its contribution to the observed monochromatic luminosity at 4020$\mathring{A}$ (X_{AGN}). We also investigate whether the AGN featureless continuum can be approximated by the usually adopted 'canonical' spectral index of $\alpha_\nu \sim -1.5$. FADO finds a range of PL spectral index values for the Seyfert 2 galaxies instead of the usually adopted 'canonical' spectral index value of $\alpha_\nu \sim -1.5$. So, there is no canonical or standard value of PL spectral index applicable for all Seyfert 2 galaxies. We note that, in general, a linear combination of power-laws having different spectral indices is not a power-law function. However, for the wavelength range of this study, 3400-8900 $\mathring{A}$, a linear combination of power-laws having different spectral indices does not deviate significantly from a power-law function. So, the spectral fitting in the UV/Optical window is not affected but the ionizing budget can change and needs to be investigated.

After extensively testing and evaluating FADO's capability on synthetic data, we apply it to a set of Seyfert 2 galaxy spectra from the Sloan Digital Sky Survey (SDSS) and evaluate the results, as described in the next chapter.

Chapter 4

Applying FADO to Seyfert 2 galaxies from the Sloan Digital Sky Survey

This chapter is devoted to the application of FADO to single-fibre Seyfert galaxy spectra from the SDSS Data Release 7 Abazajian et al. (2009). This data set contains multi-band spectrophotometric data for 926246 objects, each with a single-fibre integrated spectrum with the wavelength range of 3800-9200 Å at a resolution of $R \sim$ 1800-2200, with the fibre covering $\sim$ 5.5 kpc of the central region of an object at $z \sim 0.1$. The selection of the sample used builds upon the previous work by our team Cardoso et al. (2022) and permitted the extraction of a sample of 17000 Seyfert 2 galaxies using the classical BPT-[NII] diagnostic diagram (Baldwin et al., 1981), based on the following criteria:

- Flux of emission lines H_α, H_β, [OIII]λ5007Å and [NII]λ6584Å > 0.0
- SN of emission lines H_α, H_β, [OIII]λ5007Å and [NII]λ6584Å ≥ 3.0

Prior to spectral modelling, the SDSS sample was pre-processed. The quality of the spectra was visually checked, the spectra were corrected for Galactic foreground extinction using Schlafly and Finkbeiner (2011), and converted to the observer restframe (redshift provided by the SDSS with quality **zWARNING**=0) and rebinned using a flux-conserving technique (PyFluxconserving: Gomes 2024) so that $\Delta = 1$Å. Cardelli et al. (1989) extinction curve with Rv = 3.1 was used for the Galactic foreground extinction correction. Dr. J. M. Gomes had kindly provided me with the pre-processed spectra.

4.1 Modelling Seyfert 2 Galaxies Using FADO: Insights from the SDSS sample

Spectral fitting was carried out using BaseA (3.1.3) with the V-band extinction, stellar velocity shift and dispersion as free parameters varying within the ranges of Av=0-6 mag, $v_\star$ = -500-500 km/s and $\sigma_\star$ = 0-1500 km/s. BaseA contains 111 elements comprising of 11 single PL and 100 SSPs. The spectral index of the PL components, α_ν, is in the range of -1.0 to -2.0 in steps of 0.1. The 100 SSPs have 4 metallicities (Z = 0.004; 0.008; 0.02; 0.05 = $Z_\odot \times \{1/5; 2/5; 1; 2.5\}$) and 25 ages (between 1 Myr and 15 Gyr). For modelling the Seyfert 2 galaxies, we assumed Cardelli et al. (1989) attenuation law, which is the same as the one used for modelling the synthetic spectra for the benchmark tests.

4.2 Recovery of AGN fraction and power-law index

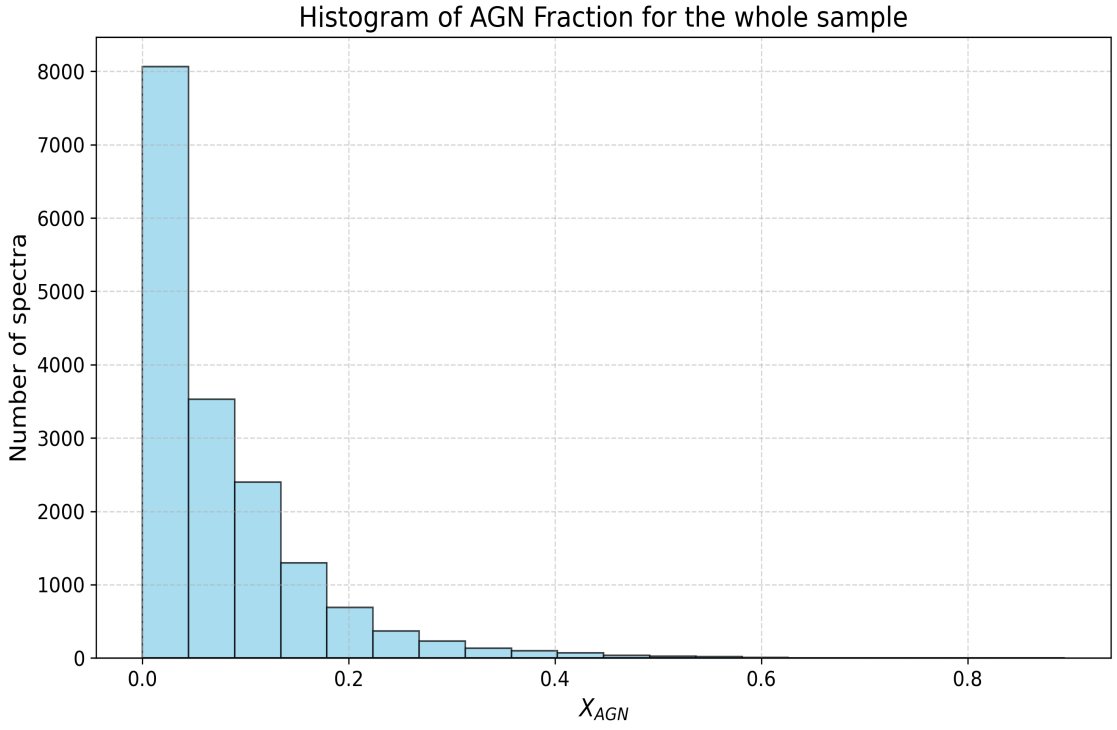

FIGURE 4.1: Distribution of the recovered X_{AGN} for the whole sample. 96% of the galaxies have $X_{AGN} \leq 0.26$. The X_{AGN} value given by FADO does not show any trend with the SN of the input spectrum.

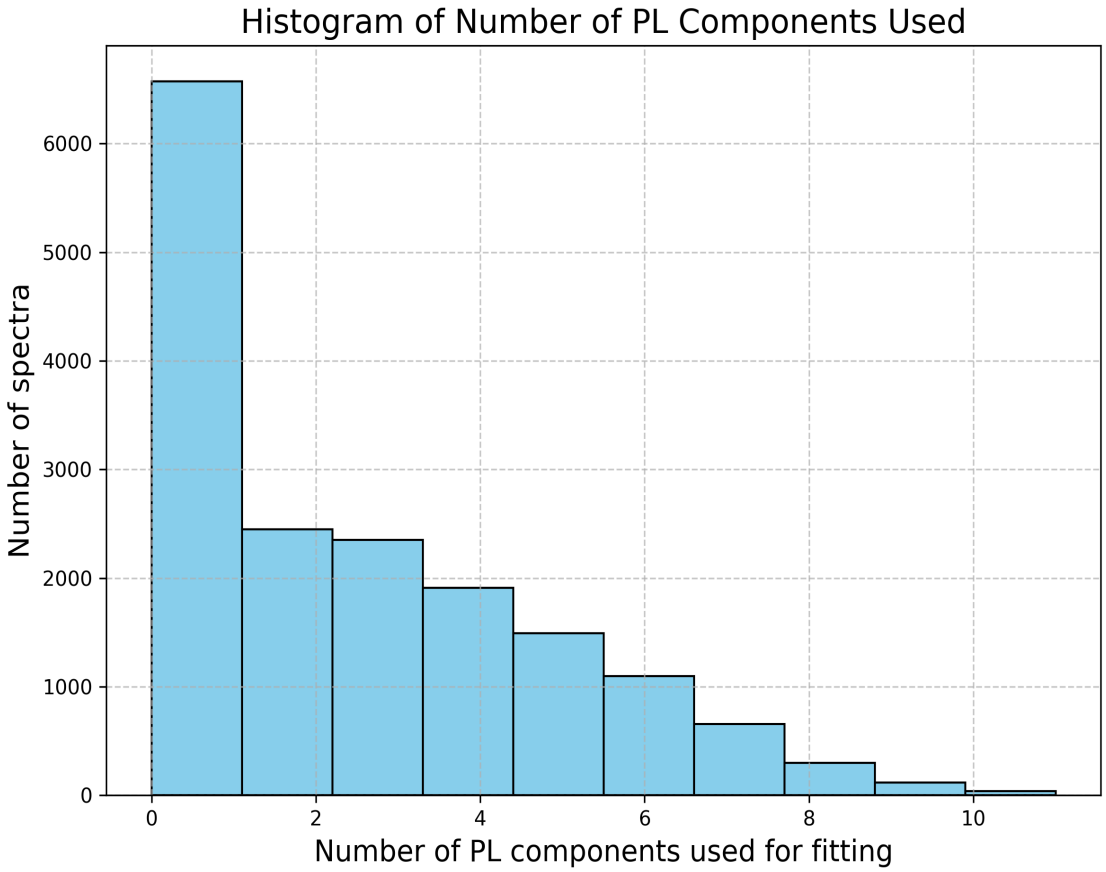

FIGURE 4.2: Number of power-law components used to fit the input spectrum for the whole sample. The number of PLs used by FADO for fitting does not depend on the SN of the input spectrum.

Figure 4.2 shows that for nearly half of the sample ($\sim$ 8500), the spectral fitting with FADO converges into one single spectral index. For around 14%, 12% and 11% of the galaxies analysed, FADO used 2, 3 and 4 power components, respectively.

The arithmetic mean and median values of the broad distribution of the average power law indices (Fig. 4.3) are -1.50 and -1.49, respectively. These values are very close to the 'canonical' value of $\alpha_\nu \sim 1.5$. A conspicuous feature in this diagram is that, around 9.3% and 6.1% of the total sample is fit with the minimum and maximum PL index allowed in the base library, respectively. The origin of this trend needs to be investigated (it might be because of a less than optimal convergence in the fit). A similar segregation towards the minimum and maximum spectral index of -2 and -1 was found when FADO used just one PL component from the base to model the input spectrum (Fig. 4.5).

As for X_{AGN}, we see from Fig. 4.1, Fig. 4.4 and Fig. 4.6 that it follows a nearly exponential distribution with $\sim$ 96%, $\sim$ 95% and $\sim$ 95%, respectively, of the galaxies in each case having $X_{AGN} < 0.26$.

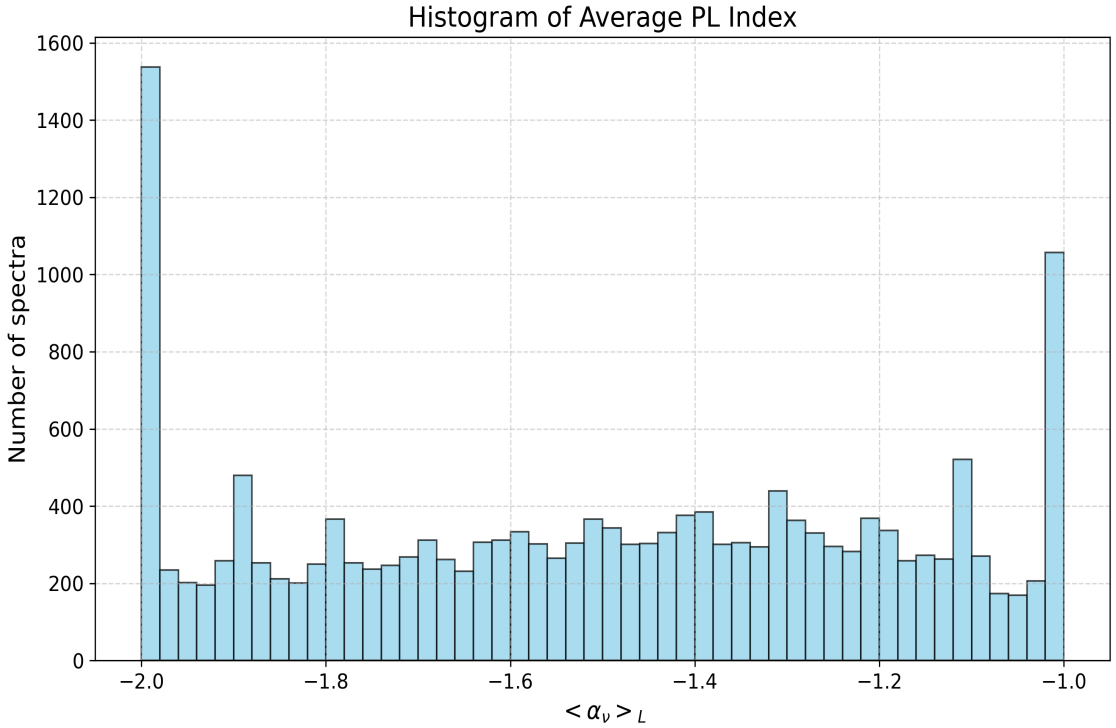

FIGURE 4.3: Range of PL components used to fit the input spectrum for the whole sample.

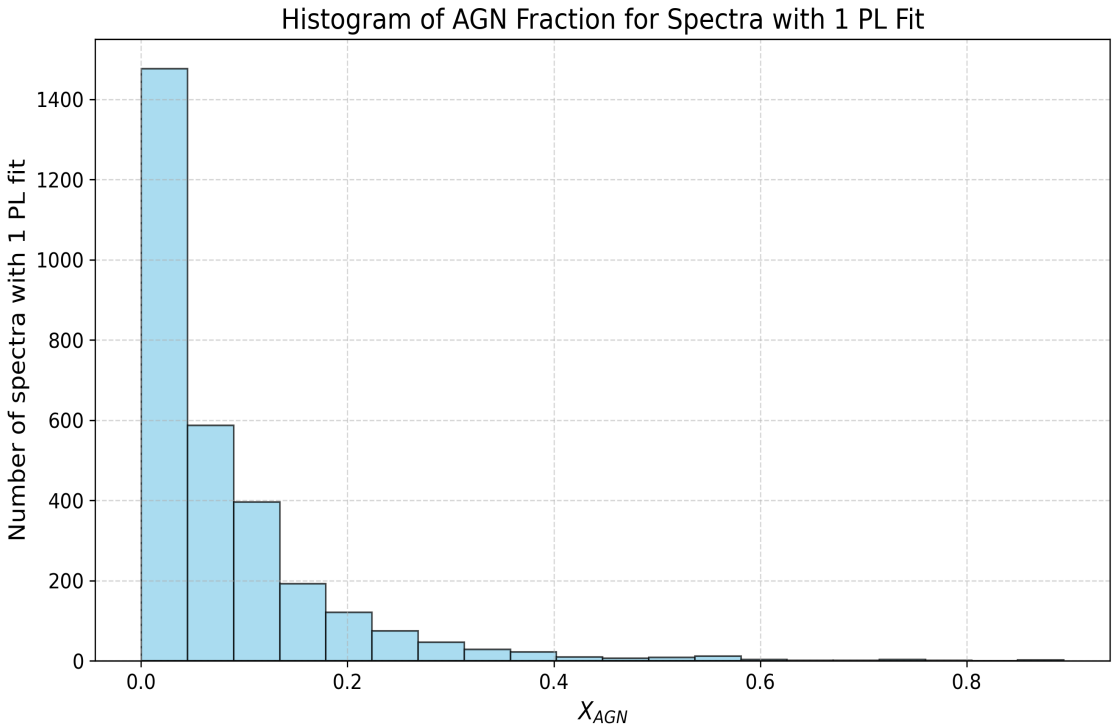

FIGURE 4.4: Distribution of the recovered X_{AGN} when only one PL was used by FADO. 95% of the galaxies of this subset have $X_{AGN} \leq 0.26$.

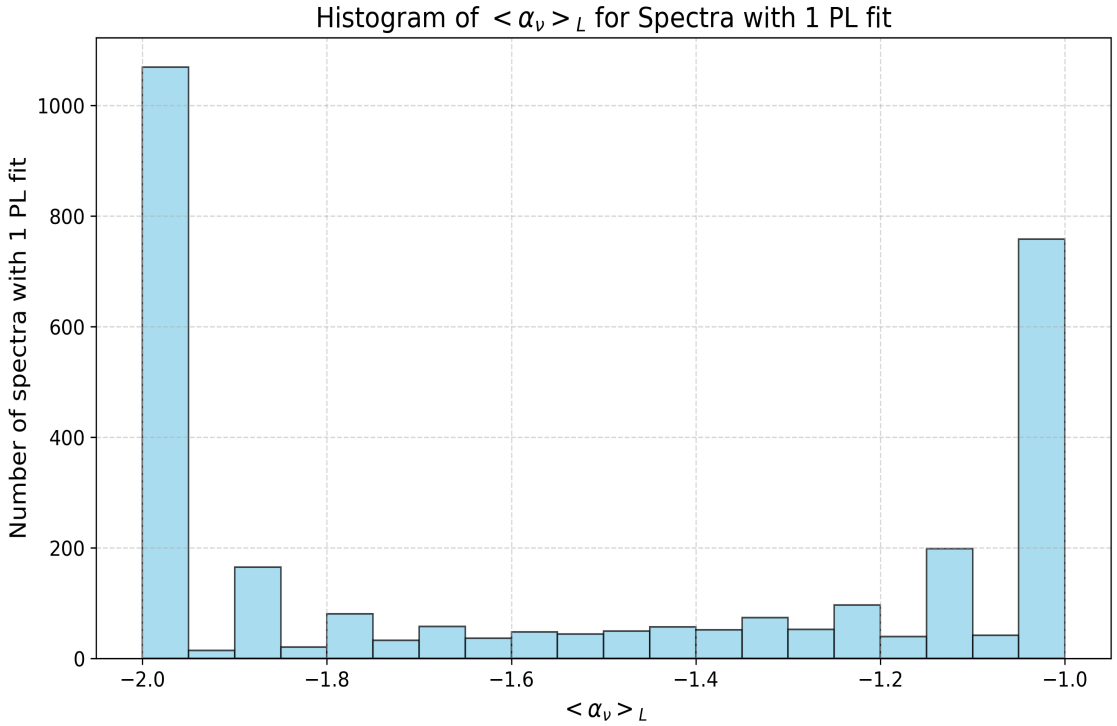

FIGURE 4.5: PL index values when only one PL was used by FADO.

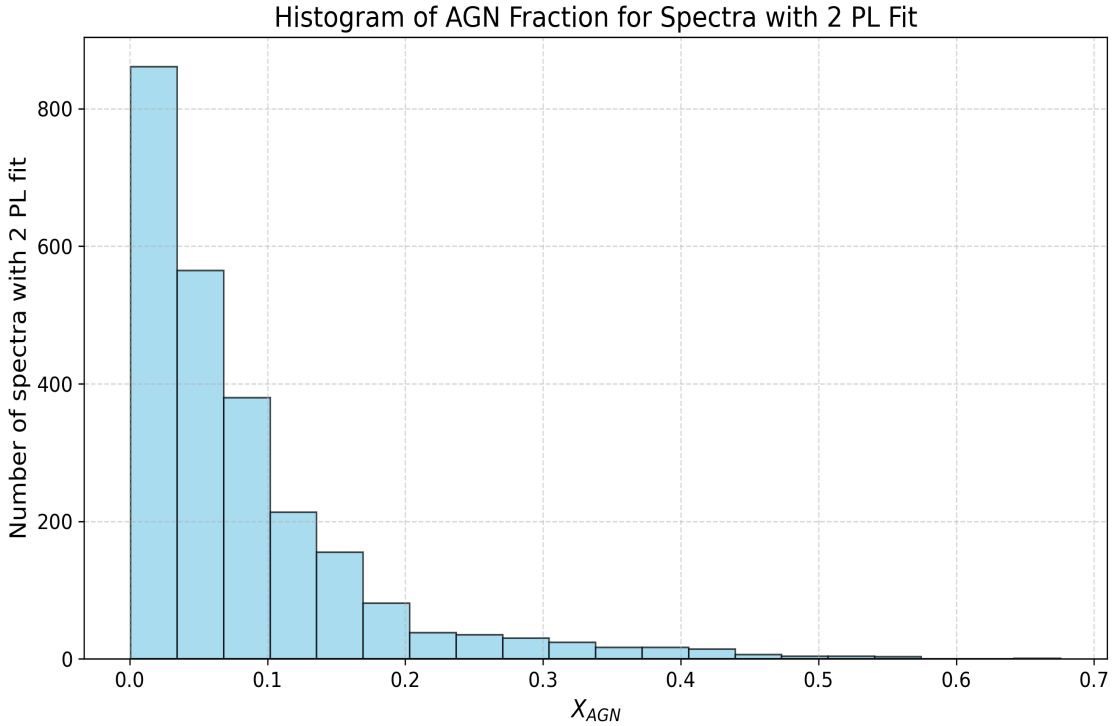

FIGURE 4.6: Distribution of the recovered X_{AGN} when two PL was used by FADO. 95% of the galaxies of this subset have $X_{AGN} \leq 0.26$.

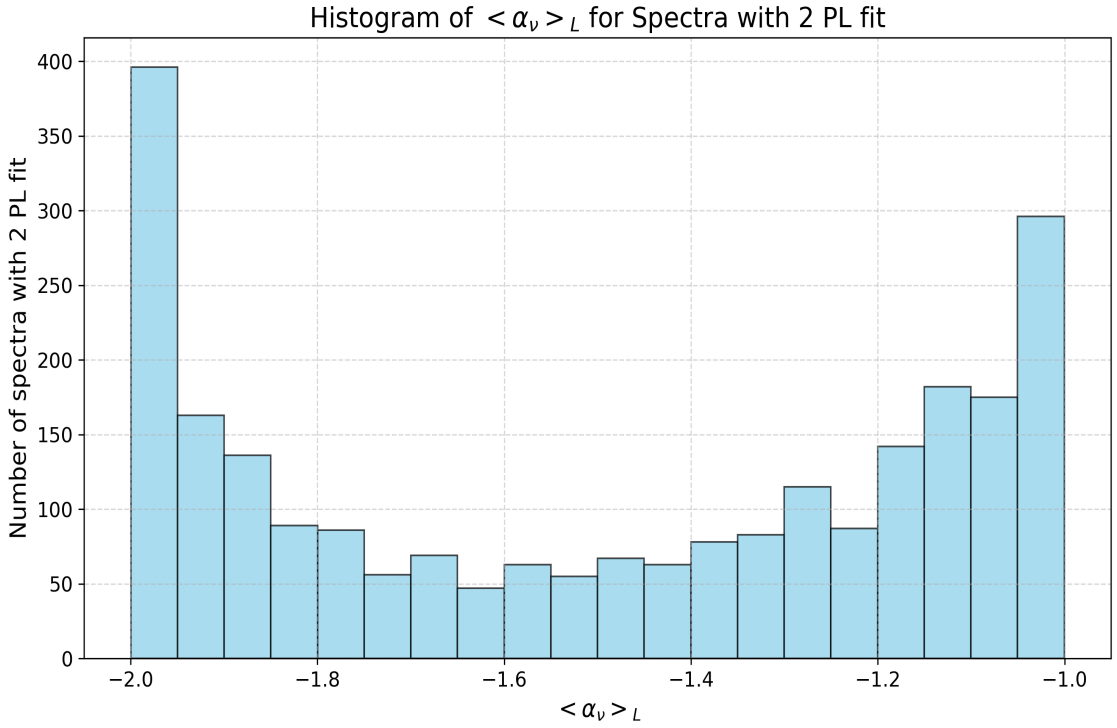

FIGURE 4.7: PL index values when 2 PLs were used by FADO

As shown in Cardoso et al. (2016), an $X_{AGN} < 0.26$ generally implies a very low, hardly detectable dilution of stellar absorption features by the AGN, in the case of an early-type galaxy where the gas density is low, thus the bulk of Lyman continuum radiation generated by the AGN escapes without being locally reprocessed into nebular emission (Gomes et al., 2016a, Papaderos et al., 2013).

In such a galaxy, and for an $X_{AGN} < 0.26$, the AGN will evade detection in the optical, prompting the interpretation of it being a 'retired' non-SF system and spectral modelling with a purely stellar base. As demonstrated in Cardoso et al. 2016, 2017 (see also the Introduction of this thesis), the neglect of the AGN power-law continuum leads to grave biases in the inferred SFH and secondary quantities, such as light- and mass-weighted age and metallicity.

Thus, the results from Fig. 4.1, Fig. 4.4 and Fig. 4.6, when taken at face value, imply that visual detection of an AGN power-law underlying the stellar and nebular continuum of a Seyfert 2 galaxy is in most cases impossible, and the presence of an AGN contribution in the optical spectral range can only be ascertained through BPT diagnostic line ratios or self-consistent spectral synthesis following the concept tested in this thesis.

4.3 Soundness of the FADO concept on AGN

4.3.1 Prominence of high-excitation emission lines

Regarding the overall soundness of the FADO concept on AGN, an elementary test that can be made involves the prominence of high-excitation emission lines (e.g., HeII 4686 Å, [NeV] 3426 Å, or [FeV] 4227 Å whose presence implies the presence of a hard ionising field with a photon energy > 54 eV corresponding to $\lambda < 228$ Å; see, e.g., Fricke et al. 2001; Izotov et al. 2004; Shirazi and Brinchmann 2012; Izotov et al. 2021) with increasing X_{AGN}. For instance, the comparatively soft radiation field produced by massive stars with approximately solar metallicity cannot lead to significant HeII emission exceeding $\sim$2% of the H_β (e.g., Schaerer and de Koter 1997), which points to the presence of an AGN or high-mass X-ray binaries (Schaerer et al., 2019). Additionally, recent advancements in stellar population models, such as the Binary Population and Spectral Synthesis (BPASS; Eldridge et al. 2017; Byrne et al. 2022) suite, incorporate binary mass transfer effects, offering improved analysis of integrated light from stellar populations and their detailed properties. It's worth noting that multiplicity (not necessarily binaries only) may abruptly change the number of ionizing continua produced and also for longer times because the evolution of stars is different than in single stars (e.g. BC03 models by Bruzual and Charlot 2003 and MILES by Vazdekis et al. 2010).

As a qualitative test, we show in Fig. 4.8 that the prominence of high-excitation lines, [NeIII] λ3967.470Å, [NeV] λ3425.881Å, HeII λ4685.710Å and H_α, increases with increasing X_{AGN}. The mean stacked spectra in Fig. 4.8 was produced as follows:

- Depending on the X_{AGN} values given by FADO, the spectra were divided into bins of X_{AGN}, 0.0-0.1, 0.1-0.2, 0.2-0.3, 0.3-0.4, 0.4-0.5, 0.5-0.6, 0.6-0.7, 0.7-0.8 and 0.8-0.9. The X_{AGN} bin 0.0-0.1, does not contain the spectra with $X_{AGN} = 0.0$ but greater than zero and up to 0.1.

- For each spectrum within a bin, the bad pixels were flagged using the corresponding error spectrum. This procedure gave us good pixels at each wavelength for each spectrum within a bin.

- We then calculated the arithmetic mean of good flux pixels at each wavelength for each bin. This gave us nine spectra, each representing, on an average, the spectral features for each X_{AGN} bin.

Figure 4.8 highlights that the prominence of high-excitation lines increases with increasing $X_{\rm AGN}$. In the low $X_{\rm AGN}$ bins ($0.0 \leq X_{\rm AGN} < 0.1$ to $0.3 \leq X_{\rm AGN} < 0.4$), the high-excitation lines

are relatively less intense, indicating a lower AGN influence. As $X_{\rm AGN}$ rises ($0.4 \leq X_{\rm AGN} < 0.5$ to $0.6 \leq X_{\rm AGN} < 0.7$), the intensity of lines such as [Ne III], [Ne V], and He II increases, reflecting a stronger AGN influence. In the highest bins ($0.7 \leq X_{\rm AGN} < 0.8$ to $0.8 \leq X_{\rm AGN} < 0.9$), the high-excitation lines are most pronounced, showing that these spectra are heavily influenced by the AGN's strong ionizing fields. This trend supports the soundness of the FADO concept by demonstrating that high-excitation emission lines, indicative of AGN activity, become more prominent with higher $X_{\rm AGN}$ values.

Figure 4.9 shows that the strength of HeII 4686 Å emission line increases with X_{AGN}. To produce Fig. 4.9, the HeII λ4686 EWs and X_{AGN} were divided into bins of X_{AGN}, 0.0-0.1, 0.1-0.2, 0.2-0.3, 0.3-0.4, 0.4-0.5, 0.5-0.6, 0.6-0.7, 0.7-0.8 and 0.8-0.9. The EW and X_{AGN} mean values were calculated for each bin and plotted. The strength of HeII λ4686 line increases with X_{AGN} implying the presence of a high-energy radiation field. The trend in the white region is not reliable due to poor statistics and low SN of the spectra.

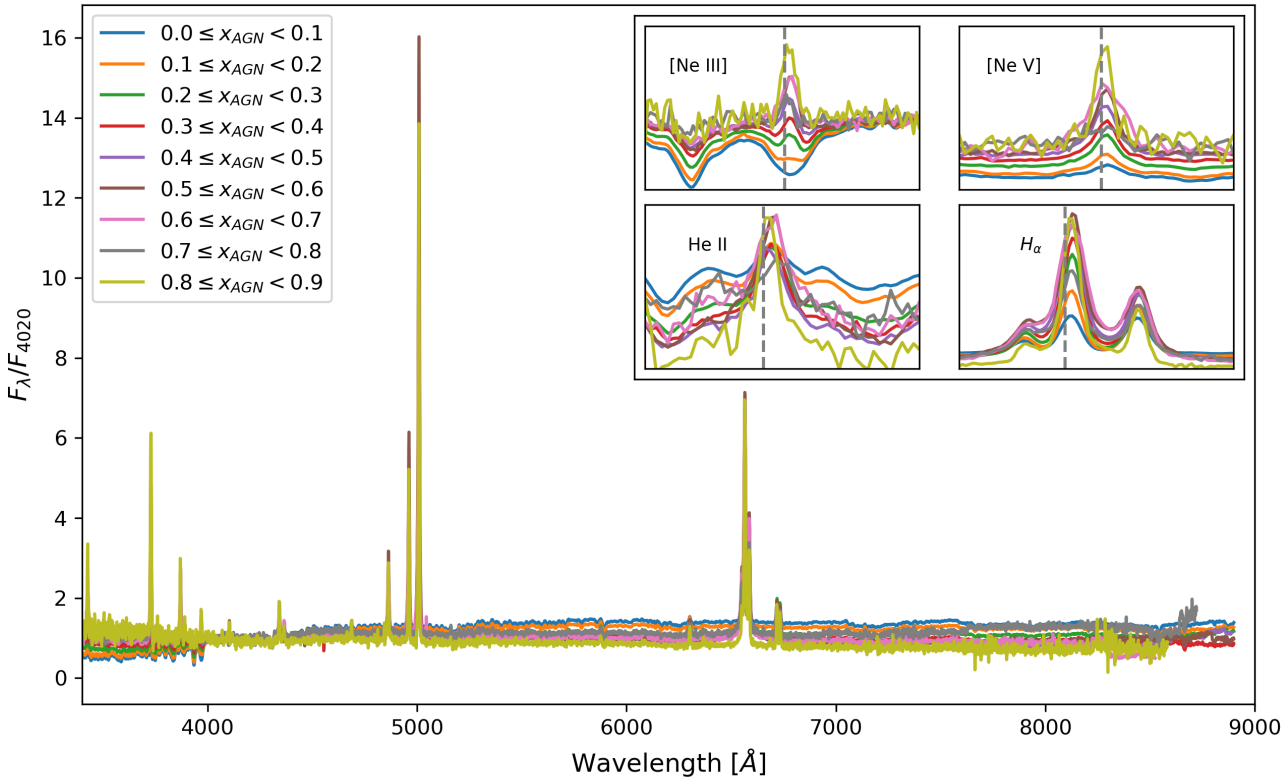

FIGURE 4.8: Mean stacked spectra displaying high excitation lines. In the upper right corner of the plot, zoom-ins of the regions around [NeIII], [NeV], HeII, and H_α are depicted. The various colors represent distinct X_{AGN} contributions, as indicated in the legend. The figure highlights that the prominence of high-excitation lines increases with increasing X_{AGN}.

4.4 An example: SDSS J023301.24+002515.0

A Seyfert 2 galaxy from our sample, SDSS J023301.24+002515.0 (or Z 388-48), present at $z \sim 0.02$, has an X_{AGN} and $< \alpha_\nu >_L = \sim 11\%$ and ~ -1.4, respectively, as calculated by FADO. Figure 4.10 shows FADO fit to the SDSS J023301.24+002515.0 spectrum along with individual components that the best-fit solution is composed of. At the normalisation wavelength of 4020 Å (vertical grey line), the flux of the observed spectrum (264.63) = flux of nebular continuum* (0.79) + flux of PLs (28.80) + flux of SSPs (235.04). Hence, PLs contribute 28.80/264.63 $\sim$ 11%, SSPs contribute 28.80/264.63 $\sim$ 88%, and nebular continuum contributes 0.79/264.63 $\sim$ 1%.

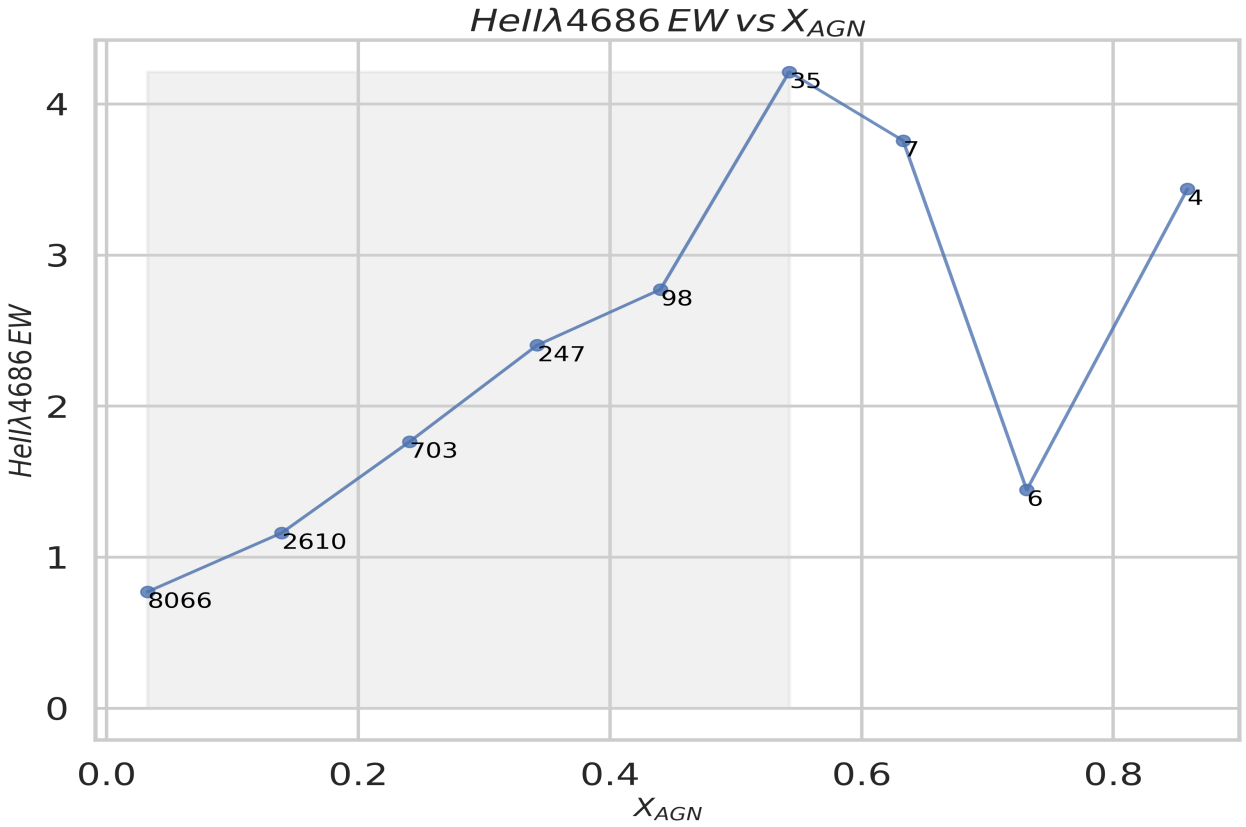

FIGURE 4.9: EW of HeII λ4686, averaged per X_{AGN} bin as a function of X_{AGN}, averaged per X_{AGN} bin. The numbers next to the data points are the number of objects in each X_{AGN} bin. The sum of these numbers is not $\sim$ 17000 because we only selected the objects having measurement of HeII λ4686 lines (11776 objects) for this plot. The strength of HeII λ4686 line increases with X_{AGN} implying the presence of a high-energy radiation field. The trend in the grey shaded region is more reliable than the white region as the number of objects per data point and the SN of the their spectra are higher.

*The nebular continuum is calculated on the fly by FADO

SDSS J023301.24+002515.0 has been previously studied in the radio by Lal (2015), where the data was taken from the radio maps from Faint Images of the Radio Sky at Twenty–Centimeters (FIRST; Becker et al. 1995) and NVSS. The author classifies the galaxy as Seyfert 2 and finds the peak flux density and integrated flux density at 1.4 GHz to be 3.89 mJy beam^{-1} and 3.98 mJy, respectively.

Goto (2006) performed a spatially resolved spectroscopy of SDSS J023301.24+002515.0 using the Apache Point Observatory (APO) 3.5-m telescope. The observation was done with the Dual Imaging Spectrograph (DIS) in the long-slit mode with 1.5-arcsec slit-width. The author investigates the spatial distribution of: 1) flux of [OIII] emission line and H_δ absorption line 2) EWs of [OIII] emission line and H_δ absorption line 3) EW of H_β and 4) [SII] / H_α flux ratio.

The author concludes that both of the AGN and post-starburst regions in SDSS J023301.24+002515.0 are centrally concentrated with, the post-starburst region being more extended towards the exterior of the galaxy than the emission-line region.

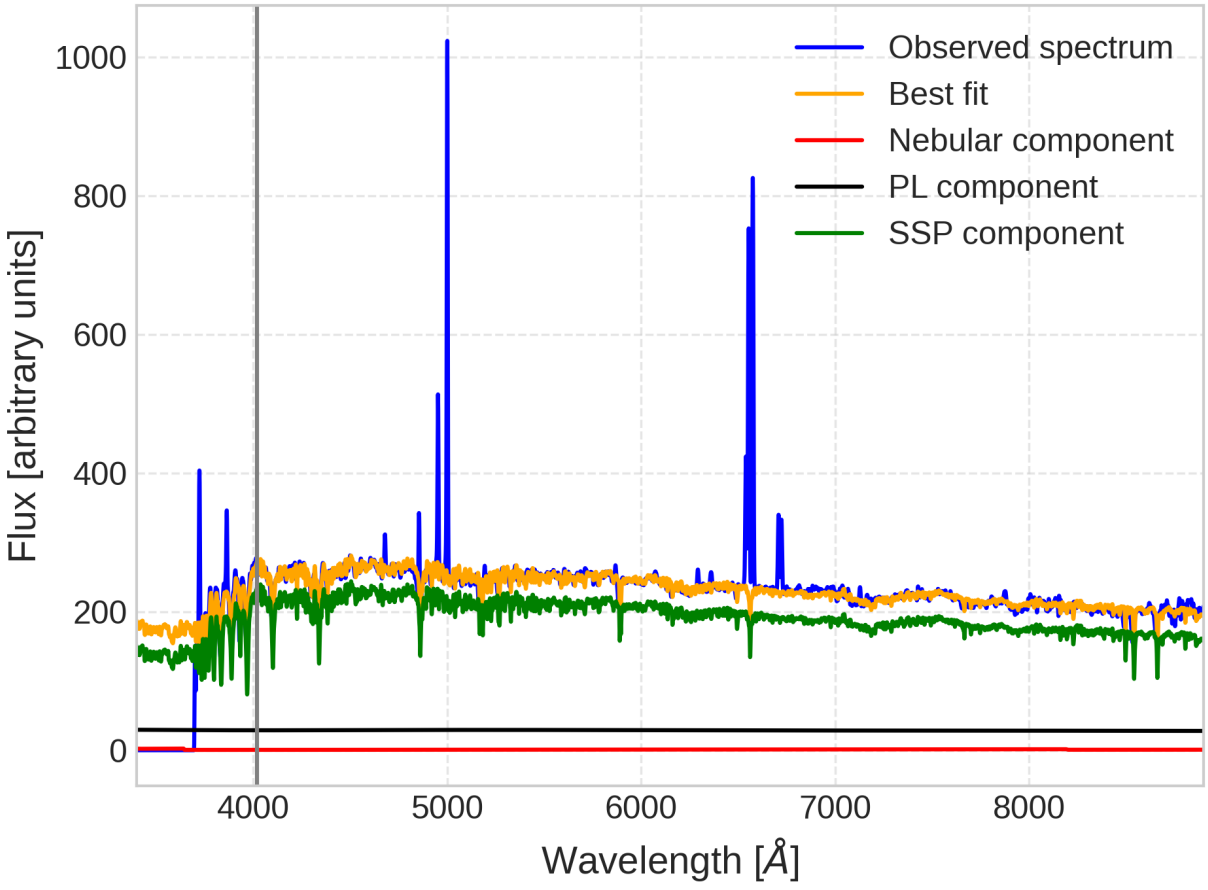

FIGURE 4.10: Modelling of SDSS J023301.24+002515.0 Seyfert 2 spectrum using FADO. The best-fit solution is composed of nebular continuum, PL continuum and SSPs. The former is calculated on the fly, while the later are selected from the templates by FADO.

4.4.1 Detection in other wavelengths

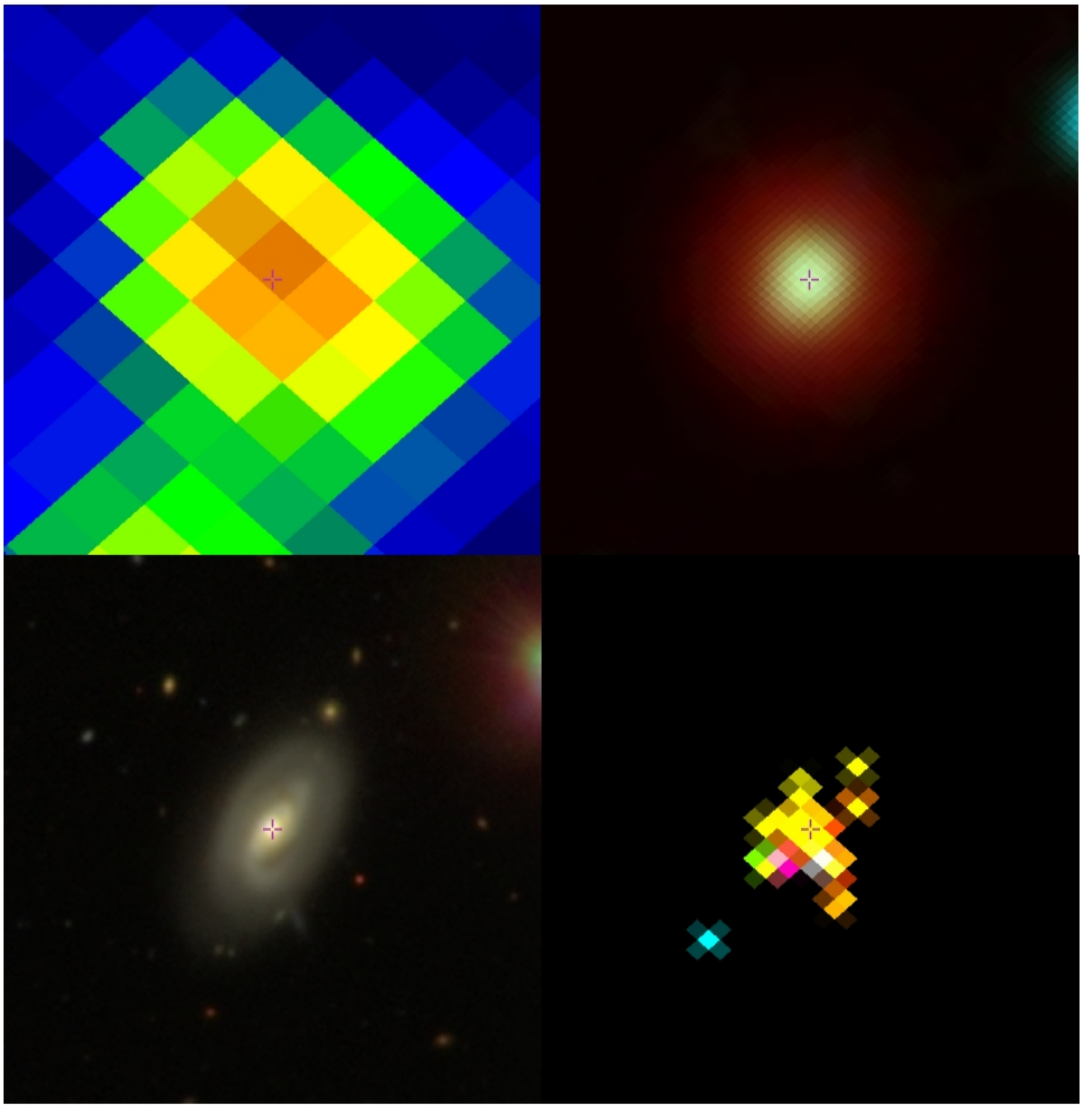

FIGURE 4.11: Multi-wavelength detection of SDSS J023301.24+002515.0 Seyfert 2. The top left image is in radio (1.4 GHz continuum) taken from NVSS - The NRAO VLA Sky Survey (intensity maps). The top right image is in IR and taken from WISE. The colours, Red, Green, Blue, correspond to W4 (22 μm), W2 (4.6 μm), and W1 (3.4 μm) bands from WISE. The bottom left image is in optical and taken from SDSS DR 9. The bottom right image is in X-ray, taken from XMM-Newton. The coloured image is made with all PN images of the 4XMM-DR12: Red=0.5-1Kev Green=1-2Kev Blue=2-4.5Kev. The images were obtained using Aladin Sky Atlas for a FOV of 1.95 arcmin.

As FADO estimates an $X_{AGN} \sim 11\%$ for this galaxy, we searched for the galaxy data in X-ray, infrared (IR) and radio wavelengths. Figure 4.11 shows the images of SDSS J023301.24+002515.0 in radio, IR, optical and X-ray, obtained by us using the Aladin Sky Atlas* for a Field Of View (FOV) of 1.95 arcmin. The radio image is in 1.4 GHz continuum, taken from NVSS - The NRAO

*https://aladin.cds.unistra.fr/AladinLite/

VLA Sky Survey (NVSS; Condon et al. 1998); the IR image is composed of observations from W1 (3.4 μm), W2 (4.6 μm), W3 (11.6 μ m) and W4 (22 μm) bands of the Wide-field Infrared Survey Explorer (WISE); the optical image is taken from SDSS DR 9; the X-ray image is a false colour image (Red=0.5-1 Kev, Green=1-2 Kev, Blue=2-4.5 Kev) taken from the 4XMM-DR12 XMM-Newton catalogue.

4.4.2 WISE MIR Colours

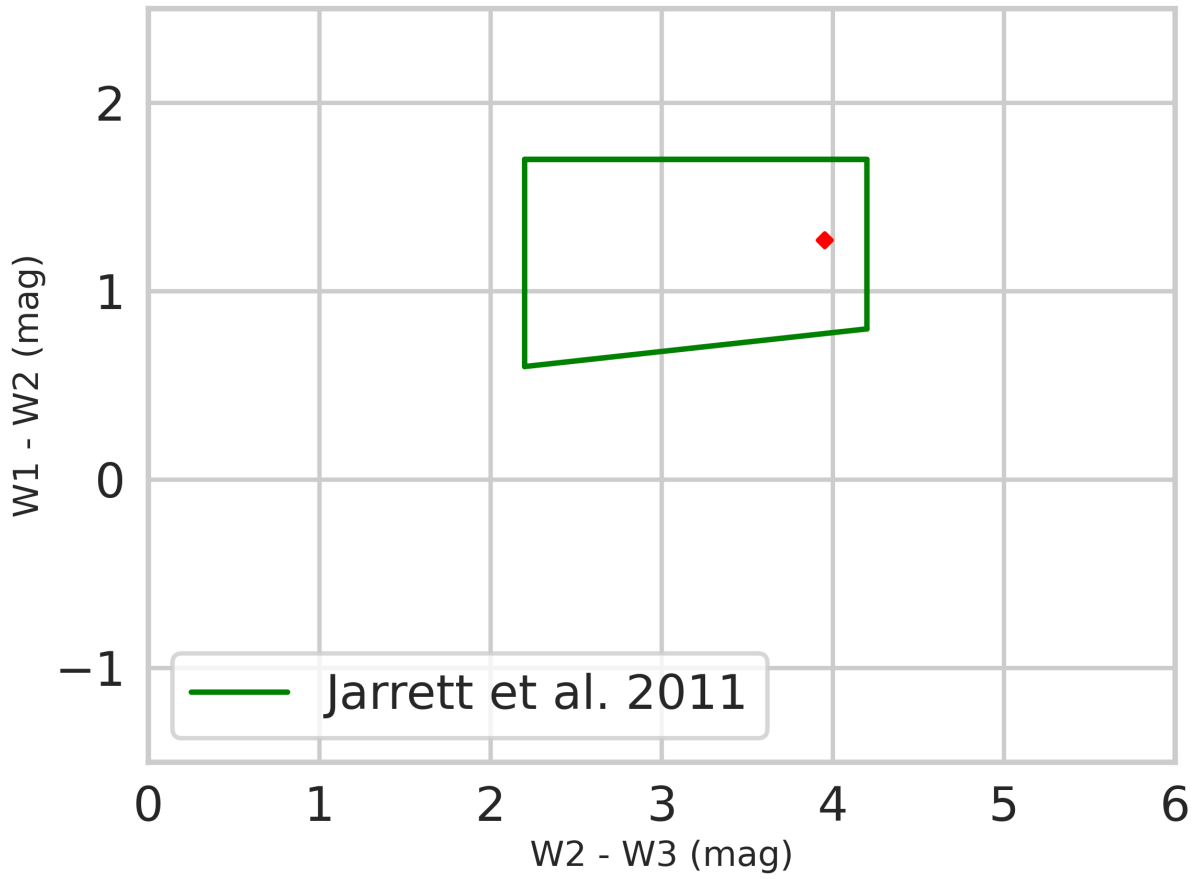

FIGURE 4.12: WISE colour-colour diagram for SDSS J023301.24+002515.0. The green quadrilateral marks the AGN region defined by Jarrett et al. (2011).

Mid-infrared (MIR) AGN diagnostics has proved beneficial in detecting hidden AGNs in various galaxies. AGNs emit a hard radiation field that leads to dust heating to high temperatures, thereby producing a strong MIR continuum and an IR SED that differs from typical star-forming galaxies.

We cross-matched SDSS J023301.24+002515.0 with AllWISE Data Release (Cutri et al., 2013) to obtain W1 (3.4 μ m), W2 (4.6 μm), W3 (11.6 μ m) and W4 (22 μ m) MIR Colours (in magnitudes),

and plotted the W1-W2 vs W2-W3 colour diagram for AGN diagnostics (see Fig. 4.12). The AGN region in the MIR colour space as defined by Jarrett et al. (2011) is as follows:

$$2.2 < [W2 - W3] < 4.2, \text{ and } (0.1 \times [W2 - W3] + 0.38) < [W1 - W2] < 1.7.$$

SDSS J023301.2+00251 (classified as a Seyfert 2 in the optical) has a $\sim$ 11% contribution at 4020 $\mathring{A}$ from PLs, as estimated by FADO. The same galaxy also shows an AGN-signature in the MIR (see Fig. 4.12) suggesting that FADO has been successful in tracing hard radiation field.

Chapter 5

Discussion and Conclusions

It is important to recall the effect of adding AGN emission on the stellar features of synthetic spectra. X_{AGN} represents the contribution of single PL model (continuum plus emission lines) at 4020 Å. The steepness of the continuum of this model depends upon α_ν. As the absolute value of α_ν decreases, the spectrum gets bluer. Hence, the increase in X_{AGN} dilutes the stellar features and makes the continuum bluer, the extent of which depends upon α_ν. As the spectrum was convolved with a Gaussian kernel of σ = 300 km/s, the spectral features suffered an additional dilution (see Fig. 5.1). Hence, even for $X_{AGN} = 0.2$, the spectral features are weaker than they would be for spectra with lower velocity broadening.

Note that the age of the system is different than the luminosity-weighted mean stellar age of the system, the latter depends on the SFH assumed for the system. SFH governs the type of stars dominating the spectra at any age of the system. For an instantaneous burst SFH, the stars are formed in an instant and evolve with the system with no new stars being added to the system. Hence, the luminosity-weighted mean stellar age of the system is close to the age of the system with its spectra being dominated by stars of age close to the age of the system. The luminosity-weighted mean stellar ages span $\sim$ 1 Myr to $\sim$ 10 Gyr for system going from 1 Myr to 10 Gyr in this case. So, models with single-burst SFH show a spectral shape diversity larger than models with constant SFH. In case of constant SFH, as new stars are continuously added to the system, the luminosity-weighted mean stellar age of the system is less than the age of the system, and differs greatly from it after $\sim$ 16 Myr. The luminosity-weighted mean stellar ages span 1 Myr to $\sim$ 0.1 Gyr for system going from 1 Myr to 10 Gyr. Figures 5.2 and 5.3 show the spectra of systems with age 1 Myr, 2.5 Myr and 6.3 Myr for models with instantaneous burst and constant SFH, respectively. The models have no AGN contribution ($X_{AGN} = 0.0$) and σ = 300 km/s. For either of the SFHs, the spectra

of the systems with age 1 Myr, 2.5 Myr and 6.3 Myr have similar continuum shape and stellar absorption features leading to degeneracy. Moreover, the inherent age-metallicity degeneracy issue, i.e., the confusion of old metal-poor with young metal-rich systems further introduces biases. The aforementioned reasons collectively contribute to the uncertainties in light-weighted quantities. The non-linear nature of mass-to-light ratio then magnifies the uncertainties in the mass-weighted quantities. On top of this, adding noise makes the situation worse.

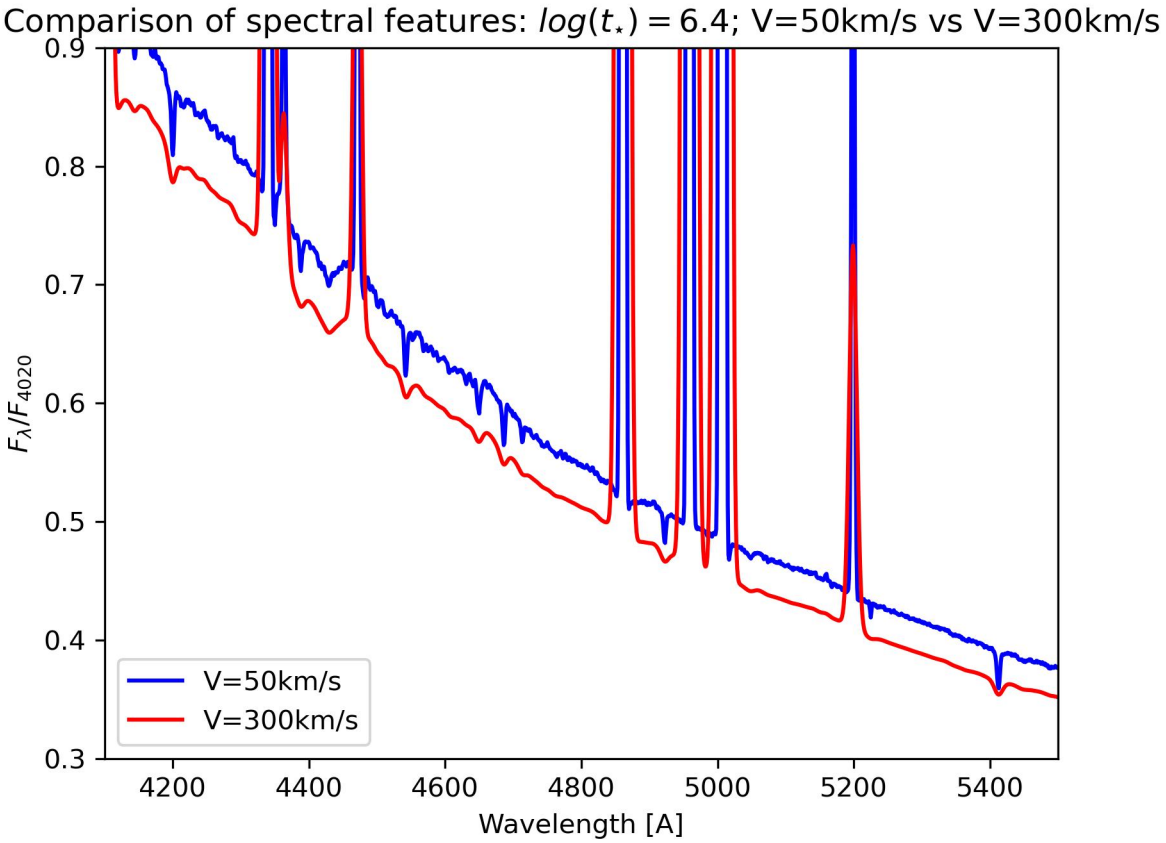

FIGURE 5.1: Comparison of the effects of broadening on a purely stellar system of age 6.4 dex (2.5 Myr) having an instantaneous burst SFH. The already weak absorption features suffer further dilution due to kinematics.

Intermediate age systems often exhibit a mix of young and old stellar characteristics, which can be complex and varied, even more due to AGN contribution. Also, such systems undergo significant evolutionary changes that can alter their spectral features. The challenges can be more pronounced in instantaneous burst SFH due to the sudden shift from young, bright stars to intermediate stages. For continuous SFH, such a shift is gradual but exists nonetheless. Hence, gaps or sparse coverage in the intermediate age range can impair FADO's ability to trace these changes,

resulting in greater scatter and MAE. Using a base containing a comprehensive range of intermediate age stellar populations with smaller age grid should reduce the errors in property recovery; although, this needs to be investigated.

The application of FADO to synthetic spectra of Seyfert 2 galaxies has shown that the concept used performs well in retrieving X_{AGN} and the spectral index, $< \alpha_\nu >_L$. However, this comes at the price of significant and systematic biases plaguing the recovery of mean stellar ages and metallicity, especially for intermediate age systems. For this reason, the current concept of FADO is not sufficient for the reconstruction of the mass assembly history of Seyfert 2 galaxies and for reliably addressing the possibly regulatory role of AGN on galaxy evolution.

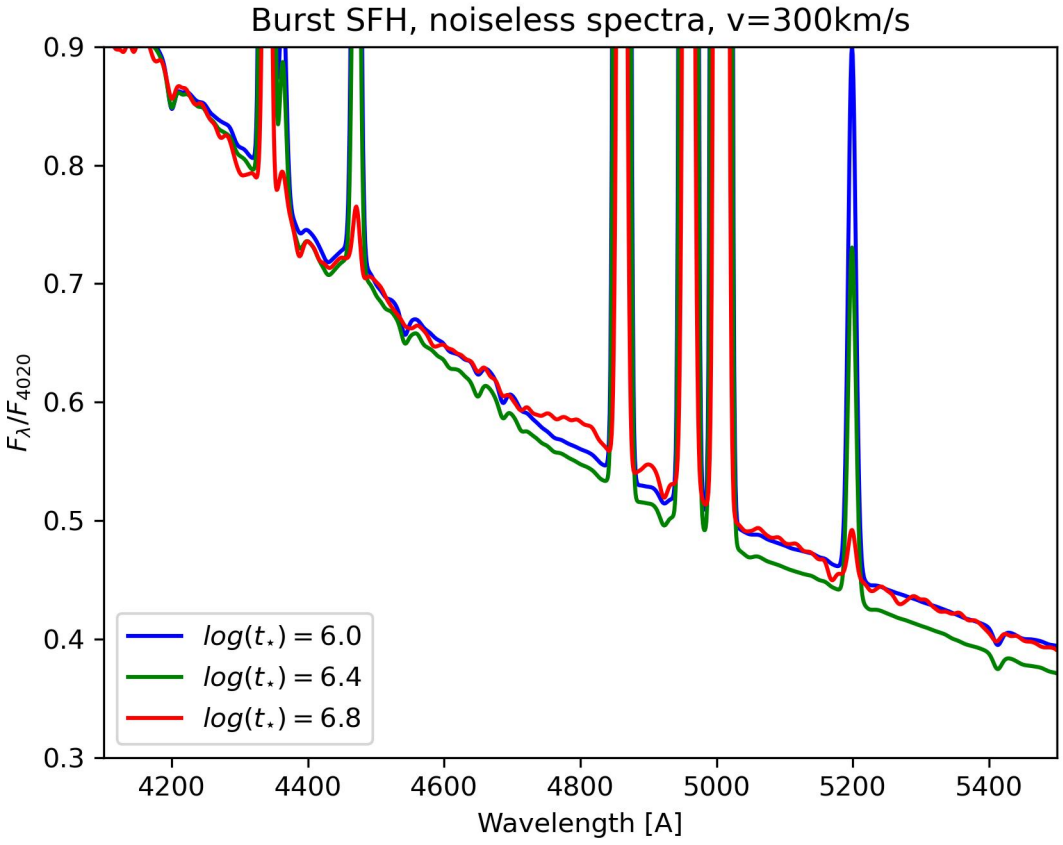

FIGURE 5.2: The spectra of a system with ages 6.0, 6.4, and 6.8 dex, convolved with a Gaussian kernel σ = 300 km/s. The absorption features are identical for the spectra. The system has an instantaneous burst SFH.

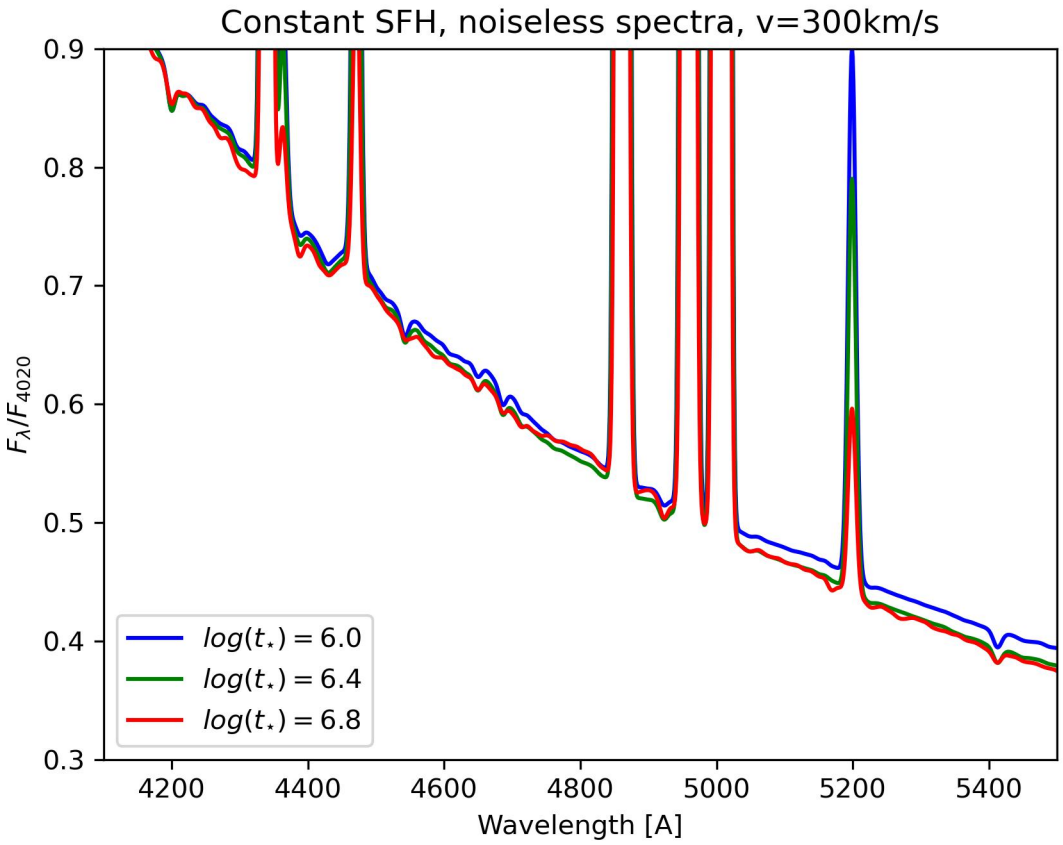

FIGURE 5.3: The spectra of a system with ages 6.0, 6.4, and 6.8 dex, convolved with a Gaussian kernel $\sigma = 300$ km/s. The absorption features are identical for the spectra. The system has constant SFH.

5.1 Conclusion

The comprehensive analysis of the mean absolute errors for various AGN and stellar properties has provided valuable insights into the performance of the FADO. The key conclusions drawn from this study are:

1. **Recovery Performance:** Overall, the recovery of AGN properties is more reliable than that of stellar properties, as evidenced by lower MAEs for $X_{\rm AGN}$ and $\langle \alpha_\nu \rangle_L$.

2. **Age Effect:** Older systems exhibit better recovery for both AGN and stellar properties, with consistently lower MAEs across all parameters under both burst and constant star formation histories.

3. **Intermediate System Challenge:** Intermediate-age systems pose the greatest challenge for recovery, showing the highest MAEs under both burst and constant star formation histories.

4. **AGN Fraction Influence:** While the input AGN fraction impacts the recovery of properties, AGN properties are less sensitive compared to stellar properties, indicating FADO's robustness in handling AGN components.

5.2 Future prospects

The FADO concept applied in this study, although oversimplified and unreliable for the recovery of mean stellar ages and metallicity, has passed an important qualitative test of tracing hard ionising radiation field. Thus, it is worth further developing and testing.

One test that might be considered involves a possible positive correlation between X_{AGN} and gas velocity dispersion, since it is to be expected that an AGN leads to a higher degree of gas turbulence through feedback (e.g., jets).

Due to lack of time, it has not been possible to thoroughly analyze the spectral synthesis output from FADO on SDSS Seyfert 2 galaxies, and study the possible influence of the spectral range fit and different compositions of the base library (e.g., with a different IMF) on the physical properties retrieved for the AGN and stellar component. It is crucial to investigate whether a base containing a comprehensive range of intermediate age stellar populations with an age grid finer than Base A reduces the errors in recovering the stellar properties.

Also, important tests to be done are:

- Study the connection between X_{AGN} and $< \alpha_\nu >_L$ with the evolutionary properties of the stellar component and the multi-wavelength characteristics of Seyfert 2 galaxies. For instance, is there a preference for X_{AGN} to increase with increasing galaxy mass, which might indicate a mass-dependence of the SMBH/$M_\star$ and/or SMBH spin parameter (see, e.g., discussion in Breda and Papaderos 2018).

- How does X_{AGN} and $< \alpha_\nu >_L$ correlate with the radio and X-ray luminosity?

Addressing such questions based on spectral fits with FADO for a sample of galaxies with existing deep radio continuum data from, e.g., the Evolutionary Map of the Universe (ASKAP) and X-ray data with Chandra, XMM/Newton and eROSITA is certainly a central task for a postdoctoral project.

Provided that it will be possible to understand and overcome the biases in modelling Seyfert 2 galaxies with FADO (see Chapter 3), a prime goal for the future will be its application to Seyfert 2 galaxies from MOONS, in order to investigate the regulatory role of AGN on galaxy evolution

since the cosmic noon ($z \sim 1.5$). One aspect in this regard that deserves special attention are aperture corrections, which are crucial for an unbiased determination of SFR and the spectroscopic classification of galaxies after BPT (Brinchmann et al. 2004; Iglesias-Páramo et al. 2013; Gomes et al. 2016b). The key importance of aperture effects may be demonstrated from integral field spectroscopy data of nearby AGN (e.g., the Circinus galaxy; Kakkad et al. 2023) showing that different gas excitation mechanisms may dominate in different areas of a galaxy, with a coexistence of an AGN nucleus with large-scale outflows whose line emission is powered by AGN photoionization or shock excitation, and even distinct regions where intense SF is taking place. Devising aperture corrections to aid the spectroscopic classification and the derivation of the physical and evolutionary properties (e.g., stellar mass, mass-weighted age) of marginally resolved galaxies observed by surveys using single-fibre spectroscopy, is clearly a timely and important future task.

Appendix A

Chapter 3 appendix: tables and figures

A.1 Tables:

A.1.1 Tables: Burst SFH, Av=0.0, SN = 15, base: BaseA

	SFH=Burst; SN=15.0; Av=0.0; Age of the system = 6.4															
	ΔX_{AGN}				$\Delta < \alpha_v >_L$				$\Delta < \log(t_\star) >_L$				$\Delta < \log(t_\star) >_M$			
X^i_{AGN}	0.2	0.4	0.6	0.8	0.2	0.4	0.6	0.8	0.2	0.4	0.6	0.8	0.2	0.4	0.6	0.8
Mean	0.0	-0.01	-0.02	-0.02	0.02	0.01	0.01	0.02	-0.06	-0.06	-0.07	-0.03	0.89	1.36	1.3	1.02
SD	0.01	0.02	0.02	0.03	0.05	0.04	0.03	0.04	0.06	0.07	0.06	0.12	1.1	1.48	1.54	1.36
MAE	0.01	0.02	0.02	0.03	0.05	0.03	0.03	0.03	0.07	0.07	0.07	0.09	0.93	1.41	1.36	1.08
MSE	0.0	0.0	0.0	0.0	0.0	0.0	0.0	0.0	0.01	0.01	0.01	0.01	2.0	4.05	4.04	2.89

	SFH=Burst; SN=15.0; Av=0.0; Age of the system = 6.4															
	$\Delta \log < Z_\star >_L$				$\Delta \log < Z_\star >_M$				$\Delta M_\star$				ΔA_v			
X^i_{AGN}	0.2	0.4	0.6	0.8	0.2	0.4	0.6	0.8	0.2	0.4	0.6	0.8	0.2	0.4	0.6	0.8
Mean	0.15	0.18	0.18	0.2	0.06	-0.01	-0.01	0.01	-0.27	-0.51	-0.52	-0.46	-0.0	-0.0	-0.0	-0.01
SD	0.06	0.06	0.07	0.08	0.11	0.21	0.18	0.21	0.38	0.59	0.64	0.63	0.0	0.01	0.03	0.04
MAE	0.15	0.18	0.18	0.2	0.1	0.15	0.14	0.17	0.28	0.52	0.53	0.48	0.0	0.0	0.0	0.01
MSE	0.03	0.04	0.04	0.05	0.02	0.04	0.03	0.05	0.21	0.62	0.68	0.61	0.0	0.0	0.0	0.0

TABLE A.2: A table showing mean, standard deviation (SD), mean absolute error (MAE) and mean square error (MSE) of Δ (output-input) of stellar and AGN properties. The top panel displays the SFH, SN, V band extinction and system age, respectively. X^i_{AGN} is the AGN fraction of the input spectrum, and spans 0.2-0.8 for each galaxy property. All the other tables follow the same format.

	SFH=Burst; SN=15.0; Av=0.0; Age of the system = 6.8															
	ΔX_{AGN}				$\Delta < \alpha_v >_L$				$\Delta < \log(t_\star) >_L$				$\Delta < \log(t_\star) >_M$			
X^i_{AGN}	0.2	0.4	0.6	0.8	0.2	0.4	0.6	0.8	0.2	0.4	0.6	0.8	0.2	0.4	0.6	0.8
Mean	0.01	0.01	0.01	0.0	0.05	0.05	0.05	0.04	0.03	0.03	0.03	0.02	0.25	0.24	0.24	0.49
SD	0.02	0.02	0.02	0.05	0.09	0.05	0.04	0.05	0.05	0.08	0.14	0.19	0.27	0.29	0.38	0.76
MAE	0.02	0.02	0.02	0.03	0.08	0.06	0.05	0.05	0.04	0.07	0.12	0.15	0.25	0.25	0.28	0.55
MSE	0.0	0.0	0.0	0.0	0.01	0.0	0.0	0.0	0.0	0.01	0.02	0.03	0.13	0.14	0.2	0.82

	SFH=Burst; SN=15.0; Av=0.0; Age of the system = 6.8															
	$\Delta \log < Z_\star >_L$				$\Delta \log < Z_\star >_M$				$\Delta M_\star$				ΔA_v			
X^i_{AGN}	0.2	0.4	0.6	0.8	0.2	0.4	0.6	0.8	0.2	0.4	0.6	0.8	0.2	0.4	0.6	0.8
Mean	-0.01	-0.04	-0.04	0.01	-0.13	-0.16	-0.18	-0.16	-0.17	-0.18	-0.2	-0.36	-0.0	-0.0	0.0	-0.0
SD	0.1	0.16	0.2	0.21	0.11	0.19	0.26	0.25	0.13	0.17	0.24	0.44	0.0	0.0	0.0	0.0
MAE	0.07	0.12	0.16	0.16	0.14	0.19	0.25	0.24	0.17	0.19	0.25	0.41	0.0	0.0	0.0	0.0
MSE	0.01	0.03	0.04	0.04	0.03	0.06	0.1	0.09	0.04	0.06	0.1	0.32	0.0	0.0	0.0	0.0

TABLE A.4

	SFH=Burst; SN=15.0; Av=0.0; Age of the system = 7.2															
	ΔX_{AGN}				$\Delta < \alpha_v >_L$				$\Delta < \log(t_\star) >_L$				$\Delta < \log(t_\star) >_M$			
X^i_{AGN}	0.2	0.4	0.6	0.8	0.2	0.4	0.6	0.8	0.2	0.4	0.6	0.8	0.2	0.4	0.6	0.8
Mean	-0.01	0.02	0.02	0.02	-0.04	0.02	0.01	0.01	-0.06	-0.12	-0.17	-0.35	1.76	1.22	0.81	0.46
SD	0.03	0.03	0.05	0.03	0.09	0.07	0.07	0.04	0.04	0.07	0.11	0.24	0.85	1.11	1.14	1.19
MAE	0.02	0.03	0.04	0.03	0.08	0.05	0.05	0.04	0.07	0.12	0.17	0.35	1.78	1.28	0.93	0.84
MSE	0.0	0.0	0.0	0.0	0.01	0.0	0.01	0.0	0.01	0.02	0.04	0.18	3.82	2.71	1.95	1.62

	SFH=Burst; SN=15.0; Av=0.0; Age of the system = 7.2															
	$\Delta \log < Z_\star >_L$				$\Delta \log < Z_\star >_M$				$\Delta M_\star$				ΔA_v			
X^i_{AGN}	0.2	0.4	0.6	0.8	0.2	0.4	0.6	0.8	0.2	0.4	0.6	0.8	0.2	0.4	0.6	0.8
Mean	-0.09	-0.12	-0.13	0.01	-0.01	-0.02	-0.14	-0.12	-0.67	-0.41	-0.22	-0.0	-0.01	-0.0	-0.0	-0.0
SD	0.06	0.07	0.13	0.26	0.19	0.15	0.19	0.29	0.4	0.56	0.58	0.68	0.05	0.01	0.01	0.0
MAE	0.09	0.12	0.15	0.22	0.13	0.11	0.19	0.26	0.69	0.52	0.46	0.52	0.01	0.0	0.0	0.0
MSE	0.01	0.02	0.03	0.07	0.04	0.02	0.05	0.1	0.6	0.48	0.39	0.46	0.0	0.0	0.0	0.0

TABLE A.6

	SFH=Burst; SN=15.0; Av=0.0; Age of the system = 7.6															
	ΔX_{AGN}				$\Delta < \alpha_v >_L$				$\Delta < \log(t_\star) >_L$				$\Delta < \log(t_\star) >_M$			
X^i_{AGN}	0.2	0.4	0.6	0.8	0.2	0.4	0.6	0.8	0.2	0.4	0.6	0.8	0.2	0.4	0.6	0.8
Mean	-0.02	-0.01	0.0	0.0	-0.04	-0.05	-0.01	0.01	-0.08	-0.23	-0.45	-0.61	1.11	1.24	1.05	0.33
SD	0.02	0.05	0.04	0.07	0.1	0.11	0.06	0.08	0.06	0.12	0.21	0.21	0.57	0.68	0.92	1.13
MAE	0.02	0.03	0.03	0.04	0.09	0.07	0.04	0.04	0.09	0.23	0.45	0.61	1.11	1.24	1.16	0.96
MSE	0.0	0.0	0.0	0.0	0.01	0.02	0.0	0.01	0.01	0.07	0.25	0.42	1.56	1.99	1.94	1.38

	SFH=Burst; SN=15.0; Av=0.0; Age of the system = 7.6															
	$\Delta \log < Z_\star >_L$				$\Delta \log < Z_\star >_M$				$\Delta M_\star$				ΔA_v			
X^i_{AGN}	0.2	0.4	0.6	0.8	0.2	0.4	0.6	0.8	0.2	0.4	0.6	0.8	0.2	0.4	0.6	0.8
Mean	-0.14	-0.25	-0.34	-0.43	-0.13	-0.14	-0.08	-0.36	-0.38	-0.38	-0.19	0.21	-0.01	-0.0	-0.0	-0.0
SD	0.07	0.1	0.13	0.2	0.17	0.26	0.29	0.24	0.25	0.36	0.5	0.73	0.02	0.01	0.03	0.01
MAE	0.14	0.25	0.34	0.44	0.18	0.25	0.26	0.39	0.38	0.42	0.44	0.67	0.01	0.0	0.0	0.0
MSE	0.02	0.07	0.13	0.23	0.05	0.09	0.09	0.19	0.2	0.27	0.28	0.57	0.0	0.0	0.0	0.0

TABLE A.8

	SFH=Burst; SN=15.0; Av=0.0; Age of the system = 8.0															
	ΔX_{AGN}				$\Delta < \alpha_v >_L$				$\Delta < \log(t_\star) >_L$				$\Delta < \log(t_\star) >_M$			
X^i_{AGN}	0.2	0.4	0.6	0.8	0.2	0.4	0.6	0.8	0.2	0.4	0.6	0.8	0.2	0.4	0.6	0.8
Mean	-0.02	-0.02	-0.01	-0.01	-0.14	-0.07	-0.02	0.02	-0.09	-0.21	-0.39	-0.66	0.32	0.29	0.27	0.36
SD	0.02	0.04	0.05	0.06	0.12	0.08	0.08	0.06	0.05	0.11	0.16	0.27	0.35	0.46	0.49	0.78
MAE	0.02	0.02	0.03	0.03	0.15	0.07	0.05	0.04	0.09	0.21	0.39	0.66	0.32	0.31	0.32	0.67
MSE	0.0	0.0	0.0	0.0	0.03	0.01	0.01	0.0	0.01	0.05	0.18	0.51	0.23	0.3	0.31	0.75

	SFH=Burst; SN=15.0; Av=0.0; Age of the system = 8.0															
	$\Delta \log < Z_\star >_L$				$\Delta \log < Z_\star >_M$				$\Delta M_\star$				ΔA_v			
X^i_{AGN}	0.2	0.4	0.6	0.8	0.2	0.4	0.6	0.8	0.2	0.4	0.6	0.8	0.2	0.4	0.6	0.8
Mean	-0.19	-0.4	-0.61	-0.65	-0.14	-0.28	-0.47	-0.5	-0.08	-0.02	0.06	0.11	-0.0	-0.0	-0.01	-0.01
SD	0.1	0.17	0.14	0.12	0.11	0.22	0.29	0.27	0.14	0.21	0.28	0.52	0.0	0.0	0.02	0.03
MAE	0.19	0.4	0.61	0.65	0.15	0.3	0.5	0.52	0.11	0.14	0.21	0.43	0.0	0.0	0.01	0.01
MSE	0.05	0.18	0.39	0.43	0.03	0.13	0.3	0.32	0.02	0.05	0.08	0.28	0.0	0.0	0.0	0.0

TABLE A.10

	SFH=Burst; SN=15.0; Av=0.0; Age of the system = 8.4															
	ΔX_{AGN}				$\Delta < \alpha_\nu >_L$				$\Delta < \log(t_\star) >_L$				$\Delta < \log(t_\star) >_M$			
X^i_{AGN}	0.2	0.4	0.6	0.8	0.2	0.4	0.6	0.8	0.2	0.4	0.6	0.8	0.2	0.4	0.6	0.8
Mean	-0.05	-0.04	-0.02	-0.02	-0.19	-0.03	0.02	0.03	-0.13	-0.2	-0.29	-0.56	0.17	0.15	0.17	0.2
SD	0.02	0.03	0.03	0.07	0.12	0.07	0.06	0.08	0.05	0.11	0.17	0.37	0.22	0.17	0.23	0.41
MAE	0.05	0.04	0.03	0.04	0.19	0.06	0.05	0.06	0.13	0.2	0.29	0.56	0.18	0.16	0.21	0.36
MSE	0.0	0.0	0.0	0.01	0.05	0.01	0.0	0.01	0.02	0.05	0.11	0.45	0.08	0.05	0.08	0.21

	SFH=Burst; SN=15.0; Av=0.0; Age of the system = 8.4															
	$\Delta \log < Z_\star >_L$				$\Delta \log < Z_\star >_M$				$\Delta M_\star$				ΔA_v			
X^i_{AGN}	0.2	0.4	0.6	0.8	0.2	0.4	0.6	0.8	0.2	0.4	0.6	0.8	0.2	0.4	0.6	0.8
Mean	-0.19	-0.34	-0.54	-0.59	-0.13	-0.21	-0.43	-0.43	-0.07	-0.04	-0.01	0.04	-0.02	-0.03	-0.03	-0.03
SD	0.07	0.15	0.17	0.15	0.07	0.15	0.22	0.3	0.09	0.08	0.14	0.31	0.03	0.04	0.04	0.05
MAE	0.19	0.34	0.54	0.59	0.13	0.21	0.44	0.46	0.07	0.07	0.1	0.24	0.02	0.03	0.03	0.03
MSE	0.04	0.14	0.33	0.37	0.02	0.07	0.24	0.27	0.01	0.01	0.02	0.1	0.0	0.0	0.0	0.0

TABLE A.12

	SFH=Burst; SN=15.0; Av=0.0; Age of the system = 8.8															
	ΔX_{AGN}				$\Delta < \alpha_v >_L$				$\Delta < \log(t_\star) >_L$				$\Delta < \log(t_\star) >_M$			
X^i_{AGN}	0.2	0.4	0.6	0.8	0.2	0.4	0.6	0.8	0.2	0.4	0.6	0.8	0.2	0.4	0.6	0.8
Mean	-0.05	-0.03	-0.04	-0.0	-0.13	-0.0	0.02	0.05	-0.13	-0.18	-0.3	-0.34	0.07	0.09	0.14	0.17
SD	0.03	0.05	0.06	0.03	0.17	0.11	0.07	0.05	0.07	0.13	0.21	0.24	0.04	0.06	0.13	0.15
MAE	0.05	0.04	0.04	0.03	0.16	0.07	0.06	0.05	0.13	0.18	0.3	0.36	0.07	0.09	0.15	0.18
MSE	0.0	0.0	0.01	0.0	0.05	0.01	0.01	0.0	0.02	0.05	0.14	0.18	0.01	0.01	0.04	0.05

	SFH=Burst; SN=15.0; Av=0.0; Age of the system = 8.8															
	$\Delta \log < Z_\star >_L$				$\Delta \log < Z_\star >_M$				$\Delta M_\star$				ΔA_v			
X^i_{AGN}	0.2	0.4	0.6	0.8	0.2	0.4	0.6	0.8	0.2	0.4	0.6	0.8	0.2	0.4	0.6	0.8
Mean	-0.11	-0.14	-0.2	-0.26	-0.05	-0.06	-0.1	-0.18	-0.05	-0.05	-0.08	-0.04	-0.0	-0.01	-0.01	-0.01
SD	0.1	0.14	0.17	0.23	0.08	0.13	0.16	0.25	0.03	0.05	0.1	0.11	0.01	0.02	0.04	0.02
MAE	0.12	0.17	0.23	0.3	0.08	0.12	0.15	0.24	0.05	0.05	0.08	0.08	0.0	0.01	0.01	0.01
MSE	0.02	0.04	0.07	0.12	0.01	0.02	0.04	0.09	0.0	0.0	0.02	0.01	0.0	0.0	0.0	0.0

TABLE A.14

	SFH=Burst; SN=15.0; Av=0.0; Age of the system = 9.2															
	ΔX_{AGN}				$\Delta < \alpha_{\nu} >_{L}$				$\Delta < \log(t_{\star}) >_{L}$				$\Delta < \log(t_{\star}) >_{M}$			
X^{i}_{AGN}	0.2	0.4	0.6	0.8	0.2	0.4	0.6	0.8	0.2	0.4	0.6	0.8	0.2	0.4	0.6	0.8
Mean	0.03	0.06	0.05	0.03	0.02	0.08	0.07	0.05	-0.06	-0.06	-0.03	-0.02	0.06	0.07	0.12	0.21
SD	0.04	0.04	0.05	0.04	0.12	0.08	0.07	0.06	0.08	0.11	0.18	0.3	0.09	0.11	0.16	0.23
MAE	0.04	0.06	0.06	0.04	0.09	0.09	0.08	0.06	0.07	0.09	0.13	0.21	0.09	0.1	0.17	0.25
MSE	0.0	0.0	0.0	0.0	0.02	0.01	0.01	0.01	0.01	0.02	0.03	0.09	0.01	0.02	0.04	0.09

	SFH=Burst; SN=15.0; Av=0.0; Age of the system = 9.2															
	$\Delta \log < Z_{\star} >_{L}$				$\Delta \log < Z_{\star} >_{M}$				$\Delta M_{\star}$				ΔA_{v}			
X^{i}_{AGN}	0.2	0.4	0.6	0.8	0.2	0.4	0.6	0.8	0.2	0.4	0.6	0.8	0.2	0.4	0.6	0.8
Mean	0.11	0.17	0.13	-0.04	0.07	0.12	0.06	-0.07	-0.02	-0.01	-0.04	-0.06	-0.0	-0.01	-0.01	-0.01
SD	0.1	0.12	0.18	0.3	0.1	0.13	0.21	0.31	0.06	0.08	0.11	0.16	0.01	0.02	0.02	0.02
MAE	0.13	0.18	0.18	0.25	0.11	0.14	0.18	0.28	0.05	0.06	0.1	0.14	0.0	0.01	0.01	0.01
MSE	0.02	0.04	0.05	0.09	0.02	0.03	0.05	0.1	0.0	0.01	0.01	0.03	0.0	0.0	0.0	0.0

TABLE A.16

	SFH=Burst; SN=15.0; Av=0.0; Age of the system = 9.6															
	ΔX_{AGN}				$\Delta < \alpha_v >_L$				$\Delta < \log(t_\star) >_L$				$\Delta < \log(t_\star) >_M$			
X^i_{AGN}	0.2	0.4	0.6	0.8	0.2	0.4	0.6	0.8	0.2	0.4	0.6	0.8	0.2	0.4	0.6	0.8
Mean	0.02	0.03	0.03	0.02	0.03	0.08	0.07	0.05	0.01	0.06	0.07	0.13	0.08	0.14	0.2	0.3
SD	0.02	0.02	0.02	0.04	0.16	0.08	0.06	0.07	0.06	0.08	0.14	0.28	0.05	0.07	0.09	0.13
MAE	0.02	0.03	0.03	0.03	0.12	0.09	0.07	0.07	0.04	0.08	0.12	0.24	0.08	0.14	0.2	0.31
MSE	0.0	0.0	0.0	0.0	0.03	0.01	0.01	0.01	0.0	0.01	0.02	0.1	0.01	0.02	0.05	0.11

	SFH=Burst; SN=15.0; Av=0.0; Age of the system = 9.6															
	$\Delta \log < Z_\star >_L$				$\Delta \log < Z_\star >_M$				$\Delta M_\star$				ΔA_v			
X^i_{AGN}	0.2	0.4	0.6	0.8	0.2	0.4	0.6	0.8	0.2	0.4	0.6	0.8	0.2	0.4	0.6	0.8
Mean	0.02	0.01	0.03	-0.06	-0.02	-0.03	-0.04	-0.12	-0.04	-0.08	-0.11	-0.16	-0.01	-0.01	-0.01	-0.02
SD	0.06	0.07	0.1	0.16	0.04	0.05	0.06	0.13	0.03	0.04	0.06	0.11	0.02	0.02	0.02	0.03
MAE	0.05	0.06	0.08	0.14	0.04	0.04	0.06	0.14	0.04	0.08	0.11	0.17	0.01	0.01	0.01	0.02
MSE	0.0	0.01	0.01	0.03	0.0	0.0	0.01	0.03	0.0	0.01	0.02	0.04	0.0	0.0	0.0	0.0

TABLE A.18

	SFH=Burst; SN=15.0; Av=0.0; Age of the system = 10.0															
	ΔX_{AGN}				$\Delta < \alpha_v >_L$				$\Delta < \log(t_\star) >_L$				$\Delta < \log(t_\star) >_M$			
X^i_{AGN}	0.2	0.4	0.6	0.8	0.2	0.4	0.6	0.8	0.2	0.4	0.6	0.8	0.2	0.4	0.6	0.8
Mean	0.01	0.02	0.02	0.0	0.06	0.08	0.08	0.04	0.0	0.02	0.04	-0.03	0.03	0.04	0.07	0.09
SD	0.01	0.01	0.01	0.05	0.14	0.08	0.06	0.08	0.04	0.04	0.06	0.33	0.04	0.04	0.05	0.06
MAE	0.01	0.02	0.02	0.02	0.12	0.09	0.09	0.07	0.03	0.04	0.06	0.18	0.03	0.05	0.07	0.1
MSE	0.0	0.0	0.0	0.0	0.02	0.01	0.01	0.01	0.0	0.0	0.0	0.11	0.0	0.0	0.01	0.01

	SFH=Burst; SN=15.0; Av=0.0; Age of the system = 10.0															
	$\Delta \log < Z_\star >_L$				$\Delta \log < Z_\star >_M$				$\Delta M_\star$				ΔA_v			
X^i_{AGN}	0.2	0.4	0.6	0.8	0.2	0.4	0.6	0.8	0.2	0.4	0.6	0.8	0.2	0.4	0.6	0.8
Mean	-0.02	-0.03	-0.04	-0.06	-0.03	-0.03	-0.04	-0.07	-0.02	-0.03	-0.06	-0.06	-0.01	-0.02	-0.03	-0.03
SD	0.03	0.03	0.04	0.08	0.01	0.02	0.03	0.1	0.03	0.03	0.04	0.07	0.02	0.02	0.03	0.03
MAE	0.03	0.04	0.05	0.07	0.03	0.03	0.04	0.07	0.03	0.04	0.06	0.08	0.01	0.02	0.03	0.03
MSE	0.0	0.0	0.0	0.01	0.0	0.0	0.0	0.01	0.0	0.0	0.0	0.01	0.0	0.0	0.0	0.0

TABLE A.20

A.1.2 Tables: Constant SFH, Av=0.0, SN = 15, base: BaseA

	SFH=Constant; SN=15.0; Av=0.0; Age of the system = 6.4															
	ΔX_{AGN}				$\Delta < \alpha_v >_L$				$\Delta < \log(t_\star) >_L$				$\Delta < \log(t_\star) >_M$			
X^i_{AGN}	0.2	0.4	0.6	0.8	0.2	0.4	0.6	0.8	0.2	0.4	0.6	0.8	0.2	0.4	0.6	0.8
Mean	-0.0	-0.01	-0.02	-0.02	0.0	-0.01	0.0	0.02	-0.01	-0.0	0.02	0.01	1.48	1.11	1.91	1.23
SD	0.01	0.01	0.02	0.02	0.06	0.04	0.03	0.04	0.09	0.09	0.08	0.11	1.37	1.39	1.59	1.51
MAE	0.01	0.02	0.03	0.03	0.04	0.03	0.02	0.03	0.07	0.07	0.06	0.08	1.52	1.13	1.92	1.28
MSE	0.0	0.0	0.0	0.0	0.0	0.0	0.0	0.0	0.01	0.01	0.01	0.01	4.05	3.15	6.15	3.79

	SFH=Constant; SN=15.0; Av=0.0; Age of the system = 6.4															
	$\Delta \log < Z_\star >_L$				$\Delta \log < Z_\star >_M$				$\Delta M_\star$				ΔA_v			
X^i_{AGN}	0.2	0.4	0.6	0.8	0.2	0.4	0.6	0.8	0.2	0.4	0.6	0.8	0.2	0.4	0.6	0.8
Mean	0.09	0.1	0.1	0.16	-0.03	-0.02	-0.02	-0.05	-0.44	-0.38	-0.74	-0.51	-0.0	-0.0	-0.0	-0.01
SD	0.07	0.05	0.08	0.08	0.14	0.18	0.23	0.24	0.45	0.53	0.69	0.68	0.0	0.0	0.0	0.03
MAE	0.1	0.1	0.11	0.16	0.09	0.11	0.15	0.17	0.46	0.38	0.75	0.53	0.0	0.0	0.0	0.01
MSE	0.01	0.01	0.02	0.03	0.02	0.03	0.05	0.06	0.4	0.42	1.03	0.73	0.0	0.0	0.0	0.0

TABLE A.22

	SFH=Constant; SN=15.0; Av=0.0; Age of the system = 6.8															
	ΔX_{AGN}				$\Delta < \alpha_v >_L$				$\Delta < \log(t_\star) >_L$				$\Delta < \log(t_\star) >_M$			
X^i_{AGN}	0.2	0.4	0.6	0.8	0.2	0.4	0.6	0.8	0.2	0.4	0.6	0.8	0.2	0.4	0.6	0.8
Mean	-0.0	0.01	0.01	0.01	0.04	0.05	0.05	0.05	0.04	0.05	0.0	-0.04	0.65	0.7	0.5	0.46
SD	0.02	0.03	0.02	0.03	0.09	0.05	0.05	0.04	0.06	0.1	0.1	0.17	0.65	0.76	0.73	0.8
MAE	0.02	0.02	0.02	0.03	0.08	0.06	0.05	0.06	0.06	0.09	0.08	0.14	0.65	0.71	0.52	0.55
MSE	0.0	0.0	0.0	0.0	0.01	0.01	0.0	0.0	0.01	0.01	0.01	0.03	0.84	1.07	0.78	0.85

	SFH=Constant; SN=15.0; Av=0.0; Age of the system = 6.8															
	$\Delta \log < Z_\star >_L$				$\Delta \log < Z_\star >_M$				$\Delta M_\star$				ΔA_v			
X^i_{AGN}	0.2	0.4	0.6	0.8	0.2	0.4	0.6	0.8	0.2	0.4	0.6	0.8	0.2	0.4	0.6	0.8
Mean	-0.0	0.05	0.08	0.14	-0.13	-0.11	-0.08	0.02	-0.25	-0.31	-0.22	-0.2	-0.0	-0.0	-0.0	-0.01
SD	0.13	0.16	0.16	0.21	0.14	0.19	0.18	0.25	0.23	0.32	0.29	0.38	0.0	0.0	0.0	0.03
MAE	0.1	0.14	0.15	0.22	0.16	0.18	0.16	0.21	0.26	0.32	0.25	0.29	0.0	0.0	0.0	0.01
MSE	0.02	0.03	0.03	0.06	0.04	0.05	0.04	0.06	0.12	0.2	0.13	0.19	0.0	0.0	0.0	0.0

TABLE A.24

	SFH=Constant; SN=15.0; Av=0.0; Age of the system = 7.2															
	ΔX_{AGN}				$\Delta < \alpha_v >_L$				$\Delta < \log(t_\star) >_L$				$\Delta < \log(t_\star) >_M$			
X^i_{AGN}	0.2	0.4	0.6	0.8	0.2	0.4	0.6	0.8	0.2	0.4	0.6	0.8	0.2	0.4	0.6	0.8
Mean	0.0	0.01	0.01	0.01	-0.04	-0.01	0.02	0.04	-0.01	-0.01	-0.04	-0.1	0.56	0.54	0.58	0.53
SD	0.02	0.03	0.03	0.02	0.13	0.09	0.06	0.04	0.06	0.09	0.1	0.18	0.92	0.83	1.05	1.02
MAE	0.02	0.02	0.02	0.02	0.1	0.07	0.05	0.05	0.05	0.08	0.09	0.16	0.62	0.61	0.67	0.72
MSE	0.0	0.0	0.0	0.0	0.02	0.01	0.0	0.0	0.0	0.01	0.01	0.04	1.16	0.99	1.44	1.32

	SFH=Constant; SN=15.0; Av=0.0; Age of the system = 7.2															
	$\Delta \log < Z_\star >_L$				$\Delta \log < Z_\star >_M$				$\Delta M_\star$				ΔA_v			
X^i_{AGN}	0.2	0.4	0.6	0.8	0.2	0.4	0.6	0.8	0.2	0.4	0.6	0.8	0.2	0.4	0.6	0.8
Mean	-0.09	-0.06	0.0	0.1	-0.11	-0.11	-0.12	-0.1	-0.17	-0.17	-0.22	-0.19	-0.0	-0.0	-0.0	-0.0
SD	0.14	0.16	0.18	0.21	0.18	0.18	0.21	0.25	0.38	0.38	0.53	0.53	0.0	0.0	0.0	0.0
MAE	0.14	0.14	0.14	0.19	0.17	0.17	0.2	0.21	0.24	0.27	0.36	0.37	0.0	0.0	0.0	0.0
MSE	0.03	0.03	0.03	0.05	0.04	0.04	0.06	0.07	0.17	0.17	0.33	0.32	0.0	0.0	0.0	0.0

TABLE A.26

	SFH=Constant; SN=15.0; Av=0.0; Age of the system = 7.6															
	ΔX_{AGN}				$\Delta < \alpha_{\nu} >_{L}$				$\Delta < \log(t_{\star}) >_{L}$				$\Delta < \log(t_{\star}) >_{M}$			
X^{i}_{AGN}	0.2	0.4	0.6	0.8	0.2	0.4	0.6	0.8	0.2	0.4	0.6	0.8	0.2	0.4	0.6	0.8
Mean	0.02	0.02	0.01	0.01	0.09	0.04	0.04	0.04	-0.13	-0.15	-0.14	-0.24	0.22	0.18	0.33	0.24
SD	0.03	0.03	0.03	0.04	0.12	0.09	0.07	0.05	0.06	0.07	0.1	0.23	0.83	0.77	0.95	0.99
MAE	0.03	0.03	0.03	0.03	0.12	0.08	0.06	0.05	0.14	0.15	0.16	0.27	0.54	0.55	0.66	0.75
MSE	0.0	0.0	0.0	0.0	0.02	0.01	0.01	0.0	0.02	0.03	0.03	0.11	0.73	0.62	1.02	1.05

	SFH=Constant; SN=15.0; Av=0.0; Age of the system = 7.6															
	$\Delta \log < Z_{\star} >_{L}$				$\Delta \log < Z_{\star} >_{M}$				$\Delta M_{\star}$				ΔA_{v}			
X^{i}_{AGN}	0.2	0.4	0.6	0.8	0.2	0.4	0.6	0.8	0.2	0.4	0.6	0.8	0.2	0.4	0.6	0.8
Mean	-0.09	-0.1	-0.05	0.09	-0.05	-0.12	-0.14	-0.05	0.09	0.09	-0.0	0.05	-0.0	-0.0	-0.0	-0.0
SD	0.11	0.17	0.14	0.22	0.14	0.16	0.19	0.26	0.33	0.32	0.46	0.57	0.0	0.0	0.0	0.02
MAE	0.11	0.16	0.11	0.21	0.11	0.16	0.17	0.21	0.27	0.27	0.34	0.44	0.0	0.0	0.0	0.0
MSE	0.02	0.04	0.02	0.06	0.02	0.04	0.06	0.07	0.12	0.11	0.21	0.33	0.0	0.0	0.0	0.0

TABLE A.28

	SFH=Constant; SN=15.0; Av=0.0; Age of the system = 8.0															
	ΔX_{AGN}				$\Delta < \alpha_v >_L$				$\Delta < \log(t_\star) >_L$				$\Delta < \log(t_\star) >_M$			
X^i_{AGN}	0.2	0.4	0.6	0.8	0.2	0.4	0.6	0.8	0.2	0.4	0.6	0.8	0.2	0.4	0.6	0.8
Mean	-0.01	0.01	0.01	0.01	-0.04	0.0	0.02	0.03	-0.24	-0.3	-0.3	-0.31	0.58	0.13	0.08	0.07
SD	0.02	0.03	0.04	0.03	0.13	0.08	0.07	0.04	0.06	0.08	0.12	0.2	0.9	0.78	0.96	1.05
MAE	0.02	0.03	0.04	0.03	0.11	0.07	0.06	0.04	0.24	0.3	0.3	0.32	0.82	0.64	0.76	0.86
MSE	0.0	0.0	0.0	0.0	0.02	0.01	0.01	0.0	0.06	0.1	0.11	0.14	1.16	0.63	0.93	1.1

	SFH=Constant; SN=15.0; Av=0.0; Age of the system = 8.0															
	$\Delta \log < Z_\star >_L$				$\Delta \log < Z_\star >_M$				$\Delta M_\star$				ΔA_v			
X^i_{AGN}	0.2	0.4	0.6	0.8	0.2	0.4	0.6	0.8	0.2	0.4	0.6	0.8	0.2	0.4	0.6	0.8
Mean	-0.19	-0.22	-0.23	-0.18	-0.11	-0.13	-0.2	-0.25	-0.02	0.22	0.22	0.22	-0.0	-0.0	-0.0	-0.0
SD	0.08	0.1	0.21	0.27	0.19	0.19	0.23	0.28	0.39	0.31	0.47	0.58	0.0	0.0	0.0	0.01
MAE	0.19	0.22	0.23	0.25	0.21	0.2	0.24	0.29	0.31	0.34	0.45	0.53	0.0	0.0	0.0	0.0
MSE	0.04	0.06	0.09	0.11	0.05	0.05	0.09	0.14	0.15	0.14	0.27	0.39	0.0	0.0	0.0	0.0

TABLE A.30

	SFH=Constant; SN=15.0; Av=0.0; Age of the system = 8.4															
	ΔX_{AGN}				$\Delta < \alpha_{\nu} >_{L}$				$\Delta < \log(t_{\star}) >_{L}$				$\Delta < \log(t_{\star}) >_{M}$			
X^{i}_{AGN}	0.2	0.4	0.6	0.8	0.2	0.4	0.6	0.8	0.2	0.4	0.6	0.8	0.2	0.4	0.6	0.8
Mean	-0.0	0.0	0.01	0.01	-0.07	-0.02	0.02	0.03	-0.22	-0.35	-0.5	-0.51	0.37	0.28	-0.06	-0.2
SD	0.02	0.03	0.03	0.03	0.11	0.07	0.04	0.04	0.06	0.13	0.13	0.19	0.58	0.72	0.87	0.92
MAE	0.02	0.02	0.03	0.03	0.09	0.06	0.04	0.04	0.22	0.35	0.5	0.52	0.5	0.58	0.7	0.82
MSE	0.0	0.0	0.0	0.0	0.02	0.01	0.0	0.0	0.05	0.14	0.27	0.3	0.48	0.59	0.76	0.89

	SFH=Constant; SN=15.0; Av=0.0; Age of the system = 8.4															
	$\Delta \log < Z_{\star} >_{L}$				$\Delta \log < Z_{\star} >_{M}$				$\Delta M_{\star}$				ΔA_{v}			
X^{i}_{AGN}	0.2	0.4	0.6	0.8	0.2	0.4	0.6	0.8	0.2	0.4	0.6	0.8	0.2	0.4	0.6	0.8
Mean	-0.22	-0.3	-0.39	-0.46	-0.13	-0.13	-0.27	-0.37	-0.0	0.11	0.36	0.43	-0.0	-0.0	-0.0	-0.0
SD	0.08	0.12	0.16	0.22	0.16	0.26	0.24	0.29	0.24	0.32	0.45	0.53	0.0	0.01	0.02	0.02
MAE	0.22	0.3	0.39	0.46	0.18	0.24	0.3	0.41	0.19	0.29	0.51	0.63	0.0	0.0	0.0	0.0
MSE	0.06	0.1	0.18	0.26	0.04	0.08	0.13	0.22	0.06	0.11	0.34	0.47	0.0	0.0	0.0	0.0

TABLE A.32

	SFH=Constant; SN=15.0; Av=0.0; Age of the system = 8.8															
	ΔX_{AGN}				$\Delta < \alpha_{\nu} >_L$				$\Delta < \log(t_{\star}) >_L$				$\Delta < \log(t_{\star}) >_M$			
X^i_{AGN}	0.2	0.4	0.6	0.8	0.2	0.4	0.6	0.8	0.2	0.4	0.6	0.8	0.2	0.4	0.6	0.8
Mean	0.02	0.02	0.03	0.02	0.02	-0.0	0.03	0.04	-0.19	-0.29	-0.46	-0.68	0.41	0.55	0.38	0.1
SD	0.03	0.03	0.03	0.04	0.09	0.06	0.04	0.04	0.07	0.13	0.21	0.2	0.44	0.49	0.63	0.97
MAE	0.03	0.03	0.04	0.04	0.08	0.05	0.04	0.05	0.19	0.29	0.46	0.68	0.49	0.62	0.59	0.84
MSE	0.0	0.0	0.0	0.0	0.01	0.0	0.0	0.0	0.04	0.1	0.25	0.5	0.36	0.54	0.53	0.95

	SFH=Constant; SN=15.0; Av=0.0; Age of the system = 8.8															
	$\Delta \log < Z_{\star} >_L$				$\Delta \log < Z_{\star} >_M$				$\Delta M_{\star}$				ΔA_v			
X^i_{AGN}	0.2	0.4	0.6	0.8	0.2	0.4	0.6	0.8	0.2	0.4	0.6	0.8	0.2	0.4	0.6	0.8
Mean	-0.24	-0.35	-0.51	-0.61	-0.12	-0.13	-0.24	-0.47	-0.04	-0.06	0.12	0.36	-0.0	-0.0	-0.0	-0.0
SD	0.08	0.15	0.19	0.15	0.14	0.24	0.32	0.3	0.2	0.23	0.34	0.61	0.0	0.0	0.01	0.01
MAE	0.24	0.35	0.51	0.61	0.15	0.23	0.35	0.51	0.17	0.19	0.3	0.6	0.0	0.0	0.0	0.0
MSE	0.06	0.15	0.3	0.4	0.03	0.08	0.16	0.31	0.04	0.05	0.13	0.51	0.0	0.0	0.0	0.0

TABLE A.34

	SFH=Constant; SN=15.0; Av=0.0; Age of the system = 9.2															
	ΔX_{AGN}				$\Delta < \alpha_v >_L$				$\Delta < \log(t_\star) >_L$				$\Delta < \log(t_\star) >_M$			
X^i_{AGN}	0.2	0.4	0.6	0.8	0.2	0.4	0.6	0.8	0.2	0.4	0.6	0.8	0.2	0.4	0.6	0.8
Mean	0.02	0.03	0.03	0.03	-0.02	0.0	0.03	0.05	-0.21	-0.3	-0.43	-0.5	0.39	0.38	0.38	0.22
SD	0.04	0.05	0.05	0.04	0.14	0.08	0.05	0.04	0.08	0.16	0.18	0.28	0.28	0.29	0.4	0.69
MAE	0.03	0.04	0.05	0.04	0.11	0.06	0.05	0.05	0.21	0.3	0.43	0.5	0.39	0.39	0.42	0.56
MSE	0.0	0.0	0.0	0.0	0.02	0.01	0.0	0.0	0.05	0.12	0.22	0.33	0.23	0.23	0.3	0.52

	SFH=Constant; SN=15.0; Av=0.0; Age of the system = 9.2															
	$\Delta \log < Z_\star >_L$				$\Delta \log < Z_\star >_M$				$\Delta M_\star$				ΔA_v			
X^i_{AGN}	0.2	0.4	0.6	0.8	0.2	0.4	0.6	0.8	0.2	0.4	0.6	0.8	0.2	0.4	0.6	0.8
Mean	-0.25	-0.34	-0.5	-0.53	-0.07	-0.13	-0.27	-0.36	-0.08	-0.02	0.01	0.19	-0.0	-0.01	-0.01	-0.01
SD	0.1	0.14	0.17	0.21	0.13	0.23	0.3	0.32	0.16	0.17	0.28	0.52	0.01	0.05	0.04	0.02
MAE	0.25	0.34	0.5	0.53	0.12	0.22	0.34	0.41	0.14	0.14	0.22	0.42	0.0	0.01	0.01	0.01
MSE	0.07	0.13	0.28	0.32	0.02	0.07	0.16	0.23	0.03	0.03	0.08	0.31	0.0	0.0	0.0	0.0

TABLE A.36

	SFH=Constant; SN=15.0; Av=0.0; Age of the system = 9.6															
	ΔX_{AGN}				$\Delta < \alpha_v >_L$				$\Delta < \log(t_\star) >_L$				$\Delta < \log(t_\star) >_M$			
X^i_{AGN}	0.2	0.4	0.6	0.8	0.2	0.4	0.6	0.8	0.2	0.4	0.6	0.8	0.2	0.4	0.6	0.8
Mean	0.03	0.03	0.03	0.02	0.02	0.0	0.02	0.03	-0.16	-0.27	-0.33	-0.39	0.38	0.42	0.28	0.14
SD	0.04	0.04	0.07	0.08	0.12	0.08	0.08	0.06	0.09	0.15	0.18	0.28	0.18	0.26	0.32	0.39
MAE	0.04	0.04	0.06	0.05	0.1	0.06	0.06	0.05	0.16	0.27	0.34	0.41	0.39	0.44	0.36	0.33
MSE	0.0	0.0	0.01	0.01	0.01	0.01	0.01	0.0	0.03	0.1	0.14	0.23	0.18	0.24	0.18	0.17

	SFH=Constant; SN=15.0; Av=0.0; Age of the system = 9.6															
	$\Delta \log < Z_\star >_L$				$\Delta \log < Z_\star >_M$				$\Delta M_\star$				ΔA_v			
X^i_{AGN}	0.2	0.4	0.6	0.8	0.2	0.4	0.6	0.8	0.2	0.4	0.6	0.8	0.2	0.4	0.6	0.8
Mean	-0.2	-0.31	-0.35	-0.44	0.0	-0.09	-0.12	-0.29	-0.12	-0.11	0.01	0.15	-0.0	-0.0	-0.01	-0.0
SD	0.1	0.14	0.21	0.22	0.14	0.2	0.28	0.33	0.12	0.19	0.24	0.36	0.0	0.0	0.02	0.01
MAE	0.2	0.31	0.36	0.44	0.11	0.17	0.24	0.38	0.14	0.19	0.21	0.32	0.0	0.0	0.01	0.0
MSE	0.05	0.12	0.17	0.24	0.02	0.05	0.09	0.19	0.03	0.05	0.06	0.16	0.0	0.0	0.0	0.0

TABLE A.38

	SFH=Constant; SN=15.0; Av=0.0; Age of the system = 10.0															
	ΔX_{AGN}				$\Delta < \alpha_{\nu} >_{L}$				$\Delta < \log(t_{\star}) >_{L}$				$\Delta < \log(t_{\star}) >_{M}$			
X^{i}_{AGN}	0.2	0.4	0.6	0.8	0.2	0.4	0.6	0.8	0.2	0.4	0.6	0.8	0.2	0.4	0.6	0.8
Mean	0.03	0.03	0.04	0.04	0.01	0.02	0.03	0.05	-0.16	-0.25	-0.32	-0.3	0.19	0.21	0.13	-0.03
SD	0.04	0.05	0.04	0.07	0.16	0.08	0.05	0.07	0.11	0.14	0.2	0.35	0.13	0.14	0.23	0.36
MAE	0.04	0.05	0.05	0.06	0.13	0.06	0.05	0.06	0.16	0.26	0.33	0.38	0.21	0.22	0.22	0.31
MSE	0.0	0.0	0.0	0.01	0.02	0.01	0.0	0.01	0.04	0.08	0.14	0.21	0.05	0.06	0.07	0.13

	SFH=Constant; SN=15.0; Av=0.0; Age of the system = 10.0															
	$\Delta \log < Z_{\star} >_{L}$				$\Delta \log < Z_{\star} >_{M}$				$\Delta M_{\star}$				ΔA_{v}			
X^{i}_{AGN}	0.2	0.4	0.6	0.8	0.2	0.4	0.6	0.8	0.2	0.4	0.6	0.8	0.2	0.4	0.6	0.8
Mean	-0.2	-0.26	-0.32	-0.34	-0.02	-0.02	-0.06	-0.15	-0.07	-0.05	0.03	0.21	-0.0	-0.01	-0.0	-0.01
SD	0.1	0.11	0.17	0.24	0.08	0.13	0.22	0.32	0.1	0.11	0.17	0.32	0.01	0.02	0.01	0.02
MAE	0.2	0.26	0.32	0.36	0.06	0.1	0.18	0.29	0.1	0.1	0.14	0.32	0.0	0.01	0.0	0.01
MSE	0.05	0.08	0.13	0.17	0.01	0.02	0.05	0.12	0.02	0.01	0.03	0.15	0.0	0.0	0.0	0.0

TABLE A.40

A.1.3 Tables: Burst SFH, Av=1.0, SN = 15, base: BaseA

	SFH=Burst; SN=15.0; Av=1.0; Age of the system = 6.0															
	ΔX_{AGN}				$\Delta < \alpha_v >_L$				$\Delta < \log(t_\star) >_L$				$\Delta < \log(t_\star) >_M$			
X^i_{AGN}	0.2	0.4	0.6	0.8	0.2	0.4	0.6	0.8	0.2	0.4	0.6	0.8	0.2	0.4	0.6	0.8
Mean	0.09	0.07	0.03	0.0	0.12	-0.08	-0.11	-0.05	0.24	0.2	0.2	0.24	1.94	2.27	2.26	1.64
SD	0.06	0.04	0.04	0.04	0.08	0.07	0.08	0.09	0.13	0.13	0.16	0.16	1.22	1.25	1.66	1.56
MAE	0.09	0.08	0.04	0.03	0.13	0.08	0.12	0.08	0.24	0.2	0.2	0.24	1.94	2.27	2.26	1.64
MSE	0.01	0.01	0.0	0.0	0.02	0.01	0.02	0.01	0.07	0.06	0.07	0.08	5.24	6.73	7.88	5.15

	SFH=Burst; SN=15.0; Av=1.0; Age of the system = 6.0															
	$\Delta \log < Z_\star >_L$				$\Delta \log < Z_\star >_M$				$\Delta M_\star$				ΔA_v			
X^i_{AGN}	0.2	0.4	0.6	0.8	0.2	0.4	0.6	0.8	0.2	0.4	0.6	0.8	0.2	0.4	0.6	0.8
Mean	-0.33	-0.33	-0.31	-0.19	-0.25	-0.18	-0.24	-0.21	-0.52	-0.66	-0.81	-0.61	0.25	0.26	0.2	0.09
SD	0.22	0.23	0.23	0.25	0.19	0.23	0.24	0.26	0.43	0.51	0.7	0.73	0.12	0.12	0.1	0.1
MAE	0.33	0.33	0.31	0.22	0.26	0.23	0.27	0.25	0.53	0.67	0.82	0.61	0.25	0.26	0.2	0.11
MSE	0.16	0.16	0.15	0.1	0.1	0.08	0.12	0.11	0.46	0.7	1.14	0.9	0.08	0.08	0.05	0.02

TABLE A.42

	SFH=Burst; SN=15.0; Av=1.0; Age of the system = 6.4															
	ΔX_{AGN}				$\Delta < \alpha_{\nu} >_{L}$				$\Delta < \log(t_{\star}) >_{L}$				$\Delta < \log(t_{\star}) >_{M}$			
X^{i}_{AGN}	0.2	0.4	0.6	0.8	0.2	0.4	0.6	0.8	0.2	0.4	0.6	0.8	0.2	0.4	0.6	0.8
Mean	0.18	0.13	0.05	0.01	0.18	-0.08	-0.13	-0.06	-0.12	-0.12	-0.1	-0.08	1.83	1.77	2.29	1.36
SD	0.07	0.05	0.04	0.04	0.06	0.07	0.08	0.1	0.13	0.12	0.14	0.15	1.3	1.34	1.46	1.63
MAE	0.18	0.13	0.05	0.03	0.18	0.09	0.13	0.09	0.14	0.14	0.13	0.14	1.88	1.82	2.35	1.44
MSE	0.04	0.02	0.0	0.0	0.04	0.01	0.02	0.01	0.03	0.03	0.03	0.03	5.03	4.92	7.41	4.5

	SFH=Burst; SN=15.0; Av=1.0; Age of the system = 6.4															
	$\Delta \log < Z_{\star} >_{L}$				$\Delta \log < Z_{\star} >_{M}$				$\Delta M_{\star}$				ΔA_{v}			
X^{i}_{AGN}	0.2	0.4	0.6	0.8	0.2	0.4	0.6	0.8	0.2	0.4	0.6	0.8	0.2	0.4	0.6	0.8
Mean	-0.15	-0.1	-0.04	0.03	-0.18	-0.14	-0.16	-0.07	-0.5	-0.5	-0.87	-0.62	0.45	0.38	0.24	0.11
SD	0.27	0.2	0.17	0.24	0.22	0.21	0.2	0.25	0.49	0.54	0.68	0.83	0.14	0.13	0.11	0.11
MAE	0.22	0.16	0.13	0.19	0.21	0.2	0.2	0.2	0.57	0.57	0.9	0.68	0.45	0.38	0.24	0.13
MSE	0.09	0.05	0.03	0.06	0.08	0.07	0.06	0.07	0.49	0.54	1.21	1.08	0.22	0.16	0.07	0.02

TABLE A.44

	SFH=Burst; SN=15.0; Av=1.0; Age of the system = 6.8															
	ΔX_{AGN}				$\Delta < \alpha_v >_L$				$\Delta < \log(t_\star) >_L$				$\Delta < \log(t_\star) >_M$			
X^i_{AGN}	0.2	0.4	0.6	0.8	0.2	0.4	0.6	0.8	0.2	0.4	0.6	0.8	0.2	0.4	0.6	0.8
Mean	0.24	0.2	0.15	0.11	0.06	-0.08	-0.1	-0.08	0.03	-0.04	-0.05	-0.16	1.06	0.42	0.58	0.6
SD	0.06	0.05	0.05	0.05	0.08	0.07	0.06	0.07	0.06	0.05	0.09	0.32	0.99	0.7	0.91	1.25
MAE	0.24	0.2	0.15	0.11	0.08	0.09	0.1	0.09	0.05	0.05	0.09	0.27	1.07	0.52	0.72	0.96
MSE	0.06	0.04	0.03	0.01	0.01	0.01	0.01	0.01	0.0	0.0	0.01	0.13	2.12	0.67	1.15	1.92

	SFH=Burst; SN=15.0; Av=1.0; Age of the system = 6.8															
	$\Delta \log < Z_\star >_L$				$\Delta \log < Z_\star >_M$				$\Delta M_\star$				ΔA_v			
X^i_{AGN}	0.2	0.4	0.6	0.8	0.2	0.4	0.6	0.8	0.2	0.4	0.6	0.8	0.2	0.4	0.6	0.8
Mean	-0.36	-0.31	-0.32	-0.39	-0.24	-0.28	-0.31	-0.37	-0.04	0.18	0.03	0.03	0.53	0.42	0.32	0.24
SD	0.21	0.24	0.26	0.31	0.25	0.24	0.27	0.3	0.44	0.23	0.37	0.76	0.11	0.11	0.08	0.08
MAE	0.36	0.31	0.32	0.42	0.29	0.3	0.32	0.4	0.33	0.26	0.29	0.51	0.53	0.42	0.32	0.24
MSE	0.17	0.16	0.17	0.25	0.12	0.14	0.16	0.23	0.19	0.08	0.14	0.58	0.29	0.19	0.11	0.06

TABLE A.46

	SFH=Burst; SN=15.0; Av=1.0; Age of the system = 7.2															
	ΔX_{AGN}				$\Delta < \alpha_v >_L$				$\Delta < \log(t_\star) >_L$				$\Delta < \log(t_\star) >_M$			
X^i_{AGN}	0.2	0.4	0.6	0.8	0.2	0.4	0.6	0.8	0.2	0.4	0.6	0.8	0.2	0.4	0.6	0.8
Mean	0.03	0.09	0.13	0.11	-0.08	-0.08	-0.13	-0.12	-0.05	-0.13	-0.2	-0.38	1.95	2.12	2.08	1.32
SD	0.05	0.05	0.07	0.05	0.11	0.09	0.11	0.08	0.05	0.08	0.11	0.29	0.66	0.7	0.97	1.34
MAE	0.05	0.09	0.13	0.11	0.1	0.09	0.14	0.12	0.06	0.13	0.2	0.41	1.95	2.13	2.12	1.63
MSE	0.0	0.01	0.02	0.01	0.02	0.01	0.03	0.02	0.01	0.02	0.05	0.23	4.23	4.99	5.26	3.53

	SFH=Burst; SN=15.0; Av=1.0; Age of the system = 7.2															
	$\Delta \log < Z_\star >_L$				$\Delta \log < Z_\star >_M$				$\Delta M_\star$				ΔA_v			
X^i_{AGN}	0.2	0.4	0.6	0.8	0.2	0.4	0.6	0.8	0.2	0.4	0.6	0.8	0.2	0.4	0.6	0.8
Mean	-0.05	-0.05	-0.02	-0.09	0.03	0.1	0.15	0.03	-0.69	-0.7	-0.63	-0.08	0.1	0.19	0.26	0.23
SD	0.06	0.06	0.13	0.27	0.15	0.18	0.23	0.28	0.34	0.42	0.63	0.89	0.11	0.1	0.12	0.08
MAE	0.05	0.06	0.1	0.21	0.11	0.15	0.24	0.22	0.7	0.74	0.81	0.78	0.13	0.19	0.27	0.23
MSE	0.01	0.01	0.02	0.08	0.02	0.04	0.08	0.08	0.6	0.67	0.8	0.79	0.02	0.05	0.08	0.06

TABLE A.48

	SFH=Burst; SN=15.0; Av=1.0; Age of the system = 7.6															
	ΔX_{AGN}				$\Delta < \alpha_v >_L$				$\Delta < \log(t_\star) >_L$				$\Delta < \log(t_\star) >_M$			
X^i_{AGN}	0.2	0.4	0.6	0.8	0.2	0.4	0.6	0.8	0.2	0.4	0.6	0.8	0.2	0.4	0.6	0.8
Mean	0.04	0.1	0.09	0.06	-0.12	-0.16	-0.14	-0.07	0.0	-0.03	-0.25	-0.45	1.52	1.79	1.58	1.27
SD	0.05	0.05	0.04	0.05	0.11	0.11	0.09	0.07	0.09	0.13	0.22	0.29	0.46	0.48	0.73	0.98
MAE	0.05	0.1	0.09	0.07	0.14	0.17	0.14	0.08	0.07	0.1	0.28	0.49	1.52	1.79	1.59	1.45
MSE	0.0	0.01	0.01	0.01	0.03	0.04	0.03	0.01	0.01	0.02	0.11	0.29	2.51	3.44	3.03	2.56

	SFH=Burst; SN=15.0; Av=1.0; Age of the system = 7.6															
	$\Delta \log < Z_\star >_L$				$\Delta \log < Z_\star >_M$				$\Delta M_\star$				ΔA_v			
X^i_{AGN}	0.2	0.4	0.6	0.8	0.2	0.4	0.6	0.8	0.2	0.4	0.6	0.8	0.2	0.4	0.6	0.8
Mean	-0.09	-0.11	-0.38	-0.52	0.01	0.12	0.02	-0.22	-0.5	-0.6	-0.4	-0.15	0.17	0.27	0.22	0.14
SD	0.08	0.16	0.19	0.22	0.2	0.22	0.32	0.35	0.21	0.29	0.49	0.66	0.11	0.12	0.09	0.08
MAE	0.1	0.16	0.39	0.53	0.16	0.21	0.26	0.35	0.5	0.6	0.56	0.57	0.18	0.27	0.22	0.15
MSE	0.01	0.04	0.18	0.31	0.04	0.06	0.11	0.17	0.3	0.44	0.4	0.46	0.04	0.09	0.06	0.03

TABLE A.50

	SFH=Burst; SN=15.0; Av=1.0; Age of the system = 8.0															
	ΔX_{AGN}				$\Delta < \alpha_v >_L$				$\Delta < \log(t_\star) >_L$				$\Delta < \log(t_\star) >_M$			
X^i_{AGN}	0.2	0.4	0.6	0.8	0.2	0.4	0.6	0.8	0.2	0.4	0.6	0.8	0.2	0.4	0.6	0.8
Mean	0.02	0.03	0.03	0.02	-0.21	-0.14	-0.05	-0.01	0.02	-0.06	-0.18	-0.31	0.82	0.68	0.34	0.36
SD	0.02	0.04	0.04	0.05	0.11	0.06	0.08	0.06	0.04	0.12	0.24	0.36	0.42	0.52	0.5	0.59
MAE	0.02	0.04	0.04	0.04	0.21	0.14	0.07	0.05	0.04	0.08	0.2	0.34	0.82	0.68	0.38	0.5
MSE	0.0	0.0	0.0	0.0	0.06	0.02	0.01	0.0	0.0	0.02	0.09	0.22	0.85	0.73	0.37	0.48

	SFH=Burst; SN=15.0; Av=1.0; Age of the system = 8.0															
	$\Delta \log < Z_\star >_L$				$\Delta \log < Z_\star >_M$				$\Delta M_\star$				ΔA_v			
X^i_{AGN}	0.2	0.4	0.6	0.8	0.2	0.4	0.6	0.8	0.2	0.4	0.6	0.8	0.2	0.4	0.6	0.8
Mean	-0.25	-0.48	-0.63	-0.65	-0.1	-0.17	-0.45	-0.49	-0.21	-0.12	0.05	0.07	0.16	0.13	0.08	0.05
SD	0.11	0.18	0.13	0.12	0.15	0.25	0.3	0.33	0.18	0.23	0.25	0.33	0.06	0.08	0.08	0.07
MAE	0.25	0.48	0.63	0.65	0.15	0.24	0.49	0.55	0.22	0.2	0.2	0.27	0.16	0.14	0.1	0.08
MSE	0.07	0.26	0.41	0.44	0.03	0.09	0.29	0.35	0.08	0.06	0.06	0.11	0.03	0.02	0.01	0.01

TABLE A.52

	SFH=Burst; SN=15.0; Av=1.0; Age of the system = 8.4															
	ΔX_{AGN}				$\Delta < \alpha_{\nu} >_L$				$\Delta < \log(t_{\star}) >_L$				$\Delta < \log(t_{\star}) >_M$			
X^i_{AGN}	0.2	0.4	0.6	0.8	0.2	0.4	0.6	0.8	0.2	0.4	0.6	0.8	0.2	0.4	0.6	0.8
Mean	-0.05	-0.05	-0.02	-0.0	-0.17	-0.05	0.02	0.03	-0.12	-0.2	-0.3	-0.44	0.17	0.22	0.2	0.21
SD	0.03	0.03	0.02	0.03	0.12	0.08	0.06	0.06	0.06	0.1	0.16	0.39	0.2	0.26	0.27	0.4
MAE	0.05	0.05	0.03	0.02	0.18	0.07	0.06	0.05	0.12	0.2	0.3	0.45	0.17	0.24	0.26	0.37
MSE	0.0	0.0	0.0	0.0	0.04	0.01	0.0	0.0	0.02	0.05	0.12	0.34	0.07	0.12	0.11	0.21

	SFH=Burst; SN=15.0; Av=1.0; Age of the system = 8.4															
	$\Delta \log < Z_{\star} >_L$				$\Delta \log < Z_{\star} >_M$				$\Delta M_{\star}$				ΔA_v			
X^i_{AGN}	0.2	0.4	0.6	0.8	0.2	0.4	0.6	0.8	0.2	0.4	0.6	0.8	0.2	0.4	0.6	0.8
Mean	-0.19	-0.36	-0.52	-0.56	-0.14	-0.23	-0.34	-0.42	-0.07	-0.08	-0.03	0.04	-0.01	-0.02	-0.03	-0.0
SD	0.07	0.14	0.17	0.2	0.08	0.14	0.26	0.3	0.09	0.13	0.15	0.31	0.06	0.06	0.06	0.06
MAE	0.19	0.36	0.52	0.56	0.15	0.23	0.36	0.45	0.08	0.1	0.11	0.22	0.05	0.05	0.05	0.05
MSE	0.04	0.15	0.3	0.36	0.03	0.07	0.18	0.27	0.01	0.02	0.02	0.09	0.0	0.0	0.0	0.0

TABLE A.54

	SFH=Burst; SN=15.0; Av=1.0; Age of the system = 8.8															
	ΔX_{AGN}				$\Delta < \alpha_{\nu} >_{L}$				$\Delta < \log(t_{\star}) >_{L}$				$\Delta < \log(t_{\star}) >_{M}$			
X^{i}_{AGN}	0.2	0.4	0.6	0.8	0.2	0.4	0.6	0.8	0.2	0.4	0.6	0.8	0.2	0.4	0.6	0.8
Mean	-0.04	-0.03	-0.01	0.0	-0.25	-0.07	-0.0	0.02	-0.07	-0.12	-0.19	-0.22	0.08	0.09	0.1	0.16
SD	0.02	0.02	0.04	0.03	0.16	0.13	0.1	0.06	0.06	0.08	0.19	0.32	0.06	0.04	0.07	0.13
MAE	0.04	0.03	0.02	0.03	0.25	0.11	0.07	0.06	0.07	0.12	0.2	0.27	0.08	0.09	0.1	0.16
MSE	0.0	0.0	0.0	0.0	0.09	0.02	0.01	0.0	0.01	0.02	0.07	0.15	0.01	0.01	0.01	0.04

	SFH=Burst; SN=15.0; Av=1.0; Age of the system = 8.8															
	$\Delta \log < Z_{\star} >_{L}$				$\Delta \log < Z_{\star} >_{M}$				$\Delta M_{\star}$				ΔA_{v}			
X^{i}_{AGN}	0.2	0.4	0.6	0.8	0.2	0.4	0.6	0.8	0.2	0.4	0.6	0.8	0.2	0.4	0.6	0.8
Mean	-0.06	-0.09	-0.1	-0.24	-0.01	-0.03	-0.03	-0.16	-0.03	-0.04	-0.04	-0.04	0.07	0.05	0.04	0.02
SD	0.1	0.12	0.19	0.26	0.08	0.09	0.16	0.25	0.04	0.03	0.05	0.09	0.05	0.07	0.1	0.05
MAE	0.1	0.12	0.18	0.3	0.07	0.08	0.13	0.24	0.03	0.04	0.05	0.07	0.08	0.07	0.07	0.05
MSE	0.01	0.02	0.05	0.12	0.01	0.01	0.03	0.09	0.0	0.0	0.0	0.01	0.01	0.01	0.01	0.0

TABLE A.56

	SFH=Burst; SN=15.0; Av=1.0; Age of the system = 9.2															
	ΔX_{AGN}				$\Delta < \alpha_v >_L$				$\Delta < \log(t_\star) >_L$				$\Delta < \log(t_\star) >_M$			
X^i_{AGN}	0.2	0.4	0.6	0.8	0.2	0.4	0.6	0.8	0.2	0.4	0.6	0.8	0.2	0.4	0.6	0.8
Mean	0.04	0.05	0.05	0.04	-0.07	0.03	0.03	0.02	-0.05	-0.05	-0.03	0.02	0.06	0.07	0.08	0.16
SD	0.03	0.03	0.03	0.02	0.15	0.1	0.08	0.06	0.06	0.09	0.11	0.19	0.08	0.13	0.16	0.22
MAE	0.05	0.06	0.05	0.04	0.12	0.08	0.07	0.05	0.06	0.08	0.09	0.14	0.08	0.11	0.15	0.2
MSE	0.0	0.0	0.0	0.0	0.03	0.01	0.01	0.0	0.01	0.01	0.01	0.04	0.01	0.02	0.03	0.07

	SFH=Burst; SN=15.0; Av=1.0; Age of the system = 9.2															
	$\Delta \log < Z_\star >_L$				$\Delta \log < Z_\star >_M$				$\Delta M_\star$				ΔA_v			
X^i_{AGN}	0.2	0.4	0.6	0.8	0.2	0.4	0.6	0.8	0.2	0.4	0.6	0.8	0.2	0.4	0.6	0.8
Mean	0.12	0.16	0.15	0.1	0.1	0.1	0.11	0.06	0.0	-0.01	0.0	-0.02	0.04	0.02	0.02	0.03
SD	0.1	0.13	0.18	0.26	0.1	0.14	0.2	0.27	0.06	0.08	0.12	0.16	0.04	0.06	0.05	0.05
MAE	0.14	0.17	0.21	0.24	0.11	0.15	0.19	0.24	0.05	0.07	0.1	0.12	0.05	0.04	0.04	0.04
MSE	0.03	0.04	0.06	0.08	0.02	0.03	0.05	0.08	0.0	0.01	0.01	0.03	0.0	0.0	0.0	0.0

TABLE A.58

	SFH=Burst; SN=15.0; Av=1.0; Age of the system = 9.6															
	ΔX_{AGN}				$\Delta < \alpha_v >_L$				$\Delta < \log(t_\star) >_L$				$\Delta < \log(t_\star) >_M$			
X^i_{AGN}	0.2	0.4	0.6	0.8	0.2	0.4	0.6	0.8	0.2	0.4	0.6	0.8	0.2	0.4	0.6	0.8
Mean	0.02	0.03	0.03	0.02	-0.09	0.06	0.05	0.03	0.02	0.06	0.12	0.14	0.11	0.15	0.23	0.29
SD	0.02	0.02	0.02	0.03	0.18	0.08	0.07	0.09	0.05	0.1	0.1	0.22	0.07	0.07	0.08	0.14
MAE	0.02	0.03	0.03	0.02	0.17	0.09	0.07	0.06	0.04	0.09	0.13	0.21	0.11	0.15	0.23	0.3
MSE	0.0	0.0	0.0	0.0	0.04	0.01	0.01	0.01	0.0	0.01	0.02	0.07	0.02	0.03	0.06	0.1

	SFH=Burst; SN=15.0; Av=1.0; Age of the system = 9.6															
	$\Delta \log < Z_\star >_L$				$\Delta \log < Z_\star >_M$				$\Delta M_\star$				ΔA_v			
X^i_{AGN}	0.2	0.4	0.6	0.8	0.2	0.4	0.6	0.8	0.2	0.4	0.6	0.8	0.2	0.4	0.6	0.8
Mean	0.02	0.02	0.0	-0.05	-0.02	-0.03	-0.05	-0.1	-0.05	-0.09	-0.13	-0.15	0.02	0.0	0.0	0.01
SD	0.06	0.08	0.1	0.13	0.03	0.04	0.06	0.1	0.04	0.04	0.05	0.11	0.03	0.03	0.03	0.08
MAE	0.05	0.06	0.08	0.11	0.03	0.04	0.06	0.1	0.05	0.09	0.13	0.17	0.03	0.03	0.03	0.04
MSE	0.0	0.01	0.01	0.02	0.0	0.0	0.01	0.02	0.0	0.01	0.02	0.04	0.0	0.0	0.0	0.01

TABLE A.60

	SFH=Burst; SN=15.0; Av=1.0; Age of the system = 10.0															
	ΔX_{AGN}				$\Delta < \alpha_v >_L$				$\Delta < \log(t_\star) >_L$				$\Delta < \log(t_\star) >_M$			
X^i_{AGN}	0.2	0.4	0.6	0.8	0.2	0.4	0.6	0.8	0.2	0.4	0.6	0.8	0.2	0.4	0.6	0.8
Mean	0.01	0.02	0.02	0.0	-0.02	0.09	0.06	0.03	-0.0	0.03	0.05	-0.04	0.03	0.04	0.07	0.09
SD	0.02	0.01	0.01	0.03	0.18	0.1	0.08	0.07	0.06	0.04	0.07	0.25	0.04	0.04	0.05	0.07
MAE	0.02	0.02	0.02	0.02	0.15	0.11	0.08	0.06	0.04	0.04	0.07	0.16	0.04	0.05	0.07	0.09
MSE	0.0	0.0	0.0	0.0	0.03	0.02	0.01	0.01	0.0	0.0	0.01	0.06	0.0	0.0	0.01	0.01

	SFH=Burst; SN=15.0; Av=1.0; Age of the system = 10.0															
	$\Delta \log < Z_\star >_L$				$\Delta \log < Z_\star >_M$				$\Delta M_\star$				ΔA_v			
X^i_{AGN}	0.2	0.4	0.6	0.8	0.2	0.4	0.6	0.8	0.2	0.4	0.6	0.8	0.2	0.4	0.6	0.8
Mean	-0.02	-0.03	-0.05	-0.08	-0.02	-0.03	-0.05	-0.07	-0.02	-0.04	-0.05	-0.06	0.0	-0.02	-0.02	-0.02
SD	0.02	0.03	0.04	0.07	0.02	0.02	0.03	0.05	0.03	0.04	0.04	0.06	0.03	0.03	0.04	0.04
MAE	0.03	0.04	0.06	0.09	0.03	0.03	0.05	0.07	0.03	0.04	0.06	0.07	0.02	0.02	0.03	0.03
MSE	0.0	0.0	0.0	0.01	0.0	0.0	0.0	0.01	0.0	0.0	0.0	0.01	0.0	0.0	0.0	0.0

TABLE A.62

A.1.4 Tables: Constant SFH, Av=1.0, SN = 15, base: BaseA

	SFH=Constant; SN=15.0; Av=1.0; Age of the system = 6.0															
	ΔX_{AGN}				$\Delta < \alpha_v >_L$				$\Delta < \log(t_\star) >_L$				$\Delta < \log(t_\star) >_M$			
X^i_{AGN}	0.2	0.4	0.6	0.8	0.2	0.4	0.6	0.8	0.2	0.4	0.6	0.8	0.2	0.4	0.6	0.8
Mean	0.09	0.09	0.03	-0.01	0.14	-0.07	-0.1	-0.04	0.24	0.22	0.22	0.25	2.29	2.13	2.33	1.57
SD	0.05	0.04	0.04	0.03	0.07	0.06	0.07	0.08	0.13	0.13	0.12	0.13	1.21	1.39	1.43	1.53
MAE	0.1	0.09	0.04	0.03	0.14	0.08	0.1	0.07	0.24	0.22	0.22	0.25	2.29	2.13	2.33	1.57
MSE	0.01	0.01	0.0	0.0	0.02	0.01	0.02	0.01	0.07	0.07	0.06	0.08	6.68	6.45	7.46	4.81

	SFH=Constant; SN=15.0; Av=1.0; Age of the system = 6.0															
	$\Delta \log < Z_\star >_L$				$\Delta \log < Z_\star >_M$				$\Delta M_\star$				ΔA_v			
X^i_{AGN}	0.2	0.4	0.6	0.8	0.2	0.4	0.6	0.8	0.2	0.4	0.6	0.8	0.2	0.4	0.6	0.8
Mean	-0.34	-0.41	-0.23	-0.11	-0.22	-0.28	-0.19	-0.18	-0.65	-0.62	-0.76	-0.59	0.27	0.28	0.17	0.06
SD	0.2	0.23	0.22	0.21	0.2	0.26	0.25	0.23	0.44	0.55	0.59	0.73	0.1	0.1	0.1	0.09
MAE	0.34	0.42	0.25	0.16	0.24	0.33	0.26	0.21	0.66	0.64	0.77	0.59	0.27	0.28	0.18	0.08
MSE	0.16	0.22	0.1	0.06	0.09	0.15	0.1	0.09	0.61	0.69	0.93	0.88	0.08	0.09	0.04	0.01

TABLE A.64

	SFH=Constant; SN=15.0; Av=1.0; Age of the system = 6.4															
	ΔX_{AGN}				$\Delta < \alpha_{\nu} >_{L}$				$\Delta < \log(t_{\star}) >_{L}$				$\Delta < \log(t_{\star}) >_{M}$			
X^{i}_{AGN}	0.2	0.4	0.6	0.8	0.2	0.4	0.6	0.8	0.2	0.4	0.6	0.8	0.2	0.4	0.6	0.8
Mean	0.14	0.12	0.05	0.0	0.16	-0.07	-0.11	-0.08	-0.04	-0.06	-0.06	-0.02	1.94	2.03	1.6	1.59
SD	0.07	0.05	0.03	0.03	0.07	0.07	0.08	0.08	0.13	0.13	0.1	0.16	1.2	1.33	1.59	1.56
MAE	0.14	0.12	0.06	0.03	0.17	0.08	0.11	0.1	0.11	0.11	0.09	0.12	1.97	2.06	1.66	1.64
MSE	0.02	0.02	0.0	0.0	0.03	0.01	0.02	0.01	0.02	0.02	0.01	0.03	5.21	5.9	5.09	4.96

	SFH=Constant; SN=15.0; Av=1.0; Age of the system = 6.4															
	$\Delta \log < Z_{\star} >_{L}$				$\Delta \log < Z_{\star} >_{M}$				$\Delta M_{\star}$				ΔA_{v}			
X^{i}_{AGN}	0.2	0.4	0.6	0.8	0.2	0.4	0.6	0.8	0.2	0.4	0.6	0.8	0.2	0.4	0.6	0.8
Mean	-0.21	-0.22	-0.09	-0.07	-0.17	-0.17	-0.19	-0.17	-0.55	-0.6	-0.56	-0.66	0.36	0.33	0.22	0.11
SD	0.26	0.27	0.2	0.22	0.23	0.25	0.23	0.26	0.45	0.53	0.68	0.74	0.15	0.12	0.1	0.1
MAE	0.25	0.26	0.16	0.17	0.21	0.24	0.23	0.23	0.59	0.65	0.61	0.68	0.36	0.33	0.22	0.13
MSE	0.11	0.12	0.05	0.05	0.08	0.09	0.09	0.1	0.5	0.64	0.77	0.98	0.15	0.13	0.06	0.02

TABLE A.66

	SFH=Constant; SN=15.0; Av=1.0; Age of the system = 6.8															
	ΔX_{AGN}				$\Delta < \alpha_{\nu} >_{L}$				$\Delta < \log(t_{\star}) >_{L}$				$\Delta < \log(t_{\star}) >_{M}$			
X^{i}_{AGN}	0.2	0.4	0.6	0.8	0.2	0.4	0.6	0.8	0.2	0.4	0.6	0.8	0.2	0.4	0.6	0.8
Mean	0.17	0.14	0.11	0.07	0.11	-0.06	-0.08	-0.06	0.03	0.02	-0.05	-0.09	1.36	0.85	0.94	0.88
SD	0.07	0.06	0.05	0.05	0.07	0.08	0.08	0.1	0.11	0.11	0.14	0.22	0.98	0.9	0.99	1.23
MAE	0.17	0.14	0.11	0.07	0.12	0.08	0.09	0.1	0.08	0.08	0.12	0.19	1.38	0.88	1.01	1.02
MSE	0.04	0.02	0.01	0.01	0.02	0.01	0.01	0.01	0.01	0.01	0.02	0.06	2.82	1.53	1.87	2.27

	SFH=Constant; SN=15.0; Av=1.0; Age of the system = 6.8															
	$\Delta \log < Z_{\star} >_{L}$				$\Delta \log < Z_{\star} >_{M}$				$\Delta M_{\star}$				ΔA_{v}			
X^{i}_{AGN}	0.2	0.4	0.6	0.8	0.2	0.4	0.6	0.8	0.2	0.4	0.6	0.8	0.2	0.4	0.6	0.8
Mean	-0.25	-0.21	-0.08	-0.17	-0.19	-0.28	-0.22	-0.22	-0.28	-0.17	-0.24	-0.28	0.44	0.35	0.25	0.18
SD	0.21	0.27	0.23	0.36	0.2	0.21	0.21	0.31	0.37	0.32	0.42	0.59	0.13	0.11	0.11	0.11
MAE	0.27	0.25	0.19	0.32	0.22	0.29	0.24	0.3	0.38	0.27	0.35	0.48	0.44	0.35	0.25	0.19
MSE	0.11	0.11	0.06	0.16	0.08	0.12	0.09	0.15	0.22	0.13	0.24	0.43	0.21	0.14	0.08	0.04

TABLE A.68

	SFH=Constant; SN=15.0; Av=1.0; Age of the system = 7.2															
	ΔX_{AGN}				$\Delta < \alpha_v >_L$				$\Delta < \log(t_\star) >_L$				$\Delta < \log(t_\star) >_M$			
X^i_{AGN}	0.2	0.4	0.6	0.8	0.2	0.4	0.6	0.8	0.2	0.4	0.6	0.8	0.2	0.4	0.6	0.8
Mean	0.18	0.15	0.11	0.09	-0.09	-0.16	-0.16	-0.09	-0.03	-0.08	-0.12	-0.21	1.58	1.33	1.16	0.78
SD	0.07	0.06	0.06	0.04	0.11	0.08	0.09	0.07	0.08	0.13	0.15	0.29	1.15	1.09	1.27	1.39
MAE	0.18	0.15	0.12	0.09	0.13	0.16	0.16	0.09	0.07	0.12	0.15	0.29	1.63	1.4	1.33	1.2
MSE	0.04	0.03	0.02	0.01	0.02	0.03	0.03	0.01	0.01	0.02	0.04	0.13	3.82	2.96	2.96	2.55

	SFH=Constant; SN=15.0; Av=1.0; Age of the system = 7.2															
	$\Delta \log < Z_\star >_L$				$\Delta \log < Z_\star >_M$				$\Delta M_\star$				ΔA_v			
X^i_{AGN}	0.2	0.4	0.6	0.8	0.2	0.4	0.6	0.8	0.2	0.4	0.6	0.8	0.2	0.4	0.6	0.8
Mean	-0.19	-0.18	-0.15	-0.18	0.04	-0.03	-0.15	-0.24	-0.34	-0.25	-0.27	-0.17	0.48	0.37	0.29	0.21
SD	0.12	0.18	0.25	0.3	0.21	0.22	0.26	0.29	0.57	0.53	0.61	0.8	0.13	0.11	0.13	0.08
MAE	0.2	0.2	0.21	0.26	0.18	0.18	0.23	0.3	0.52	0.46	0.51	0.63	0.48	0.37	0.29	0.21
MSE	0.05	0.06	0.09	0.12	0.04	0.05	0.09	0.14	0.44	0.35	0.45	0.67	0.25	0.15	0.1	0.05

TABLE A.70

	SFH=Constant; SN=15.0; Av=1.0; Age of the system = 7.6															
	ΔX_{AGN}				$\Delta < \alpha_v >_L$				$\Delta < \log(t_\star) >_L$				$\Delta < \log(t_\star) >_M$			
X^i_{AGN}	0.2	0.4	0.6	0.8	0.2	0.4	0.6	0.8	0.2	0.4	0.6	0.8	0.2	0.4	0.6	0.8
Mean	0.16	0.17	0.11	0.09	-0.07	-0.15	-0.14	-0.1	-0.12	-0.2	-0.2	-0.37	1.6	0.7	1.07	0.62
SD	0.04	0.05	0.06	0.05	0.13	0.08	0.09	0.07	0.05	0.09	0.12	0.25	1.06	1.14	1.14	1.3
MAE	0.16	0.17	0.11	0.1	0.12	0.15	0.14	0.1	0.12	0.2	0.21	0.38	1.63	1.04	1.29	1.19
MSE	0.03	0.03	0.02	0.01	0.02	0.03	0.03	0.02	0.02	0.05	0.05	0.2	3.68	1.79	2.46	2.06

	SFH=Constant; SN=15.0; Av=1.0; Age of the system = 7.6															
	$\Delta \log < Z_\star >_L$				$\Delta \log < Z_\star >_M$				$\Delta M_\star$				ΔA_v			
X^i_{AGN}	0.2	0.4	0.6	0.8	0.2	0.4	0.6	0.8	0.2	0.4	0.6	0.8	0.2	0.4	0.6	0.8
Mean	-0.18	-0.2	-0.15	-0.21	0.13	-0.02	-0.05	-0.25	-0.32	0.14	-0.12	0.12	0.42	0.37	0.26	0.21
SD	0.08	0.14	0.18	0.34	0.2	0.24	0.22	0.29	0.58	0.52	0.61	0.73	0.11	0.11	0.12	0.09
MAE	0.18	0.2	0.18	0.32	0.21	0.19	0.18	0.31	0.56	0.47	0.55	0.66	0.42	0.37	0.26	0.21
MSE	0.04	0.06	0.06	0.16	0.06	0.06	0.05	0.15	0.44	0.29	0.39	0.56	0.19	0.15	0.08	0.05

TABLE A.72

	SFH=Constant; SN=15.0; Av=1.0; Age of the system = 8.0															
	ΔX_{AGN}				$\Delta < \alpha_v >_L$				$\Delta < \log(t_\star) >_L$				$\Delta < \log(t_\star) >_M$			
X^i_{AGN}	0.2	0.4	0.6	0.8	0.2	0.4	0.6	0.8	0.2	0.4	0.6	0.8	0.2	0.4	0.6	0.8
Mean	0.1	0.11	0.11	0.08	-0.11	-0.18	-0.15	-0.09	-0.15	-0.28	-0.36	-0.46	1.51	1.82	1.19	0.36
SD	0.04	0.05	0.05	0.05	0.13	0.09	0.08	0.09	0.08	0.1	0.13	0.25	0.77	0.67	1.05	1.35
MAE	0.1	0.11	0.11	0.09	0.14	0.18	0.15	0.1	0.15	0.28	0.36	0.47	1.54	1.84	1.38	1.24
MSE	0.01	0.01	0.01	0.01	0.03	0.04	0.03	0.02	0.03	0.09	0.15	0.27	2.88	3.75	2.51	1.94

	SFH=Constant; SN=15.0; Av=1.0; Age of the system = 8.0															
	$\Delta \log < Z_\star >_L$				$\Delta \log < Z_\star >_M$				$\Delta M_\star$				ΔA_v			
X^i_{AGN}	0.2	0.4	0.6	0.8	0.2	0.4	0.6	0.8	0.2	0.4	0.6	0.8	0.2	0.4	0.6	0.8
Mean	-0.24	-0.32	-0.4	-0.39	0.1	0.13	-0.0	-0.29	-0.37	-0.44	-0.04	0.45	0.3	0.29	0.26	0.19
SD	0.09	0.14	0.21	0.26	0.2	0.27	0.31	0.34	0.44	0.43	0.59	1.38	0.12	0.09	0.1	0.08
MAE	0.24	0.32	0.4	0.4	0.19	0.26	0.28	0.38	0.48	0.54	0.5	0.93	0.3	0.29	0.26	0.19
MSE	0.07	0.12	0.21	0.22	0.05	0.09	0.1	0.2	0.32	0.37	0.35	2.12	0.1	0.09	0.07	0.04

TABLE A.74

	SFH=Constant; SN=15.0; Av=1.0; Age of the system = 8.4															
	ΔX_{AGN}				$\Delta < \alpha_{\nu} >_{L}$				$\Delta < \log(t_{\star}) >_{L}$				$\Delta < \log(t_{\star}) >_{M}$			
X^{i}_{AGN}	0.2	0.4	0.6	0.8	0.2	0.4	0.6	0.8	0.2	0.4	0.6	0.8	0.2	0.4	0.6	0.8
Mean	0.11	0.09	0.08	0.05	-0.17	-0.16	-0.1	-0.05	-0.07	-0.21	-0.37	-0.38	1.31	1.18	0.8	0.59
SD	0.05	0.04	0.04	0.05	0.11	0.08	0.07	0.07	0.12	0.15	0.17	0.35	0.47	0.6	0.83	0.95
MAE	0.11	0.09	0.08	0.06	0.17	0.16	0.11	0.07	0.11	0.22	0.38	0.47	1.32	1.2	0.93	0.95
MSE	0.01	0.01	0.01	0.0	0.04	0.03	0.02	0.01	0.02	0.06	0.17	0.26	1.95	1.76	1.33	1.26

	SFH=Constant; SN=15.0; Av=1.0; Age of the system = 8.4															
	$\Delta \log < Z_{\star} >_{L}$				$\Delta \log < Z_{\star} >_{M}$				$\Delta M_{\star}$				ΔA_{v}			
X^{i}_{AGN}	0.2	0.4	0.6	0.8	0.2	0.4	0.6	0.8	0.2	0.4	0.6	0.8	0.2	0.4	0.6	0.8
Mean	-0.25	-0.35	-0.51	-0.58	0.11	0.03	-0.21	-0.37	-0.32	-0.23	0.01	0.11	0.33	0.25	0.17	0.12
SD	0.12	0.2	0.19	0.18	0.17	0.3	0.33	0.31	0.27	0.35	0.52	0.62	0.13	0.08	0.08	0.07
MAE	0.25	0.35	0.51	0.58	0.17	0.27	0.34	0.41	0.36	0.35	0.44	0.51	0.33	0.25	0.18	0.13
MSE	0.08	0.16	0.3	0.37	0.04	0.09	0.15	0.24	0.18	0.18	0.27	0.4	0.12	0.07	0.04	0.02

TABLE A.76

	SFH=Constant; SN=15.0; Av=1.0; Age of the system = 8.8															
	ΔX_{AGN}				$\Delta < \alpha_v >_L$				$\Delta < \log(t_\star) >_L$				$\Delta < \log(t_\star) >_M$			
X^i_{AGN}	0.2	0.4	0.6	0.8	0.2	0.4	0.6	0.8	0.2	0.4	0.6	0.8	0.2	0.4	0.6	0.8
Mean	0.08	0.1	0.08	0.06	-0.15	-0.11	-0.05	-0.02	-0.03	-0.07	-0.25	-0.25	0.87	0.71	0.55	0.32
SD	0.05	0.05	0.04	0.04	0.11	0.07	0.08	0.07	0.12	0.19	0.25	0.43	0.32	0.47	0.59	0.82
MAE	0.08	0.1	0.08	0.06	0.16	0.11	0.07	0.06	0.09	0.16	0.3	0.42	0.87	0.72	0.63	0.71
MSE	0.01	0.01	0.01	0.01	0.04	0.02	0.01	0.01	0.01	0.04	0.13	0.25	0.87	0.73	0.65	0.77

	SFH=Constant; SN=15.0; Av=1.0; Age of the system = 8.8															
	$\Delta \log < Z_\star >_L$				$\Delta \log < Z_\star >_M$				$\Delta M_\star$				ΔA_v			
X^i_{AGN}	0.2	0.4	0.6	0.8	0.2	0.4	0.6	0.8	0.2	0.4	0.6	0.8	0.2	0.4	0.6	0.8
Mean	-0.25	-0.37	-0.51	-0.57	-0.02	-0.07	-0.21	-0.42	-0.21	-0.1	0.02	0.13	0.25	0.21	0.13	0.1
SD	0.13	0.16	0.2	0.16	0.18	0.2	0.33	0.29	0.19	0.27	0.36	0.56	0.1	0.08	0.08	0.07
MAE	0.25	0.37	0.51	0.57	0.15	0.18	0.33	0.44	0.24	0.24	0.29	0.46	0.25	0.21	0.13	0.1
MSE	0.08	0.16	0.3	0.35	0.03	0.05	0.15	0.26	0.08	0.09	0.13	0.33	0.07	0.05	0.02	0.01

TABLE A.78

	SFH=Constant; SN=15.0; Av=1.0; Age of the system = 9.2															
	ΔX_{AGN}				$\Delta < \alpha_v >_L$				$\Delta < \log(t_\star) >_L$				$\Delta < \log(t_\star) >_M$			
X^i_{AGN}	0.2	0.4	0.6	0.8	0.2	0.4	0.6	0.8	0.2	0.4	0.6	0.8	0.2	0.4	0.6	0.8
Mean	0.08	0.09	0.06	0.05	-0.16	-0.07	-0.04	-0.0	0.0	-0.1	-0.2	-0.19	0.56	0.45	0.46	0.34
SD	0.05	0.06	0.06	0.04	0.15	0.09	0.08	0.08	0.12	0.2	0.28	0.41	0.24	0.35	0.34	0.47
MAE	0.08	0.09	0.07	0.05	0.18	0.09	0.07	0.06	0.09	0.18	0.28	0.37	0.56	0.47	0.46	0.46
MSE	0.01	0.01	0.01	0.0	0.05	0.01	0.01	0.01	0.01	0.05	0.12	0.21	0.37	0.33	0.32	0.33

	SFH=Constant; SN=15.0; Av=1.0; Age of the system = 9.2															
	$\Delta \log < Z_\star >_L$				$\Delta \log < Z_\star >_M$				$\Delta M_\star$				ΔA_v			
X^i_{AGN}	0.2	0.4	0.6	0.8	0.2	0.4	0.6	0.8	0.2	0.4	0.6	0.8	0.2	0.4	0.6	0.8
Mean	-0.24	-0.31	-0.4	-0.52	-0.02	-0.07	-0.13	-0.34	-0.11	-0.04	-0.04	0.07	0.21	0.15	0.1	0.07
SD	0.1	0.16	0.2	0.19	0.14	0.21	0.26	0.26	0.14	0.22	0.23	0.37	0.09	0.08	0.1	0.08
MAE	0.24	0.31	0.41	0.53	0.11	0.18	0.23	0.37	0.15	0.18	0.19	0.28	0.21	0.15	0.12	0.08
MSE	0.07	0.12	0.2	0.31	0.02	0.05	0.08	0.18	0.03	0.05	0.05	0.15	0.05	0.03	0.02	0.01

TABLE A.80

	SFH=Constant; SN=15.0; Av=1.0; Age of the system = 9.6															
	ΔX_{AGN}				$\Delta < \alpha_{\nu} >_{L}$				$\Delta < \log(t_{\star}) >_{L}$				$\Delta < \log(t_{\star}) >_{M}$			
X^{i}_{AGN}	0.2	0.4	0.6	0.8	0.2	0.4	0.6	0.8	0.2	0.4	0.6	0.8	0.2	0.4	0.6	0.8
Mean	0.09	0.07	0.07	0.05	-0.13	-0.06	-0.02	-0.0	-0.03	-0.14	-0.12	-0.03	0.47	0.37	0.31	0.19
SD	0.05	0.05	0.05	0.04	0.15	0.1	0.08	0.06	0.13	0.2	0.29	0.46	0.17	0.22	0.3	0.36
MAE	0.09	0.08	0.08	0.06	0.17	0.09	0.07	0.05	0.11	0.2	0.25	0.37	0.47	0.38	0.37	0.32
MSE	0.01	0.01	0.01	0.0	0.04	0.01	0.01	0.0	0.02	0.06	0.1	0.22	0.25	0.19	0.19	0.17

	SFH=Constant; SN=15.0; Av=1.0; Age of the system = 9.6															
	$\Delta \log < Z_{\star} >_{L}$				$\Delta \log < Z_{\star} >_{M}$				$\Delta M_{\star}$				ΔA_{v}			
X^{i}_{AGN}	0.2	0.4	0.6	0.8	0.2	0.4	0.6	0.8	0.2	0.4	0.6	0.8	0.2	0.4	0.6	0.8
Mean	-0.18	-0.27	-0.35	-0.4	0.04	0.01	-0.1	-0.24	-0.12	-0.05	0.01	0.08	0.16	0.11	0.09	0.07
SD	0.1	0.14	0.2	0.26	0.1	0.15	0.29	0.34	0.13	0.16	0.22	0.3	0.09	0.09	0.08	0.06
MAE	0.19	0.27	0.36	0.42	0.08	0.12	0.25	0.35	0.14	0.14	0.18	0.26	0.17	0.12	0.1	0.08
MSE	0.04	0.09	0.17	0.22	0.01	0.02	0.09	0.17	0.03	0.03	0.05	0.09	0.04	0.02	0.01	0.01

TABLE A.82

	SFH=Constant; SN=15.0; Av=1.0; Age of the system = 10.0															
	ΔX_{AGN}				$\Delta < \alpha_v >_L$				$\Delta < \log(t_\star) >_L$				$\Delta < \log(t_\star) >_M$			
X^i_{AGN}	0.2	0.4	0.6	0.8	0.2	0.4	0.6	0.8	0.2	0.4	0.6	0.8	0.2	0.4	0.6	0.8
Mean	0.06	0.06	0.05	0.06	-0.09	-0.05	-0.02	-0.01	-0.05	-0.13	-0.18	0.06	0.25	0.21	0.12	-0.09
SD	0.05	0.05	0.05	0.05	0.15	0.09	0.08	0.07	0.13	0.19	0.25	0.44	0.12	0.14	0.25	0.33
MAE	0.07	0.06	0.06	0.06	0.14	0.08	0.06	0.06	0.12	0.19	0.25	0.36	0.25	0.22	0.23	0.3
MSE	0.01	0.01	0.01	0.01	0.03	0.01	0.01	0.0	0.02	0.06	0.1	0.19	0.08	0.06	0.08	0.12

	SFH=Constant; SN=15.0; Av=1.0; Age of the system = 10.0															
	$\Delta \log < Z_\star >_L$				$\Delta \log < Z_\star >_M$				$\Delta M_\star$				ΔA_v			
X^i_{AGN}	0.2	0.4	0.6	0.8	0.2	0.4	0.6	0.8	0.2	0.4	0.6	0.8	0.2	0.4	0.6	0.8
Mean	-0.21	-0.22	-0.25	-0.26	-0.02	-0.01	-0.0	-0.15	-0.08	-0.03	0.05	0.24	0.1	0.08	0.06	0.07
SD	0.1	0.11	0.22	0.33	0.06	0.1	0.23	0.34	0.09	0.11	0.18	0.27	0.1	0.08	0.08	0.06
MAE	0.21	0.22	0.29	0.36	0.05	0.07	0.17	0.32	0.1	0.1	0.15	0.3	0.12	0.09	0.09	0.08
MSE	0.05	0.06	0.11	0.18	0.0	0.01	0.05	0.14	0.01	0.01	0.03	0.13	0.02	0.01	0.01	0.01

TABLE A.84

A.1.5 Tables: Burst SFH, Av=2.0, SN = 15, base: BaseA

	SFH=Burst; SN=15.0; Av=2.0; Age of the system = 6.0															
	ΔX_{AGN}				$\Delta < \alpha_v >_L$				$\Delta < \log(t_\star) >_L$				$\Delta < \log(t_\star) >_M$			
X^i_{AGN}	0.2	0.4	0.6	0.8	0.2	0.4	0.6	0.8	0.2	0.4	0.6	0.8	0.2	0.4	0.6	0.8
Mean	0.09	0.08	0.03	0.0	0.13	-0.08	-0.11	-0.06	0.2	0.23	0.22	0.24	2.15	2.44	2.32	1.94
SD	0.05	0.04	0.04	0.03	0.07	0.06	0.08	0.07	0.13	0.13	0.15	0.17	1.17	1.27	1.53	1.62
MAE	0.09	0.08	0.04	0.02	0.13	0.08	0.11	0.08	0.2	0.23	0.22	0.24	2.15	2.44	2.32	1.94
MSE	0.01	0.01	0.0	0.0	0.02	0.01	0.02	0.01	0.06	0.07	0.07	0.09	5.96	7.56	7.74	6.41

	SFH=Burst; SN=15.0; Av=2.0; Age of the system = 6.0															
	$\Delta \log < Z_\star >_L$				$\Delta \log < Z_\star >_M$				$\Delta M_\star$				ΔA_v			
X^i_{AGN}	0.2	0.4	0.6	0.8	0.2	0.4	0.6	0.8	0.2	0.4	0.6	0.8	0.2	0.4	0.6	0.8
Mean	-0.3	-0.4	-0.28	-0.16	-0.26	-0.26	-0.23	-0.2	-0.58	-0.71	-0.79	-0.74	0.25	0.27	0.18	0.09
SD	0.2	0.23	0.27	0.25	0.18	0.28	0.27	0.26	0.41	0.48	0.64	0.74	0.1	0.12	0.11	0.08
MAE	0.3	0.4	0.3	0.22	0.27	0.33	0.28	0.26	0.59	0.72	0.8	0.74	0.25	0.27	0.18	0.1
MSE	0.13	0.21	0.15	0.09	0.1	0.15	0.13	0.11	0.5	0.73	1.03	1.08	0.07	0.08	0.04	0.02

TABLE A.86

	SFH=Burst; SN=15.0; Av=2.0; Age of the system = 6.4															
	ΔX_{AGN}				$\Delta < \alpha_{\nu} >_{L}$				$\Delta < \log(t_{\star}) >_{L}$				$\Delta < \log(t_{\star}) >_{M}$			
X^{i}_{AGN}	0.2	0.4	0.6	0.8	0.2	0.4	0.6	0.8	0.2	0.4	0.6	0.8	0.2	0.4	0.6	0.8
Mean	0.15	0.13	0.06	0.01	0.18	-0.09	-0.11	-0.05	-0.15	-0.16	-0.13	-0.12	1.56	1.8	1.42	1.21
SD	0.07	0.05	0.03	0.04	0.06	0.07	0.08	0.09	0.11	0.12	0.11	0.14	1.08	1.46	1.54	1.49
MAE	0.15	0.13	0.06	0.03	0.18	0.09	0.11	0.08	0.16	0.17	0.14	0.15	1.59	1.87	1.51	1.31
MSE	0.03	0.02	0.01	0.0	0.03	0.01	0.02	0.01	0.04	0.04	0.03	0.04	3.6	5.37	4.38	3.69

	SFH=Burst; SN=15.0; Av=2.0; Age of the system = 6.4															
	$\Delta \log < Z_{\star} >_{L}$				$\Delta \log < Z_{\star} >_{M}$				$\Delta M_{\star}$				ΔA_{v}			
X^{i}_{AGN}	0.2	0.4	0.6	0.8	0.2	0.4	0.6	0.8	0.2	0.4	0.6	0.8	0.2	0.4	0.6	0.8
Mean	-0.08	-0.13	-0.05	0.05	-0.14	-0.16	-0.14	-0.07	-0.38	-0.54	-0.49	-0.51	0.36	0.37	0.23	0.09
SD	0.22	0.22	0.19	0.2	0.2	0.22	0.18	0.24	0.41	0.55	0.63	0.71	0.14	0.13	0.09	0.1
MAE	0.16	0.19	0.14	0.16	0.16	0.2	0.16	0.18	0.43	0.61	0.55	0.55	0.36	0.37	0.23	0.11
MSE	0.06	0.06	0.04	0.04	0.06	0.08	0.05	0.06	0.31	0.59	0.64	0.77	0.15	0.15	0.06	0.02

TABLE A.88

	SFH=Burst; SN=15.0; Av=2.0; Age of the system = 6.8															
	ΔX_{AGN}				$\Delta < \alpha_v >_L$				$\Delta < \log(t_\star) >_L$				$\Delta < \log(t_\star) >_M$			
X^i_{AGN}	0.2	0.4	0.6	0.8	0.2	0.4	0.6	0.8	0.2	0.4	0.6	0.8	0.2	0.4	0.6	0.8
Mean	0.22	0.19	0.15	0.1	0.09	-0.08	-0.11	-0.08	0.02	-0.02	-0.03	-0.09	1.18	0.38	0.45	0.34
SD	0.05	0.06	0.06	0.05	0.08	0.07	0.07	0.08	0.05	0.07	0.11	0.26	1.0	0.61	0.81	0.88
MAE	0.22	0.19	0.15	0.11	0.1	0.09	0.11	0.09	0.04	0.06	0.09	0.22	1.19	0.46	0.59	0.61
MSE	0.05	0.04	0.03	0.01	0.01	0.01	0.02	0.01	0.0	0.0	0.01	0.08	2.41	0.51	0.85	0.88

	SFH=Burst; SN=15.0; Av=2.0; Age of the system = 6.8															
	$\Delta \log < Z_\star >_L$				$\Delta \log < Z_\star >_M$				$\Delta M_\star$				ΔA_v			
X^i_{AGN}	0.2	0.4	0.6	0.8	0.2	0.4	0.6	0.8	0.2	0.4	0.6	0.8	0.2	0.4	0.6	0.8
Mean	-0.25	-0.35	-0.38	-0.36	-0.13	-0.32	-0.34	-0.38	-0.11	0.16	0.07	0.1	0.45	0.42	0.33	0.23
SD	0.16	0.25	0.26	0.32	0.2	0.22	0.26	0.28	0.43	0.28	0.37	0.62	0.08	0.11	0.09	0.09
MAE	0.25	0.35	0.38	0.39	0.19	0.32	0.36	0.41	0.34	0.28	0.32	0.46	0.45	0.42	0.33	0.23
MSE	0.09	0.18	0.21	0.23	0.05	0.15	0.19	0.23	0.2	0.1	0.14	0.39	0.21	0.18	0.12	0.06

TABLE A.90

	SFH=Burst; SN=15.0; Av=2.0; Age of the system = 7.2															
	ΔX_{AGN}				$\Delta < \alpha_{\nu} >_{L}$				$\Delta < \log(t_{\star}) >_{L}$				$\Delta < \log(t_{\star}) >_{M}$			
X^{i}_{AGN}	0.2	0.4	0.6	0.8	0.2	0.4	0.6	0.8	0.2	0.4	0.6	0.8	0.2	0.4	0.6	0.8
Mean	0.03	0.1	0.12	0.09	-0.06	-0.1	-0.13	-0.09	-0.04	-0.11	-0.23	-0.24	1.98	2.22	1.72	1.24
SD	0.04	0.05	0.07	0.06	0.09	0.09	0.09	0.07	0.05	0.07	0.14	0.45	0.73	0.63	1.12	1.28
MAE	0.04	0.1	0.12	0.1	0.09	0.11	0.13	0.09	0.05	0.12	0.23	0.38	1.98	2.22	1.8	1.44
MSE	0.0	0.01	0.02	0.01	0.01	0.02	0.03	0.01	0.0	0.02	0.07	0.27	4.43	5.32	4.22	3.17

	SFH=Burst; SN=15.0; Av=2.0; Age of the system = 7.2															
	$\Delta \log < Z_{\star} >_{L}$				$\Delta \log < Z_{\star} >_{M}$				$\Delta M_{\star}$				ΔA_{v}			
X^{i}_{AGN}	0.2	0.4	0.6	0.8	0.2	0.4	0.6	0.8	0.2	0.4	0.6	0.8	0.2	0.4	0.6	0.8
Mean	-0.05	-0.04	-0.05	-0.02	0.02	0.11	0.1	-0.02	-0.71	-0.74	-0.44	-0.08	0.1	0.21	0.24	0.18
SD	0.05	0.06	0.12	0.25	0.14	0.16	0.22	0.27	0.37	0.38	0.67	0.89	0.09	0.09	0.1	0.09
MAE	0.05	0.05	0.1	0.2	0.1	0.15	0.2	0.22	0.72	0.76	0.7	0.79	0.12	0.21	0.24	0.19
MSE	0.0	0.0	0.02	0.06	0.02	0.04	0.06	0.07	0.65	0.69	0.63	0.79	0.02	0.05	0.07	0.04

TABLE A.92

	SFH=Burst; SN=15.0; Av=2.0; Age of the system = 7.6															
	ΔX_{AGN}				$\Delta < \alpha_{\nu} >_L$				$\Delta < \log(t_{\star}) >_L$				$\Delta < \log(t_{\star}) >_M$			
X^i_{AGN}	0.2	0.4	0.6	0.8	0.2	0.4	0.6	0.8	0.2	0.4	0.6	0.8	0.2	0.4	0.6	0.8
Mean	0.04	0.08	0.08	0.07	-0.12	-0.14	-0.13	-0.07	-0.0	-0.09	-0.27	-0.35	1.59	1.68	1.74	1.17
SD	0.04	0.04	0.05	0.05	0.13	0.08	0.09	0.07	0.09	0.15	0.26	0.39	0.49	0.49	0.59	1.02
MAE	0.05	0.08	0.08	0.07	0.14	0.14	0.14	0.07	0.07	0.13	0.31	0.46	1.59	1.68	1.74	1.31
MSE	0.0	0.01	0.01	0.01	0.03	0.03	0.03	0.01	0.01	0.03	0.14	0.28	2.76	3.08	3.36	2.42

	SFH=Burst; SN=15.0; Av=2.0; Age of the system = 7.6															
	$\Delta \log < Z_{\star} >_L$				$\Delta \log < Z_{\star} >_M$				$\Delta M_{\star}$				ΔA_v			
X^i_{AGN}	0.2	0.4	0.6	0.8	0.2	0.4	0.6	0.8	0.2	0.4	0.6	0.8	0.2	0.4	0.6	0.8
Mean	-0.1	-0.14	-0.38	-0.54	0.02	0.11	0.07	-0.36	-0.55	-0.53	-0.48	-0.11	0.16	0.23	0.2	0.14
SD	0.07	0.16	0.22	0.21	0.18	0.21	0.3	0.35	0.25	0.29	0.42	0.75	0.1	0.08	0.09	0.07
MAE	0.1	0.16	0.39	0.54	0.15	0.2	0.27	0.44	0.55	0.54	0.55	0.63	0.17	0.23	0.2	0.14
MSE	0.02	0.04	0.19	0.33	0.03	0.06	0.1	0.25	0.37	0.37	0.41	0.57	0.04	0.06	0.05	0.03

TABLE A.94

	SFH=Burst; SN=15.0; Av=2.0; Age of the system = 8.0															
	ΔX_{AGN}				$\Delta < \alpha_v >_L$				$\Delta < \log(t_\star) >_L$				$\Delta < \log(t_\star) >_M$			
X^i_{AGN}	0.2	0.4	0.6	0.8	0.2	0.4	0.6	0.8	0.2	0.4	0.6	0.8	0.2	0.4	0.6	0.8
Mean	0.02	0.03	0.02	0.02	-0.19	-0.13	-0.05	-0.03	0.03	-0.05	-0.21	-0.28	0.74	0.68	0.45	0.44
SD	0.02	0.03	0.04	0.04	0.1	0.06	0.07	0.07	0.05	0.1	0.24	0.37	0.4	0.53	0.54	0.6
MAE	0.03	0.04	0.04	0.04	0.19	0.13	0.07	0.06	0.04	0.07	0.22	0.32	0.74	0.68	0.47	0.54
MSE	0.0	0.0	0.0	0.0	0.05	0.02	0.01	0.01	0.0	0.01	0.1	0.22	0.72	0.74	0.5	0.56

	SFH=Burst; SN=15.0; Av=2.0; Age of the system = 8.0															
	$\Delta \log < Z_\star >_L$				$\Delta \log < Z_\star >_M$				$\Delta M_\star$				ΔA_v			
X^i_{AGN}	0.2	0.4	0.6	0.8	0.2	0.4	0.6	0.8	0.2	0.4	0.6	0.8	0.2	0.4	0.6	0.8
Mean	-0.23	-0.48	-0.62	-0.64	-0.13	-0.18	-0.4	-0.54	-0.18	-0.11	0.02	0.05	0.16	0.13	0.07	0.07
SD	0.12	0.19	0.15	0.16	0.12	0.26	0.33	0.28	0.17	0.22	0.25	0.33	0.06	0.06	0.08	0.08
MAE	0.23	0.48	0.62	0.64	0.16	0.25	0.46	0.57	0.2	0.2	0.22	0.26	0.16	0.14	0.09	0.09
MSE	0.07	0.26	0.41	0.43	0.03	0.1	0.27	0.37	0.06	0.06	0.06	0.11	0.03	0.02	0.01	0.01

TABLE A.96

	SFH=Burst; SN=15.0; Av=2.0; Age of the system = 8.4															
	ΔX_{AGN}				$\Delta < \alpha_v >_L$				$\Delta < \log(t_\star) >_L$				$\Delta < \log(t_\star) >_M$			
X^i_{AGN}	0.2	0.4	0.6	0.8	0.2	0.4	0.6	0.8	0.2	0.4	0.6	0.8	0.2	0.4	0.6	0.8
Mean	-0.05	-0.04	-0.02	-0.02	-0.18	-0.05	0.01	0.01	-0.13	-0.18	-0.29	-0.43	0.18	0.17	0.16	0.28
SD	0.02	0.02	0.03	0.04	0.1	0.08	0.06	0.06	0.06	0.11	0.17	0.38	0.21	0.18	0.25	0.36
MAE	0.05	0.04	0.03	0.03	0.18	0.07	0.05	0.05	0.13	0.18	0.29	0.44	0.19	0.18	0.21	0.38
MSE	0.0	0.0	0.0	0.0	0.04	0.01	0.0	0.0	0.02	0.04	0.11	0.33	0.08	0.06	0.09	0.21

	SFH=Burst; SN=15.0; Av=2.0; Age of the system = 8.4															
	$\Delta \log < Z_\star >_L$				$\Delta \log < Z_\star >_M$				$\Delta M_\star$				ΔA_v			
X^i_{AGN}	0.2	0.4	0.6	0.8	0.2	0.4	0.6	0.8	0.2	0.4	0.6	0.8	0.2	0.4	0.6	0.8
Mean	-0.2	-0.35	-0.49	-0.59	-0.14	-0.23	-0.33	-0.49	-0.07	-0.05	-0.02	-0.03	-0.01	-0.01	-0.03	0.0
SD	0.07	0.16	0.19	0.17	0.08	0.17	0.28	0.27	0.09	0.08	0.14	0.25	0.06	0.07	0.07	0.07
MAE	0.2	0.35	0.49	0.59	0.15	0.24	0.37	0.52	0.07	0.07	0.1	0.18	0.05	0.06	0.06	0.06
MSE	0.04	0.15	0.28	0.38	0.03	0.08	0.19	0.32	0.01	0.01	0.02	0.06	0.0	0.0	0.01	0.01

TABLE A.98

	SFH=Burst; SN=15.0; Av=2.0; Age of the system = 8.8															
	ΔX_{AGN}				$\Delta < \alpha_v >_L$				$\Delta < \log(t_\star) >_L$				$\Delta < \log(t_\star) >_M$			
X^i_{AGN}	0.2	0.4	0.6	0.8	0.2	0.4	0.6	0.8	0.2	0.4	0.6	0.8	0.2	0.4	0.6	0.8
Mean	-0.03	-0.03	-0.01	-0.0	-0.24	-0.06	0.01	0.01	-0.07	-0.12	-0.18	-0.2	0.07	0.1	0.11	0.17
SD	0.03	0.05	0.03	0.03	0.16	0.11	0.07	0.07	0.07	0.11	0.2	0.32	0.03	0.1	0.05	0.13
MAE	0.03	0.04	0.03	0.02	0.24	0.1	0.06	0.05	0.07	0.12	0.19	0.28	0.07	0.1	0.11	0.18
MSE	0.0	0.0	0.0	0.0	0.09	0.02	0.01	0.0	0.01	0.03	0.07	0.14	0.01	0.02	0.01	0.05

	SFH=Burst; SN=15.0; Av=2.0; Age of the system = 8.8															
	$\Delta \log < Z_\star >_L$				$\Delta \log < Z_\star >_M$				$\Delta M_\star$				ΔA_v			
X^i_{AGN}	0.2	0.4	0.6	0.8	0.2	0.4	0.6	0.8	0.2	0.4	0.6	0.8	0.2	0.4	0.6	0.8
Mean	-0.04	-0.1	-0.13	-0.24	-0.01	-0.03	-0.04	-0.16	-0.02	-0.05	-0.05	-0.07	0.07	0.04	0.02	0.02
SD	0.09	0.14	0.15	0.23	0.07	0.11	0.13	0.24	0.02	0.09	0.04	0.11	0.04	0.1	0.06	0.07
MAE	0.08	0.16	0.17	0.28	0.06	0.09	0.11	0.22	0.03	0.05	0.05	0.08	0.07	0.07	0.06	0.06
MSE	0.01	0.03	0.04	0.11	0.01	0.01	0.02	0.08	0.0	0.01	0.0	0.02	0.01	0.01	0.0	0.0

TABLE A.100

	SFH=Burst; SN=15.0; Av=2.0; Age of the system = 9.2															
	ΔX_{AGN}				$\Delta < \alpha_v >_L$				$\Delta < \log(t_\star) >_L$				$\Delta < \log(t_\star) >_M$			
X^i_{AGN}	0.2	0.4	0.6	0.8	0.2	0.4	0.6	0.8	0.2	0.4	0.6	0.8	0.2	0.4	0.6	0.8
Mean	0.04	0.06	0.05	0.03	-0.05	-0.01	0.01	0.02	-0.03	-0.05	-0.04	0.04	0.07	0.05	0.11	0.21
SD	0.02	0.02	0.03	0.03	0.1	0.1	0.08	0.06	0.06	0.08	0.13	0.2	0.09	0.11	0.15	0.22
MAE	0.04	0.06	0.05	0.03	0.09	0.07	0.06	0.05	0.06	0.08	0.1	0.17	0.09	0.1	0.15	0.25
MSE	0.0	0.0	0.0	0.0	0.01	0.01	0.01	0.0	0.0	0.01	0.02	0.04	0.01	0.01	0.04	0.09

	SFH=Burst; SN=15.0; Av=2.0; Age of the system = 9.2															
	$\Delta \log < Z_\star >_L$				$\Delta \log < Z_\star >_M$				$\Delta M_\star$				ΔA_v			
X^i_{AGN}	0.2	0.4	0.6	0.8	0.2	0.4	0.6	0.8	0.2	0.4	0.6	0.8	0.2	0.4	0.6	0.8
Mean	0.12	0.2	0.15	-0.0	0.08	0.15	0.1	-0.04	-0.01	0.02	-0.02	-0.07	0.03	0.04	0.03	0.02
SD	0.11	0.13	0.16	0.3	0.11	0.14	0.19	0.29	0.06	0.08	0.11	0.16	0.03	0.05	0.05	0.05
MAE	0.14	0.21	0.18	0.26	0.12	0.18	0.18	0.24	0.05	0.07	0.1	0.14	0.04	0.05	0.05	0.04
MSE	0.03	0.05	0.05	0.09	0.02	0.04	0.05	0.08	0.0	0.01	0.01	0.03	0.0	0.0	0.0	0.0

TABLE A.102

	SFH=Burst; SN=15.0; Av=2.0; Age of the system = 9.6															
	ΔX_{AGN}				$\Delta < \alpha_v >_L$				$\Delta < \log(t_\star) >_L$				$\Delta < \log(t_\star) >_M$			
X^i_{AGN}	0.2	0.4	0.6	0.8	0.2	0.4	0.6	0.8	0.2	0.4	0.6	0.8	0.2	0.4	0.6	0.8
Mean	0.02	0.03	0.03	0.01	-0.03	0.03	0.04	0.03	0.02	0.07	0.08	0.09	0.12	0.16	0.2	0.27
SD	0.03	0.01	0.02	0.02	0.16	0.08	0.08	0.06	0.08	0.07	0.12	0.23	0.08	0.06	0.08	0.12
MAE	0.02	0.03	0.03	0.02	0.13	0.07	0.07	0.05	0.05	0.08	0.12	0.2	0.12	0.16	0.2	0.28
MSE	0.0	0.0	0.0	0.0	0.03	0.01	0.01	0.0	0.01	0.01	0.02	0.06	0.02	0.03	0.05	0.09

	SFH=Burst; SN=15.0; Av=2.0; Age of the system = 9.6															
	$\Delta \log < Z_\star >_L$				$\Delta \log < Z_\star >_M$				$\Delta M_\star$				ΔA_v			
X^i_{AGN}	0.2	0.4	0.6	0.8	0.2	0.4	0.6	0.8	0.2	0.4	0.6	0.8	0.2	0.4	0.6	0.8
Mean	0.02	0.04	0.01	-0.05	-0.02	-0.02	-0.04	-0.1	-0.06	-0.08	-0.1	-0.15	0.01	0.01	-0.0	0.0
SD	0.06	0.07	0.12	0.18	0.04	0.04	0.07	0.14	0.04	0.04	0.06	0.1	0.04	0.03	0.04	0.04
MAE	0.05	0.07	0.1	0.16	0.03	0.03	0.07	0.13	0.06	0.08	0.11	0.15	0.03	0.03	0.03	0.03
MSE	0.0	0.01	0.01	0.04	0.0	0.0	0.01	0.03	0.01	0.01	0.01	0.03	0.0	0.0	0.0	0.0

TABLE A.104

	SFH=Burst; SN=15.0; Av=2.0; Age of the system = 10.0															
	ΔX_{AGN}				$\Delta < \alpha_v >_L$				$\Delta < \log(t_\star) >_L$				$\Delta < \log(t_\star) >_M$			
X^i_{AGN}	0.2	0.4	0.6	0.8	0.2	0.4	0.6	0.8	0.2	0.4	0.6	0.8	0.2	0.4	0.6	0.8
Mean	0.01	0.01	0.01	0.0	0.04	0.07	0.04	0.03	-0.0	0.02	0.01	-0.06	0.03	0.04	0.06	0.09
SD	0.01	0.02	0.06	0.02	0.18	0.1	0.08	0.06	0.04	0.06	0.19	0.28	0.04	0.04	0.07	0.08
MAE	0.01	0.02	0.02	0.02	0.15	0.1	0.07	0.05	0.03	0.04	0.09	0.18	0.03	0.04	0.07	0.1
MSE	0.0	0.0	0.0	0.0	0.03	0.01	0.01	0.0	0.0	0.0	0.04	0.08	0.0	0.0	0.01	0.01

	SFH=Burst; SN=15.0; Av=2.0; Age of the system = 10.0															
	$\Delta \log < Z_\star >_L$				$\Delta \log < Z_\star >_M$				$\Delta M_\star$				ΔA_v			
X^i_{AGN}	0.2	0.4	0.6	0.8	0.2	0.4	0.6	0.8	0.2	0.4	0.6	0.8	0.2	0.4	0.6	0.8
Mean	-0.02	-0.03	-0.05	-0.06	-0.03	-0.03	-0.04	-0.06	-0.02	-0.03	-0.05	-0.05	-0.01	-0.02	-0.02	-0.02
SD	0.03	0.03	0.05	0.09	0.02	0.02	0.03	0.06	0.03	0.03	0.05	0.07	0.03	0.03	0.05	0.05
MAE	0.03	0.04	0.06	0.08	0.03	0.03	0.04	0.06	0.03	0.04	0.05	0.08	0.02	0.03	0.04	0.04
MSE	0.0	0.0	0.01	0.01	0.0	0.0	0.0	0.01	0.0	0.0	0.0	0.01	0.0	0.0	0.0	0.0

TABLE A.106

A.1.6 Tables: Constant SFH, Av=2.0, SN = 15, base: BaseA

	SFH=Constant; SN=15.0; Av=2.0; Age of the system = 6.0															
	ΔX_{AGN}				$\Delta < \alpha_v >_L$				$\Delta < \log(t_\star) >_L$				$\Delta < \log(t_\star) >_M$			
X^i_{AGN}	0.2	0.4	0.6	0.8	0.2	0.4	0.6	0.8	0.2	0.4	0.6	0.8	0.2	0.4	0.6	0.8
Mean	0.09	0.06	0.03	0.0	0.13	-0.06	-0.11	-0.05	0.18	0.22	0.26	0.23	2.14	2.14	2.53	1.52
SD	0.05	0.05	0.04	0.03	0.06	0.06	0.08	0.07	0.12	0.12	0.15	0.15	1.21	1.46	1.51	1.63
MAE	0.09	0.07	0.04	0.02	0.14	0.07	0.12	0.07	0.18	0.22	0.26	0.23	2.14	2.14	2.53	1.52
MSE	0.01	0.01	0.0	0.0	0.02	0.01	0.02	0.01	0.05	0.06	0.09	0.08	6.05	6.7	8.68	4.95

	SFH=Constant; SN=15.0; Av=2.0; Age of the system = 6.0															
	$\Delta \log < Z_\star >_L$				$\Delta \log < Z_\star >_M$				$\Delta M_\star$				ΔA_v			
X^i_{AGN}	0.2	0.4	0.6	0.8	0.2	0.4	0.6	0.8	0.2	0.4	0.6	0.8	0.2	0.4	0.6	0.8
Mean	-0.29	-0.32	-0.31	-0.17	-0.23	-0.22	-0.2	-0.23	-0.59	-0.64	-0.92	-0.58	0.25	0.23	0.21	0.09
SD	0.19	0.22	0.23	0.25	0.21	0.24	0.25	0.26	0.43	0.55	0.72	0.74	0.11	0.12	0.11	0.08
MAE	0.29	0.32	0.32	0.22	0.25	0.26	0.25	0.27	0.6	0.66	0.93	0.59	0.25	0.23	0.21	0.1
MSE	0.12	0.15	0.15	0.09	0.1	0.11	0.1	0.12	0.53	0.71	1.36	0.88	0.07	0.07	0.05	0.01

TABLE A.108

	SFH=Constant; SN=15.0; Av=2.0; Age of the system = 6.4															
	ΔX_{AGN}				$\Delta < \alpha_{\nu} >_{L}$				$\Delta < \log(t_{\star}) >_{L}$				$\Delta < \log(t_{\star}) >_{M}$			
X^{i}_{AGN}	0.2	0.4	0.6	0.8	0.2	0.4	0.6	0.8	0.2	0.4	0.6	0.8	0.2	0.4	0.6	0.8
Mean	0.14	0.11	0.05	0.01	0.18	-0.06	-0.11	-0.07	-0.06	-0.08	-0.06	-0.03	1.75	1.86	1.65	1.49
SD	0.06	0.05	0.04	0.04	0.05	0.07	0.07	0.09	0.13	0.12	0.14	0.16	1.28	1.43	1.58	1.51
MAE	0.14	0.11	0.05	0.03	0.18	0.08	0.11	0.09	0.13	0.12	0.12	0.13	1.8	1.92	1.7	1.56
MSE	0.02	0.01	0.0	0.0	0.03	0.01	0.02	0.01	0.02	0.02	0.02	0.03	4.73	5.53	5.2	4.5

	SFH=Constant; SN=15.0; Av=2.0; Age of the system = 6.4															
	$\Delta \log < Z_{\star} >_{L}$				$\Delta \log < Z_{\star} >_{M}$				$\Delta M_{\star}$				ΔA_{v}			
X^{i}_{AGN}	0.2	0.4	0.6	0.8	0.2	0.4	0.6	0.8	0.2	0.4	0.6	0.8	0.2	0.4	0.6	0.8
Mean	-0.19	-0.19	-0.1	-0.05	-0.16	-0.21	-0.18	-0.17	-0.49	-0.56	-0.62	-0.59	0.35	0.31	0.21	0.1
SD	0.23	0.24	0.2	0.26	0.23	0.24	0.24	0.26	0.48	0.53	0.73	0.69	0.13	0.12	0.1	0.11
MAE	0.21	0.22	0.15	0.2	0.21	0.25	0.24	0.25	0.54	0.61	0.66	0.6	0.35	0.31	0.21	0.12
MSE	0.09	0.09	0.05	0.07	0.08	0.1	0.09	0.1	0.47	0.6	0.91	0.82	0.14	0.11	0.05	0.02

TABLE A.110

	SFH=Constant; SN=15.0; Av=2.0; Age of the system = 6.8															
	ΔX_{AGN}				$\Delta < \alpha_v >_L$				$\Delta < \log(t_\star) >_L$				$\Delta < \log(t_\star) >_M$			
X^i_{AGN}	0.2	0.4	0.6	0.8	0.2	0.4	0.6	0.8	0.2	0.4	0.6	0.8	0.2	0.4	0.6	0.8
Mean	0.16	0.14	0.11	0.07	0.13	-0.04	-0.08	-0.07	0.03	0.01	-0.04	-0.11	1.05	0.93	0.65	1.1
SD	0.06	0.06	0.06	0.05	0.07	0.06	0.1	0.07	0.09	0.11	0.16	0.24	0.86	0.9	0.91	1.34
MAE	0.16	0.14	0.11	0.08	0.13	0.06	0.1	0.08	0.07	0.09	0.13	0.22	1.06	0.96	0.73	1.28
MSE	0.03	0.02	0.02	0.01	0.02	0.01	0.02	0.01	0.01	0.01	0.03	0.07	1.83	1.66	1.26	3.0

	SFH=Constant; SN=15.0; Av=2.0; Age of the system = 6.8															
	$\Delta \log < Z_\star >_L$				$\Delta \log < Z_\star >_M$				$\Delta M_\star$				ΔA_v			
X^i_{AGN}	0.2	0.4	0.6	0.8	0.2	0.4	0.6	0.8	0.2	0.4	0.6	0.8	0.2	0.4	0.6	0.8
Mean	-0.21	-0.22	-0.21	-0.2	-0.22	-0.25	-0.29	-0.33	-0.19	-0.2	-0.16	-0.4	0.4	0.35	0.27	0.19
SD	0.21	0.23	0.28	0.32	0.19	0.22	0.24	0.28	0.31	0.33	0.38	0.64	0.12	0.1	0.13	0.09
MAE	0.24	0.25	0.27	0.29	0.24	0.27	0.31	0.37	0.27	0.28	0.28	0.53	0.4	0.35	0.28	0.2
MSE	0.09	0.1	0.12	0.14	0.09	0.11	0.14	0.19	0.13	0.15	0.17	0.57	0.17	0.13	0.09	0.05

TABLE A.112

	SFH=Constant; SN=15.0; Av=2.0; Age of the system = 7.2															
	ΔX_{AGN}				$\Delta < \alpha_v >_L$				$\Delta < \log(t_\star) >_L$				$\Delta < \log(t_\star) >_M$			
X^i_{AGN}	0.2	0.4	0.6	0.8	0.2	0.4	0.6	0.8	0.2	0.4	0.6	0.8	0.2	0.4	0.6	0.8
Mean	0.17	0.15	0.13	0.08	-0.07	-0.17	-0.15	-0.1	-0.02	-0.05	-0.11	-0.25	1.39	1.22	0.84	0.8
SD	0.06	0.06	0.06	0.06	0.1	0.08	0.08	0.08	0.09	0.12	0.15	0.26	1.12	1.22	1.2	1.17
MAE	0.17	0.15	0.13	0.09	0.1	0.17	0.15	0.11	0.08	0.11	0.15	0.31	1.43	1.35	1.05	1.09
MSE	0.03	0.03	0.02	0.01	0.02	0.03	0.03	0.02	0.01	0.02	0.03	0.13	3.19	2.97	2.15	2.01

	SFH=Constant; SN=15.0; Av=2.0; Age of the system = 7.2															
	$\Delta \log < Z_\star >_L$				$\Delta \log < Z_\star >_M$				$\Delta M_\star$				ΔA_v			
X^i_{AGN}	0.2	0.4	0.6	0.8	0.2	0.4	0.6	0.8	0.2	0.4	0.6	0.8	0.2	0.4	0.6	0.8
Mean	-0.21	-0.23	-0.18	-0.17	0.03	-0.07	-0.15	-0.2	-0.23	-0.23	-0.11	-0.1	0.45	0.37	0.3	0.2
SD	0.12	0.17	0.2	0.31	0.2	0.22	0.23	0.28	0.49	0.6	0.59	0.62	0.13	0.12	0.11	0.11
MAE	0.22	0.24	0.21	0.26	0.17	0.19	0.22	0.27	0.44	0.51	0.45	0.47	0.45	0.37	0.3	0.21
MSE	0.06	0.08	0.07	0.13	0.04	0.05	0.08	0.12	0.3	0.41	0.36	0.4	0.22	0.15	0.1	0.05

TABLE A.114

	SFH=Constant; SN=15.0; Av=2.0; Age of the system = 7.6															
	ΔX_{AGN}				$\Delta < \alpha_{\nu} >_{L}$				$\Delta < \log(t_{\star}) >_{L}$				$\Delta < \log(t_{\star}) >_{M}$			
X^{i}_{AGN}	0.2	0.4	0.6	0.8	0.2	0.4	0.6	0.8	0.2	0.4	0.6	0.8	0.2	0.4	0.6	0.8
Mean	0.15	0.15	0.13	0.09	-0.03	-0.15	-0.14	-0.1	-0.12	-0.17	-0.22	-0.36	1.31	0.94	0.75	0.73
SD	0.04	0.07	0.06	0.05	0.12	0.09	0.09	0.08	0.05	0.1	0.16	0.26	1.11	1.26	1.25	1.43
MAE	0.15	0.15	0.13	0.1	0.1	0.15	0.14	0.11	0.12	0.18	0.23	0.39	1.4	1.22	1.11	1.31
MSE	0.02	0.03	0.02	0.01	0.02	0.03	0.03	0.02	0.02	0.04	0.07	0.2	2.97	2.47	2.11	2.58

	SFH=Constant; SN=15.0; Av=2.0; Age of the system = 7.6															
	$\Delta \log < Z_{\star} >_{L}$				$\Delta \log < Z_{\star} >_{M}$				$\Delta M_{\star}$				ΔA_{v}			
X^{i}_{AGN}	0.2	0.4	0.6	0.8	0.2	0.4	0.6	0.8	0.2	0.4	0.6	0.8	0.2	0.4	0.6	0.8
Mean	-0.16	-0.18	-0.21	-0.21	0.09	-0.02	-0.15	-0.2	-0.15	-0.03	0.03	-0.0	0.37	0.35	0.28	0.21
SD	0.08	0.12	0.21	0.32	0.19	0.21	0.27	0.34	0.53	0.66	0.63	0.81	0.08	0.12	0.12	0.09
MAE	0.16	0.18	0.24	0.29	0.18	0.17	0.25	0.32	0.48	0.58	0.54	0.71	0.37	0.35	0.28	0.21
MSE	0.03	0.04	0.09	0.14	0.04	0.04	0.09	0.15	0.31	0.44	0.4	0.66	0.14	0.14	0.09	0.05

TABLE A.116

	SFH=Constant; SN=15.0; Av=2.0; Age of the system = 8.0															
	ΔX_{AGN}				$\Delta < \alpha_{\nu} >_L$				$\Delta < \log(t_{\star}) >_L$				$\Delta < \log(t_{\star}) >_M$			
X^i_{AGN}	0.2	0.4	0.6	0.8	0.2	0.4	0.6	0.8	0.2	0.4	0.6	0.8	0.2	0.4	0.6	0.8
Mean	0.09	0.12	0.11	0.09	-0.12	-0.17	-0.15	-0.06	-0.17	-0.28	-0.33	-0.33	1.54	1.61	0.92	0.42
SD	0.05	0.05	0.04	0.05	0.14	0.08	0.08	0.08	0.09	0.11	0.16	0.51	0.71	0.87	1.18	1.13
MAE	0.09	0.12	0.11	0.09	0.14	0.17	0.15	0.08	0.17	0.28	0.35	0.46	1.55	1.7	1.3	1.01
MSE	0.01	0.02	0.01	0.01	0.03	0.04	0.03	0.01	0.04	0.09	0.14	0.36	2.88	3.35	2.24	1.45

	SFH=Constant; SN=15.0; Av=2.0; Age of the system = 8.0															
	$\Delta \log < Z_{\star} >_L$				$\Delta \log < Z_{\star} >_M$				$\Delta M_{\star}$				ΔA_v			
X^i_{AGN}	0.2	0.4	0.6	0.8	0.2	0.4	0.6	0.8	0.2	0.4	0.6	0.8	0.2	0.4	0.6	0.8
Mean	-0.23	-0.34	-0.41	-0.37	0.11	0.13	-0.13	-0.23	-0.38	-0.33	0.03	0.43	0.27	0.3	0.27	0.17
SD	0.11	0.17	0.19	0.3	0.17	0.24	0.35	0.29	0.42	0.49	0.67	1.05	0.12	0.1	0.08	0.09
MAE	0.23	0.35	0.41	0.41	0.17	0.24	0.32	0.3	0.46	0.51	0.59	0.74	0.27	0.3	0.27	0.17
MSE	0.06	0.15	0.21	0.23	0.04	0.08	0.14	0.14	0.32	0.35	0.45	1.27	0.09	0.1	0.08	0.04

TABLE A.118

	SFH=Constant; SN=15.0; Av=2.0; Age of the system = 8.4															
	ΔX_{AGN}				$\Delta < \alpha_v >_L$				$\Delta < \log(t_\star) >_L$				$\Delta < \log(t_\star) >_M$			
X^i_{AGN}	0.2	0.4	0.6	0.8	0.2	0.4	0.6	0.8	0.2	0.4	0.6	0.8	0.2	0.4	0.6	0.8
Mean	0.08	0.09	0.08	0.07	-0.17	-0.15	-0.09	-0.05	-0.1	-0.23	-0.36	-0.27	1.29	1.1	0.81	0.49
SD	0.05	0.05	0.05	0.05	0.12	0.07	0.06	0.07	0.09	0.16	0.21	0.33	0.43	0.67	0.84	0.88
MAE	0.08	0.09	0.08	0.08	0.17	0.15	0.09	0.06	0.11	0.23	0.37	0.36	1.29	1.12	0.99	0.83
MSE	0.01	0.01	0.01	0.01	0.04	0.03	0.01	0.01	0.02	0.08	0.17	0.18	1.85	1.65	1.36	1.02

	SFH=Constant; SN=15.0; Av=2.0; Age of the system = 8.4															
	$\Delta \log < Z_\star >_L$				$\Delta \log < Z_\star >_M$				$\Delta M_\star$				ΔA_v			
X^i_{AGN}	0.2	0.4	0.6	0.8	0.2	0.4	0.6	0.8	0.2	0.4	0.6	0.8	0.2	0.4	0.6	0.8
Mean	-0.21	-0.38	-0.5	-0.54	0.08	0.05	-0.16	-0.4	-0.33	-0.18	0.01	0.21	0.27	0.23	0.17	0.14
SD	0.09	0.16	0.16	0.22	0.17	0.25	0.33	0.32	0.26	0.34	0.45	0.63	0.1	0.08	0.09	0.07
MAE	0.21	0.38	0.5	0.54	0.16	0.22	0.3	0.44	0.35	0.33	0.37	0.52	0.27	0.23	0.17	0.15
MSE	0.05	0.17	0.28	0.34	0.04	0.06	0.13	0.26	0.17	0.15	0.2	0.45	0.08	0.06	0.04	0.03

TABLE A.120

	SFH=Constant; SN=15.0; Av=2.0; Age of the system = 8.8															
	ΔX_{AGN}				$\Delta < \alpha_{\nu} >_L$				$\Delta < \log(t_{\star}) >_L$				$\Delta < \log(t_{\star}) >_M$			
X^i_{AGN}	0.2	0.4	0.6	0.8	0.2	0.4	0.6	0.8	0.2	0.4	0.6	0.8	0.2	0.4	0.6	0.8
Mean	0.08	0.08	0.08	0.04	-0.14	-0.11	-0.06	-0.02	-0.02	-0.13	-0.24	-0.34	0.84	0.7	0.56	0.54
SD	0.04	0.06	0.04	0.04	0.12	0.08	0.08	0.06	0.11	0.18	0.24	0.39	0.39	0.44	0.55	0.73
MAE	0.08	0.08	0.08	0.05	0.15	0.11	0.08	0.05	0.09	0.18	0.27	0.43	0.84	0.71	0.65	0.76
MSE	0.01	0.01	0.01	0.0	0.03	0.02	0.01	0.0	0.01	0.05	0.12	0.27	0.85	0.69	0.62	0.82

	SFH=Constant; SN=15.0; Av=2.0; Age of the system = 8.8															
	$\Delta \log < Z_{\star} >_L$				$\Delta \log < Z_{\star} >_M$				$\Delta M_{\star}$				ΔA_v			
X^i_{AGN}	0.2	0.4	0.6	0.8	0.2	0.4	0.6	0.8	0.2	0.4	0.6	0.8	0.2	0.4	0.6	0.8
Mean	-0.23	-0.37	-0.52	-0.58	-0.03	-0.06	-0.23	-0.33	-0.2	-0.09	0.04	0.01	0.24	0.17	0.13	0.08
SD	0.11	0.16	0.17	0.15	0.13	0.23	0.28	0.32	0.2	0.24	0.3	0.51	0.09	0.09	0.08	0.07
MAE	0.24	0.37	0.52	0.58	0.1	0.19	0.3	0.41	0.24	0.21	0.25	0.4	0.24	0.18	0.14	0.09
MSE	0.07	0.16	0.3	0.36	0.02	0.06	0.13	0.21	0.08	0.07	0.09	0.27	0.07	0.04	0.02	0.01

TABLE A.122

	SFH=Constant; SN=15.0; Av=2.0; Age of the system = 9.2															
	ΔX_{AGN}				$\Delta < \alpha_v >_L$				$\Delta < \log(t_\star) >_L$				$\Delta < \log(t_\star) >_M$			
X^i_{AGN}	0.2	0.4	0.6	0.8	0.2	0.4	0.6	0.8	0.2	0.4	0.6	0.8	0.2	0.4	0.6	0.8
Mean	0.07	0.09	0.07	0.05	-0.11	-0.09	-0.04	-0.01	-0.04	-0.04	-0.17	-0.22	0.55	0.49	0.38	0.27
SD	0.04	0.04	0.05	0.04	0.13	0.09	0.08	0.07	0.1	0.17	0.27	0.46	0.26	0.29	0.35	0.45
MAE	0.07	0.09	0.08	0.05	0.13	0.1	0.07	0.06	0.08	0.14	0.26	0.43	0.55	0.49	0.4	0.41
MSE	0.01	0.01	0.01	0.0	0.03	0.02	0.01	0.01	0.01	0.03	0.1	0.26	0.37	0.32	0.27	0.27

	SFH=Constant; SN=15.0; Av=2.0; Age of the system = 9.2															
	$\Delta \log < Z_\star >_L$				$\Delta \log < Z_\star >_M$				$\Delta M_\star$				ΔA_v			
X^i_{AGN}	0.2	0.4	0.6	0.8	0.2	0.4	0.6	0.8	0.2	0.4	0.6	0.8	0.2	0.4	0.6	0.8
Mean	-0.24	-0.32	-0.41	-0.49	-0.04	-0.08	-0.15	-0.31	-0.12	-0.05	0.03	0.12	0.17	0.17	0.11	0.07
SD	0.12	0.14	0.19	0.23	0.14	0.2	0.24	0.33	0.16	0.16	0.25	0.4	0.08	0.08	0.09	0.08
MAE	0.24	0.32	0.41	0.49	0.11	0.17	0.23	0.38	0.16	0.14	0.2	0.28	0.18	0.17	0.12	0.09
MSE	0.07	0.12	0.2	0.29	0.02	0.05	0.08	0.2	0.04	0.03	0.06	0.17	0.04	0.04	0.02	0.01

TABLE A.124

	SFH=Constant; SN=15.0; Av=2.0; Age of the system = 9.6															
	ΔX_{AGN}				$\Delta < \alpha_v >_L$				$\Delta < \log(t_\star) >_L$				$\Delta < \log(t_\star) >_M$			
X^i_{AGN}	0.2	0.4	0.6	0.8	0.2	0.4	0.6	0.8	0.2	0.4	0.6	0.8	0.2	0.4	0.6	0.8
Mean	0.07	0.08	0.08	0.06	-0.11	-0.05	-0.02	-0.01	-0.07	-0.12	-0.1	0.01	0.44	0.44	0.31	0.1
SD	0.05	0.04	0.05	0.04	0.13	0.09	0.08	0.06	0.13	0.2	0.28	0.49	0.16	0.21	0.32	0.47
MAE	0.07	0.08	0.08	0.06	0.13	0.08	0.06	0.04	0.12	0.18	0.24	0.39	0.44	0.45	0.37	0.32
MSE	0.01	0.01	0.01	0.0	0.03	0.01	0.01	0.0	0.02	0.06	0.09	0.24	0.22	0.24	0.2	0.24

	SFH=Constant; SN=15.0; Av=2.0; Age of the system = 9.6															
	$\Delta \log < Z_\star >_L$				$\Delta \log < Z_\star >_M$				$\Delta M_\star$				ΔA_v			
X^i_{AGN}	0.2	0.4	0.6	0.8	0.2	0.4	0.6	0.8	0.2	0.4	0.6	0.8	0.2	0.4	0.6	0.8
Mean	-0.21	-0.27	-0.25	-0.33	-0.0	-0.01	-0.01	-0.17	-0.12	-0.1	0.0	0.13	0.12	0.1	0.09	0.08
SD	0.09	0.12	0.21	0.29	0.1	0.17	0.23	0.34	0.1	0.16	0.23	0.37	0.09	0.09	0.07	0.07
MAE	0.21	0.27	0.28	0.38	0.08	0.14	0.19	0.32	0.13	0.16	0.2	0.29	0.13	0.12	0.1	0.09
MSE	0.05	0.09	0.11	0.19	0.01	0.03	0.05	0.15	0.03	0.04	0.06	0.15	0.02	0.02	0.01	0.01

TABLE A.126

	SFH=Constant; SN=15.0; Av=2.0; Age of the system = 10.0															
	ΔX_{AGN}				$\Delta < \alpha_v >_L$				$\Delta < \log(t_\star) >_L$				$\Delta < \log(t_\star) >_M$			
X^i_{AGN}	0.2	0.4	0.6	0.8	0.2	0.4	0.6	0.8	0.2	0.4	0.6	0.8	0.2	0.4	0.6	0.8
Mean	0.07	0.08	0.06	0.05	-0.1	-0.05	-0.02	-0.0	-0.06	-0.09	-0.14	0.05	0.24	0.19	0.13	0.03
SD	0.05	0.04	0.04	0.05	0.17	0.09	0.07	0.06	0.13	0.18	0.29	0.49	0.12	0.15	0.21	0.36
MAE	0.07	0.08	0.07	0.06	0.15	0.08	0.06	0.04	0.12	0.17	0.26	0.42	0.25	0.22	0.21	0.31
MSE	0.01	0.01	0.01	0.01	0.04	0.01	0.01	0.0	0.02	0.04	0.1	0.24	0.07	0.06	0.06	0.13

	SFH=Constant; SN=15.0; Av=2.0; Age of the system = 10.0															
	$\Delta \log < Z_\star >_L$				$\Delta \log < Z_\star >_M$				$\Delta M_\star$				ΔA_v			
X^i_{AGN}	0.2	0.4	0.6	0.8	0.2	0.4	0.6	0.8	0.2	0.4	0.6	0.8	0.2	0.4	0.6	0.8
Mean	-0.2	-0.21	-0.28	-0.34	0.0	0.03	-0.03	-0.26	-0.07	-0.01	0.06	0.17	0.1	0.1	0.07	0.06
SD	0.09	0.12	0.15	0.25	0.07	0.14	0.17	0.31	0.08	0.13	0.15	0.31	0.09	0.07	0.06	0.08
MAE	0.2	0.21	0.28	0.36	0.06	0.11	0.14	0.35	0.09	0.11	0.12	0.27	0.12	0.1	0.07	0.08
MSE	0.05	0.06	0.1	0.18	0.01	0.02	0.03	0.16	0.01	0.02	0.03	0.12	0.02	0.01	0.01	0.01

TABLE A.128

A.1.7 Tables: Instantaneous burst SFH, SN=5, Av=0.0, base: BaseA

	SFH=Burst; SN=5.0; Av=0.0; Age of the system = 6.0															
	ΔX_{AGN}				$\Delta < \alpha_v >_L$				$\Delta < \log(t_\star) >_L$				$\Delta < \log(t_\star) >_M$			
X^i_{AGN}	0.2	0.4	0.6	0.8	0.2	0.4	0.6	0.8	0.2	0.4	0.6	0.8	0.2	0.4	0.6	0.8
Mean	-0.02	-0.05	-0.04	-0.04	0.0	-0.05	-0.0	0.01	0.19	0.28	0.27	0.27	1.26	1.59	1.38	0.98
SD	0.04	0.05	0.04	0.05	0.18	0.12	0.07	0.06	0.12	0.17	0.14	0.16	1.37	1.58	1.51	1.22
MAE	0.03	0.05	0.04	0.04	0.14	0.09	0.05	0.05	0.19	0.28	0.27	0.27	1.26	1.59	1.38	0.98
MSE	0.0	0.0	0.0	0.0	0.03	0.02	0.0	0.0	0.05	0.11	0.1	0.1	3.47	5.0	4.19	2.45

	SFH=Burst; SN=5.0; Av=0.0; Age of the system = 6.0															
	$\Delta \log < Z_\star >_L$				$\Delta \log < Z_\star >_M$				$\Delta M_\star$				ΔA_v			
X^i_{AGN}	0.2	0.4	0.6	0.8	0.2	0.4	0.6	0.8	0.2	0.4	0.6	0.8	0.2	0.4	0.6	0.8
Mean	-0.06	-0.04	-0.02	-0.01	-0.14	-0.22	-0.17	-0.13	-0.42	-0.61	-0.53	-0.37	-0.0	-0.0	-0.0	-0.01
SD	0.08	0.1	0.1	0.17	0.2	0.24	0.22	0.2	0.54	0.7	0.7	0.52	0.0	0.01	0.01	0.05
MAE	0.07	0.08	0.08	0.14	0.17	0.23	0.19	0.17	0.42	0.61	0.53	0.38	0.0	0.0	0.0	0.01
MSE	0.01	0.01	0.01	0.03	0.06	0.11	0.08	0.06	0.46	0.85	0.76	0.41	0.0	0.0	0.0	0.0

TABLE A.130

	SFH=Burst; SN=5.0; Av=0.0; Age of the system = 6.4															
	ΔX_{AGN}				$\Delta < \alpha_v >_L$				$\Delta < \log(t_\star) >_L$				$\Delta < \log(t_\star) >_M$			
X^i_{AGN}	0.2	0.4	0.6	0.8	0.2	0.4	0.6	0.8	0.2	0.4	0.6	0.8	0.2	0.4	0.6	0.8
Mean	-0.01	-0.02	-0.04	-0.04	0.01	-0.0	-0.01	0.01	-0.04	-0.02	-0.01	-0.01	1.22	0.73	0.74	0.86
SD	0.03	0.04	0.05	0.04	0.12	0.1	0.06	0.07	0.08	0.11	0.12	0.14	1.35	1.25	1.32	1.24
MAE	0.03	0.03	0.04	0.04	0.1	0.07	0.05	0.05	0.07	0.09	0.09	0.1	1.25	0.79	0.8	0.9
MSE	0.0	0.0	0.0	0.0	0.01	0.01	0.0	0.0	0.01	0.01	0.01	0.02	3.31	2.09	2.28	2.28

	SFH=Burst; SN=5.0; Av=0.0; Age of the system = 6.4															
	$\Delta \log < Z_\star >_L$				$\Delta \log < Z_\star >_M$				$\Delta M_\star$				ΔA_v			
X^i_{AGN}	0.2	0.4	0.6	0.8	0.2	0.4	0.6	0.8	0.2	0.4	0.6	0.8	0.2	0.4	0.6	0.8
Mean	0.14	0.1	0.11	0.13	-0.09	-0.04	-0.02	0.01	-0.44	-0.3	-0.36	-0.38	-0.0	-0.0	-0.0	-0.01
SD	0.09	0.14	0.13	0.16	0.23	0.25	0.24	0.23	0.54	0.56	0.68	0.62	0.0	0.0	0.0	0.03
MAE	0.14	0.15	0.14	0.17	0.16	0.18	0.17	0.18	0.46	0.34	0.39	0.44	0.0	0.0	0.0	0.01
MSE	0.03	0.03	0.03	0.04	0.06	0.06	0.06	0.05	0.48	0.41	0.59	0.53	0.0	0.0	0.0	0.0

TABLE A.132

	SFH=Burst; SN=5.0; Av=0.0; Age of the system = 6.8															
	ΔX_{AGN}				$\Delta < \alpha_{\nu} >_L$				$\Delta < \log(t_{\star}) >_L$				$\Delta < \log(t_{\star}) >_M$			
X^i_{AGN}	0.2	0.4	0.6	0.8	0.2	0.4	0.6	0.8	0.2	0.4	0.6	0.8	0.2	0.4	0.6	0.8
Mean	-0.0	0.0	-0.02	-0.01	0.03	0.04	0.0	0.03	0.09	0.09	0.09	-0.02	0.33	0.45	0.63	0.35
SD	0.05	0.06	0.06	0.1	0.19	0.11	0.09	0.09	0.09	0.14	0.16	0.26	0.31	0.57	0.88	0.74
MAE	0.04	0.04	0.04	0.05	0.14	0.09	0.07	0.06	0.11	0.14	0.15	0.22	0.33	0.47	0.66	0.54
MSE	0.0	0.0	0.0	0.01	0.04	0.01	0.01	0.01	0.02	0.03	0.03	0.07	0.2	0.53	1.16	0.67

	SFH=Burst; SN=5.0; Av=0.0; Age of the system = 6.8															
	$\Delta \log < Z_{\star} >_L$				$\Delta \log < Z_{\star} >_M$				$\Delta M_{\star}$				ΔA_v			
X^i_{AGN}	0.2	0.4	0.6	0.8	0.2	0.4	0.6	0.8	0.2	0.4	0.6	0.8	0.2	0.4	0.6	0.8
Mean	-0.14	-0.11	-0.12	-0.06	-0.27	-0.26	-0.2	-0.15	-0.27	-0.33	-0.44	-0.32	-0.0	-0.0	-0.0	-0.0
SD	0.18	0.24	0.26	0.32	0.2	0.25	0.26	0.33	0.16	0.35	0.49	0.51	0.0	0.0	0.0	0.01
MAE	0.17	0.2	0.2	0.26	0.28	0.3	0.27	0.3	0.28	0.36	0.46	0.4	0.0	0.0	0.0	0.0
MSE	0.05	0.07	0.08	0.11	0.11	0.13	0.11	0.13	0.1	0.23	0.43	0.36	0.0	0.0	0.0	0.0

TABLE A.134

	SFH=Burst; SN=5.0; Av=0.0; Age of the system = 7.2															
	ΔX_{AGN}				$\Delta < \alpha_v >_L$				$\Delta < \log(t_\star) >_L$				$\Delta < \log(t_\star) >_M$			
X^i_{AGN}	0.2	0.4	0.6	0.8	0.2	0.4	0.6	0.8	0.2	0.4	0.6	0.8	0.2	0.4	0.6	0.8
Mean	-0.03	-0.01	-0.01	-0.04	-0.16	-0.08	-0.05	-0.05	-0.05	-0.11	-0.17	-0.26	1.92	1.72	1.29	1.08
SD	0.05	0.06	0.07	0.12	0.21	0.14	0.1	0.12	0.1	0.13	0.2	0.31	1.0	1.06	1.28	1.3
MAE	0.05	0.05	0.05	0.07	0.2	0.11	0.08	0.08	0.09	0.13	0.2	0.32	1.93	1.76	1.41	1.29
MSE	0.0	0.0	0.01	0.02	0.07	0.02	0.01	0.02	0.01	0.03	0.07	0.17	4.68	4.08	3.29	2.84

	SFH=Burst; SN=5.0; Av=0.0; Age of the system = 7.2															
	$\Delta \log < Z_\star >_L$				$\Delta \log < Z_\star >_M$				$\Delta M_\star$				ΔA_v			
X^i_{AGN}	0.2	0.4	0.6	0.8	0.2	0.4	0.6	0.8	0.2	0.4	0.6	0.8	0.2	0.4	0.6	0.8
Mean	-0.14	-0.16	-0.12	-0.12	-0.18	-0.18	-0.2	-0.19	-0.84	-0.7	-0.53	-0.39	-0.02	-0.0	-0.01	-0.0
SD	0.09	0.14	0.19	0.32	0.27	0.25	0.26	0.32	0.56	0.59	0.8	0.85	0.06	0.02	0.03	0.01
MAE	0.14	0.18	0.18	0.28	0.25	0.24	0.25	0.28	0.87	0.76	0.75	0.69	0.02	0.0	0.01	0.0
MSE	0.03	0.04	0.05	0.12	0.11	0.09	0.11	0.14	1.02	0.84	0.93	0.88	0.0	0.0	0.0	0.0

TABLE A.136

	SFH=Burst; SN=5.0; Av=0.0; Age of the system = 7.6															
	ΔX_{AGN}				$\Delta < \alpha_v >_L$				$\Delta < \log(t_\star) >_L$				$\Delta < \log(t_\star) >_M$			
X^i_{AGN}	0.2	0.4	0.6	0.8	0.2	0.4	0.6	0.8	0.2	0.4	0.6	0.8	0.2	0.4	0.6	0.8
Mean	-0.03	-0.05	-0.03	-0.02	-0.16	-0.15	-0.07	-0.02	-0.13	-0.27	-0.44	-0.52	0.98	1.33	1.15	0.52
SD	0.05	0.06	0.08	0.09	0.19	0.14	0.08	0.1	0.09	0.15	0.22	0.29	0.78	0.86	0.93	1.15
MAE	0.05	0.07	0.06	0.06	0.18	0.16	0.08	0.07	0.13	0.27	0.44	0.52	0.99	1.35	1.24	0.99
MSE	0.0	0.01	0.01	0.01	0.06	0.04	0.01	0.01	0.02	0.09	0.24	0.35	1.57	2.51	2.19	1.58

	SFH=Burst; SN=5.0; Av=0.0; Age of the system = 7.6															
	$\Delta \log < Z_\star >_L$				$\Delta \log < Z_\star >_M$				$\Delta M_\star$				ΔA_v			
X^i_{AGN}	0.2	0.4	0.6	0.8	0.2	0.4	0.6	0.8	0.2	0.4	0.6	0.8	0.2	0.4	0.6	0.8
Mean	-0.21	-0.36	-0.47	-0.43	-0.21	-0.22	-0.34	-0.36	-0.36	-0.52	-0.3	-0.01	-0.03	-0.01	-0.01	-0.0
SD	0.11	0.18	0.18	0.26	0.22	0.27	0.32	0.32	0.38	0.51	0.57	0.81	0.07	0.05	0.04	0.01
MAE	0.21	0.36	0.47	0.44	0.25	0.28	0.41	0.41	0.39	0.57	0.53	0.66	0.03	0.01	0.01	0.0
MSE	0.06	0.16	0.25	0.25	0.09	0.12	0.22	0.23	0.28	0.53	0.42	0.65	0.0	0.0	0.0	0.0

TABLE A.138

	SFH=Burst; SN=5.0; Av=0.0; Age of the system = 8.0															
	ΔX_{AGN}				$\Delta < \alpha_v >_L$				$\Delta < \log(t_\star) >_L$				$\Delta < \log(t_\star) >_M$			
X^i_{AGN}	0.2	0.4	0.6	0.8	0.2	0.4	0.6	0.8	0.2	0.4	0.6	0.8	0.2	0.4	0.6	0.8
Mean	-0.04	-0.04	-0.07	-0.04	-0.24	-0.11	-0.09	-0.01	-0.1	-0.22	-0.43	-0.6	0.32	0.41	0.49	0.58
SD	0.04	0.07	0.09	0.1	0.18	0.14	0.12	0.11	0.07	0.12	0.19	0.34	0.47	0.55	0.61	0.87
MAE	0.04	0.06	0.07	0.07	0.24	0.14	0.1	0.06	0.1	0.22	0.43	0.6	0.34	0.44	0.55	0.84
MSE	0.0	0.01	0.01	0.01	0.09	0.03	0.02	0.01	0.02	0.06	0.22	0.47	0.32	0.47	0.62	1.11

	SFH=Burst; SN=5.0; Av=0.0; Age of the system = 8.0															
	$\Delta \log < Z_\star >_L$				$\Delta \log < Z_\star >_M$				$\Delta M_\star$				ΔA_v			
X^i_{AGN}	0.2	0.4	0.6	0.8	0.2	0.4	0.6	0.8	0.2	0.4	0.6	0.8	0.2	0.4	0.6	0.8
Mean	-0.3	-0.48	-0.56	-0.58	-0.29	-0.44	-0.44	-0.44	-0.09	-0.1	-0.12	-0.16	-0.01	-0.02	-0.02	-0.01
SD	0.18	0.19	0.15	0.17	0.2	0.21	0.26	0.3	0.21	0.28	0.39	0.68	0.04	0.07	0.04	0.03
MAE	0.3	0.48	0.56	0.58	0.3	0.45	0.46	0.48	0.15	0.2	0.29	0.58	0.01	0.02	0.02	0.01
MSE	0.12	0.27	0.33	0.37	0.12	0.24	0.27	0.28	0.05	0.09	0.17	0.49	0.0	0.01	0.0	0.0

TABLE A.140

	SFH=Burst; SN=5.0; Av=0.0; Age of the system = 8.4															
	ΔX_{AGN}				$\Delta < \alpha_v >_L$				$\Delta < \log(t_\star) >_L$				$\Delta < \log(t_\star) >_M$			
X^i_{AGN}	0.2	0.4	0.6	0.8	0.2	0.4	0.6	0.8	0.2	0.4	0.6	0.8	0.2	0.4	0.6	0.8
Mean	-0.08	-0.08	-0.08	-0.07	-0.25	-0.06	-0.02	-0.02	-0.18	-0.26	-0.38	-0.64	0.32	0.37	0.52	0.41
SD	0.04	0.06	0.09	0.11	0.21	0.13	0.11	0.1	0.1	0.13	0.23	0.32	0.39	0.41	0.46	0.62
MAE	0.08	0.08	0.09	0.09	0.27	0.12	0.08	0.07	0.18	0.26	0.38	0.64	0.34	0.42	0.55	0.62
MSE	0.01	0.01	0.02	0.02	0.1	0.02	0.01	0.01	0.04	0.08	0.2	0.51	0.25	0.3	0.48	0.56

	SFH=Burst; SN=5.0; Av=0.0; Age of the system = 8.4															
	$\Delta \log < Z_\star >_L$				$\Delta \log < Z_\star >_M$				$\Delta M_\star$				ΔA_v			
X^i_{AGN}	0.2	0.4	0.6	0.8	0.2	0.4	0.6	0.8	0.2	0.4	0.6	0.8	0.2	0.4	0.6	0.8
Mean	-0.34	-0.49	-0.52	-0.6	-0.25	-0.37	-0.38	-0.49	-0.16	-0.18	-0.27	-0.18	-0.07	-0.07	-0.05	-0.02
SD	0.19	0.2	0.18	0.15	0.2	0.25	0.3	0.27	0.18	0.21	0.29	0.55	0.09	0.08	0.08	0.05
MAE	0.34	0.49	0.52	0.6	0.26	0.39	0.43	0.51	0.17	0.21	0.3	0.47	0.07	0.07	0.05	0.02
MSE	0.15	0.28	0.31	0.39	0.1	0.2	0.23	0.32	0.06	0.08	0.16	0.33	0.01	0.01	0.01	0.0

TABLE A.142

	SFH=Burst; SN=5.0; Av=0.0; Age of the system = 8.8															
	ΔX_{AGN}				$\Delta < \alpha_v >_L$				$\Delta < \log(t_\star) >_L$				$\Delta < \log(t_\star) >_M$			
X^i_{AGN}	0.2	0.4	0.6	0.8	0.2	0.4	0.6	0.8	0.2	0.4	0.6	0.8	0.2	0.4	0.6	0.8
Mean	-0.07	-0.07	-0.07	-0.05	-0.21	-0.04	0.0	0.01	-0.17	-0.26	-0.36	-0.55	0.11	0.17	0.28	0.33
SD	0.05	0.07	0.09	0.12	0.26	0.14	0.13	0.11	0.11	0.18	0.27	0.41	0.13	0.2	0.24	0.3
MAE	0.07	0.08	0.08	0.08	0.26	0.11	0.09	0.08	0.17	0.26	0.37	0.57	0.12	0.18	0.28	0.35
MSE	0.01	0.01	0.01	0.02	0.11	0.02	0.02	0.01	0.04	0.1	0.2	0.48	0.03	0.07	0.14	0.2

	SFH=Burst; SN=5.0; Av=0.0; Age of the system = 8.8															
	$\Delta \log < Z_\star >_L$				$\Delta \log < Z_\star >_M$				$\Delta M_\star$				ΔA_v			
X^i_{AGN}	0.2	0.4	0.6	0.8	0.2	0.4	0.6	0.8	0.2	0.4	0.6	0.8	0.2	0.4	0.6	0.8
Mean	-0.14	-0.21	-0.29	-0.4	-0.08	-0.13	-0.22	-0.33	-0.08	-0.1	-0.17	-0.17	-0.02	-0.03	-0.03	-0.04
SD	0.18	0.2	0.23	0.26	0.18	0.21	0.25	0.3	0.08	0.12	0.19	0.32	0.04	0.06	0.06	0.07
MAE	0.18	0.25	0.33	0.42	0.15	0.2	0.27	0.38	0.08	0.11	0.17	0.26	0.02	0.03	0.03	0.04
MSE	0.05	0.08	0.14	0.23	0.04	0.06	0.11	0.2	0.01	0.03	0.06	0.13	0.0	0.0	0.0	0.01

TABLE A.144

	SFH=Burst; SN=5.0; Av=0.0; Age of the system = 9.2															
	ΔX_{AGN}				$\Delta < \alpha_v >_L$				$\Delta < \log(t_\star) >_L$				$\Delta < \log(t_\star) >_M$			
X^i_{AGN}	0.2	0.4	0.6	0.8	0.2	0.4	0.6	0.8	0.2	0.4	0.6	0.8	0.2	0.4	0.6	0.8
Mean	0.01	-0.0	0.0	-0.0	-0.08	-0.02	0.03	0.03	-0.15	-0.15	-0.15	-0.15	0.08	0.1	0.19	0.29
SD	0.07	0.09	0.08	0.1	0.19	0.15	0.11	0.09	0.18	0.24	0.26	0.47	0.16	0.16	0.23	0.25
MAE	0.06	0.06	0.06	0.06	0.17	0.11	0.08	0.07	0.17	0.19	0.23	0.38	0.14	0.16	0.24	0.31
MSE	0.0	0.01	0.01	0.01	0.04	0.02	0.01	0.01	0.05	0.08	0.09	0.24	0.03	0.04	0.09	0.15

	SFH=Burst; SN=5.0; Av=0.0; Age of the system = 9.2															
	$\Delta \log < Z_\star >_L$				$\Delta \log < Z_\star >_M$				$\Delta M_\star$				ΔA_v			
X^i_{AGN}	0.2	0.4	0.6	0.8	0.2	0.4	0.6	0.8	0.2	0.4	0.6	0.8	0.2	0.4	0.6	0.8
Mean	0.06	-0.01	-0.12	-0.24	0.05	-0.01	-0.11	-0.22	-0.03	-0.04	-0.08	-0.12	-0.01	-0.02	-0.02	-0.02
SD	0.2	0.26	0.33	0.37	0.21	0.27	0.34	0.39	0.11	0.12	0.17	0.22	0.02	0.07	0.05	0.04
MAE	0.18	0.22	0.3	0.37	0.18	0.23	0.31	0.39	0.09	0.1	0.15	0.19	0.01	0.02	0.02	0.02
MSE	0.04	0.07	0.12	0.19	0.05	0.08	0.13	0.2	0.01	0.02	0.04	0.06	0.0	0.01	0.0	0.0

TABLE A.146

	SFH=Burst; SN=5.0; Av=0.0; Age of the system = 9.6															
	ΔX_{AGN}				$\Delta < \alpha_v >_L$				$\Delta < \log(t_\star) >_L$				$\Delta < \log(t_\star) >_M$			
X^i_{AGN}	0.2	0.4	0.6	0.8	0.2	0.4	0.6	0.8	0.2	0.4	0.6	0.8	0.2	0.4	0.6	0.8
Mean	-0.0	-0.01	-0.01	-0.02	-0.07	-0.03	-0.01	0.01	-0.05	-0.08	-0.05	-0.14	0.14	0.17	0.23	0.2
SD	0.06	0.09	0.09	0.09	0.17	0.17	0.13	0.11	0.13	0.23	0.31	0.51	0.11	0.11	0.17	0.26
MAE	0.04	0.05	0.06	0.05	0.16	0.12	0.09	0.07	0.1	0.17	0.23	0.38	0.15	0.17	0.26	0.28
MSE	0.0	0.01	0.01	0.01	0.03	0.03	0.02	0.01	0.02	0.06	0.1	0.28	0.03	0.04	0.08	0.11

	SFH=Burst; SN=5.0; Av=0.0; Age of the system = 9.6															
	$\Delta \log < Z_\star >_L$				$\Delta \log < Z_\star >_M$				$\Delta M_\star$				ΔA_v			
X^i_{AGN}	0.2	0.4	0.6	0.8	0.2	0.4	0.6	0.8	0.2	0.4	0.6	0.8	0.2	0.4	0.6	0.8
Mean	0.02	0.02	-0.06	-0.16	-0.03	-0.03	-0.11	-0.16	-0.07	-0.09	-0.11	-0.07	-0.01	-0.02	-0.02	-0.04
SD	0.12	0.14	0.21	0.3	0.08	0.1	0.17	0.28	0.07	0.09	0.13	0.23	0.03	0.04	0.04	0.05
MAE	0.1	0.12	0.17	0.28	0.06	0.08	0.16	0.26	0.08	0.1	0.14	0.19	0.01	0.02	0.02	0.04
MSE	0.02	0.02	0.05	0.12	0.01	0.01	0.04	0.1	0.01	0.01	0.03	0.06	0.0	0.0	0.0	0.0

TABLE A.148

	SFH=Burst; SN=5.0; Av=0.0; Age of the system = 10.0															
	ΔX_{AGN}				$\Delta < \alpha_{\nu} >_{L}$				$\Delta < \log(t_{\star}) >_{L}$				$\Delta < \log(t_{\star}) >_{M}$			
X^{i}_{AGN}	0.2	0.4	0.6	0.8	0.2	0.4	0.6	0.8	0.2	0.4	0.6	0.8	0.2	0.4	0.6	0.8
Mean	0.0	-0.01	-0.04	-0.01	-0.08	-0.02	-0.01	0.02	-0.03	-0.08	-0.21	-0.23	0.05	0.05	0.05	0.06
SD	0.03	0.07	0.11	0.08	0.15	0.17	0.16	0.11	0.1	0.21	0.4	0.46	0.07	0.08	0.1	0.13
MAE	0.02	0.04	0.06	0.04	0.14	0.13	0.12	0.08	0.08	0.15	0.28	0.32	0.07	0.08	0.09	0.11
MSE	0.0	0.0	0.01	0.01	0.03	0.03	0.03	0.01	0.01	0.05	0.21	0.26	0.01	0.01	0.01	0.02

	SFH=Burst; SN=5.0; Av=0.0; Age of the system = 10.0															
	$\Delta \log < Z_{\star} >_{L}$				$\Delta \log < Z_{\star} >_{M}$				$\Delta M_{\star}$				ΔA_{v}			
X^{i}_{AGN}	0.2	0.4	0.6	0.8	0.2	0.4	0.6	0.8	0.2	0.4	0.6	0.8	0.2	0.4	0.6	0.8
Mean	-0.03	-0.05	-0.07	-0.08	-0.03	-0.05	-0.07	-0.1	-0.03	-0.03	-0.02	-0.01	-0.02	-0.03	-0.04	-0.05
SD	0.07	0.08	0.13	0.16	0.03	0.05	0.09	0.19	0.05	0.06	0.1	0.13	0.03	0.06	0.04	0.06
MAE	0.06	0.07	0.11	0.13	0.04	0.05	0.08	0.13	0.05	0.05	0.08	0.1	0.02	0.03	0.04	0.05
MSE	0.01	0.01	0.02	0.03	0.0	0.0	0.01	0.05	0.0	0.0	0.01	0.02	0.0	0.0	0.0	0.01

TABLE A.150

A.1.8 Tables: Instantaneous burst SFH, SN=5, Av=1.0, base: BaseA

	SFH=Burst; SN=5.0; Av=1.0; Age of the system = 6.0															
	ΔX_{AGN}				$\Delta < \alpha_v >_L$				$\Delta < \log(t_\star) >_L$				$\Delta < \log(t_\star) >_M$			
X^i_{AGN}	0.2	0.4	0.6	0.8	0.2	0.4	0.6	0.8	0.2	0.4	0.6	0.8	0.2	0.4	0.6	0.8
Mean	0.08	0.07	0.05	0.02	0.07	-0.14	-0.19	-0.13	0.34	0.3	0.28	0.36	2.52	1.81	1.82	1.54
SD	0.08	0.08	0.06	0.06	0.14	0.1	0.1	0.11	0.18	0.23	0.23	0.24	1.2	1.49	1.48	1.44
MAE	0.09	0.09	0.07	0.05	0.13	0.15	0.19	0.15	0.34	0.3	0.28	0.36	2.52	1.81	1.82	1.54
MSE	0.01	0.01	0.01	0.0	0.03	0.03	0.04	0.03	0.15	0.14	0.13	0.19	7.76	5.52	5.51	4.45

	SFH=Burst; SN=5.0; Av=1.0; Age of the system = 6.0															
	$\Delta \log < Z_\star >_L$				$\Delta \log < Z_\star >_M$				$\Delta M_\star$				ΔA_v			
X^i_{AGN}	0.2	0.4	0.6	0.8	0.2	0.4	0.6	0.8	0.2	0.4	0.6	0.8	0.2	0.4	0.6	0.8
Mean	-0.57	-0.52	-0.51	-0.47	-0.39	-0.45	-0.44	-0.4	-0.83	-0.57	-0.58	-0.51	0.36	0.33	0.29	0.18
SD	0.18	0.23	0.26	0.3	0.26	0.28	0.27	0.28	0.54	0.65	0.67	0.73	0.12	0.15	0.13	0.13
MAE	0.57	0.52	0.52	0.5	0.42	0.48	0.47	0.42	0.83	0.62	0.62	0.57	0.36	0.34	0.3	0.2
MSE	0.35	0.32	0.33	0.31	0.22	0.28	0.27	0.24	0.98	0.74	0.79	0.79	0.15	0.13	0.1	0.05

TABLE A.152

	SFH=Burst; SN=5.0; Av=1.0; Age of the system = 6.4															
	ΔX_{AGN}				$\Delta < \alpha_\nu >_L$				$\Delta < \log(t_\star) >_L$				$\Delta < \log(t_\star) >_M$			
X^i_{AGN}	0.2	0.4	0.6	0.8	0.2	0.4	0.6	0.8	0.2	0.4	0.6	0.8	0.2	0.4	0.6	0.8
Mean	0.22	0.16	0.1	0.03	0.13	-0.16	-0.22	-0.17	-0.04	-0.09	-0.15	-0.03	1.47	1.18	0.58	0.82
SD	0.09	0.08	0.05	0.05	0.1	0.09	0.12	0.12	0.22	0.16	0.17	0.36	1.49	1.39	1.15	1.2
MAE	0.22	0.17	0.1	0.05	0.14	0.16	0.22	0.18	0.18	0.14	0.18	0.24	1.56	1.27	0.75	0.97
MSE	0.05	0.03	0.01	0.0	0.03	0.03	0.06	0.04	0.05	0.03	0.05	0.13	4.39	3.32	1.67	2.11

	SFH=Burst; SN=5.0; Av=1.0; Age of the system = 6.4															
	$\Delta \log < Z_\star >_L$				$\Delta \log < Z_\star >_M$				$\Delta M_\star$				ΔA_v			
X^i_{AGN}	0.2	0.4	0.6	0.8	0.2	0.4	0.6	0.8	0.2	0.4	0.6	0.8	0.2	0.4	0.6	0.8
Mean	-0.49	-0.44	-0.41	-0.36	-0.46	-0.38	-0.41	-0.36	-0.43	-0.29	-0.16	-0.34	0.59	0.49	0.38	0.24
SD	0.25	0.25	0.32	0.33	0.23	0.25	0.29	0.28	0.64	0.58	0.47	0.62	0.16	0.15	0.13	0.12
MAE	0.5	0.45	0.44	0.41	0.47	0.4	0.42	0.39	0.58	0.47	0.27	0.41	0.59	0.49	0.38	0.24
MSE	0.3	0.25	0.27	0.24	0.27	0.21	0.25	0.21	0.59	0.42	0.24	0.5	0.37	0.26	0.16	0.07

TABLE A.154

	SFH=Burst; SN=5.0; Av=1.0; Age of the system = 6.8															
	ΔX_{AGN}				$\Delta < \alpha_v >_L$				$\Delta < \log(t_\star) >_L$				$\Delta < \log(t_\star) >_M$			
X^i_{AGN}	0.2	0.4	0.6	0.8	0.2	0.4	0.6	0.8	0.2	0.4	0.6	0.8	0.2	0.4	0.6	0.8
Mean	0.24	0.2	0.17	0.1	-0.0	-0.13	-0.15	-0.14	0.13	0.01	-0.07	-0.03	1.26	1.0	0.99	1.21
SD	0.1	0.08	0.08	0.07	0.13	0.16	0.11	0.14	0.14	0.17	0.23	0.37	1.11	1.17	1.13	1.34
MAE	0.24	0.2	0.17	0.1	0.1	0.17	0.15	0.16	0.14	0.11	0.16	0.27	1.3	1.07	1.12	1.42
MSE	0.07	0.05	0.04	0.01	0.02	0.04	0.03	0.04	0.04	0.03	0.06	0.14	2.82	2.37	2.26	3.25

	SFH=Burst; SN=5.0; Av=1.0; Age of the system = 6.8															
	$\Delta \log < Z_\star >_L$				$\Delta \log < Z_\star >_M$				$\Delta M_\star$				ΔA_v			
X^i_{AGN}	0.2	0.4	0.6	0.8	0.2	0.4	0.6	0.8	0.2	0.4	0.6	0.8	0.2	0.4	0.6	0.8
Mean	-0.44	-0.38	-0.41	-0.32	-0.35	-0.29	-0.31	-0.22	-0.22	-0.12	-0.12	-0.21	0.58	0.47	0.38	0.27
SD	0.22	0.28	0.3	0.35	0.27	0.26	0.3	0.36	0.59	0.57	0.54	0.98	0.17	0.17	0.14	0.13
MAE	0.44	0.41	0.43	0.4	0.39	0.32	0.35	0.34	0.47	0.43	0.44	0.72	0.58	0.47	0.38	0.28
MSE	0.24	0.23	0.26	0.23	0.19	0.15	0.18	0.18	0.4	0.34	0.31	1.01	0.36	0.25	0.16	0.09

TABLE A.156

	SFH=Burst; SN=5.0; Av=1.0; Age of the system = 7.2															
	ΔX_{AGN}				$\Delta < \alpha_v >_L$				$\Delta < \log(t_\star) >_L$				$\Delta < \log(t_\star) >_M$			
X^i_{AGN}	0.2	0.4	0.6	0.8	0.2	0.4	0.6	0.8	0.2	0.4	0.6	0.8	0.2	0.4	0.6	0.8
Mean	0.06	0.12	0.13	0.09	-0.33	-0.26	-0.27	-0.21	0.01	-0.09	-0.22	-0.26	2.2	2.01	1.65	1.35
SD	0.11	0.09	0.1	0.06	0.18	0.16	0.18	0.16	0.12	0.14	0.29	0.54	0.84	1.0	1.15	1.42
MAE	0.1	0.12	0.15	0.09	0.34	0.26	0.28	0.22	0.09	0.15	0.28	0.48	2.2	2.04	1.77	1.67
MSE	0.01	0.02	0.03	0.01	0.14	0.09	0.1	0.07	0.01	0.03	0.13	0.36	5.54	5.03	4.06	3.84

	SFH=Burst; SN=5.0; Av=1.0; Age of the system = 7.2															
	$\Delta \log < Z_\star >_L$				$\Delta \log < Z_\star >_M$				$\Delta M_\star$				ΔA_v			
X^i_{AGN}	0.2	0.4	0.6	0.8	0.2	0.4	0.6	0.8	0.2	0.4	0.6	0.8	0.2	0.4	0.6	0.8
Mean	-0.07	-0.08	-0.1	-0.33	0.01	-0.02	-0.05	-0.19	-0.91	-0.67	-0.32	-0.17	0.26	0.32	0.35	0.28
SD	0.11	0.17	0.27	0.33	0.21	0.3	0.28	0.38	0.49	0.66	0.84	1.27	0.26	0.15	0.19	0.16
MAE	0.11	0.15	0.23	0.39	0.15	0.23	0.22	0.34	0.94	0.84	0.74	0.97	0.31	0.32	0.36	0.28
MSE	0.02	0.04	0.08	0.22	0.04	0.09	0.08	0.18	1.06	0.88	0.8	1.64	0.13	0.12	0.16	0.1

TABLE A.158

	SFH=Burst; SN=5.0; Av=1.0; Age of the system = 7.6															
	ΔX_{AGN}				$\Delta < \alpha_v >_L$				$\Delta < \log(t_\star) >_L$				$\Delta < \log(t_\star) >_M$			
X^i_{AGN}	0.2	0.4	0.6	0.8	0.2	0.4	0.6	0.8	0.2	0.4	0.6	0.8	0.2	0.4	0.6	0.8
Mean	0.06	0.08	0.05	0.04	-0.25	-0.29	-0.18	-0.1	0.05	-0.0	-0.24	-0.41	1.61	1.59	1.29	1.19
SD	0.08	0.11	0.1	0.08	0.23	0.16	0.12	0.11	0.17	0.23	0.3	0.49	0.69	0.76	0.88	1.17
MAE	0.09	0.11	0.09	0.08	0.29	0.29	0.19	0.12	0.14	0.18	0.31	0.53	1.61	1.59	1.37	1.51
MSE	0.01	0.02	0.01	0.01	0.11	0.11	0.05	0.02	0.03	0.05	0.15	0.41	3.06	3.09	2.43	2.79

	SFH=Burst; SN=5.0; Av=1.0; Age of the system = 7.6															
	$\Delta \log < Z_\star >_L$				$\Delta \log < Z_\star >_M$				$\Delta M_\star$				ΔA_v			
X^i_{AGN}	0.2	0.4	0.6	0.8	0.2	0.4	0.6	0.8	0.2	0.4	0.6	0.8	0.2	0.4	0.6	0.8
Mean	-0.13	-0.25	-0.43	-0.43	-0.11	-0.09	-0.3	-0.28	-0.56	-0.51	-0.3	-0.21	0.26	0.31	0.19	0.15
SD	0.16	0.22	0.23	0.28	0.27	0.29	0.32	0.35	0.38	0.44	0.57	0.95	0.24	0.21	0.17	0.11
MAE	0.17	0.28	0.45	0.46	0.23	0.26	0.38	0.37	0.59	0.59	0.51	0.82	0.3	0.33	0.23	0.16
MSE	0.04	0.11	0.24	0.26	0.08	0.09	0.19	0.2	0.46	0.46	0.42	0.94	0.13	0.14	0.07	0.03

TABLE A.160

	SFH=Burst; SN=5.0; Av=1.0; Age of the system = 8.0															
	ΔX_{AGN}				$\Delta < \alpha_v >_L$				$\Delta < \log(t_\star) >_L$				$\Delta < \log(t_\star) >_M$			
X^i_{AGN}	0.2	0.4	0.6	0.8	0.2	0.4	0.6	0.8	0.2	0.4	0.6	0.8	0.2	0.4	0.6	0.8
Mean	0.01	0.01	-0.03	-0.03	-0.3	-0.24	-0.15	-0.09	0.01	-0.06	-0.21	-0.38	0.72	0.6	0.72	0.95
SD	0.05	0.05	0.1	0.07	0.19	0.14	0.15	0.16	0.12	0.19	0.35	0.45	0.64	0.53	0.57	0.76
MAE	0.04	0.04	0.07	0.06	0.3	0.24	0.17	0.13	0.1	0.12	0.3	0.47	0.73	0.62	0.75	1.02
MSE	0.0	0.0	0.01	0.01	0.12	0.08	0.05	0.03	0.01	0.04	0.17	0.34	0.93	0.65	0.85	1.49

	SFH=Burst; SN=5.0; Av=1.0; Age of the system = 8.0															
	$\Delta \log < Z_\star >_L$				$\Delta \log < Z_\star >_M$				$\Delta M_\star$				ΔA_v			
X^i_{AGN}	0.2	0.4	0.6	0.8	0.2	0.4	0.6	0.8	0.2	0.4	0.6	0.8	0.2	0.4	0.6	0.8
Mean	-0.4	-0.54	-0.59	-0.51	-0.28	-0.38	-0.4	-0.36	-0.19	-0.1	-0.2	-0.39	0.17	0.17	0.1	0.09
SD	0.21	0.16	0.16	0.19	0.27	0.27	0.29	0.29	0.31	0.27	0.32	0.65	0.14	0.13	0.2	0.17
MAE	0.4	0.54	0.59	0.51	0.32	0.42	0.43	0.4	0.27	0.21	0.29	0.6	0.18	0.19	0.17	0.13
MSE	0.2	0.32	0.37	0.3	0.15	0.22	0.24	0.22	0.13	0.08	0.14	0.57	0.05	0.05	0.05	0.04

TABLE A.162

	SFH=Burst; SN=5.0; Av=1.0; Age of the system = 8.4															
	ΔX_{AGN}				$\Delta < \alpha_{\nu} >_{L}$				$\Delta < \log(t_{\star}) >_{L}$				$\Delta < \log(t_{\star}) >_{M}$			
X^{i}_{AGN}	0.2	0.4	0.6	0.8	0.2	0.4	0.6	0.8	0.2	0.4	0.6	0.8	0.2	0.4	0.6	0.8
Mean	-0.07	-0.08	-0.06	-0.05	-0.27	-0.14	-0.07	-0.08	-0.15	-0.22	-0.27	-0.4	0.27	0.34	0.38	0.6
SD	0.05	0.06	0.06	0.06	0.18	0.16	0.14	0.14	0.14	0.18	0.27	0.46	0.33	0.42	0.44	0.51
MAE	0.07	0.08	0.06	0.06	0.27	0.17	0.12	0.13	0.16	0.23	0.29	0.47	0.31	0.39	0.45	0.68
MSE	0.01	0.01	0.01	0.01	0.11	0.04	0.03	0.03	0.04	0.08	0.14	0.36	0.18	0.29	0.33	0.62

	SFH=Burst; SN=5.0; Av=1.0; Age of the system = 8.4															
	$\Delta \log < Z_{\star} >_{L}$				$\Delta \log < Z_{\star} >_{M}$				$\Delta M_{\star}$				ΔA_{v}			
X^{i}_{AGN}	0.2	0.4	0.6	0.8	0.2	0.4	0.6	0.8	0.2	0.4	0.6	0.8	0.2	0.4	0.6	0.8
Mean	-0.29	-0.45	-0.52	-0.54	-0.19	-0.34	-0.4	-0.39	-0.12	-0.15	-0.16	-0.31	-0.03	-0.02	0.02	0.06
SD	0.21	0.24	0.19	0.2	0.21	0.25	0.26	0.31	0.16	0.21	0.26	0.41	0.16	0.15	0.15	0.14
MAE	0.3	0.45	0.52	0.54	0.22	0.36	0.41	0.44	0.14	0.18	0.22	0.4	0.14	0.12	0.12	0.12
MSE	0.13	0.26	0.31	0.33	0.08	0.18	0.23	0.25	0.04	0.07	0.09	0.26	0.03	0.02	0.02	0.02

TABLE A.164

	SFH=Burst; SN=5.0; Av=1.0; Age of the system = 8.8															
	ΔX_{AGN}				$\Delta < \alpha_{\nu} >_L$				$\Delta < \log(t_{\star}) >_L$				$\Delta < \log(t_{\star}) >_M$			
X^i_{AGN}	0.2	0.4	0.6	0.8	0.2	0.4	0.6	0.8	0.2	0.4	0.6	0.8	0.2	0.4	0.6	0.8
Mean	-0.05	-0.07	-0.05	-0.04	-0.23	-0.15	-0.05	-0.06	-0.1	-0.18	-0.24	-0.26	0.14	0.19	0.25	0.36
SD	0.05	0.05	0.07	0.11	0.22	0.2	0.13	0.13	0.11	0.19	0.36	0.41	0.16	0.19	0.21	0.26
MAE	0.06	0.07	0.06	0.06	0.27	0.2	0.11	0.11	0.11	0.21	0.29	0.36	0.14	0.2	0.25	0.36
MSE	0.01	0.01	0.01	0.01	0.1	0.06	0.02	0.02	0.02	0.07	0.19	0.24	0.04	0.07	0.1	0.19

	SFH=Burst; SN=5.0; Av=1.0; Age of the system = 8.8															
	$\Delta \log < Z_{\star} >_L$				$\Delta \log < Z_{\star} >_M$				$\Delta M_{\star}$				ΔA_v			
X^i_{AGN}	0.2	0.4	0.6	0.8	0.2	0.4	0.6	0.8	0.2	0.4	0.6	0.8	0.2	0.4	0.6	0.8
Mean	-0.11	-0.2	-0.3	-0.33	-0.06	-0.12	-0.24	-0.3	-0.06	-0.1	-0.11	-0.18	0.05	0.05	0.02	0.05
SD	0.19	0.2	0.27	0.3	0.17	0.21	0.28	0.33	0.1	0.12	0.15	0.23	0.1	0.13	0.13	0.19
MAE	0.18	0.24	0.36	0.36	0.14	0.19	0.3	0.36	0.08	0.11	0.12	0.22	0.09	0.11	0.1	0.12
MSE	0.05	0.08	0.17	0.2	0.03	0.06	0.14	0.2	0.01	0.02	0.03	0.08	0.01	0.02	0.02	0.04

TABLE A.166

	SFH=Burst; SN=5.0; Av=1.0; Age of the system = 9.2															
	ΔX_{AGN}				$\Delta < \alpha_{\nu} >_{L}$				$\Delta < \log(t_{\star}) >_{L}$				$\Delta < \log(t_{\star}) >_{M}$			
X^{i}_{AGN}	0.2	0.4	0.6	0.8	0.2	0.4	0.6	0.8	0.2	0.4	0.6	0.8	0.2	0.4	0.6	0.8
Mean	0.02	0.01	0.02	0.01	-0.25	-0.13	-0.04	-0.04	-0.05	-0.07	0.01	0.07	0.14	0.15	0.25	0.3
SD	0.05	0.08	0.06	0.06	0.25	0.18	0.17	0.14	0.14	0.19	0.21	0.34	0.16	0.18	0.22	0.27
MAE	0.04	0.06	0.05	0.04	0.29	0.17	0.13	0.1	0.11	0.16	0.16	0.27	0.17	0.2	0.28	0.33
MSE	0.0	0.01	0.0	0.0	0.12	0.05	0.03	0.02	0.02	0.04	0.04	0.12	0.05	0.06	0.11	0.16

	SFH=Burst; SN=5.0; Av=1.0; Age of the system = 9.2															
	$\Delta \log < Z_{\star} >_{L}$				$\Delta \log < Z_{\star} >_{M}$				$\Delta M_{\star}$				ΔA_{v}			
X^{i}_{AGN}	0.2	0.4	0.6	0.8	0.2	0.4	0.6	0.8	0.2	0.4	0.6	0.8	0.2	0.4	0.6	0.8
Mean	0.06	0.0	-0.12	-0.26	0.04	-0.01	-0.14	-0.26	-0.04	-0.05	-0.1	-0.12	0.08	0.06	0.04	0.05
SD	0.17	0.26	0.3	0.39	0.18	0.25	0.3	0.4	0.1	0.14	0.16	0.22	0.07	0.09	0.11	0.13
MAE	0.15	0.22	0.27	0.4	0.15	0.22	0.27	0.42	0.08	0.12	0.15	0.2	0.09	0.08	0.09	0.09
MSE	0.03	0.07	0.1	0.22	0.03	0.06	0.11	0.23	0.01	0.02	0.03	0.06	0.01	0.01	0.01	0.02

TABLE A.168

	SFH=Burst; SN=5.0; Av=1.0; Age of the system = 9.6															
	ΔX_{AGN}				$\Delta < \alpha_v >_L$				$\Delta < \log(t_\star) >_L$				$\Delta < \log(t_\star) >_M$			
X^i_{AGN}	0.2	0.4	0.6	0.8	0.2	0.4	0.6	0.8	0.2	0.4	0.6	0.8	0.2	0.4	0.6	0.8
Mean	0.01	-0.0	0.01	0.01	-0.21	-0.12	-0.02	-0.02	0.01	-0.02	0.08	-0.0	0.18	0.21	0.28	0.27
SD	0.03	0.06	0.03	0.06	0.26	0.2	0.16	0.16	0.12	0.19	0.21	0.36	0.12	0.13	0.14	0.23
MAE	0.03	0.04	0.03	0.04	0.28	0.18	0.12	0.11	0.09	0.15	0.18	0.29	0.18	0.21	0.28	0.32
MSE	0.0	0.0	0.0	0.0	0.11	0.05	0.03	0.03	0.01	0.04	0.05	0.13	0.05	0.06	0.1	0.13

	SFH=Burst; SN=5.0; Av=1.0; Age of the system = 9.6															
	$\Delta \log < Z_\star >_L$				$\Delta \log < Z_\star >_M$				$\Delta M_\star$				ΔA_v			
X^i_{AGN}	0.2	0.4	0.6	0.8	0.2	0.4	0.6	0.8	0.2	0.4	0.6	0.8	0.2	0.4	0.6	0.8
Mean	0.03	0.01	-0.05	-0.13	-0.03	-0.04	-0.09	-0.16	-0.06	-0.09	-0.14	-0.1	0.04	0.03	0.02	0.01
SD	0.12	0.14	0.18	0.31	0.09	0.12	0.14	0.28	0.08	0.09	0.1	0.22	0.08	0.07	0.1	0.12
MAE	0.1	0.11	0.15	0.29	0.07	0.08	0.13	0.24	0.09	0.11	0.15	0.19	0.07	0.06	0.08	0.08
MSE	0.01	0.02	0.03	0.11	0.01	0.02	0.03	0.1	0.01	0.02	0.03	0.06	0.01	0.01	0.01	0.01

TABLE A.170

	SFH=Burst; SN=5.0; Av=1.0; Age of the system = 10.0															
	ΔX_{AGN}				$\Delta < \alpha_{\nu} >_{L}$				$\Delta < \log(t_{\star}) >_{L}$				$\Delta < \log(t_{\star}) >_{M}$			
X^{i}_{AGN}	0.2	0.4	0.6	0.8	0.2	0.4	0.6	0.8	0.2	0.4	0.6	0.8	0.2	0.4	0.6	0.8
Mean	-0.0	0.0	0.0	-0.0	-0.16	-0.15	-0.01	-0.03	-0.03	-0.04	-0.05	-0.14	0.06	0.06	0.07	0.05
SD	0.04	0.03	0.03	0.04	0.22	0.22	0.18	0.15	0.13	0.16	0.2	0.3	0.07	0.09	0.09	0.12
MAE	0.03	0.02	0.03	0.03	0.23	0.2	0.13	0.11	0.09	0.12	0.15	0.23	0.07	0.1	0.09	0.11
MSE	0.0	0.0	0.0	0.0	0.07	0.07	0.03	0.02	0.02	0.03	0.04	0.11	0.01	0.01	0.01	0.02

	SFH=Burst; SN=5.0; Av=1.0; Age of the system = 10.0															
	$\Delta \log < Z_{\star} >_{L}$				$\Delta \log < Z_{\star} >_{M}$				$\Delta M_{\star}$				ΔA_{v}			
X^{i}_{AGN}	0.2	0.4	0.6	0.8	0.2	0.4	0.6	0.8	0.2	0.4	0.6	0.8	0.2	0.4	0.6	0.8
Mean	-0.03	-0.03	-0.05	-0.11	-0.03	-0.03	-0.06	-0.11	-0.03	-0.02	-0.02	0.03	0.0	0.01	-0.01	-0.0
SD	0.07	0.08	0.14	0.17	0.04	0.05	0.11	0.14	0.05	0.06	0.09	0.13	0.05	0.08	0.09	0.1
MAE	0.06	0.07	0.1	0.15	0.04	0.04	0.08	0.12	0.05	0.05	0.08	0.11	0.04	0.06	0.07	0.08
MSE	0.01	0.01	0.02	0.04	0.0	0.0	0.02	0.03	0.0	0.0	0.01	0.02	0.0	0.01	0.01	0.01

TABLE A.172

A.1.9 Tables: Instantaneous burst SFH, SN=5, Av=2.0, base: BaseA

	SFH=Burst; SN=5.0; Av=2.0; Age of the system = 6.0															
	ΔX_{AGN}				$\Delta < \alpha_{\nu} >_{L}$				$\Delta < \log(t_{\star}) >_{L}$				$\Delta < \log(t_{\star}) >_{M}$			
X^{i}_{AGN}	0.2	0.4	0.6	0.8	0.2	0.4	0.6	0.8	0.2	0.4	0.6	0.8	0.2	0.4	0.6	0.8
Mean	0.12	0.1	0.06	0.01	0.12	-0.14	-0.17	-0.13	0.35	0.26	0.3	0.32	2.4	1.7	1.55	1.29
SD	0.1	0.06	0.07	0.09	0.17	0.11	0.1	0.12	0.19	0.2	0.25	0.28	1.4	1.5	1.54	1.38
MAE	0.14	0.1	0.07	0.06	0.18	0.14	0.17	0.15	0.35	0.26	0.3	0.32	2.4	1.7	1.55	1.29
MSE	0.03	0.01	0.01	0.01	0.04	0.03	0.04	0.03	0.16	0.11	0.15	0.18	7.7	5.12	4.77	3.57

	SFH=Burst; SN=5.0; Av=2.0; Age of the system = 6.0															
	$\Delta \log < Z_{\star} >_{L}$				$\Delta \log < Z_{\star} >_{M}$				$\Delta M_{\star}$				ΔA_{v}			
X^{i}_{AGN}	0.2	0.4	0.6	0.8	0.2	0.4	0.6	0.8	0.2	0.4	0.6	0.8	0.2	0.4	0.6	0.8
Mean	-0.51	-0.58	-0.5	-0.48	-0.41	-0.44	-0.44	-0.47	-0.76	-0.51	-0.51	-0.47	0.38	0.37	0.27	0.18
SD	0.22	0.19	0.24	0.29	0.28	0.31	0.3	0.26	0.58	0.63	0.71	0.74	0.16	0.1	0.12	0.13
MAE	0.52	0.58	0.5	0.5	0.44	0.47	0.48	0.47	0.78	0.56	0.57	0.51	0.38	0.37	0.28	0.2
MSE	0.31	0.37	0.31	0.32	0.25	0.29	0.29	0.28	0.92	0.65	0.77	0.77	0.17	0.15	0.09	0.05

TABLE A.174

	SFH=Burst; SN=5.0; Av=2.0; Age of the system = 6.4															
	ΔX_{AGN}				$\Delta < \alpha_{\nu} >_{L}$				$\Delta < \log(t_{\star}) >_{L}$				$\Delta < \log(t_{\star}) >_{M}$			
X^{i}_{AGN}	0.2	0.4	0.6	0.8	0.2	0.4	0.6	0.8	0.2	0.4	0.6	0.8	0.2	0.4	0.6	0.8
Mean	0.21	0.15	0.09	0.04	0.12	-0.13	-0.22	-0.17	-0.05	-0.11	-0.07	-0.05	1.52	1.02	1.11	1.05
SD	0.1	0.08	0.08	0.06	0.15	0.1	0.14	0.11	0.19	0.15	0.19	0.24	1.35	1.39	1.31	1.4
MAE	0.21	0.15	0.1	0.06	0.16	0.14	0.23	0.18	0.16	0.15	0.16	0.2	1.6	1.13	1.2	1.21
MSE	0.05	0.03	0.01	0.01	0.04	0.03	0.07	0.04	0.04	0.04	0.04	0.06	4.13	2.97	2.93	3.08

	SFH=Burst; SN=5.0; Av=2.0; Age of the system = 6.4															
	$\Delta \log < Z_{\star} >_{L}$				$\Delta \log < Z_{\star} >_{M}$				$\Delta M_{\star}$				ΔA_{v}			
X^{i}_{AGN}	0.2	0.4	0.6	0.8	0.2	0.4	0.6	0.8	0.2	0.4	0.6	0.8	0.2	0.4	0.6	0.8
Mean	-0.48	-0.42	-0.34	-0.38	-0.43	-0.38	-0.32	-0.37	-0.42	-0.29	-0.33	-0.39	0.57	0.46	0.37	0.25
SD	0.26	0.32	0.3	0.32	0.27	0.3	0.3	0.32	0.59	0.61	0.58	0.73	0.16	0.18	0.17	0.11
MAE	0.49	0.47	0.37	0.42	0.45	0.41	0.36	0.4	0.55	0.43	0.42	0.54	0.57	0.47	0.38	0.26
MSE	0.3	0.28	0.21	0.25	0.26	0.23	0.19	0.23	0.52	0.45	0.44	0.69	0.35	0.24	0.17	0.08

TABLE A.176

	SFH=Burst; SN=5.0; Av=2.0; Age of the system = 6.8															
	ΔX_{AGN}				$\Delta < \alpha_v >_L$				$\Delta < \log(t_\star) >_L$				$\Delta < \log(t_\star) >_M$			
X^i_{AGN}	0.2	0.4	0.6	0.8	0.2	0.4	0.6	0.8	0.2	0.4	0.6	0.8	0.2	0.4	0.6	0.8
Mean	0.23	0.19	0.15	0.08	0.03	-0.12	-0.15	-0.12	0.09	0.02	0.01	-0.09	1.09	0.99	1.06	1.04
SD	0.09	0.08	0.08	0.08	0.13	0.12	0.11	0.11	0.13	0.16	0.25	0.52	1.02	1.24	1.21	1.24
MAE	0.23	0.19	0.15	0.1	0.11	0.13	0.16	0.13	0.11	0.12	0.18	0.37	1.1	1.08	1.17	1.28
MSE	0.06	0.04	0.03	0.01	0.02	0.03	0.04	0.03	0.02	0.03	0.06	0.28	2.23	2.52	2.59	2.62

	SFH=Burst; SN=5.0; Av=2.0; Age of the system = 6.8															
	$\Delta \log < Z_\star >_L$				$\Delta \log < Z_\star >_M$				$\Delta M_\star$				ΔA_v			
X^i_{AGN}	0.2	0.4	0.6	0.8	0.2	0.4	0.6	0.8	0.2	0.4	0.6	0.8	0.2	0.4	0.6	0.8
Mean	-0.4	-0.38	-0.37	-0.42	-0.31	-0.29	-0.26	-0.31	-0.11	-0.16	-0.26	-0.31	0.54	0.45	0.36	0.23
SD	0.22	0.26	0.29	0.3	0.26	0.31	0.29	0.28	0.49	0.7	0.68	0.67	0.16	0.14	0.14	0.14
MAE	0.4	0.39	0.41	0.46	0.36	0.36	0.33	0.35	0.39	0.54	0.55	0.57	0.54	0.45	0.36	0.24
MSE	0.2	0.21	0.22	0.27	0.16	0.19	0.16	0.18	0.25	0.51	0.53	0.54	0.31	0.22	0.15	0.07

TABLE A.178

	SFH=Burst; SN=5.0; Av=2.0; Age of the system = 7.2															
	ΔX_{AGN}				$\Delta < \alpha_v >_L$				$\Delta < \log(t_\star) >_L$				$\Delta < \log(t_\star) >_M$			
X^i_{AGN}	0.2	0.4	0.6	0.8	0.2	0.4	0.6	0.8	0.2	0.4	0.6	0.8	0.2	0.4	0.6	0.8
Mean	0.06	0.11	0.14	0.1	-0.28	-0.23	-0.21	-0.18	0.01	-0.11	-0.21	-0.33	2.16	1.62	1.73	1.16
SD	0.09	0.1	0.09	0.06	0.22	0.2	0.13	0.13	0.11	0.17	0.27	0.62	0.7	1.17	1.17	1.5
MAE	0.09	0.13	0.15	0.1	0.3	0.25	0.21	0.19	0.09	0.16	0.28	0.56	2.16	1.71	1.79	1.58
MSE	0.01	0.02	0.03	0.01	0.12	0.09	0.06	0.05	0.01	0.04	0.12	0.49	5.18	4.0	4.36	3.59

	SFH=Burst; SN=5.0; Av=2.0; Age of the system = 7.2															
	$\Delta \log < Z_\star >_L$				$\Delta \log < Z_\star >_M$				$\Delta M_\star$				ΔA_v			
X^i_{AGN}	0.2	0.4	0.6	0.8	0.2	0.4	0.6	0.8	0.2	0.4	0.6	0.8	0.2	0.4	0.6	0.8
Mean	-0.06	-0.04	-0.05	-0.16	-0.01	-0.04	-0.08	-0.15	-0.85	-0.46	-0.44	-0.07	0.25	0.3	0.31	0.27
SD	0.11	0.16	0.24	0.38	0.2	0.24	0.32	0.37	0.39	0.77	0.81	1.1	0.21	0.2	0.16	0.12
MAE	0.09	0.14	0.19	0.34	0.14	0.19	0.25	0.33	0.85	0.79	0.79	0.95	0.27	0.31	0.32	0.27
MSE	0.02	0.03	0.06	0.17	0.04	0.06	0.11	0.16	0.87	0.81	0.85	1.21	0.11	0.13	0.12	0.09

TABLE A.180

	SFH=Burst; SN=5.0; Av=2.0; Age of the system = 7.6															
	ΔX_{AGN}				$\Delta < \alpha_v >_L$				$\Delta < \log(t_\star) >_L$				$\Delta < \log(t_\star) >_M$			
X^i_{AGN}	0.2	0.4	0.6	0.8	0.2	0.4	0.6	0.8	0.2	0.4	0.6	0.8	0.2	0.4	0.6	0.8
Mean	0.03	0.06	0.06	0.05	-0.28	-0.25	-0.21	-0.14	-0.01	-0.0	-0.26	-0.31	1.38	1.63	1.25	1.08
SD	0.11	0.12	0.1	0.07	0.23	0.17	0.12	0.12	0.2	0.2	0.37	0.57	0.82	0.7	0.89	1.11
MAE	0.09	0.11	0.09	0.08	0.3	0.26	0.21	0.15	0.15	0.16	0.39	0.54	1.39	1.64	1.31	1.38
MSE	0.01	0.02	0.01	0.01	0.13	0.09	0.06	0.04	0.04	0.04	0.21	0.42	2.58	3.16	2.37	2.39

	SFH=Burst; SN=5.0; Av=2.0; Age of the system = 7.6															
	$\Delta \log < Z_\star >_L$				$\Delta \log < Z_\star >_M$				$\Delta M_\star$				ΔA_v			
X^i_{AGN}	0.2	0.4	0.6	0.8	0.2	0.4	0.6	0.8	0.2	0.4	0.6	0.8	0.2	0.4	0.6	0.8
Mean	-0.15	-0.22	-0.43	-0.5	-0.15	-0.06	-0.22	-0.39	-0.5	-0.59	-0.26	-0.01	0.17	0.27	0.21	0.18
SD	0.14	0.22	0.23	0.27	0.24	0.28	0.34	0.34	0.38	0.45	0.63	1.17	0.29	0.22	0.15	0.12
MAE	0.17	0.26	0.44	0.52	0.24	0.24	0.34	0.43	0.52	0.62	0.54	0.76	0.27	0.31	0.22	0.18
MSE	0.04	0.1	0.24	0.33	0.08	0.08	0.16	0.27	0.39	0.55	0.46	1.38	0.11	0.12	0.07	0.05

TABLE A.182

	SFH=Burst; SN=5.0; Av=2.0; Age of the system = 8.0															
	ΔX_{AGN}				$\Delta < \alpha_v >_L$				$\Delta < \log(t_\star) >_L$				$\Delta < \log(t_\star) >_M$			
X^i_{AGN}	0.2	0.4	0.6	0.8	0.2	0.4	0.6	0.8	0.2	0.4	0.6	0.8	0.2	0.4	0.6	0.8
Mean	0.01	0.01	-0.01	-0.02	-0.28	-0.18	-0.12	-0.07	0.02	-0.06	-0.18	-0.33	0.6	0.71	0.67	0.78
SD	0.05	0.07	0.07	0.12	0.22	0.14	0.12	0.12	0.11	0.18	0.31	0.5	0.53	0.56	0.57	0.72
MAE	0.04	0.05	0.05	0.06	0.3	0.19	0.13	0.1	0.08	0.14	0.26	0.45	0.61	0.72	0.72	0.88
MSE	0.0	0.0	0.01	0.02	0.13	0.05	0.03	0.02	0.01	0.04	0.13	0.36	0.65	0.82	0.78	1.13

	SFH=Burst; SN=5.0; Av=2.0; Age of the system = 8.0															
	$\Delta \log < Z_\star >_L$				$\Delta \log < Z_\star >_M$				$\Delta M_\star$				ΔA_v			
X^i_{AGN}	0.2	0.4	0.6	0.8	0.2	0.4	0.6	0.8	0.2	0.4	0.6	0.8	0.2	0.4	0.6	0.8
Mean	-0.32	-0.5	-0.58	-0.62	-0.24	-0.37	-0.45	-0.45	-0.13	-0.17	-0.17	-0.2	0.17	0.13	0.09	0.06
SD	0.22	0.23	0.17	0.15	0.25	0.28	0.26	0.3	0.24	0.28	0.33	0.56	0.15	0.12	0.13	0.21
MAE	0.33	0.5	0.58	0.62	0.28	0.41	0.47	0.49	0.19	0.25	0.28	0.49	0.19	0.15	0.13	0.14
MSE	0.15	0.3	0.36	0.41	0.12	0.21	0.27	0.29	0.07	0.11	0.14	0.35	0.05	0.03	0.03	0.05

TABLE A.184

	SFH=Burst; SN=5.0; Av=2.0; Age of the system = 8.4															
	ΔX_{AGN}				$\Delta < \alpha_v >_L$				$\Delta < \log(t_\star) >_L$				$\Delta < \log(t_\star) >_M$			
X^i_{AGN}	0.2	0.4	0.6	0.8	0.2	0.4	0.6	0.8	0.2	0.4	0.6	0.8	0.2	0.4	0.6	0.8
Mean	-0.07	-0.08	-0.08	-0.03	-0.24	-0.11	-0.05	-0.03	-0.15	-0.23	-0.38	-0.34	0.27	0.35	0.44	0.55
SD	0.04	0.07	0.11	0.06	0.25	0.17	0.14	0.13	0.15	0.18	0.3	0.44	0.36	0.37	0.43	0.48
MAE	0.07	0.08	0.09	0.05	0.29	0.15	0.12	0.11	0.17	0.24	0.39	0.41	0.31	0.38	0.49	0.61
MSE	0.01	0.01	0.02	0.01	0.12	0.04	0.02	0.02	0.04	0.08	0.23	0.31	0.2	0.26	0.38	0.53

	SFH=Burst; SN=5.0; Av=2.0; Age of the system = 8.4															
	$\Delta \log < Z_\star >_L$				$\Delta \log < Z_\star >_M$				$\Delta M_\star$				ΔA_v			
X^i_{AGN}	0.2	0.4	0.6	0.8	0.2	0.4	0.6	0.8	0.2	0.4	0.6	0.8	0.2	0.4	0.6	0.8
Mean	-0.32	-0.44	-0.5	-0.56	-0.23	-0.35	-0.33	-0.44	-0.12	-0.17	-0.22	-0.23	-0.04	-0.04	-0.04	0.04
SD	0.2	0.24	0.21	0.2	0.21	0.26	0.32	0.28	0.16	0.23	0.3	0.36	0.17	0.17	0.17	0.12
MAE	0.32	0.46	0.5	0.57	0.25	0.39	0.4	0.46	0.14	0.19	0.27	0.34	0.15	0.12	0.12	0.1
MSE	0.14	0.26	0.29	0.36	0.1	0.19	0.21	0.27	0.04	0.08	0.14	0.18	0.03	0.03	0.03	0.02

TABLE A.186

	SFH=Burst; SN=5.0; Av=2.0; Age of the system = 8.8															
	ΔX_{AGN}				$\Delta < \alpha_v >_L$				$\Delta < \log(t_\star) >_L$				$\Delta < \log(t_\star) >_M$			
X^i_{AGN}	0.2	0.4	0.6	0.8	0.2	0.4	0.6	0.8	0.2	0.4	0.6	0.8	0.2	0.4	0.6	0.8
Mean	-0.05	-0.04	-0.06	-0.02	-0.24	-0.12	-0.02	-0.02	-0.11	-0.12	-0.3	-0.28	0.12	0.18	0.24	0.3
SD	0.04	0.05	0.1	0.07	0.22	0.14	0.15	0.13	0.09	0.13	0.36	0.44	0.15	0.18	0.19	0.26
MAE	0.05	0.05	0.07	0.05	0.27	0.14	0.12	0.11	0.11	0.14	0.32	0.39	0.13	0.18	0.24	0.3
MSE	0.0	0.0	0.01	0.0	0.11	0.04	0.02	0.02	0.02	0.03	0.22	0.27	0.04	0.07	0.09	0.16

	SFH=Burst; SN=5.0; Av=2.0; Age of the system = 8.8															
	$\Delta \log < Z_\star >_L$				$\Delta \log < Z_\star >_M$				$\Delta M_\star$				ΔA_v			
X^i_{AGN}	0.2	0.4	0.6	0.8	0.2	0.4	0.6	0.8	0.2	0.4	0.6	0.8	0.2	0.4	0.6	0.8
Mean	-0.09	-0.14	-0.33	-0.34	-0.04	-0.08	-0.25	-0.26	-0.05	-0.08	-0.12	-0.14	0.04	0.07	-0.02	0.04
SD	0.2	0.23	0.26	0.29	0.18	0.21	0.3	0.33	0.09	0.11	0.14	0.22	0.12	0.1	0.18	0.1
MAE	0.17	0.23	0.37	0.37	0.14	0.17	0.32	0.34	0.07	0.09	0.13	0.17	0.1	0.1	0.12	0.08
MSE	0.05	0.07	0.17	0.2	0.04	0.05	0.15	0.18	0.01	0.02	0.04	0.07	0.02	0.01	0.03	0.01

TABLE A.188

	SFH=Burst; SN=5.0; Av=2.0; Age of the system = 9.2															
	ΔX_{AGN}				$\Delta < \alpha_v >_L$				$\Delta < \log(t_\star) >_L$				$\Delta < \log(t_\star) >_M$			
X^i_{AGN}	0.2	0.4	0.6	0.8	0.2	0.4	0.6	0.8	0.2	0.4	0.6	0.8	0.2	0.4	0.6	0.8
Mean	-0.0	0.0	-0.02	-0.01	-0.19	-0.14	-0.03	-0.02	-0.1	-0.05	-0.08	-0.01	0.14	0.17	0.21	0.31
SD	0.08	0.1	0.18	0.15	0.28	0.19	0.15	0.11	0.18	0.2	0.36	0.46	0.17	0.21	0.21	0.29
MAE	0.06	0.06	0.1	0.06	0.27	0.19	0.12	0.09	0.15	0.16	0.25	0.34	0.18	0.22	0.24	0.35
MSE	0.01	0.01	0.03	0.02	0.11	0.06	0.02	0.01	0.04	0.04	0.14	0.22	0.05	0.08	0.09	0.19

	SFH=Burst; SN=5.0; Av=2.0; Age of the system = 9.2															
	$\Delta \log < Z_\star >_L$				$\Delta \log < Z_\star >_M$				$\Delta M_\star$				ΔA_v			
X^i_{AGN}	0.2	0.4	0.6	0.8	0.2	0.4	0.6	0.8	0.2	0.4	0.6	0.8	0.2	0.4	0.6	0.8
Mean	0.05	-0.01	-0.13	-0.23	0.03	-0.02	-0.12	-0.22	-0.05	-0.06	-0.11	-0.14	0.04	0.06	-0.03	-0.01
SD	0.19	0.26	0.35	0.35	0.2	0.26	0.33	0.36	0.11	0.15	0.22	0.27	0.1	0.09	0.21	0.24
MAE	0.17	0.22	0.32	0.37	0.17	0.22	0.3	0.37	0.11	0.13	0.17	0.23	0.08	0.09	0.12	0.11
MSE	0.04	0.07	0.14	0.18	0.04	0.07	0.12	0.18	0.02	0.03	0.06	0.09	0.01	0.01	0.04	0.06

TABLE A.190

	SFH=Burst; SN=5.0; Av=2.0; Age of the system = 9.6															
	ΔX_{AGN}				$\Delta < \alpha_v >_L$				$\Delta < \log(t_\star) >_L$				$\Delta < \log(t_\star) >_M$			
X^i_{AGN}	0.2	0.4	0.6	0.8	0.2	0.4	0.6	0.8	0.2	0.4	0.6	0.8	0.2	0.4	0.6	0.8
Mean	0.0	-0.01	0.01	-0.01	-0.17	-0.08	-0.01	-0.03	-0.01	-0.03	0.05	0.03	0.14	0.2	0.25	0.29
SD	0.05	0.09	0.04	0.09	0.26	0.21	0.16	0.17	0.15	0.25	0.21	0.37	0.12	0.17	0.18	0.25
MAE	0.04	0.05	0.03	0.04	0.24	0.18	0.13	0.12	0.12	0.18	0.17	0.31	0.15	0.22	0.27	0.35
MSE	0.0	0.01	0.0	0.01	0.09	0.05	0.03	0.03	0.02	0.06	0.05	0.14	0.03	0.07	0.09	0.15

	SFH=Burst; SN=5.0; Av=2.0; Age of the system = 9.6															
	$\Delta \log < Z_\star >_L$				$\Delta \log < Z_\star >_M$				$\Delta M_\star$				ΔA_v			
X^i_{AGN}	0.2	0.4	0.6	0.8	0.2	0.4	0.6	0.8	0.2	0.4	0.6	0.8	0.2	0.4	0.6	0.8
Mean	0.02	-0.0	-0.05	-0.13	-0.02	-0.04	-0.09	-0.18	-0.06	-0.1	-0.12	-0.11	0.02	0.01	0.01	0.02
SD	0.13	0.17	0.21	0.29	0.09	0.13	0.17	0.27	0.08	0.11	0.14	0.25	0.07	0.11	0.1	0.12
MAE	0.11	0.13	0.17	0.25	0.07	0.1	0.14	0.24	0.08	0.13	0.16	0.23	0.05	0.08	0.09	0.09
MSE	0.02	0.03	0.04	0.1	0.01	0.02	0.04	0.11	0.01	0.02	0.03	0.08	0.01	0.01	0.01	0.01

TABLE A.192

	SFH=Burst; SN=5.0; Av=2.0; Age of the system = 10.0															
	ΔX_{AGN}				$\Delta < \alpha_v >_L$				$\Delta < \log(t_\star) >_L$				$\Delta < \log(t_\star) >_M$			
X^i_{AGN}	0.2	0.4	0.6	0.8	0.2	0.4	0.6	0.8	0.2	0.4	0.6	0.8	0.2	0.4	0.6	0.8
Mean	-0.01	-0.05	-0.02	-0.01	-0.16	-0.08	-0.03	0.0	-0.09	-0.12	-0.11	-0.12	0.04	0.03	0.05	0.06
SD	0.06	0.13	0.08	0.11	0.25	0.19	0.2	0.11	0.17	0.3	0.27	0.34	0.09	0.1	0.09	0.1
MAE	0.04	0.07	0.04	0.04	0.23	0.16	0.15	0.08	0.13	0.19	0.18	0.21	0.08	0.09	0.09	0.11
MSE	0.0	0.02	0.01	0.01	0.09	0.04	0.04	0.01	0.04	0.1	0.09	0.13	0.01	0.01	0.01	0.02

	SFH=Burst; SN=5.0; Av=2.0; Age of the system = 10.0															
	$\Delta \log < Z_\star >_L$				$\Delta \log < Z_\star >_M$				$\Delta M_\star$				ΔA_v			
X^i_{AGN}	0.2	0.4	0.6	0.8	0.2	0.4	0.6	0.8	0.2	0.4	0.6	0.8	0.2	0.4	0.6	0.8
Mean	-0.01	-0.07	-0.07	-0.13	-0.02	-0.06	-0.07	-0.12	-0.02	-0.02	-0.02	0.0	-0.01	-0.03	-0.03	-0.03
SD	0.06	0.1	0.11	0.19	0.03	0.08	0.07	0.17	0.06	0.06	0.09	0.12	0.07	0.12	0.1	0.14
MAE	0.05	0.09	0.1	0.16	0.03	0.07	0.07	0.15	0.05	0.05	0.07	0.09	0.05	0.09	0.08	0.08
MSE	0.0	0.02	0.02	0.05	0.0	0.01	0.01	0.05	0.0	0.0	0.01	0.01	0.0	0.02	0.01	0.02

TABLE A.194

A.1.10 Tables: Constant SFH, SN=5, Av=0.0, base: BaseA

	SFH=Constant; SN=5.0; Av=0.0; Age of the system = 6.0															
	ΔX_{AGN}				$\Delta < \alpha_v >_L$				$\Delta < \log(t_\star) >_L$				$\Delta < \log(t_\star) >_M$			
X^i_{AGN}	0.2	0.4	0.6	0.8	0.2	0.4	0.6	0.8	0.2	0.4	0.6	0.8	0.2	0.4	0.6	0.8
Mean	-0.03	-0.03	-0.04	-0.05	-0.06	-0.01	-0.01	-0.0	0.25	0.24	0.29	0.36	1.64	1.44	1.27	1.44
SD	0.04	0.04	0.04	0.05	0.17	0.1	0.07	0.07	0.14	0.13	0.15	0.17	1.61	1.51	1.42	1.52
MAE	0.04	0.04	0.04	0.06	0.13	0.07	0.06	0.05	0.25	0.24	0.29	0.36	1.64	1.44	1.27	1.44
MSE	0.0	0.0	0.0	0.0	0.03	0.01	0.01	0.0	0.08	0.07	0.1	0.16	5.26	4.36	3.62	4.39

	SFH=Constant; SN=5.0; Av=0.0; Age of the system = 6.0															
	$\Delta \log < Z_\star >_L$				$\Delta \log < Z_\star >_M$				$\Delta M_\star$				ΔA_v			
X^i_{AGN}	0.2	0.4	0.6	0.8	0.2	0.4	0.6	0.8	0.2	0.4	0.6	0.8	0.2	0.4	0.6	0.8
Mean	-0.07	-0.04	-0.02	-0.05	-0.2	-0.12	-0.16	-0.18	-0.59	-0.52	-0.46	-0.64	-0.0	-0.0	-0.0	-0.0
SD	0.07	0.11	0.13	0.16	0.2	0.24	0.23	0.24	0.66	0.64	0.63	0.79	0.02	0.0	0.0	0.01
MAE	0.08	0.08	0.1	0.13	0.21	0.19	0.19	0.21	0.59	0.52	0.46	0.65	0.0	0.0	0.0	0.0
MSE	0.01	0.01	0.02	0.03	0.08	0.07	0.08	0.09	0.79	0.68	0.6	1.03	0.0	0.0	0.0	0.0

TABLE A.196

	SFH=Constant; SN=5.0; Av=0.0; Age of the system = 6.4															
	ΔX_{AGN}				$\Delta < \alpha_v >_L$				$\Delta < \log(t_\star) >_L$				$\Delta < \log(t_\star) >_M$			
X^i_{AGN}	0.2	0.4	0.6	0.8	0.2	0.4	0.6	0.8	0.2	0.4	0.6	0.8	0.2	0.4	0.6	0.8
Mean	-0.02	-0.02	-0.03	-0.04	0.0	0.01	0.0	0.02	0.04	0.04	0.06	0.08	1.07	0.81	0.85	0.6
SD	0.03	0.04	0.04	0.05	0.14	0.09	0.06	0.06	0.09	0.1	0.12	0.12	1.3	1.26	1.31	1.05
MAE	0.03	0.03	0.04	0.04	0.12	0.07	0.05	0.05	0.07	0.09	0.09	0.09	1.08	0.85	0.88	0.62
MSE	0.0	0.0	0.0	0.0	0.02	0.01	0.0	0.0	0.01	0.01	0.02	0.02	2.83	2.25	2.45	1.46

	SFH=Constant; SN=5.0; Av=0.0; Age of the system = 6.4															
	$\Delta \log < Z_\star >_L$				$\Delta \log < Z_\star >_M$				$\Delta M_\star$				ΔA_v			
X^i_{AGN}	0.2	0.4	0.6	0.8	0.2	0.4	0.6	0.8	0.2	0.4	0.6	0.8	0.2	0.4	0.6	0.8
Mean	0.03	0.03	0.04	0.1	-0.09	-0.11	-0.07	-0.01	-0.4	-0.32	-0.37	-0.27	-0.0	-0.0	-0.0	-0.01
SD	0.11	0.12	0.14	0.15	0.21	0.22	0.19	0.18	0.55	0.55	0.65	0.59	0.0	0.01	0.01	0.03
MAE	0.08	0.1	0.11	0.15	0.14	0.16	0.12	0.14	0.41	0.34	0.39	0.33	0.0	0.0	0.0	0.01
MSE	0.01	0.02	0.02	0.03	0.05	0.06	0.04	0.03	0.46	0.41	0.56	0.42	0.0	0.0	0.0	0.0

TABLE A.198

	SFH=Constant; SN=5.0; Av=0.0; Age of the system = 6.8															
	ΔX_{AGN}				$\Delta < \alpha_v >_L$				$\Delta < \log(t_\star) >_L$				$\Delta < \log(t_\star) >_M$			
X^i_{AGN}	0.2	0.4	0.6	0.8	0.2	0.4	0.6	0.8	0.2	0.4	0.6	0.8	0.2	0.4	0.6	0.8
Mean	0.02	0.02	0.01	-0.01	0.13	0.09	0.06	0.04	0.04	0.03	0.01	-0.02	0.49	0.49	0.56	0.59
SD	0.04	0.05	0.04	0.04	0.14	0.11	0.07	0.06	0.08	0.11	0.12	0.17	0.71	0.63	0.73	0.89
MAE	0.03	0.04	0.03	0.03	0.16	0.12	0.08	0.06	0.06	0.08	0.09	0.14	0.5	0.51	0.58	0.66
MSE	0.0	0.0	0.0	0.0	0.04	0.02	0.01	0.01	0.01	0.01	0.02	0.03	0.75	0.65	0.85	1.14

	SFH=Constant; SN=5.0; Av=0.0; Age of the system = 6.8															
	$\Delta \log < Z_\star >_L$				$\Delta \log < Z_\star >_M$				$\Delta M_\star$				ΔA_v			
X^i_{AGN}	0.2	0.4	0.6	0.8	0.2	0.4	0.6	0.8	0.2	0.4	0.6	0.8	0.2	0.4	0.6	0.8
Mean	-0.04	-0.07	0.02	0.08	-0.13	-0.15	-0.08	-0.0	-0.18	-0.19	-0.19	-0.26	-0.0	-0.0	-0.0	-0.0
SD	0.18	0.22	0.22	0.25	0.18	0.2	0.22	0.27	0.33	0.29	0.31	0.45	0.0	0.03	0.0	0.0
MAE	0.15	0.18	0.18	0.21	0.17	0.2	0.18	0.21	0.22	0.23	0.24	0.34	0.0	0.0	0.0	0.0
MSE	0.03	0.05	0.05	0.07	0.05	0.06	0.06	0.07	0.14	0.12	0.13	0.27	0.0	0.0	0.0	0.0

TABLE A.200

	SFH=Constant; SN=5.0; Av=0.0; Age of the system = 7.2															
	ΔX_{AGN}				$\Delta < \alpha_v >_L$				$\Delta < \log(t_\star) >_L$				$\Delta < \log(t_\star) >_M$			
X^i_{AGN}	0.2	0.4	0.6	0.8	0.2	0.4	0.6	0.8	0.2	0.4	0.6	0.8	0.2	0.4	0.6	0.8
Mean	0.01	0.01	0.01	-0.01	-0.09	-0.01	0.02	0.02	-0.04	-0.06	-0.09	-0.09	0.46	0.4	0.38	0.47
SD	0.04	0.05	0.04	0.06	0.19	0.12	0.09	0.08	0.09	0.11	0.14	0.26	0.64	0.81	0.85	1.1
MAE	0.03	0.04	0.04	0.04	0.16	0.1	0.07	0.06	0.08	0.1	0.14	0.24	0.51	0.51	0.56	0.72
MSE	0.0	0.0	0.0	0.0	0.04	0.02	0.01	0.01	0.01	0.02	0.03	0.07	0.63	0.82	0.86	1.43

	SFH=Constant; SN=5.0; Av=0.0; Age of the system = 7.2															
	$\Delta \log < Z_\star >_L$				$\Delta \log < Z_\star >_M$				$\Delta M_\star$				ΔA_v			
X^i_{AGN}	0.2	0.4	0.6	0.8	0.2	0.4	0.6	0.8	0.2	0.4	0.6	0.8	0.2	0.4	0.6	0.8
Mean	-0.06	-0.02	-0.01	0.06	-0.13	-0.08	-0.1	-0.04	-0.1	-0.08	-0.06	-0.21	-0.0	-0.0	-0.0	-0.0
SD	0.18	0.2	0.25	0.23	0.17	0.21	0.26	0.28	0.29	0.34	0.41	0.67	0.0	0.0	0.03	0.01
MAE	0.15	0.17	0.2	0.2	0.16	0.19	0.22	0.22	0.18	0.24	0.27	0.43	0.0	0.0	0.0	0.0
MSE	0.04	0.04	0.06	0.06	0.05	0.05	0.08	0.08	0.09	0.12	0.17	0.49	0.0	0.0	0.0	0.0

TABLE A.202

	SFH=Constant; SN=5.0; Av=0.0; Age of the system = 7.6															
	ΔX_{AGN}				$\Delta < \alpha_{\nu} >_{L}$				$\Delta < \log(t_{\star}) >_{L}$				$\Delta < \log(t_{\star}) >_{M}$			
X^{i}_{AGN}	0.2	0.4	0.6	0.8	0.2	0.4	0.6	0.8	0.2	0.4	0.6	0.8	0.2	0.4	0.6	0.8
Mean	0.01	0.02	-0.0	-0.02	-0.04	0.01	-0.02	-0.0	-0.14	-0.17	-0.16	-0.2	0.21	0.38	0.34	0.36
SD	0.05	0.06	0.07	0.08	0.2	0.15	0.11	0.08	0.08	0.14	0.17	0.27	0.94	1.07	0.88	1.06
MAE	0.04	0.05	0.05	0.05	0.16	0.11	0.08	0.06	0.15	0.19	0.2	0.28	0.62	0.72	0.63	0.8
MSE	0.0	0.0	0.0	0.01	0.04	0.02	0.01	0.01	0.03	0.05	0.06	0.11	0.92	1.28	0.9	1.24

	SFH=Constant; SN=5.0; Av=0.0; Age of the system = 7.6															
	$\Delta \log < Z_{\star} >_{L}$				$\Delta \log < Z_{\star} >_{M}$				$\Delta M_{\star}$				ΔA_{v}			
X^{i}_{AGN}	0.2	0.4	0.6	0.8	0.2	0.4	0.6	0.8	0.2	0.4	0.6	0.8	0.2	0.4	0.6	0.8
Mean	-0.09	-0.04	-0.09	-0.01	-0.18	-0.17	-0.19	-0.12	0.06	-0.0	0.01	-0.08	-0.0	-0.01	-0.01	-0.0
SD	0.16	0.22	0.26	0.28	0.19	0.24	0.26	0.28	0.45	0.57	0.44	0.67	0.03	0.03	0.05	0.02
MAE	0.15	0.18	0.23	0.23	0.2	0.24	0.24	0.24	0.34	0.41	0.32	0.45	0.0	0.01	0.01	0.0
MSE	0.04	0.05	0.08	0.08	0.07	0.09	0.1	0.09	0.2	0.32	0.2	0.45	0.0	0.0	0.0	0.0

TABLE A.204

	SFH=Constant; SN=5.0; Av=0.0; Age of the system = 8.0															
	ΔX_{AGN}				$\Delta < \alpha_v >_L$				$\Delta < \log(t_\star) >_L$				$\Delta < \log(t_\star) >_M$			
X^i_{AGN}	0.2	0.4	0.6	0.8	0.2	0.4	0.6	0.8	0.2	0.4	0.6	0.8	0.2	0.4	0.6	0.8
Mean	-0.0	0.01	-0.0	-0.01	-0.06	-0.04	-0.02	0.01	-0.24	-0.29	-0.3	-0.3	0.6	0.24	0.16	0.06
SD	0.05	0.07	0.07	0.09	0.22	0.14	0.1	0.08	0.1	0.12	0.16	0.27	1.03	1.07	1.09	1.07
MAE	0.04	0.05	0.05	0.05	0.18	0.12	0.08	0.06	0.24	0.29	0.31	0.35	0.93	0.84	0.89	0.89
MSE	0.0	0.0	0.0	0.01	0.05	0.02	0.01	0.01	0.07	0.1	0.12	0.16	1.42	1.2	1.21	1.15

	SFH=Constant; SN=5.0; Av=0.0; Age of the system = 8.0															
	$\Delta \log < Z_\star >_L$				$\Delta \log < Z_\star >_M$				$\Delta M_\star$				ΔA_v			
X^i_{AGN}	0.2	0.4	0.6	0.8	0.2	0.4	0.6	0.8	0.2	0.4	0.6	0.8	0.2	0.4	0.6	0.8
Mean	-0.2	-0.26	-0.26	-0.18	-0.23	-0.23	-0.25	-0.23	-0.07	0.13	0.11	0.14	-0.01	-0.0	-0.0	-0.0
SD	0.13	0.2	0.24	0.27	0.2	0.24	0.27	0.3	0.51	0.53	0.64	0.71	0.04	0.01	0.0	0.02
MAE	0.2	0.27	0.29	0.25	0.27	0.29	0.3	0.3	0.39	0.47	0.54	0.6	0.01	0.0	0.0	0.0
MSE	0.06	0.11	0.13	0.11	0.09	0.11	0.14	0.14	0.27	0.29	0.42	0.52	0.0	0.0	0.0	0.0

TABLE A.206

	SFH=Constant; SN=5.0; Av=0.0; Age of the system = 8.4															
	ΔX_{AGN}				$\Delta < \alpha_v >_L$				$\Delta < \log(t_\star) >_L$				$\Delta < \log(t_\star) >_M$			
X^i_{AGN}	0.2	0.4	0.6	0.8	0.2	0.4	0.6	0.8	0.2	0.4	0.6	0.8	0.2	0.4	0.6	0.8
Mean	-0.01	-0.01	0.0	-0.02	-0.15	-0.08	-0.01	-0.0	-0.29	-0.37	-0.5	-0.55	0.5	0.31	0.02	0.09
SD	0.06	0.06	0.07	0.1	0.21	0.14	0.1	0.1	0.14	0.18	0.21	0.26	0.86	0.86	0.99	1.21
MAE	0.04	0.05	0.05	0.07	0.2	0.12	0.07	0.07	0.29	0.37	0.5	0.55	0.77	0.69	0.82	1.07
MSE	0.0	0.0	0.01	0.01	0.07	0.03	0.01	0.01	0.11	0.17	0.3	0.37	0.99	0.84	0.97	1.46

	SFH=Constant; SN=5.0; Av=0.0; Age of the system = 8.4															
	$\Delta \log < Z_\star >_L$				$\Delta \log < Z_\star >_M$				$\Delta M_\star$				ΔA_v			
X^i_{AGN}	0.2	0.4	0.6	0.8	0.2	0.4	0.6	0.8	0.2	0.4	0.6	0.8	0.2	0.4	0.6	0.8
Mean	-0.27	-0.37	-0.47	-0.36	-0.23	-0.31	-0.34	-0.28	-0.05	0.08	0.31	0.21	-0.01	-0.0	-0.01	-0.0
SD	0.15	0.2	0.2	0.3	0.24	0.28	0.27	0.27	0.43	0.48	0.58	0.85	0.05	0.01	0.04	0.01
MAE	0.27	0.37	0.47	0.39	0.29	0.36	0.38	0.32	0.36	0.4	0.57	0.77	0.01	0.0	0.01	0.0
MSE	0.09	0.17	0.26	0.22	0.11	0.18	0.19	0.15	0.19	0.24	0.44	0.76	0.0	0.0	0.0	0.0

TABLE A.208

	SFH=Constant; SN=5.0; Av=0.0; Age of the system = 8.8															
	ΔX_{AGN}				$\Delta < \alpha_v >_L$				$\Delta < \log(t_\star) >_L$				$\Delta < \log(t_\star) >_M$			
X^i_{AGN}	0.2	0.4	0.6	0.8	0.2	0.4	0.6	0.8	0.2	0.4	0.6	0.8	0.2	0.4	0.6	0.8
Mean	0.01	0.0	0.0	-0.04	-0.07	-0.03	0.01	-0.01	-0.18	-0.31	-0.45	-0.6	0.31	0.39	0.24	0.33
SD	0.06	0.07	0.08	0.12	0.23	0.12	0.08	0.13	0.12	0.18	0.24	0.29	0.6	0.66	0.68	0.98
MAE	0.05	0.06	0.06	0.07	0.19	0.1	0.07	0.08	0.19	0.31	0.45	0.6	0.48	0.6	0.61	0.9
MSE	0.0	0.01	0.01	0.02	0.06	0.01	0.01	0.02	0.05	0.13	0.26	0.44	0.45	0.59	0.52	1.06

	SFH=Constant; SN=5.0; Av=0.0; Age of the system = 8.8															
	$\Delta \log < Z_\star >_L$				$\Delta \log < Z_\star >_M$				$\Delta M_\star$				ΔA_v			
X^i_{AGN}	0.2	0.4	0.6	0.8	0.2	0.4	0.6	0.8	0.2	0.4	0.6	0.8	0.2	0.4	0.6	0.8
Mean	-0.32	-0.44	-0.5	-0.52	-0.25	-0.32	-0.38	-0.4	-0.02	-0.02	0.11	0.01	-0.01	-0.02	-0.02	-0.02
SD	0.17	0.2	0.21	0.24	0.24	0.25	0.27	0.32	0.33	0.4	0.45	0.75	0.02	0.04	0.08	0.05
MAE	0.33	0.44	0.5	0.52	0.29	0.35	0.41	0.45	0.25	0.33	0.37	0.61	0.01	0.02	0.02	0.02
MSE	0.13	0.23	0.3	0.32	0.12	0.17	0.22	0.26	0.11	0.16	0.21	0.57	0.0	0.0	0.01	0.0

TABLE A.210

	SFH=Constant; SN=5.0; Av=0.0; Age of the system = 9.2															
	ΔX_{AGN}				$\Delta < \alpha_v >_L$				$\Delta < \log(t_\star) >_L$				$\Delta < \log(t_\star) >_M$			
X^i_{AGN}	0.2	0.4	0.6	0.8	0.2	0.4	0.6	0.8	0.2	0.4	0.6	0.8	0.2	0.4	0.6	0.8
Mean	0.01	-0.01	-0.01	-0.01	-0.05	-0.04	-0.0	0.0	-0.19	-0.33	-0.39	-0.52	0.45	0.37	0.45	0.04
SD	0.08	0.11	0.12	0.16	0.25	0.15	0.11	0.14	0.16	0.21	0.24	0.41	0.47	0.41	0.52	0.8
MAE	0.06	0.09	0.08	0.09	0.2	0.12	0.08	0.08	0.21	0.34	0.4	0.55	0.51	0.42	0.59	0.61
MSE	0.01	0.01	0.01	0.02	0.06	0.02	0.01	0.02	0.06	0.15	0.21	0.43	0.42	0.3	0.47	0.64

	SFH=Constant; SN=5.0; Av=0.0; Age of the system = 9.2															
	$\Delta \log < Z_\star >_L$				$\Delta \log < Z_\star >_M$				$\Delta M_\star$				ΔA_v			
X^i_{AGN}	0.2	0.4	0.6	0.8	0.2	0.4	0.6	0.8	0.2	0.4	0.6	0.8	0.2	0.4	0.6	0.8
Mean	-0.39	-0.45	-0.53	-0.56	-0.26	-0.3	-0.38	-0.45	-0.12	-0.05	-0.11	0.25	-0.02	-0.04	-0.03	-0.02
SD	0.15	0.18	0.16	0.22	0.22	0.23	0.28	0.31	0.29	0.27	0.42	0.75	0.05	0.1	0.07	0.07
MAE	0.39	0.46	0.53	0.57	0.28	0.31	0.42	0.49	0.23	0.22	0.34	0.63	0.02	0.04	0.03	0.02
MSE	0.18	0.24	0.3	0.36	0.12	0.15	0.23	0.3	0.1	0.08	0.19	0.62	0.0	0.01	0.01	0.01

TABLE A.212

	SFH=Constant; SN=5.0; Av=0.0; Age of the system = 9.6															
	ΔX_{AGN}				$\Delta < \alpha_v >_L$				$\Delta < \log(t_\star) >_L$				$\Delta < \log(t_\star) >_M$			
X^i_{AGN}	0.2	0.4	0.6	0.8	0.2	0.4	0.6	0.8	0.2	0.4	0.6	0.8	0.2	0.4	0.6	0.8
Mean	0.03	0.02	0.01	-0.01	-0.02	0.01	0.01	0.0	-0.2	-0.24	-0.31	-0.46	0.29	0.27	0.19	0.06
SD	0.08	0.09	0.12	0.14	0.21	0.11	0.13	0.11	0.15	0.2	0.31	0.41	0.33	0.34	0.42	0.62
MAE	0.06	0.07	0.09	0.09	0.17	0.09	0.09	0.07	0.21	0.27	0.36	0.5	0.37	0.37	0.37	0.46
MSE	0.01	0.01	0.01	0.02	0.05	0.01	0.02	0.01	0.06	0.1	0.19	0.37	0.19	0.19	0.21	0.38

	SFH=Constant; SN=5.0; Av=0.0; Age of the system = 9.6															
	$\Delta \log < Z_\star >_L$				$\Delta \log < Z_\star >_M$				$\Delta M_\star$				ΔA_v			
X^i_{AGN}	0.2	0.4	0.6	0.8	0.2	0.4	0.6	0.8	0.2	0.4	0.6	0.8	0.2	0.4	0.6	0.8
Mean	-0.32	-0.39	-0.44	-0.41	-0.12	-0.22	-0.32	-0.3	-0.05	-0.02	0.03	0.18	-0.03	-0.03	-0.02	-0.01
SD	0.14	0.19	0.24	0.26	0.21	0.27	0.33	0.36	0.24	0.25	0.38	0.65	0.11	0.06	0.06	0.06
MAE	0.32	0.4	0.46	0.44	0.19	0.28	0.39	0.4	0.2	0.21	0.32	0.5	0.03	0.03	0.02	0.01
MSE	0.12	0.19	0.25	0.24	0.06	0.12	0.21	0.22	0.06	0.06	0.15	0.46	0.01	0.0	0.0	0.0

TABLE A.214

	SFH=Constant; SN=5.0; Av=0.0; Age of the system = 10.0															
	ΔX_{AGN}				$\Delta < \alpha_{\nu} >_{L}$				$\Delta < \log(t_{\star}) >_{L}$				$\Delta < \log(t_{\star}) >_{M}$			
X^{i}_{AGN}	0.2	0.4	0.6	0.8	0.2	0.4	0.6	0.8	0.2	0.4	0.6	0.8	0.2	0.4	0.6	0.8
Mean	0.02	0.03	0.01	-0.01	-0.02	0.02	0.01	-0.01	-0.2	-0.2	-0.33	-0.34	0.11	0.07	-0.02	-0.0
SD	0.09	0.11	0.09	0.14	0.28	0.15	0.1	0.11	0.17	0.26	0.26	0.42	0.25	0.31	0.38	0.4
MAE	0.08	0.09	0.07	0.1	0.22	0.12	0.08	0.08	0.21	0.27	0.37	0.46	0.24	0.28	0.32	0.34
MSE	0.01	0.01	0.01	0.02	0.08	0.02	0.01	0.01	0.07	0.11	0.17	0.29	0.08	0.1	0.14	0.16

	SFH=Constant; SN=5.0; Av=0.0; Age of the system = 10.0															
	$\Delta \log < Z_{\star} >_{L}$				$\Delta \log < Z_{\star} >_{M}$				$\Delta M_{\star}$				ΔA_{v}			
X^{i}_{AGN}	0.2	0.4	0.6	0.8	0.2	0.4	0.6	0.8	0.2	0.4	0.6	0.8	0.2	0.4	0.6	0.8
Mean	-0.27	-0.34	-0.44	-0.47	-0.09	-0.14	-0.29	-0.45	0.0	0.06	0.12	0.19	-0.04	-0.04	-0.03	-0.01
SD	0.18	0.21	0.21	0.26	0.21	0.29	0.32	0.31	0.19	0.25	0.33	0.51	0.09	0.09	0.05	0.02
MAE	0.28	0.36	0.45	0.49	0.17	0.26	0.36	0.49	0.16	0.2	0.28	0.46	0.04	0.04	0.03	0.01
MSE	0.1	0.16	0.24	0.29	0.05	0.11	0.19	0.29	0.04	0.07	0.12	0.3	0.01	0.01	0.0	0.0

TABLE A.216

A.1.11 Tables: Constant SFH, SN=5, Av=1.0, base: BaseA

	SFH=Constant; SN=5.0; Av=1.0; Age of the system = 6.0															
	ΔX_{AGN}				$\Delta < \alpha_v >_L$				$\Delta < \log(t_\star) >_L$				$\Delta < \log(t_\star) >_M$			
X^i_{AGN}	0.2	0.4	0.6	0.8	0.2	0.4	0.6	0.8	0.2	0.4	0.6	0.8	0.2	0.4	0.6	0.8
Mean	0.1	0.11	0.04	0.01	0.08	-0.15	-0.2	-0.16	0.33	0.3	0.3	0.35	2.21	1.9	1.69	1.67
SD	0.09	0.07	0.06	0.05	0.14	0.11	0.1	0.13	0.19	0.21	0.19	0.28	1.41	1.58	1.55	1.49
MAE	0.11	0.11	0.06	0.04	0.14	0.16	0.2	0.18	0.33	0.3	0.3	0.35	2.21	1.9	1.69	1.67
MSE	0.02	0.02	0.01	0.0	0.03	0.04	0.05	0.04	0.15	0.13	0.12	0.2	6.87	6.1	5.27	5.03

	SFH=Constant; SN=5.0; Av=1.0; Age of the system = 6.0															
	$\Delta \log < Z_\star >_L$				$\Delta \log < Z_\star >_M$				$\Delta M_\star$				ΔA_v			
X^i_{AGN}	0.2	0.4	0.6	0.8	0.2	0.4	0.6	0.8	0.2	0.4	0.6	0.8	0.2	0.4	0.6	0.8
Mean	-0.58	-0.6	-0.54	-0.48	-0.45	-0.49	-0.43	-0.42	-0.72	-0.56	-0.59	-0.62	0.37	0.4	0.29	0.2
SD	0.15	0.17	0.22	0.27	0.25	0.25	0.27	0.3	0.59	0.65	0.73	0.73	0.15	0.11	0.12	0.12
MAE	0.58	0.6	0.54	0.5	0.46	0.5	0.45	0.45	0.74	0.63	0.63	0.66	0.37	0.4	0.29	0.21
MSE	0.36	0.39	0.34	0.3	0.26	0.3	0.25	0.26	0.86	0.74	0.88	0.92	0.16	0.17	0.1	0.05

TABLE A.218

	SFH=Constant; SN=5.0; Av=1.0; Age of the system = 6.4															
	ΔX_{AGN}				$\Delta < \alpha_{\nu} >_{L}$				$\Delta < \log(t_{\star}) >_{L}$				$\Delta < \log(t_{\star}) >_{M}$			
X^{i}_{AGN}	0.2	0.4	0.6	0.8	0.2	0.4	0.6	0.8	0.2	0.4	0.6	0.8	0.2	0.4	0.6	0.8
Mean	0.19	0.12	0.08	0.02	0.15	-0.14	-0.23	-0.16	0.04	-0.02	0.02	0.05	1.83	1.36	1.34	1.12
SD	0.1	0.07	0.06	0.05	0.13	0.1	0.13	0.13	0.2	0.2	0.22	0.23	1.33	1.43	1.48	1.41
MAE	0.19	0.13	0.09	0.05	0.17	0.15	0.24	0.17	0.16	0.15	0.15	0.18	1.87	1.44	1.4	1.19
MSE	0.05	0.02	0.01	0.0	0.04	0.03	0.07	0.04	0.04	0.04	0.05	0.06	5.09	3.87	3.98	3.26

	SFH=Constant; SN=5.0; Av=1.0; Age of the system = 6.4															
	$\Delta \log < Z_{\star} >_{L}$				$\Delta \log < Z_{\star} >_{M}$				$\Delta M_{\star}$				ΔA_{v}			
X^{i}_{AGN}	0.2	0.4	0.6	0.8	0.2	0.4	0.6	0.8	0.2	0.4	0.6	0.8	0.2	0.4	0.6	0.8
Mean	-0.53	-0.46	-0.45	-0.45	-0.43	-0.39	-0.41	-0.41	-0.51	-0.4	-0.43	-0.48	0.51	0.42	0.37	0.23
SD	0.21	0.28	0.31	0.31	0.23	0.24	0.3	0.29	0.61	0.6	0.67	0.75	0.15	0.16	0.14	0.13
MAE	0.53	0.47	0.48	0.48	0.44	0.4	0.44	0.42	0.59	0.5	0.52	0.55	0.51	0.43	0.38	0.24
MSE	0.33	0.29	0.29	0.3	0.24	0.21	0.26	0.25	0.63	0.52	0.64	0.79	0.29	0.2	0.16	0.07

TABLE A.220

	SFH=Constant; SN=5.0; Av=1.0; Age of the system = 6.8															
	ΔX_{AGN}				$\Delta < \alpha_v >_L$				$\Delta < \log(t_\star) >_L$				$\Delta < \log(t_\star) >_M$			
X^i_{AGN}	0.2	0.4	0.6	0.8	0.2	0.4	0.6	0.8	0.2	0.4	0.6	0.8	0.2	0.4	0.6	0.8
Mean	0.25	0.2	0.14	0.07	0.11	-0.13	-0.17	-0.14	-0.0	-0.07	-0.15	-0.09	0.9	0.89	0.74	1.07
SD	0.1	0.08	0.09	0.06	0.14	0.12	0.12	0.14	0.17	0.16	0.23	0.33	1.13	1.07	1.15	1.38
MAE	0.25	0.2	0.15	0.08	0.15	0.15	0.18	0.16	0.13	0.13	0.2	0.28	1.02	0.97	0.94	1.26
MSE	0.07	0.04	0.03	0.01	0.03	0.03	0.04	0.04	0.03	0.03	0.07	0.12	2.09	1.93	1.87	3.05

	SFH=Constant; SN=5.0; Av=1.0; Age of the system = 6.8															
	$\Delta \log < Z_\star >_L$				$\Delta \log < Z_\star >_M$				$\Delta M_\star$				ΔA_v			
X^i_{AGN}	0.2	0.4	0.6	0.8	0.2	0.4	0.6	0.8	0.2	0.4	0.6	0.8	0.2	0.4	0.6	0.8
Mean	-0.48	-0.45	-0.34	-0.37	-0.39	-0.33	-0.34	-0.33	-0.09	-0.12	-0.16	-0.38	0.59	0.5	0.37	0.25
SD	0.26	0.27	0.31	0.36	0.27	0.27	0.26	0.34	0.45	0.43	0.53	0.77	0.18	0.14	0.18	0.12
MAE	0.51	0.45	0.39	0.45	0.42	0.36	0.36	0.41	0.37	0.33	0.35	0.58	0.59	0.5	0.39	0.25
MSE	0.3	0.27	0.21	0.27	0.23	0.18	0.18	0.22	0.21	0.2	0.3	0.74	0.38	0.27	0.17	0.08

TABLE A.222

	SFH=Constant; SN=5.0; Av=1.0; Age of the system = 7.2															
	ΔX_{AGN}				$\Delta < \alpha_{\nu} >_{L}$				$\Delta < \log(t_{\star}) >_{L}$				$\Delta < \log(t_{\star}) >_{M}$			
X^{i}_{AGN}	0.2	0.4	0.6	0.8	0.2	0.4	0.6	0.8	0.2	0.4	0.6	0.8	0.2	0.4	0.6	0.8
Mean	0.23	0.22	0.15	0.07	-0.21	-0.24	-0.23	-0.15	-0.05	-0.16	-0.22	-0.15	1.18	0.72	0.65	0.84
SD	0.09	0.07	0.07	0.07	0.16	0.14	0.13	0.14	0.12	0.16	0.2	0.49	1.21	1.16	1.21	1.37
MAE	0.23	0.22	0.15	0.08	0.22	0.24	0.23	0.16	0.1	0.19	0.26	0.38	1.26	0.98	0.95	1.22
MSE	0.06	0.05	0.03	0.01	0.07	0.08	0.07	0.04	0.02	0.05	0.09	0.26	2.84	1.85	1.87	2.59

	SFH=Constant; SN=5.0; Av=1.0; Age of the system = 7.2															
	$\Delta \log < Z_{\star} >_{L}$				$\Delta \log < Z_{\star} >_{M}$				$\Delta M_{\star}$				ΔA_{v}			
X^{i}_{AGN}	0.2	0.4	0.6	0.8	0.2	0.4	0.6	0.8	0.2	0.4	0.6	0.8	0.2	0.4	0.6	0.8
Mean	-0.33	-0.29	-0.3	-0.33	-0.16	-0.23	-0.26	-0.3	-0.07	0.09	0.02	-0.17	0.61	0.5	0.38	0.24
SD	0.21	0.29	0.29	0.36	0.24	0.27	0.3	0.36	0.55	0.49	0.56	0.83	0.16	0.14	0.14	0.13
MAE	0.33	0.34	0.34	0.4	0.24	0.28	0.33	0.41	0.47	0.43	0.43	0.61	0.61	0.5	0.38	0.24
MSE	0.15	0.17	0.18	0.24	0.08	0.13	0.16	0.22	0.31	0.25	0.31	0.72	0.39	0.27	0.16	0.07

TABLE A.224

	SFH=Constant; SN=5.0; Av=1.0; Age of the system = 7.6															
	ΔX_{AGN}				$\Delta < \alpha_v >_L$				$\Delta < \log(t_\star) >_L$				$\Delta < \log(t_\star) >_M$			
X^i_{AGN}	0.2	0.4	0.6	0.8	0.2	0.4	0.6	0.8	0.2	0.4	0.6	0.8	0.2	0.4	0.6	0.8
Mean	0.21	0.15	0.15	0.08	-0.19	-0.27	-0.25	-0.16	-0.13	-0.19	-0.27	-0.33	1.36	1.28	0.64	0.65
SD	0.08	0.09	0.07	0.07	0.19	0.16	0.13	0.15	0.14	0.16	0.24	0.4	1.24	1.17	1.34	1.38
MAE	0.21	0.16	0.15	0.09	0.22	0.28	0.26	0.18	0.16	0.21	0.31	0.44	1.54	1.45	1.16	1.27
MSE	0.05	0.03	0.03	0.01	0.07	0.1	0.08	0.05	0.04	0.06	0.13	0.27	3.38	3.02	2.22	2.33

	SFH=Constant; SN=5.0; Av=1.0; Age of the system = 7.6															
	$\Delta \log < Z_\star >_L$				$\Delta \log < Z_\star >_M$				$\Delta M_\star$				ΔA_v			
X^i_{AGN}	0.2	0.4	0.6	0.8	0.2	0.4	0.6	0.8	0.2	0.4	0.6	0.8	0.2	0.4	0.6	0.8
Mean	-0.25	-0.23	-0.32	-0.31	-0.03	-0.12	-0.24	-0.24	-0.15	-0.15	0.12	0.03	0.53	0.42	0.38	0.24
SD	0.13	0.22	0.27	0.35	0.24	0.26	0.31	0.33	0.69	0.64	0.76	0.86	0.16	0.21	0.14	0.14
MAE	0.25	0.25	0.34	0.39	0.19	0.23	0.31	0.32	0.61	0.55	0.65	0.7	0.53	0.43	0.38	0.25
MSE	0.08	0.1	0.17	0.22	0.06	0.08	0.15	0.17	0.49	0.43	0.59	0.75	0.31	0.22	0.17	0.08

TABLE A.226

	SFH=Constant; SN=5.0; Av=1.0; Age of the system = 8.0															
	ΔX_{AGN}				$\Delta < \alpha_v >_L$				$\Delta < \log(t_\star) >_L$				$\Delta < \log(t_\star) >_M$			
X^i_{AGN}	0.2	0.4	0.6	0.8	0.2	0.4	0.6	0.8	0.2	0.4	0.6	0.8	0.2	0.4	0.6	0.8
Mean	0.17	0.13	0.11	0.05	-0.21	-0.23	-0.16	-0.14	-0.09	-0.21	-0.26	-0.25	1.23	1.16	0.93	0.63
SD	0.09	0.09	0.08	0.1	0.21	0.14	0.12	0.13	0.17	0.19	0.28	0.51	0.97	1.13	1.18	1.2
MAE	0.17	0.15	0.12	0.08	0.24	0.24	0.17	0.16	0.16	0.24	0.32	0.48	1.31	1.39	1.29	1.15
MSE	0.04	0.03	0.02	0.01	0.09	0.08	0.04	0.04	0.04	0.08	0.15	0.32	2.46	2.63	2.26	1.84

	SFH=Constant; SN=5.0; Av=1.0; Age of the system = 8.0															
	$\Delta \log < Z_\star >_L$				$\Delta \log < Z_\star >_M$				$\Delta M_\star$				ΔA_v			
X^i_{AGN}	0.2	0.4	0.6	0.8	0.2	0.4	0.6	0.8	0.2	0.4	0.6	0.8	0.2	0.4	0.6	0.8
Mean	-0.32	-0.37	-0.4	-0.47	-0.12	-0.21	-0.24	-0.32	-0.17	-0.14	-0.03	0.11	0.43	0.36	0.27	0.19
SD	0.18	0.24	0.27	0.28	0.3	0.32	0.34	0.33	0.52	0.7	0.71	0.99	0.17	0.16	0.13	0.15
MAE	0.33	0.38	0.42	0.5	0.26	0.32	0.34	0.39	0.45	0.63	0.6	0.79	0.43	0.36	0.28	0.22
MSE	0.14	0.2	0.23	0.3	0.1	0.15	0.17	0.21	0.3	0.51	0.5	0.98	0.22	0.15	0.09	0.06

Table A.228

	SFH=Constant; SN=5.0; Av=1.0; Age of the system = 8.4															
	ΔX_{AGN}				$\Delta < \alpha_v >_L$				$\Delta < \log(t_\star) >_L$				$\Delta < \log(t_\star) >_M$			
X^i_{AGN}	0.2	0.4	0.6	0.8	0.2	0.4	0.6	0.8	0.2	0.4	0.6	0.8	0.2	0.4	0.6	0.8
Mean	0.14	0.09	0.06	0.04	-0.24	-0.19	-0.12	-0.09	0.01	-0.15	-0.27	-0.39	1.0	0.87	0.9	0.55
SD	0.09	0.09	0.07	0.1	0.17	0.13	0.14	0.13	0.18	0.24	0.32	0.56	0.7	0.73	0.92	1.18
MAE	0.14	0.11	0.08	0.08	0.25	0.2	0.14	0.11	0.14	0.23	0.35	0.57	1.02	0.95	1.07	1.17
MSE	0.03	0.02	0.01	0.01	0.09	0.05	0.03	0.03	0.03	0.08	0.17	0.47	1.48	1.29	1.66	1.7

	SFH=Constant; SN=5.0; Av=1.0; Age of the system = 8.4															
	$\Delta \log < Z_\star >_L$				$\Delta \log < Z_\star >_M$				$\Delta M_\star$				ΔA_v			
X^i_{AGN}	0.2	0.4	0.6	0.8	0.2	0.4	0.6	0.8	0.2	0.4	0.6	0.8	0.2	0.4	0.6	0.8
Mean	-0.29	-0.42	-0.47	-0.51	-0.12	-0.24	-0.28	-0.36	-0.15	-0.08	-0.13	0.14	0.39	0.26	0.17	0.14
SD	0.21	0.22	0.21	0.25	0.3	0.33	0.3	0.32	0.4	0.43	0.63	0.82	0.18	0.17	0.14	0.15
MAE	0.31	0.43	0.47	0.52	0.27	0.35	0.35	0.4	0.35	0.34	0.55	0.68	0.4	0.27	0.19	0.17
MSE	0.13	0.23	0.27	0.32	0.11	0.17	0.17	0.23	0.18	0.19	0.42	0.7	0.19	0.1	0.05	0.04

TABLE A.230

	SFH=Constant; SN=5.0; Av=1.0; Age of the system = 8.8															
	ΔX_{AGN}				$\Delta < \alpha_v >_L$				$\Delta < \log(t_\star) >_L$				$\Delta < \log(t_\star) >_M$			
X^i_{AGN}	0.2	0.4	0.6	0.8	0.2	0.4	0.6	0.8	0.2	0.4	0.6	0.8	0.2	0.4	0.6	0.8
Mean	0.1	0.1	0.03	0.05	-0.16	-0.16	-0.13	-0.09	0.0	-0.02	-0.2	-0.19	0.73	0.64	0.55	0.54
SD	0.09	0.08	0.09	0.07	0.21	0.15	0.17	0.13	0.22	0.27	0.37	0.59	0.54	0.59	0.58	0.83
MAE	0.12	0.11	0.08	0.07	0.21	0.18	0.16	0.12	0.18	0.23	0.35	0.49	0.75	0.71	0.68	0.85
MSE	0.02	0.02	0.01	0.01	0.07	0.05	0.05	0.03	0.05	0.07	0.17	0.38	0.83	0.75	0.64	0.98

	SFH=Constant; SN=5.0; Av=1.0; Age of the system = 8.8															
	$\Delta \log < Z_\star >_L$				$\Delta \log < Z_\star >_M$				$\Delta M_\star$				ΔA_v			
X^i_{AGN}	0.2	0.4	0.6	0.8	0.2	0.4	0.6	0.8	0.2	0.4	0.6	0.8	0.2	0.4	0.6	0.8
Mean	-0.37	-0.47	-0.51	-0.53	-0.19	-0.28	-0.31	-0.36	-0.13	-0.06	-0.05	-0.0	0.27	0.24	0.14	0.14
SD	0.21	0.2	0.23	0.24	0.3	0.28	0.31	0.34	0.33	0.37	0.39	0.71	0.16	0.15	0.2	0.11
MAE	0.38	0.48	0.53	0.54	0.27	0.32	0.38	0.44	0.28	0.31	0.33	0.58	0.28	0.25	0.2	0.15
MSE	0.18	0.26	0.32	0.33	0.13	0.16	0.19	0.25	0.13	0.14	0.16	0.5	0.1	0.08	0.06	0.03

TABLE A.232

	SFH=Constant; SN=5.0; Av=1.0; Age of the system = 9.2															
	ΔX_{AGN}				$\Delta < \alpha_v >_L$				$\Delta < \log(t_\star) >_L$				$\Delta < \log(t_\star) >_M$			
X^i_{AGN}	0.2	0.4	0.6	0.8	0.2	0.4	0.6	0.8	0.2	0.4	0.6	0.8	0.2	0.4	0.6	0.8
Mean	0.1	0.08	0.06	0.03	-0.14	-0.1	-0.08	-0.06	0.01	-0.03	-0.07	-0.06	0.52	0.46	0.41	0.24
SD	0.09	0.09	0.08	0.12	0.21	0.16	0.14	0.14	0.23	0.29	0.4	0.68	0.43	0.44	0.5	0.71
MAE	0.11	0.1	0.09	0.09	0.21	0.15	0.13	0.11	0.18	0.23	0.34	0.54	0.54	0.5	0.52	0.59
MSE	0.02	0.01	0.01	0.02	0.06	0.04	0.03	0.02	0.05	0.09	0.17	0.46	0.46	0.4	0.42	0.56

	SFH=Constant; SN=5.0; Av=1.0; Age of the system = 9.2															
	$\Delta \log < Z_\star >_L$				$\Delta \log < Z_\star >_M$				$\Delta M_\star$				ΔA_v			
X^i_{AGN}	0.2	0.4	0.6	0.8	0.2	0.4	0.6	0.8	0.2	0.4	0.6	0.8	0.2	0.4	0.6	0.8
Mean	-0.37	-0.44	-0.47	-0.45	-0.17	-0.28	-0.31	-0.34	-0.09	-0.05	-0.01	0.07	0.2	0.15	0.12	0.09
SD	0.18	0.23	0.24	0.3	0.23	0.31	0.35	0.35	0.29	0.34	0.37	0.65	0.16	0.15	0.14	0.17
MAE	0.38	0.45	0.48	0.49	0.21	0.35	0.4	0.41	0.27	0.28	0.3	0.51	0.23	0.18	0.15	0.14
MSE	0.17	0.25	0.27	0.3	0.08	0.17	0.22	0.23	0.1	0.12	0.14	0.43	0.07	0.04	0.04	0.04

TABLE A.234

	SFH=Constant; SN=5.0; Av=1.0; Age of the system = 9.6															
	ΔX_{AGN}				$\Delta < \alpha_v >_L$				$\Delta < \log(t_\star) >_L$				$\Delta < \log(t_\star) >_M$			
X^i_{AGN}	0.2	0.4	0.6	0.8	0.2	0.4	0.6	0.8	0.2	0.4	0.6	0.8	0.2	0.4	0.6	0.8
Mean	0.08	0.08	0.04	0.04	-0.15	-0.11	-0.07	-0.05	-0.0	-0.03	-0.15	0.0	0.4	0.23	0.31	0.18
SD	0.09	0.08	0.08	0.08	0.26	0.14	0.14	0.12	0.29	0.26	0.41	0.72	0.32	0.33	0.41	0.57
MAE	0.11	0.1	0.08	0.08	0.25	0.13	0.12	0.1	0.24	0.22	0.37	0.57	0.45	0.32	0.41	0.46
MSE	0.01	0.01	0.01	0.01	0.09	0.03	0.02	0.02	0.08	0.07	0.19	0.51	0.26	0.16	0.27	0.36

	SFH=Constant; SN=5.0; Av=1.0; Age of the system = 9.6															
	$\Delta \log < Z_\star >_L$				$\Delta \log < Z_\star >_M$				$\Delta M_\star$				ΔA_v			
X^i_{AGN}	0.2	0.4	0.6	0.8	0.2	0.4	0.6	0.8	0.2	0.4	0.6	0.8	0.2	0.4	0.6	0.8
Mean	-0.33	-0.36	-0.44	-0.48	-0.11	-0.14	-0.28	-0.38	-0.07	0.05	-0.03	0.14	0.14	0.13	0.08	0.08
SD	0.18	0.19	0.24	0.25	0.2	0.27	0.32	0.33	0.24	0.25	0.38	0.56	0.23	0.12	0.14	0.11
MAE	0.33	0.37	0.46	0.49	0.18	0.24	0.37	0.45	0.21	0.22	0.33	0.43	0.22	0.15	0.13	0.1
MSE	0.14	0.17	0.25	0.29	0.05	0.09	0.18	0.25	0.06	0.07	0.14	0.34	0.07	0.03	0.03	0.02

TABLE A.236

	SFH=Constant; SN=5.0; Av=1.0; Age of the system = 10.0															
	ΔX_{AGN}				$\Delta < \alpha_v >_L$				$\Delta < \log(t_\star) >_L$				$\Delta < \log(t_\star) >_M$			
X^i_{AGN}	0.2	0.4	0.6	0.8	0.2	0.4	0.6	0.8	0.2	0.4	0.6	0.8	0.2	0.4	0.6	0.8
Mean	0.07	0.05	0.05	0.05	-0.14	-0.11	-0.04	-0.08	-0.01	-0.1	-0.05	0.18	0.14	0.09	0.01	-0.09
SD	0.11	0.11	0.08	0.07	0.26	0.19	0.15	0.14	0.3	0.36	0.42	0.62	0.24	0.33	0.34	0.43
MAE	0.11	0.1	0.08	0.07	0.23	0.17	0.12	0.12	0.26	0.3	0.35	0.5	0.23	0.3	0.3	0.39
MSE	0.02	0.01	0.01	0.01	0.09	0.05	0.02	0.03	0.09	0.14	0.18	0.41	0.08	0.11	0.11	0.2

	SFH=Constant; SN=5.0; Av=1.0; Age of the system = 10.0															
	$\Delta \log < Z_\star >_L$				$\Delta \log < Z_\star >_M$				$\Delta M_\star$				ΔA_v			
X^i_{AGN}	0.2	0.4	0.6	0.8	0.2	0.4	0.6	0.8	0.2	0.4	0.6	0.8	0.2	0.4	0.6	0.8
Mean	-0.24	-0.29	-0.43	-0.35	-0.02	-0.09	-0.28	-0.24	0.02	0.06	0.15	0.26	0.09	0.07	0.06	0.11
SD	0.18	0.21	0.2	0.3	0.16	0.25	0.29	0.37	0.19	0.27	0.32	0.42	0.18	0.17	0.13	0.11
MAE	0.27	0.31	0.43	0.4	0.12	0.19	0.34	0.38	0.14	0.22	0.28	0.42	0.17	0.16	0.11	0.13
MSE	0.09	0.13	0.23	0.21	0.03	0.07	0.17	0.19	0.04	0.08	0.12	0.24	0.04	0.04	0.02	0.02

TABLE A.238

A.1.12 Tables: Constant SFH, SN=5, Av=2.0, base: BaseA

	SFH=Constant; SN=5.0; Av=2.0; Age of the system = 6.0															
	ΔX_{AGN}				$\Delta < \alpha_v >_L$				$\Delta < \log(t_\star) >_L$				$\Delta < \log(t_\star) >_M$			
X^i_{AGN}	0.2	0.4	0.6	0.8	0.2	0.4	0.6	0.8	0.2	0.4	0.6	0.8	0.2	0.4	0.6	0.8
Mean	0.1	0.1	0.05	0.0	0.1	-0.1	-0.17	-0.15	0.33	0.28	0.29	0.38	2.09	1.83	1.66	1.56
SD	0.09	0.08	0.06	0.07	0.11	0.12	0.1	0.13	0.24	0.22	0.19	0.35	1.4	1.51	1.54	1.52
MAE	0.11	0.1	0.07	0.05	0.13	0.12	0.17	0.18	0.33	0.28	0.29	0.38	2.09	1.83	1.66	1.56
MSE	0.02	0.02	0.01	0.0	0.02	0.02	0.04	0.04	0.17	0.13	0.12	0.26	6.34	5.61	5.15	4.77

	SFH=Constant; SN=5.0; Av=2.0; Age of the system = 6.0															
	$\Delta \log < Z_\star >_L$				$\Delta \log < Z_\star >_M$				$\Delta M_\star$				ΔA_v			
X^i_{AGN}	0.2	0.4	0.6	0.8	0.2	0.4	0.6	0.8	0.2	0.4	0.6	0.8	0.2	0.4	0.6	0.8
Mean	-0.51	-0.51	-0.49	-0.48	-0.43	-0.39	-0.37	-0.43	-0.65	-0.54	-0.54	-0.61	0.36	0.34	0.27	0.19
SD	0.25	0.25	0.26	0.28	0.28	0.28	0.36	0.3	0.58	0.62	0.68	0.79	0.16	0.14	0.12	0.13
MAE	0.53	0.51	0.5	0.5	0.45	0.42	0.46	0.46	0.67	0.6	0.58	0.66	0.36	0.34	0.28	0.21
MSE	0.32	0.32	0.31	0.31	0.26	0.24	0.27	0.28	0.75	0.69	0.76	0.99	0.15	0.13	0.09	0.05

TABLE A.240

	SFH=Constant; SN=5.0; Av=2.0; Age of the system = 6.4															
	ΔX_{AGN}				$\Delta < \alpha_v >_L$				$\Delta < \log(t_\star) >_L$				$\Delta < \log(t_\star) >_M$			
X^i_{AGN}	0.2	0.4	0.6	0.8	0.2	0.4	0.6	0.8	0.2	0.4	0.6	0.8	0.2	0.4	0.6	0.8
Mean	0.17	0.13	0.08	0.03	0.11	-0.17	-0.19	-0.15	0.07	0.01	-0.05	-0.01	1.99	1.52	0.95	0.94
SD	0.1	0.06	0.06	0.06	0.15	0.12	0.13	0.11	0.19	0.21	0.21	0.19	1.32	1.46	1.3	1.29
MAE	0.17	0.13	0.09	0.05	0.16	0.18	0.2	0.16	0.16	0.17	0.17	0.14	2.02	1.6	1.03	1.01
MSE	0.04	0.02	0.01	0.0	0.03	0.04	0.05	0.03	0.04	0.04	0.05	0.04	5.73	4.45	2.59	2.55

	SFH=Constant; SN=5.0; Av=2.0; Age of the system = 6.4															
	$\Delta \log < Z_\star >_L$				$\Delta \log < Z_\star >_M$				$\Delta M_\star$				ΔA_v			
X^i_{AGN}	0.2	0.4	0.6	0.8	0.2	0.4	0.6	0.8	0.2	0.4	0.6	0.8	0.2	0.4	0.6	0.8
Mean	-0.5	-0.52	-0.44	-0.37	-0.43	-0.45	-0.37	-0.37	-0.61	-0.47	-0.3	-0.33	0.49	0.46	0.33	0.22
SD	0.24	0.22	0.27	0.32	0.28	0.24	0.25	0.28	0.57	0.64	0.59	0.65	0.16	0.13	0.14	0.12
MAE	0.5	0.52	0.44	0.4	0.45	0.46	0.39	0.38	0.67	0.57	0.4	0.43	0.49	0.46	0.33	0.22
MSE	0.3	0.32	0.26	0.24	0.26	0.26	0.2	0.22	0.7	0.63	0.44	0.52	0.27	0.22	0.13	0.06

TABLE A.242

	SFH=Constant; SN=5.0; Av=2.0; Age of the system = 6.8															
	ΔX_{AGN}				$\Delta < \alpha_v >_L$				$\Delta < \log(t_\star) >_L$				$\Delta < \log(t_\star) >_M$			
X^i_{AGN}	0.2	0.4	0.6	0.8	0.2	0.4	0.6	0.8	0.2	0.4	0.6	0.8	0.2	0.4	0.6	0.8
Mean	0.23	0.2	0.14	0.08	0.07	-0.12	-0.15	-0.13	0.03	-0.07	-0.1	-0.06	0.91	0.79	0.84	0.85
SD	0.09	0.08	0.08	0.05	0.14	0.12	0.12	0.11	0.16	0.2	0.19	0.36	0.93	1.15	1.07	1.3
MAE	0.23	0.2	0.14	0.08	0.12	0.15	0.17	0.14	0.11	0.16	0.17	0.29	0.96	0.95	0.95	1.04
MSE	0.06	0.05	0.03	0.01	0.02	0.03	0.04	0.03	0.03	0.04	0.05	0.13	1.68	1.94	1.84	2.41

	SFH=Constant; SN=5.0; Av=2.0; Age of the system = 6.8															
	$\Delta \log < Z_\star >_L$				$\Delta \log < Z_\star >_M$				$\Delta M_\star$				ΔA_v			
X^i_{AGN}	0.2	0.4	0.6	0.8	0.2	0.4	0.6	0.8	0.2	0.4	0.6	0.8	0.2	0.4	0.6	0.8
Mean	-0.47	-0.46	-0.34	-0.45	-0.4	-0.4	-0.31	-0.39	-0.06	-0.11	-0.16	-0.28	0.57	0.5	0.36	0.25
SD	0.25	0.26	0.32	0.31	0.23	0.25	0.28	0.31	0.38	0.48	0.49	0.68	0.18	0.15	0.15	0.11
MAE	0.48	0.48	0.39	0.47	0.4	0.42	0.34	0.43	0.28	0.36	0.35	0.47	0.57	0.51	0.36	0.25
MSE	0.29	0.28	0.22	0.29	0.21	0.23	0.18	0.24	0.15	0.25	0.26	0.54	0.35	0.28	0.15	0.07

TABLE A.244

	SFH=Constant; SN=5.0; Av=2.0; Age of the system = 7.2															
	ΔX_{AGN}				$\Delta < \alpha_v >_L$				$\Delta < \log(t_\star) >_L$				$\Delta < \log(t_\star) >_M$			
X^i_{AGN}	0.2	0.4	0.6	0.8	0.2	0.4	0.6	0.8	0.2	0.4	0.6	0.8	0.2	0.4	0.6	0.8
Mean	0.23	0.18	0.14	0.07	-0.21	-0.26	-0.22	-0.18	-0.08	-0.08	-0.17	-0.19	1.27	1.24	0.9	0.75
SD	0.1	0.08	0.09	0.07	0.15	0.13	0.14	0.15	0.14	0.16	0.23	0.33	1.23	1.23	1.27	1.36
MAE	0.23	0.18	0.15	0.08	0.22	0.26	0.23	0.19	0.13	0.15	0.23	0.31	1.43	1.38	1.19	1.12
MSE	0.06	0.04	0.03	0.01	0.07	0.09	0.07	0.05	0.03	0.03	0.08	0.15	3.14	3.03	2.42	2.41

	SFH=Constant; SN=5.0; Av=2.0; Age of the system = 7.2															
	$\Delta \log < Z_\star >_L$				$\Delta \log < Z_\star >_M$				$\Delta M_\star$				ΔA_v			
X^i_{AGN}	0.2	0.4	0.6	0.8	0.2	0.4	0.6	0.8	0.2	0.4	0.6	0.8	0.2	0.4	0.6	0.8
Mean	-0.31	-0.35	-0.35	-0.4	-0.18	-0.21	-0.26	-0.34	-0.13	-0.2	-0.11	-0.19	0.59	0.48	0.37	0.26
SD	0.22	0.24	0.33	0.3	0.26	0.29	0.34	0.31	0.6	0.61	0.66	0.79	0.18	0.13	0.17	0.14
MAE	0.32	0.35	0.41	0.44	0.26	0.29	0.35	0.39	0.51	0.5	0.51	0.58	0.59	0.48	0.37	0.27
MSE	0.14	0.18	0.23	0.25	0.1	0.13	0.18	0.21	0.38	0.41	0.45	0.66	0.38	0.25	0.17	0.09

TABLE A.246

	SFH=Constant; SN=5.0; Av=2.0; Age of the system = 7.6															
	ΔX_{AGN}				$\Delta < \alpha_v >_L$				$\Delta < \log(t_\star) >_L$				$\Delta < \log(t_\star) >_M$			
X^i_{AGN}	0.2	0.4	0.6	0.8	0.2	0.4	0.6	0.8	0.2	0.4	0.6	0.8	0.2	0.4	0.6	0.8
Mean	0.16	0.15	0.15	0.09	-0.21	-0.25	-0.25	-0.17	-0.1	-0.16	-0.24	-0.25	1.27	1.05	0.88	0.81
SD	0.1	0.08	0.07	0.06	0.22	0.17	0.13	0.11	0.15	0.15	0.23	0.42	1.19	1.31	1.4	1.41
MAE	0.17	0.15	0.15	0.09	0.24	0.26	0.25	0.17	0.15	0.18	0.28	0.43	1.44	1.34	1.32	1.33
MSE	0.04	0.03	0.03	0.01	0.09	0.09	0.08	0.04	0.03	0.05	0.11	0.24	3.03	2.82	2.75	2.63

	SFH=Constant; SN=5.0; Av=2.0; Age of the system = 7.6															
	$\Delta \log < Z_\star >_L$				$\Delta \log < Z_\star >_M$				$\Delta M_\star$				ΔA_v			
X^i_{AGN}	0.2	0.4	0.6	0.8	0.2	0.4	0.6	0.8	0.2	0.4	0.6	0.8	0.2	0.4	0.6	0.8
Mean	-0.25	-0.29	-0.34	-0.34	-0.16	-0.16	-0.26	-0.22	-0.14	-0.09	-0.03	-0.04	0.44	0.41	0.38	0.26
SD	0.18	0.25	0.3	0.32	0.27	0.29	0.34	0.35	0.58	0.69	0.81	0.96	0.24	0.18	0.13	0.11
MAE	0.26	0.3	0.39	0.39	0.24	0.27	0.37	0.33	0.52	0.59	0.7	0.8	0.45	0.41	0.38	0.26
MSE	0.09	0.15	0.21	0.22	0.1	0.11	0.19	0.17	0.36	0.48	0.65	0.92	0.25	0.2	0.16	0.08

TABLE A.248

	SFH=Constant; SN=5.0; Av=2.0; Age of the system = 8.0															
	ΔX_{AGN}				$\Delta < \alpha_v >_L$				$\Delta < \log(t_\star) >_L$				$\Delta < \log(t_\star) >_M$			
X^i_{AGN}	0.2	0.4	0.6	0.8	0.2	0.4	0.6	0.8	0.2	0.4	0.6	0.8	0.2	0.4	0.6	0.8
Mean	0.13	0.14	0.11	0.07	-0.22	-0.25	-0.19	-0.16	-0.11	-0.23	-0.31	-0.26	1.22	1.09	0.7	0.76
SD	0.1	0.09	0.09	0.08	0.25	0.15	0.15	0.11	0.18	0.19	0.27	0.61	0.97	1.04	1.17	1.41
MAE	0.14	0.14	0.12	0.09	0.27	0.25	0.2	0.17	0.17	0.25	0.36	0.54	1.34	1.23	1.13	1.41
MSE	0.03	0.03	0.02	0.01	0.11	0.09	0.06	0.04	0.04	0.09	0.17	0.44	2.43	2.28	1.86	2.56

	SFH=Constant; SN=5.0; Av=2.0; Age of the system = 8.0															
	$\Delta \log < Z_\star >_L$				$\Delta \log < Z_\star >_M$				$\Delta M_\star$				ΔA_v			
X^i_{AGN}	0.2	0.4	0.6	0.8	0.2	0.4	0.6	0.8	0.2	0.4	0.6	0.8	0.2	0.4	0.6	0.8
Mean	-0.29	-0.4	-0.44	-0.47	-0.13	-0.21	-0.28	-0.39	-0.2	-0.05	0.09	0.03	0.38	0.37	0.28	0.23
SD	0.19	0.21	0.24	0.27	0.28	0.32	0.29	0.34	0.5	0.65	0.76	1.23	0.22	0.17	0.13	0.14
MAE	0.3	0.4	0.45	0.48	0.25	0.33	0.34	0.45	0.44	0.56	0.64	0.91	0.39	0.38	0.29	0.25
MSE	0.12	0.2	0.25	0.29	0.09	0.15	0.16	0.27	0.29	0.43	0.58	1.51	0.19	0.17	0.1	0.07

TABLE A.250

	SFH=Constant; SN=5.0; Av=2.0; Age of the system = 8.4															
	ΔX_{AGN}				$\Delta < \alpha_v >_L$				$\Delta < \log(t_\star) >_L$				$\Delta < \log(t_\star) >_M$			
X^i_{AGN}	0.2	0.4	0.6	0.8	0.2	0.4	0.6	0.8	0.2	0.4	0.6	0.8	0.2	0.4	0.6	0.8
Mean	0.15	0.09	0.05	0.05	-0.25	-0.21	-0.14	-0.1	0.04	-0.11	-0.32	-0.3	1.06	0.79	0.82	0.52
SD	0.1	0.09	0.08	0.07	0.2	0.15	0.14	0.13	0.23	0.25	0.3	0.58	0.69	0.74	0.92	1.14
MAE	0.16	0.11	0.08	0.07	0.28	0.22	0.16	0.12	0.19	0.22	0.38	0.54	1.08	0.88	1.06	1.09
MSE	0.03	0.02	0.01	0.01	0.11	0.07	0.04	0.03	0.06	0.07	0.19	0.43	1.6	1.16	1.52	1.57

	SFH=Constant; SN=5.0; Av=2.0; Age of the system = 8.4															
	$\Delta \log < Z_\star >_L$				$\Delta \log < Z_\star >_M$				$\Delta M_\star$				ΔA_v			
X^i_{AGN}	0.2	0.4	0.6	0.8	0.2	0.4	0.6	0.8	0.2	0.4	0.6	0.8	0.2	0.4	0.6	0.8
Mean	-0.32	-0.42	-0.49	-0.51	-0.12	-0.26	-0.31	-0.35	-0.17	-0.06	-0.09	0.07	0.42	0.27	0.17	0.16
SD	0.21	0.22	0.2	0.23	0.28	0.29	0.26	0.31	0.39	0.4	0.58	0.82	0.21	0.18	0.15	0.13
MAE	0.34	0.42	0.49	0.52	0.25	0.31	0.33	0.4	0.34	0.33	0.49	0.67	0.44	0.29	0.2	0.18
MSE	0.15	0.22	0.28	0.32	0.09	0.15	0.16	0.22	0.18	0.16	0.35	0.68	0.22	0.11	0.05	0.04

TABLE A.252

	SFH=Constant; SN=5.0; Av=2.0; Age of the system = 8.8															
	ΔX_{AGN}				$\Delta < \alpha_v >_L$				$\Delta < \log(t_\star) >_L$				$\Delta < \log(t_\star) >_M$			
X^i_{AGN}	0.2	0.4	0.6	0.8	0.2	0.4	0.6	0.8	0.2	0.4	0.6	0.8	0.2	0.4	0.6	0.8
Mean	0.09	0.08	0.04	0.05	-0.17	-0.13	-0.11	-0.07	-0.0	-0.1	-0.13	-0.22	0.69	0.51	0.56	0.56
SD	0.09	0.09	0.12	0.06	0.22	0.15	0.14	0.1	0.23	0.34	0.33	0.55	0.54	0.56	0.68	0.79
MAE	0.11	0.1	0.1	0.06	0.22	0.16	0.13	0.1	0.18	0.27	0.29	0.51	0.76	0.62	0.72	0.82
MSE	0.02	0.01	0.02	0.01	0.08	0.04	0.03	0.01	0.05	0.13	0.13	0.35	0.77	0.57	0.78	0.94

	SFH=Constant; SN=5.0; Av=2.0; Age of the system = 8.8															
	$\Delta \log < Z_\star >_L$				$\Delta \log < Z_\star >_M$				$\Delta M_\star$				ΔA_v			
X^i_{AGN}	0.2	0.4	0.6	0.8	0.2	0.4	0.6	0.8	0.2	0.4	0.6	0.8	0.2	0.4	0.6	0.8
Mean	-0.35	-0.47	-0.46	-0.53	-0.23	-0.28	-0.3	-0.4	-0.1	0.02	-0.08	0.09	0.24	0.17	0.14	0.12
SD	0.19	0.18	0.23	0.24	0.25	0.28	0.3	0.3	0.3	0.31	0.48	0.77	0.2	0.19	0.2	0.09
MAE	0.36	0.47	0.46	0.55	0.26	0.33	0.36	0.43	0.25	0.24	0.39	0.52	0.28	0.21	0.19	0.13
MSE	0.16	0.25	0.26	0.34	0.11	0.15	0.18	0.25	0.1	0.1	0.24	0.6	0.1	0.07	0.06	0.02

TABLE A.254

	SFH=Constant; SN=5.0; Av=2.0; Age of the system = 9.2															
	ΔX_{AGN}				$\Delta < \alpha_v >_L$				$\Delta < \log(t_\star) >_L$				$\Delta < \log(t_\star) >_M$			
X^i_{AGN}	0.2	0.4	0.6	0.8	0.2	0.4	0.6	0.8	0.2	0.4	0.6	0.8	0.2	0.4	0.6	0.8
Mean	0.11	0.06	0.03	0.04	-0.18	-0.14	-0.07	-0.04	0.08	-0.03	-0.14	-0.14	0.54	0.46	0.56	0.39
SD	0.1	0.09	0.11	0.06	0.2	0.17	0.14	0.14	0.25	0.3	0.34	0.58	0.39	0.43	0.45	0.62
MAE	0.12	0.1	0.09	0.06	0.21	0.18	0.12	0.11	0.22	0.25	0.31	0.48	0.55	0.49	0.61	0.61
MSE	0.02	0.01	0.01	0.01	0.07	0.05	0.03	0.02	0.07	0.09	0.14	0.35	0.44	0.4	0.52	0.53

	SFH=Constant; SN=5.0; Av=2.0; Age of the system = 9.2															
	$\Delta \log < Z_\star >_L$				$\Delta \log < Z_\star >_M$				$\Delta M_\star$				ΔA_v			
X^i_{AGN}	0.2	0.4	0.6	0.8	0.2	0.4	0.6	0.8	0.2	0.4	0.6	0.8	0.2	0.4	0.6	0.8
Mean	-0.36	-0.46	-0.43	-0.51	-0.16	-0.31	-0.25	-0.37	-0.07	-0.07	-0.16	-0.02	0.25	0.16	0.09	0.09
SD	0.19	0.2	0.24	0.24	0.24	0.26	0.3	0.33	0.27	0.31	0.36	0.54	0.17	0.15	0.16	0.13
MAE	0.37	0.46	0.45	0.54	0.22	0.34	0.32	0.44	0.23	0.26	0.31	0.42	0.27	0.19	0.15	0.12
MSE	0.17	0.25	0.24	0.32	0.08	0.17	0.15	0.25	0.08	0.1	0.16	0.3	0.09	0.05	0.03	0.02

TABLE A.256

	SFH=Constant; SN=5.0; Av=2.0; Age of the system = 9.6															
	ΔX_{AGN}				$\Delta < \alpha_v >_L$				$\Delta < \log(t_\star) >_L$				$\Delta < \log(t_\star) >_M$			
X^i_{AGN}	0.2	0.4	0.6	0.8	0.2	0.4	0.6	0.8	0.2	0.4	0.6	0.8	0.2	0.4	0.6	0.8
Mean	0.06	0.05	0.05	0.02	-0.13	-0.11	-0.09	-0.06	-0.04	-0.1	-0.03	-0.1	0.34	0.33	0.25	0.22
SD	0.1	0.09	0.09	0.08	0.28	0.15	0.14	0.13	0.23	0.3	0.34	0.55	0.34	0.33	0.34	0.58
MAE	0.1	0.09	0.09	0.07	0.25	0.15	0.13	0.11	0.19	0.24	0.29	0.43	0.41	0.4	0.34	0.49
MSE	0.01	0.01	0.01	0.01	0.1	0.04	0.03	0.02	0.05	0.1	0.12	0.31	0.23	0.22	0.17	0.38

	SFH=Constant; SN=5.0; Av=2.0; Age of the system = 9.6															
	$\Delta \log < Z_\star >_L$				$\Delta \log < Z_\star >_M$				$\Delta M_\star$				ΔA_v			
X^i_{AGN}	0.2	0.4	0.6	0.8	0.2	0.4	0.6	0.8	0.2	0.4	0.6	0.8	0.2	0.4	0.6	0.8
Mean	-0.31	-0.41	-0.44	-0.41	-0.08	-0.2	-0.29	-0.28	-0.06	-0.03	0.03	0.04	0.1	0.09	0.1	0.09
SD	0.17	0.19	0.27	0.28	0.22	0.27	0.31	0.36	0.24	0.26	0.26	0.52	0.19	0.17	0.14	0.14
MAE	0.31	0.41	0.47	0.44	0.18	0.27	0.36	0.39	0.22	0.22	0.22	0.42	0.17	0.16	0.13	0.13
MSE	0.12	0.2	0.26	0.24	0.06	0.12	0.18	0.21	0.06	0.07	0.07	0.28	0.05	0.04	0.03	0.03

TABLE A.258

	SFH=Constant; SN=5.0; Av=2.0; Age of the system = 10.0															
	ΔX_{AGN}				$\Delta < \alpha_v >_L$				$\Delta < \log(t_\star) >_L$				$\Delta < \log(t_\star) >_M$			
X^i_{AGN}	0.2	0.4	0.6	0.8	0.2	0.4	0.6	0.8	0.2	0.4	0.6	0.8	0.2	0.4	0.6	0.8
Mean	0.09	0.07	0.07	0.02	-0.08	-0.12	-0.07	-0.08	0.02	-0.02	0.07	0.19	0.09	0.06	-0.04	-0.02
SD	0.09	0.1	0.12	0.13	0.27	0.2	0.16	0.13	0.26	0.34	0.39	0.64	0.27	0.38	0.39	0.41
MAE	0.1	0.1	0.11	0.09	0.23	0.18	0.13	0.11	0.21	0.29	0.34	0.56	0.25	0.33	0.34	0.36
MSE	0.02	0.02	0.02	0.02	0.08	0.05	0.03	0.02	0.07	0.12	0.16	0.44	0.08	0.15	0.15	0.17

	SFH=Constant; SN=5.0; Av=2.0; Age of the system = 10.0															
	$\Delta \log < Z_\star >_L$				$\Delta \log < Z_\star >_M$				$\Delta M_\star$				ΔA_v			
X^i_{AGN}	0.2	0.4	0.6	0.8	0.2	0.4	0.6	0.8	0.2	0.4	0.6	0.8	0.2	0.4	0.6	0.8
Mean	-0.26	-0.32	-0.4	-0.4	-0.06	-0.13	-0.28	-0.32	0.06	0.11	0.2	0.19	0.07	0.1	0.08	0.08
SD	0.16	0.21	0.24	0.3	0.18	0.27	0.3	0.36	0.21	0.3	0.34	0.49	0.16	0.18	0.16	0.18
MAE	0.26	0.34	0.42	0.44	0.13	0.23	0.35	0.43	0.17	0.26	0.31	0.42	0.14	0.16	0.13	0.13
MSE	0.09	0.15	0.22	0.25	0.04	0.09	0.17	0.23	0.05	0.1	0.16	0.27	0.03	0.04	0.03	0.04

TABLE A.260

A.1.13 Tables: Burst SFH, SN=15, Av=0.0, base: BaseD (just one PL in the base)

	SFH=Burst; SN=15.0; Av=0.0; Age of the system = 6.0															
	ΔX_{AGN}				$\Delta < \alpha_v >_L$				$\Delta < \log(t_\star) >_L$				$\Delta < \log(t_\star) >_M$			
X^i_{AGN}	0.2	0.4	0.6	0.8	0.2	0.4	0.6	0.8	0.2	0.4	0.6	0.8	0.2	0.4	0.6	0.8
Mean	0.05	0.04	-0.02	-0.04	-0.0	-0.0	-0.0	-0.0	0.35	0.53	0.58	0.61	2.58	1.76	2.18	2.17
SD	0.08	0.06	0.07	0.06	0.16	0.16	0.16	0.16	0.19	0.21	0.24	0.26	1.31	1.31	1.38	1.51
MAE	0.08	0.06	0.06	0.05	0.13	0.13	0.13	0.13	0.35	0.53	0.58	0.61	2.58	1.76	2.18	2.17
MSE	0.01	0.01	0.01	0.01	0.03	0.03	0.03	0.03	0.16	0.32	0.39	0.44	8.39	4.81	6.66	6.96

	SFH=Burst; SN=15.0; Av=0.0; Age of the system = 6.0															
	$\Delta \log < Z_\star >_L$				$\Delta \log < Z_\star >_M$				$\Delta M_\star$				ΔA_v			
X^i_{AGN}	0.2	0.4	0.6	0.8	0.2	0.4	0.6	0.8	0.2	0.4	0.6	0.8	0.2	0.4	0.6	0.8
Mean	-0.17	-0.59	-0.62	-0.52	-0.53	-0.61	-0.53	-0.68	-0.79	-0.57	-0.88	-1.02	0.29	0.14	0.01	-0.02
SD	0.2	0.48	0.72	0.7	0.37	0.52	0.66	0.65	0.55	0.47	0.64	0.74	0.14	0.23	0.22	0.19
MAE	0.21	0.61	0.66	0.57	0.55	0.68	0.63	0.72	0.81	0.58	0.89	1.02	0.29	0.22	0.18	0.16
MSE	0.07	0.57	0.9	0.76	0.42	0.64	0.73	0.89	0.92	0.55	1.2	1.58	0.1	0.07	0.05	0.04

TABLE A.262

	SFH=Burst; SN=15.0; Av=0.0; Age of the system = 6.4															
	ΔX_{AGN}				$\Delta < \alpha_{\nu} >_{L}$				$\Delta < \log(t_{\star}) >_{L}$				$\Delta < \log(t_{\star}) >_{M}$			
X^{i}_{AGN}	0.2	0.4	0.6	0.8	0.2	0.4	0.6	0.8	0.2	0.4	0.6	0.8	0.2	0.4	0.6	0.8
Mean	0.07	0.05	0.01	-0.03	-0.0	-0.0	-0.0	-0.0	0.01	0.16	0.23	0.29	1.99	1.65	1.55	1.49
SD	0.06	0.06	0.06	0.06	0.16	0.16	0.16	0.16	0.12	0.23	0.22	0.28	1.39	1.42	1.33	1.33
MAE	0.07	0.06	0.05	0.04	0.13	0.13	0.13	0.13	0.1	0.23	0.27	0.34	2.02	1.67	1.56	1.51
MSE	0.01	0.01	0.0	0.0	0.03	0.03	0.03	0.03	0.02	0.08	0.1	0.16	5.88	4.75	4.18	3.99

	SFH=Burst; SN=15.0; Av=0.0; Age of the system = 6.4															
	$\Delta \log < Z_{\star} >_{L}$				$\Delta \log < Z_{\star} >_{M}$				$\Delta M_{\star}$				ΔA_{v}			
X^{i}_{AGN}	0.2	0.4	0.6	0.8	0.2	0.4	0.6	0.8	0.2	0.4	0.6	0.8	0.2	0.4	0.6	0.8
Mean	0.02	-0.28	-0.28	-0.48	-0.52	-0.48	-0.46	-0.8	-0.67	-0.71	-0.77	-0.87	0.32	0.16	0.03	-0.01
SD	0.12	0.47	0.42	0.67	0.47	0.46	0.46	0.58	0.57	0.52	0.58	0.63	0.13	0.23	0.23	0.18
MAE	0.11	0.37	0.35	0.54	0.53	0.53	0.52	0.82	0.71	0.73	0.79	0.88	0.32	0.23	0.19	0.15
MSE	0.02	0.29	0.25	0.68	0.49	0.43	0.42	0.98	0.78	0.78	0.93	1.16	0.12	0.08	0.05	0.03

TABLE A.264

	SFH=Burst; SN=15.0; Av=0.0; Age of the system = 6.8															
	ΔX_{AGN}				$\Delta < \alpha_v >_L$				$\Delta < \log(t_\star) >_L$				$\Delta < \log(t_\star) >_M$			
X^i_{AGN}	0.2	0.4	0.6	0.8	0.2	0.4	0.6	0.8	0.2	0.4	0.6	0.8	0.2	0.4	0.6	0.8
Mean	0.15	0.15	0.09	0.04	-0.0	-0.0	-0.0	-0.0	0.17	0.28	0.31	0.2	1.46	0.72	0.48	0.62
SD	0.04	0.06	0.07	0.05	0.16	0.16	0.16	0.16	0.12	0.21	0.22	0.29	0.99	0.53	0.3	0.89
MAE	0.15	0.15	0.09	0.06	0.13	0.13	0.13	0.13	0.18	0.28	0.33	0.31	1.46	0.75	0.52	0.7
MSE	0.02	0.02	0.01	0.0	0.03	0.03	0.03	0.03	0.05	0.12	0.15	0.13	3.12	0.81	0.32	1.19

	SFH=Burst; SN=15.0; Av=0.0; Age of the system = 6.8															
	$\Delta \log < Z_\star >_L$				$\Delta \log < Z_\star >_M$				$\Delta M_\star$				ΔA_v			
X^i_{AGN}	0.2	0.4	0.6	0.8	0.2	0.4	0.6	0.8	0.2	0.4	0.6	0.8	0.2	0.4	0.6	0.8
Mean	-0.34	-0.5	-0.7	-0.64	-0.52	-0.69	-0.94	-0.87	-0.47	-0.35	-0.45	-0.58	0.42	0.25	0.12	0.07
SD	0.26	0.34	0.56	0.64	0.39	0.35	0.54	0.59	0.46	0.33	0.38	0.49	0.1	0.19	0.21	0.18
MAE	0.34	0.51	0.71	0.65	0.54	0.69	0.94	0.87	0.5	0.43	0.53	0.6	0.42	0.26	0.21	0.17
MSE	0.18	0.37	0.81	0.81	0.42	0.6	1.18	1.1	0.43	0.23	0.34	0.57	0.18	0.1	0.06	0.04

TABLE A.266

	SFH=Burst; SN=15.0; Av=0.0; Age of the system = 7.2															
	ΔX_{AGN}				$\Delta < \alpha_{\nu} >_{L}$				$\Delta < \log(t_{\star}) >_{L}$				$\Delta < \log(t_{\star}) >_{M}$			
X^{i}_{AGN}	0.2	0.4	0.6	0.8	0.2	0.4	0.6	0.8	0.2	0.4	0.6	0.8	0.2	0.4	0.6	0.8
Mean	-0.01	0.04	0.04	0.02	-0.0	-0.0	-0.0	-0.0	-0.02	-0.08	-0.14	-0.21	1.99	1.73	1.06	0.67
SD	0.04	0.09	0.13	0.11	0.16	0.16	0.16	0.16	0.06	0.14	0.16	0.3	0.78	0.96	1.16	1.27
MAE	0.03	0.08	0.11	0.08	0.13	0.13	0.13	0.13	0.06	0.13	0.19	0.3	2.0	1.73	1.13	0.94
MSE	0.0	0.01	0.02	0.01	0.03	0.03	0.03	0.03	0.0	0.02	0.05	0.14	4.57	3.91	2.47	2.05

	SFH=Burst; SN=15.0; Av=0.0; Age of the system = 7.2															
	$\Delta \log < Z_{\star} >_{L}$				$\Delta \log < Z_{\star} >_{M}$				$\Delta M_{\star}$				ΔA_{v}			
X^{i}_{AGN}	0.2	0.4	0.6	0.8	0.2	0.4	0.6	0.8	0.2	0.4	0.6	0.8	0.2	0.4	0.6	0.8
Mean	-0.1	-0.08	-0.11	-0.14	-0.1	-0.1	-0.15	-0.24	-0.84	-0.6	-0.32	-0.23	-0.0	0.07	0.04	0.04
SD	0.07	0.09	0.13	0.23	0.25	0.39	0.36	0.43	0.39	0.58	0.76	0.79	0.1	0.15	0.23	0.16
MAE	0.1	0.09	0.12	0.19	0.18	0.23	0.28	0.37	0.84	0.67	0.58	0.55	0.08	0.14	0.19	0.14
MSE	0.01	0.01	0.03	0.07	0.07	0.16	0.15	0.24	0.85	0.7	0.67	0.68	0.01	0.03	0.05	0.03

TABLE A.268

	SFH=Burst; SN=15.0; Av=0.0; Age of the system = 7.6															
	ΔX_{AGN}				$\Delta < \alpha_{\nu} >_L$				$\Delta < \log(t_{\star}) >_L$				$\Delta < \log(t_{\star}) >_M$			
X^i_{AGN}	0.2	0.4	0.6	0.8	0.2	0.4	0.6	0.8	0.2	0.4	0.6	0.8	0.2	0.4	0.6	0.8
Mean	-0.03	-0.02	0.0	0.02	-0.0	-0.0	-0.0	-0.0	0.03	0.08	0.05	-0.28	1.4	1.77	1.76	0.86
SD	0.07	0.11	0.12	0.1	0.16	0.16	0.16	0.16	0.06	0.13	0.16	0.33	0.61	0.59	0.66	1.06
MAE	0.05	0.07	0.08	0.07	0.13	0.13	0.13	0.13	0.05	0.11	0.13	0.31	1.4	1.77	1.76	1.01
MSE	0.0	0.01	0.01	0.01	0.03	0.03	0.03	0.03	0.0	0.02	0.03	0.18	2.34	3.48	3.54	1.87

	SFH=Burst; SN=15.0; Av=0.0; Age of the system = 7.6															
	$\Delta \log < Z_{\star} >_L$				$\Delta \log < Z_{\star} >_M$				$\Delta M_{\star}$				ΔA_v			
X^i_{AGN}	0.2	0.4	0.6	0.8	0.2	0.4	0.6	0.8	0.2	0.4	0.6	0.8	0.2	0.4	0.6	0.8
Mean	-0.16	-0.33	-0.47	-0.85	-0.24	-0.35	-0.24	-0.79	-0.59	-0.83	-0.85	-0.24	0.0	0.01	0.02	0.02
SD	0.1	0.11	0.21	0.64	0.29	0.49	0.52	0.73	0.33	0.4	0.49	0.72	0.13	0.2	0.18	0.21
MAE	0.16	0.33	0.47	0.85	0.29	0.47	0.43	0.88	0.59	0.83	0.85	0.56	0.1	0.16	0.16	0.17
MSE	0.03	0.12	0.27	1.13	0.14	0.36	0.33	1.15	0.45	0.84	0.96	0.57	0.02	0.04	0.03	0.04

TABLE A.270

	SFH=Burst; SN=15.0; Av=0.0; Age of the system = 8.0															
	ΔX_{AGN}				$\Delta < \alpha_{\nu} >_{L}$				$\Delta < \log(t_{\star}) >_{L}$				$\Delta < \log(t_{\star}) >_{M}$			
X^{i}_{AGN}	0.2	0.4	0.6	0.8	0.2	0.4	0.6	0.8	0.2	0.4	0.6	0.8	0.2	0.4	0.6	0.8
Mean	0.0	-0.04	-0.06	-0.03	-0.0	-0.0	-0.0	-0.0	0.09	0.09	0.06	-0.24	1.01	1.11	1.31	1.03
SD	0.04	0.08	0.08	0.08	0.16	0.16	0.16	0.16	0.05	0.11	0.11	0.42	0.5	0.64	0.47	0.81
MAE	0.03	0.05	0.07	0.05	0.13	0.13	0.13	0.13	0.09	0.12	0.1	0.31	1.01	1.12	1.31	1.16
MSE	0.0	0.01	0.01	0.01	0.03	0.03	0.03	0.03	0.01	0.02	0.02	0.23	1.27	1.65	1.94	1.72

	SFH=Burst; SN=15.0; Av=0.0; Age of the system = 8.0															
	$\Delta \log < Z_{\star} >_{L}$				$\Delta \log < Z_{\star} >_{M}$				$\Delta M_{\star}$				ΔA_{v}			
X^{i}_{AGN}	0.2	0.4	0.6	0.8	0.2	0.4	0.6	0.8	0.2	0.4	0.6	0.8	0.2	0.4	0.6	0.8
Mean	-0.21	-0.62	-1.16	-1.51	-0.19	-0.37	-0.6	-1.21	-0.39	-0.55	-0.69	-0.46	0.03	-0.06	-0.06	-0.01
SD	0.11	0.37	0.49	0.7	0.28	0.39	0.65	0.86	0.25	0.36	0.38	0.65	0.08	0.17	0.18	0.17
MAE	0.21	0.62	1.16	1.51	0.28	0.4	0.67	1.27	0.39	0.55	0.69	0.67	0.07	0.14	0.15	0.14
MSE	0.05	0.52	1.59	2.76	0.11	0.29	0.79	2.2	0.21	0.43	0.62	0.63	0.01	0.03	0.04	0.03

TABLE A.272

	SFH=Burst; SN=15.0; Av=0.0; Age of the system = 8.4															
	ΔX_{AGN}				$\Delta < \alpha_v >_L$				$\Delta < \log(t_\star) >_L$				$\Delta < \log(t_\star) >_M$			
X^i_{AGN}	0.2	0.4	0.6	0.8	0.2	0.4	0.6	0.8	0.2	0.4	0.6	0.8	0.2	0.4	0.6	0.8
Mean	-0.06	-0.09	-0.1	-0.09	-0.0	-0.0	-0.0	-0.0	-0.0	-0.04	-0.06	-0.33	0.55	0.58	0.73	0.77
SD	0.04	0.07	0.13	0.13	0.16	0.16	0.16	0.16	0.06	0.11	0.14	0.33	0.28	0.33	0.42	0.52
MAE	0.06	0.09	0.1	0.09	0.13	0.13	0.13	0.13	0.05	0.1	0.11	0.35	0.55	0.59	0.73	0.81
MSE	0.01	0.01	0.03	0.02	0.03	0.03	0.03	0.03	0.0	0.01	0.02	0.22	0.39	0.45	0.7	0.88

	SFH=Burst; SN=15.0; Av=0.0; Age of the system = 8.4															
	$\Delta \log < Z_\star >_L$				$\Delta \log < Z_\star >_M$				$\Delta M_\star$				ΔA_v			
X^i_{AGN}	0.2	0.4	0.6	0.8	0.2	0.4	0.6	0.8	0.2	0.4	0.6	0.8	0.2	0.4	0.6	0.8
Mean	-0.25	-0.5	-1.04	-1.37	-0.21	-0.42	-0.8	-1.25	-0.3	-0.38	-0.5	-0.5	-0.09	-0.12	-0.12	-0.05
SD	0.13	0.24	0.42	0.61	0.16	0.26	0.59	0.69	0.15	0.24	0.4	0.54	0.09	0.17	0.24	0.18
MAE	0.25	0.5	1.04	1.37	0.23	0.43	0.81	1.27	0.3	0.38	0.5	0.52	0.1	0.15	0.18	0.15
MSE	0.08	0.31	1.26	2.26	0.07	0.24	0.99	2.05	0.12	0.2	0.41	0.54	0.02	0.04	0.07	0.03

TABLE A.274

	SFH=Burst; SN=15.0; Av=0.0; Age of the system = 8.8															
	ΔX_{AGN}				$\Delta < \alpha_v >_L$				$\Delta < \log(t_\star) >_L$				$\Delta < \log(t_\star) >_M$			
X^i_{AGN}	0.2	0.4	0.6	0.8	0.2	0.4	0.6	0.8	0.2	0.4	0.6	0.8	0.2	0.4	0.6	0.8
Mean	-0.05	-0.07	-0.1	-0.07	-0.0	-0.0	-0.0	-0.0	-0.1	-0.21	-0.33	-0.48	0.13	0.19	0.38	0.51
SD	0.05	0.1	0.14	0.15	0.16	0.16	0.16	0.16	0.06	0.17	0.22	0.38	0.12	0.21	0.31	0.38
MAE	0.05	0.07	0.11	0.08	0.13	0.13	0.13	0.13	0.1	0.22	0.33	0.49	0.13	0.19	0.38	0.51
MSE	0.01	0.01	0.03	0.03	0.03	0.03	0.03	0.03	0.01	0.07	0.16	0.38	0.03	0.08	0.24	0.4

	SFH=Burst; SN=15.0; Av=0.0; Age of the system = 8.8															
	$\Delta \log < Z_\star >_L$				$\Delta \log < Z_\star >_M$				$\Delta M_\star$				ΔA_v			
X^i_{AGN}	0.2	0.4	0.6	0.8	0.2	0.4	0.6	0.8	0.2	0.4	0.6	0.8	0.2	0.4	0.6	0.8
Mean	-0.09	-0.19	-0.36	-0.43	-0.05	-0.12	-0.33	-0.46	-0.1	-0.14	-0.27	-0.31	-0.04	-0.08	-0.1	-0.05
SD	0.09	0.2	0.23	0.36	0.1	0.21	0.36	0.49	0.09	0.17	0.33	0.41	0.09	0.14	0.24	0.2
MAE	0.11	0.23	0.39	0.46	0.09	0.18	0.36	0.49	0.1	0.15	0.28	0.32	0.07	0.11	0.16	0.15
MSE	0.02	0.07	0.18	0.31	0.01	0.06	0.24	0.45	0.02	0.05	0.18	0.26	0.01	0.02	0.07	0.04

TABLE A.276

	SFH=Burst; SN=15.0; Av=0.0; Age of the system = 9.2															
	ΔX_{AGN}				$\Delta < \alpha_v >_L$				$\Delta < \log(t_\star) >_L$				$\Delta < \log(t_\star) >_M$			
X^i_{AGN}	0.2	0.4	0.6	0.8	0.2	0.4	0.6	0.8	0.2	0.4	0.6	0.8	0.2	0.4	0.6	0.8
Mean	-0.01	-0.0	0.01	-0.02	-0.0	-0.01	-0.0	-0.0	-0.01	-0.04	-0.05	0.05	0.21	0.24	0.3	0.52
SD	0.06	0.08	0.08	0.09	0.16	0.16	0.16	0.16	0.11	0.17	0.24	0.32	0.12	0.12	0.2	0.24
MAE	0.04	0.04	0.04	0.05	0.13	0.13	0.13	0.13	0.07	0.13	0.19	0.25	0.21	0.24	0.31	0.53
MSE	0.0	0.01	0.01	0.01	0.03	0.03	0.03	0.03	0.01	0.03	0.06	0.1	0.06	0.07	0.13	0.33

	SFH=Burst; SN=15.0; Av=0.0; Age of the system = 9.2															
	$\Delta \log < Z_\star >_L$				$\Delta \log < Z_\star >_M$				$\Delta M_\star$				ΔA_v			
X^i_{AGN}	0.2	0.4	0.6	0.8	0.2	0.4	0.6	0.8	0.2	0.4	0.6	0.8	0.2	0.4	0.6	0.8
Mean	0.04	0.05	0.02	-0.21	0.0	0.01	-0.03	-0.26	-0.11	-0.12	-0.15	-0.29	0.02	0.01	0.02	0.01
SD	0.12	0.16	0.2	0.32	0.11	0.16	0.24	0.34	0.09	0.12	0.17	0.22	0.05	0.08	0.1	0.12
MAE	0.11	0.15	0.18	0.28	0.09	0.13	0.2	0.32	0.11	0.13	0.18	0.31	0.04	0.06	0.08	0.1
MSE	0.02	0.03	0.04	0.14	0.01	0.02	0.06	0.18	0.02	0.03	0.05	0.13	0.0	0.01	0.01	0.02

TABLE A.278

	SFH=Burst; SN=15.0; Av=0.0; Age of the system = 9.6															
	ΔX_{AGN}				$\Delta < \alpha_{\nu} >_{L}$				$\Delta < \log(t_{\star}) >_{L}$				$\Delta < \log(t_{\star}) >_{M}$			
X^{i}_{AGN}	0.2	0.4	0.6	0.8	0.2	0.4	0.6	0.8	0.2	0.4	0.6	0.8	0.2	0.4	0.6	0.8
Mean	-0.0	-0.0	-0.01	-0.06	-0.0	-0.0	-0.0	-0.0	0.05	0.05	0.01	-0.14	0.14	0.2	0.26	0.34
SD	0.03	0.05	0.08	0.15	0.16	0.16	0.16	0.16	0.08	0.14	0.19	0.43	0.08	0.09	0.09	0.09
MAE	0.02	0.03	0.04	0.08	0.13	0.13	0.13	0.13	0.07	0.1	0.13	0.31	0.14	0.2	0.26	0.34
MSE	0.0	0.0	0.01	0.03	0.03	0.03	0.03	0.03	0.01	0.02	0.04	0.21	0.03	0.05	0.08	0.12

	SFH=Burst; SN=15.0; Av=0.0; Age of the system = 9.6															
	$\Delta \log < Z_{\star} >_{L}$				$\Delta \log < Z_{\star} >_{M}$				$\Delta M_{\star}$				ΔA_{v}			
X^{i}_{AGN}	0.2	0.4	0.6	0.8	0.2	0.4	0.6	0.8	0.2	0.4	0.6	0.8	0.2	0.4	0.6	0.8
Mean	-0.03	-0.04	-0.04	-0.16	-0.03	-0.05	-0.05	-0.14	-0.08	-0.12	-0.16	-0.23	0.01	0.01	0.01	-0.03
SD	0.06	0.08	0.12	0.14	0.03	0.05	0.07	0.11	0.05	0.05	0.1	0.14	0.03	0.06	0.09	0.19
MAE	0.06	0.08	0.1	0.18	0.04	0.05	0.07	0.15	0.08	0.12	0.16	0.23	0.03	0.05	0.07	0.12
MSE	0.01	0.01	0.02	0.05	0.0	0.0	0.01	0.03	0.01	0.02	0.04	0.07	0.0	0.0	0.01	0.04

TABLE A.280

	SFH=Burst; SN=15.0; Av=0.0; Age of the system = 10.0															
	ΔX_{AGN}				$\Delta < \alpha_v >_L$				$\Delta < \log(t_\star) >_L$				$\Delta < \log(t_\star) >_M$			
X^i_{AGN}	0.2	0.4	0.6	0.8	0.2	0.4	0.6	0.8	0.2	0.4	0.6	0.8	0.2	0.4	0.6	0.8
Mean	0.0	-0.0	-0.02	-0.05	-0.0	-0.0	-0.0	-0.0	-0.01	-0.01	-0.08	-0.31	0.04	0.06	0.07	0.1
SD	0.02	0.04	0.1	0.13	0.16	0.16	0.16	0.16	0.04	0.08	0.24	0.45	0.04	0.06	0.05	0.06
MAE	0.02	0.02	0.04	0.07	0.13	0.13	0.13	0.13	0.03	0.06	0.13	0.38	0.04	0.06	0.07	0.11
MSE	0.0	0.0	0.01	0.02	0.03	0.03	0.03	0.03	0.0	0.01	0.07	0.3	0.0	0.01	0.01	0.01

	SFH=Burst; SN=15.0; Av=0.0; Age of the system = 10.0															
	$\Delta \log < Z_\star >_L$				$\Delta \log < Z_\star >_M$				$\Delta M_\star$				ΔA_v			
X^i_{AGN}	0.2	0.4	0.6	0.8	0.2	0.4	0.6	0.8	0.2	0.4	0.6	0.8	0.2	0.4	0.6	0.8
Mean	-0.03	-0.05	-0.08	-0.1	-0.03	-0.03	-0.04	-0.06	-0.03	-0.04	-0.06	-0.08	-0.01	-0.01	-0.02	-0.02
SD	0.03	0.05	0.08	0.08	0.01	0.02	0.03	0.07	0.04	0.05	0.07	0.1	0.03	0.05	0.11	0.12
MAE	0.04	0.05	0.08	0.1	0.03	0.03	0.04	0.07	0.03	0.05	0.07	0.1	0.02	0.04	0.07	0.1
MSE	0.0	0.0	0.01	0.02	0.0	0.0	0.0	0.01	0.0	0.0	0.01	0.02	0.0	0.0	0.01	0.01

TABLE A.282

A.2 Figures:

A.2.1 Figures: Instantaneous burst SFH, Av=0.0, SN = 15.0, base: BaseA

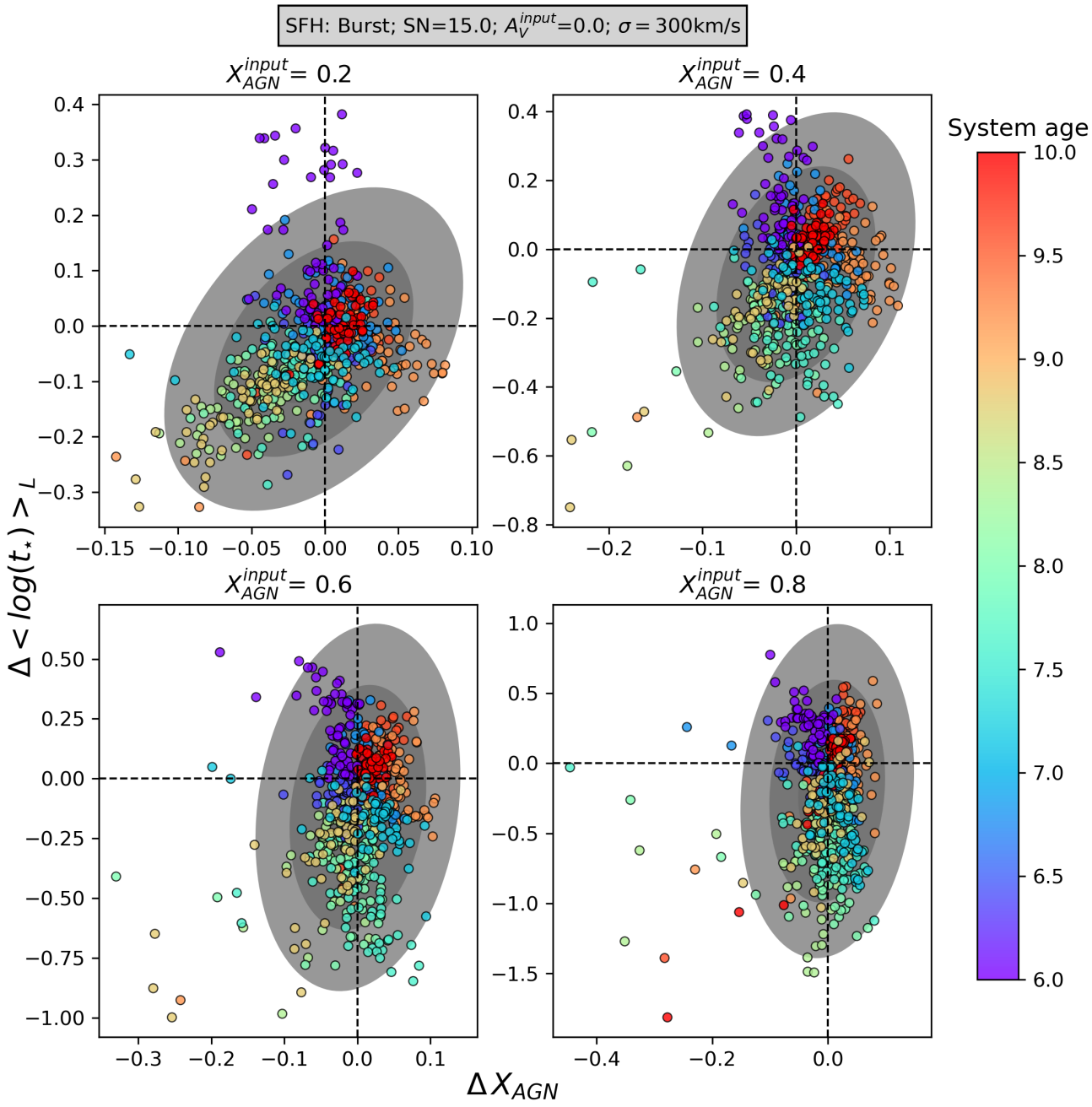

FIGURE A.1: $\Delta < log(t_\star) >_L$ vs ΔX_{AGN}; SFH: Burst, SN = 15.0, base: BaseA

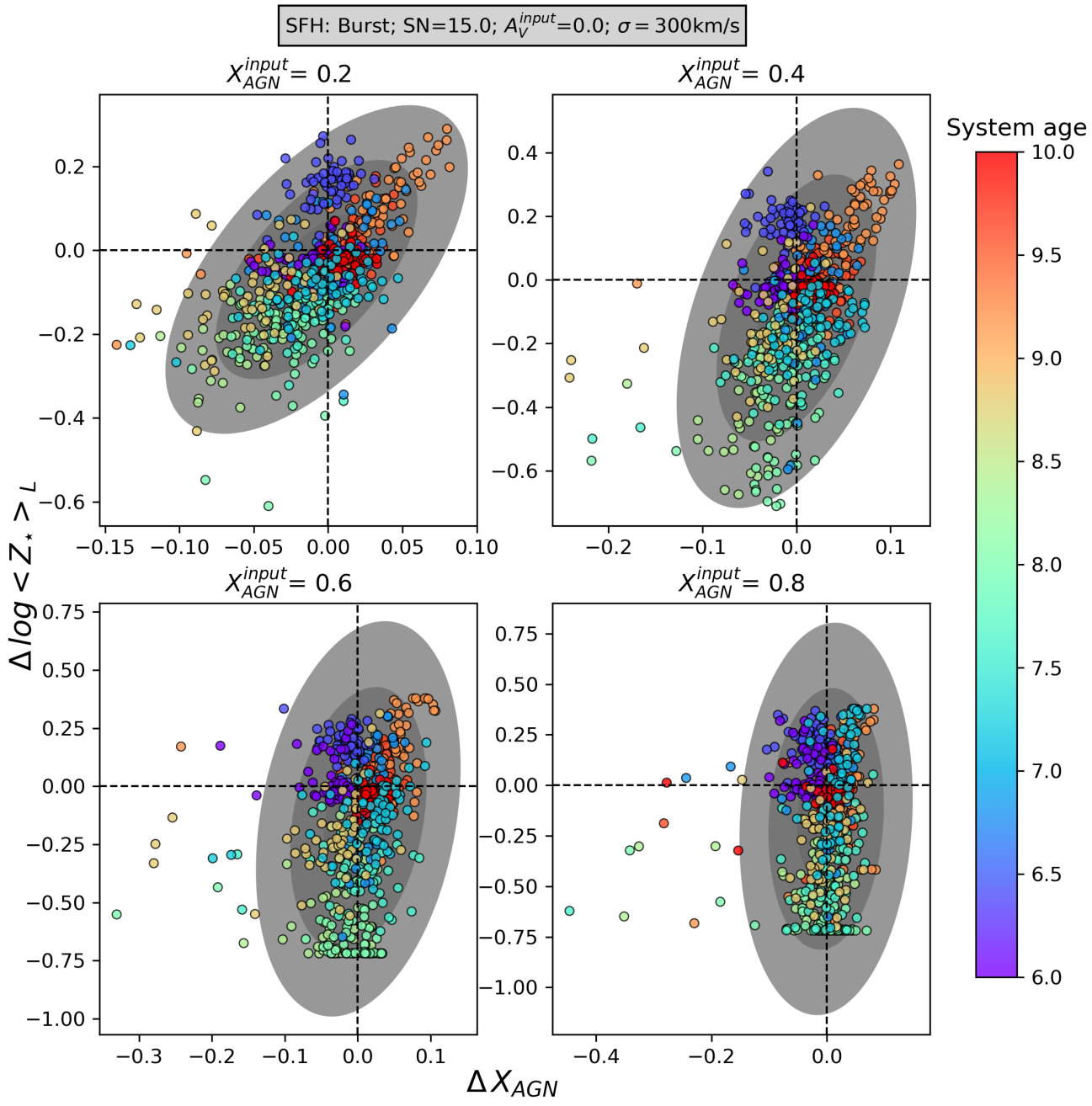

FIGURE A.2: $\Delta log < Z_\star >_L$ vs ΔX_{AGN}; SFH: Burst, SN = 15.0, base: BaseA

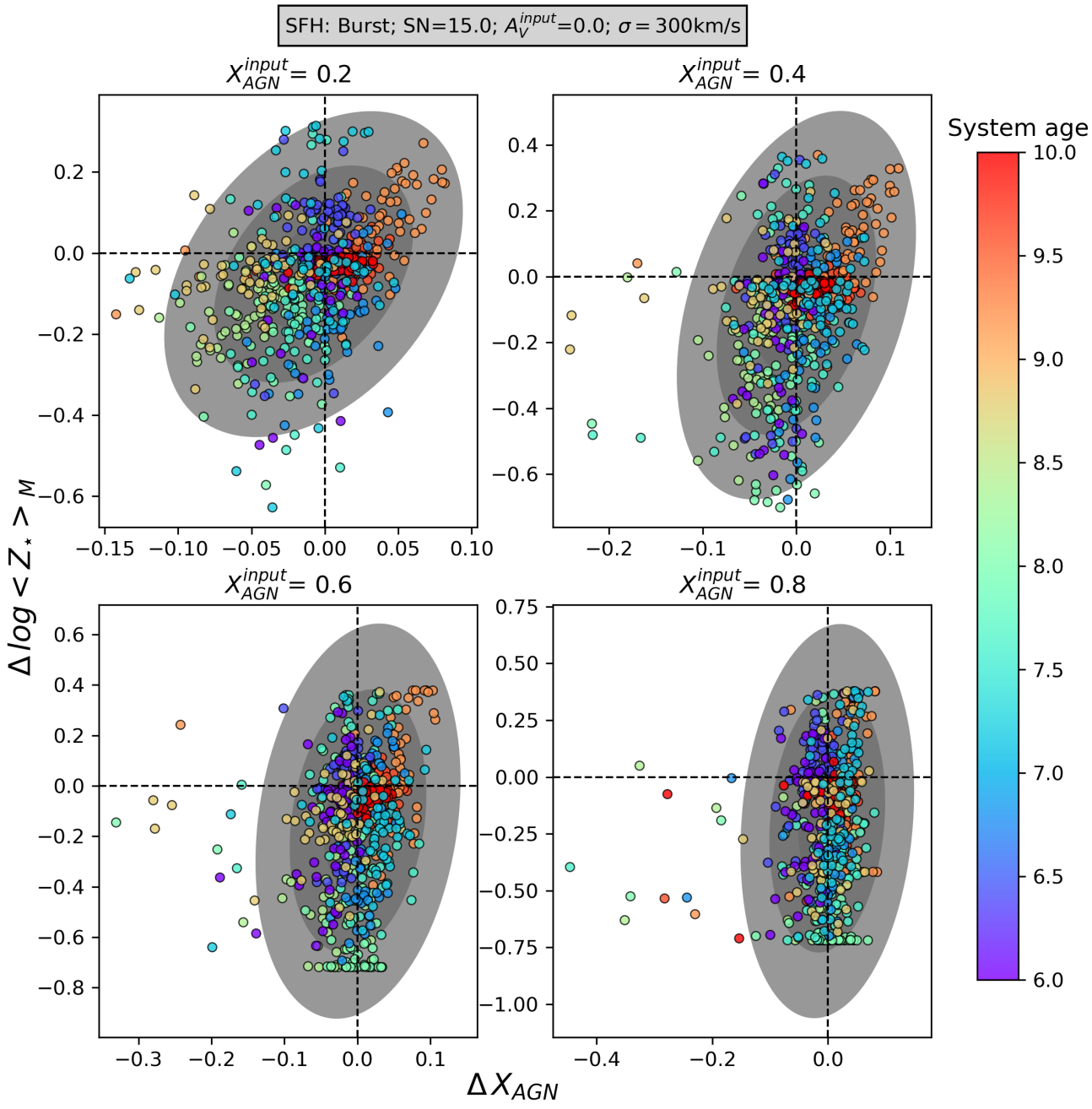

FIGURE A.3: $\Delta log < Z_\star >_M$ vs vs ΔX_{AGN}; SFH: Burst, SN = 15.0, base: BaseA

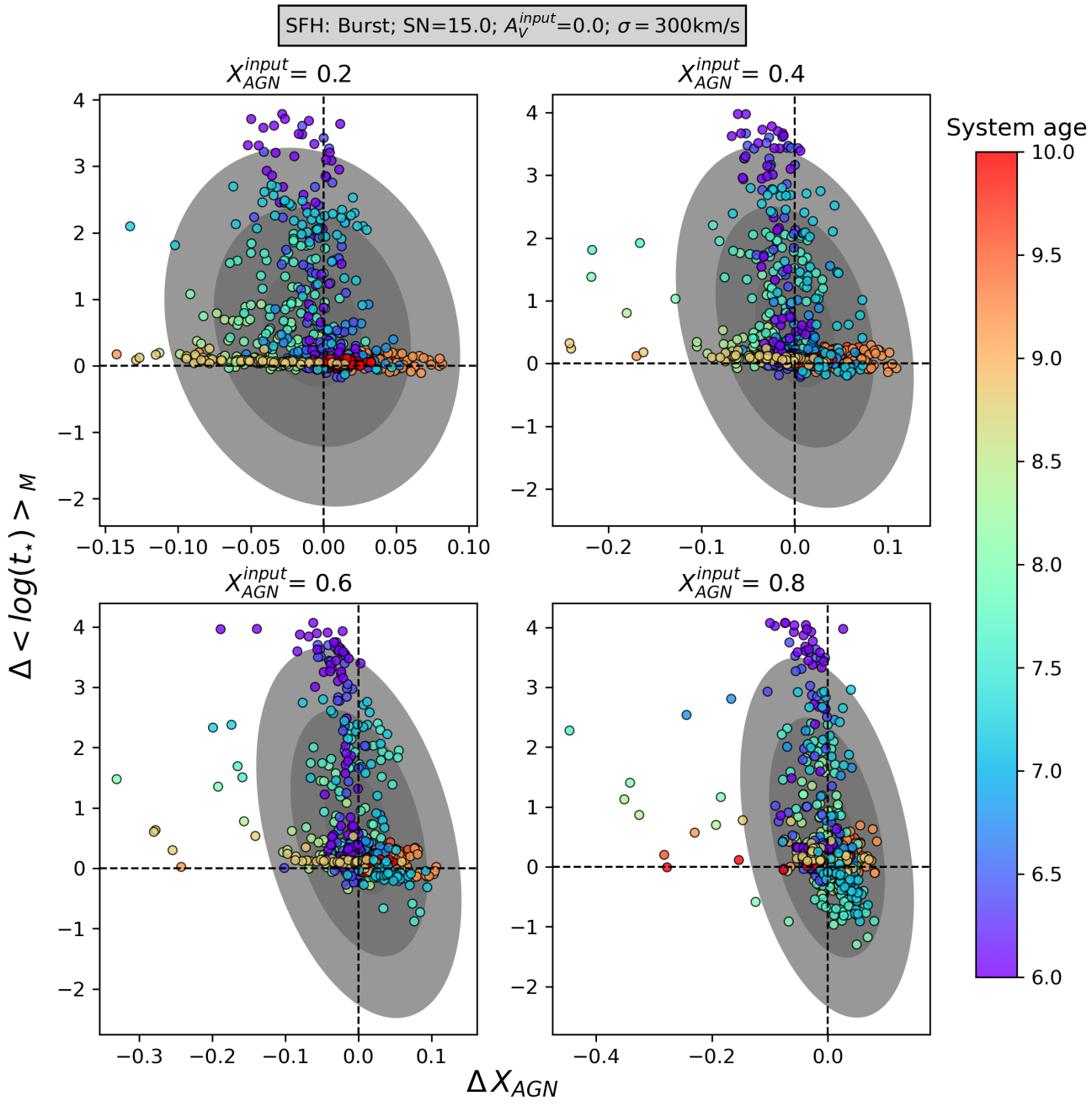

FIGURE A.4: $\Delta < log(t_\star) >_M$ vs ΔX_{AGN}; SFH: Burst, SN = 15.0, base: BaseA

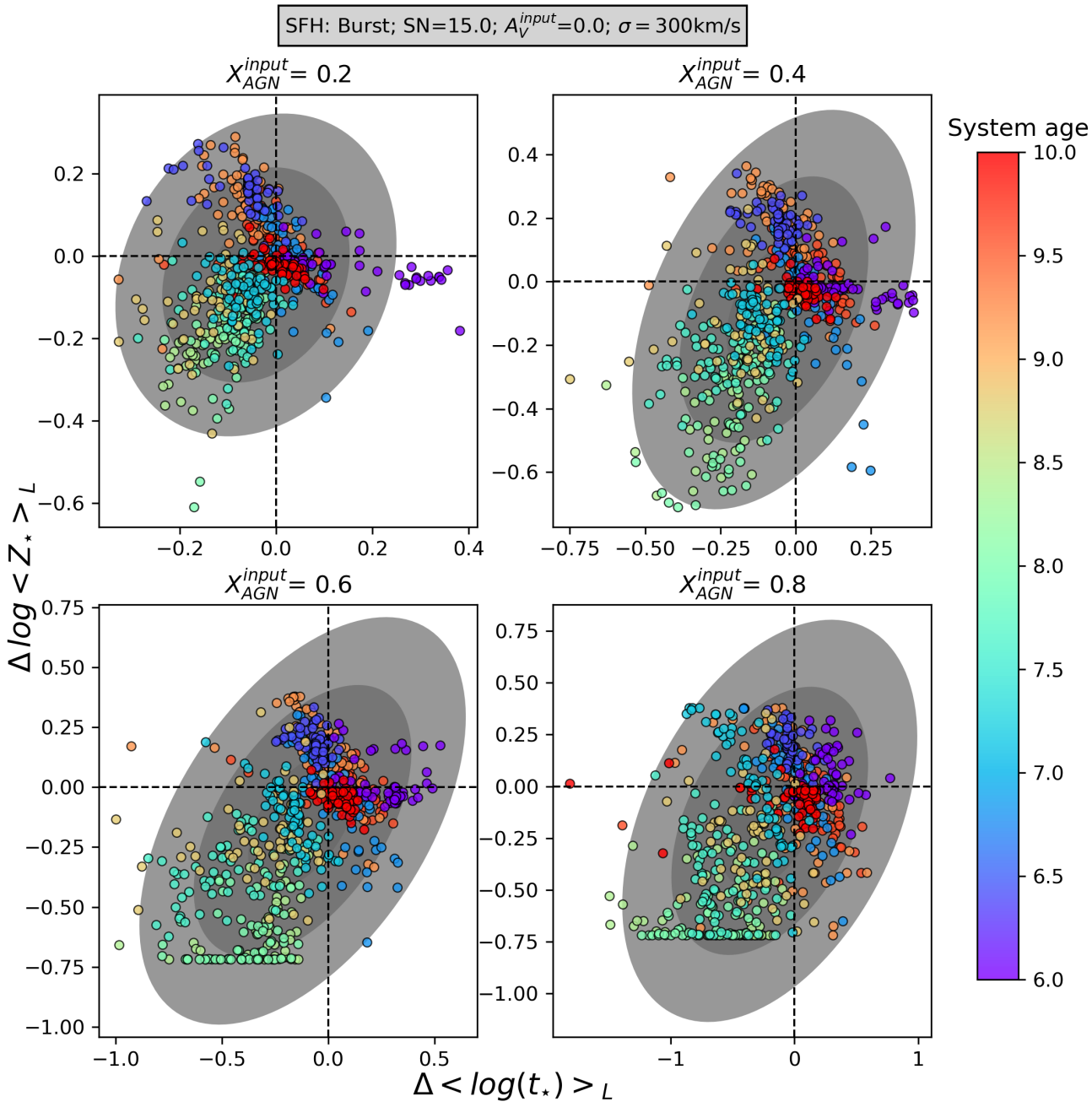

FIGURE A.5: $\Delta log < Z_\star >_L$ vs $\Delta < log(t_\star) >_L$; SFH: Burst, SN = 15.0, base: BaseA

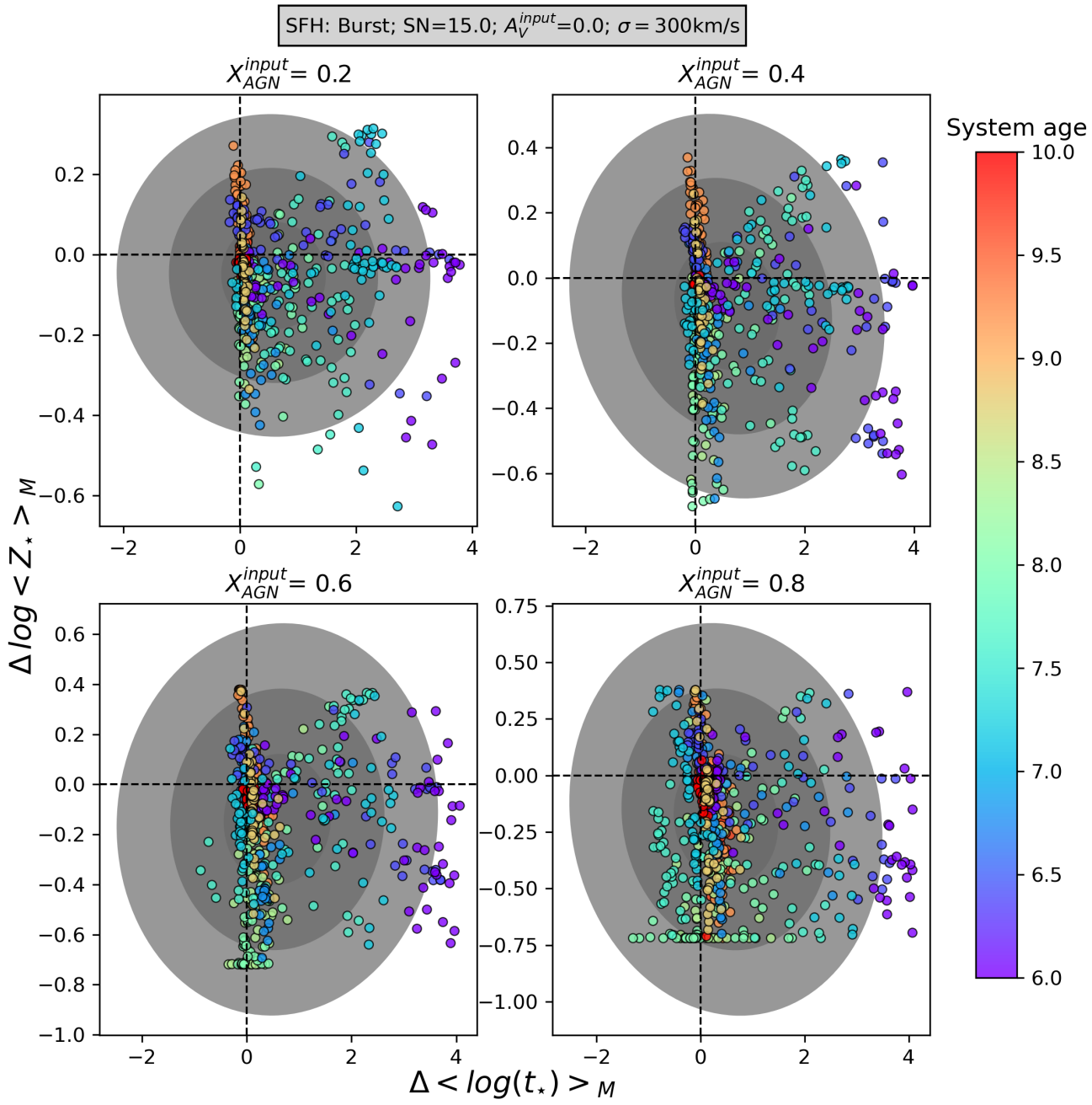

FIGURE A.6: $\Delta log < Z_\star >_M$ vs $\Delta < log(t_\star) >_M$; SFH: Burst, SN = 15.0, base: BaseA

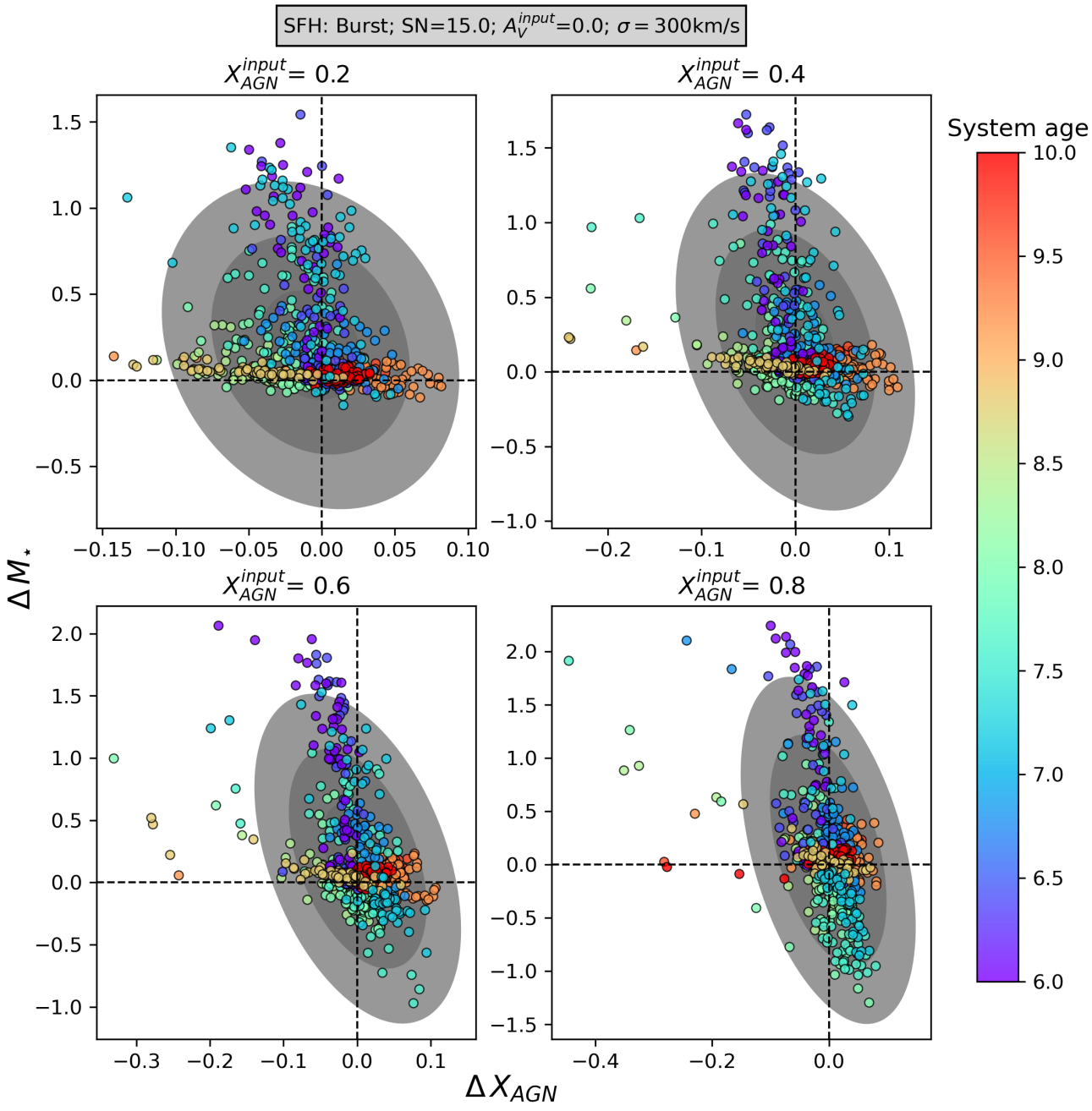

FIGURE A.7: $\Delta M_\star$ vs ΔX_{AGN}; SFH: Burst, SN = 15.0, base: BaseA

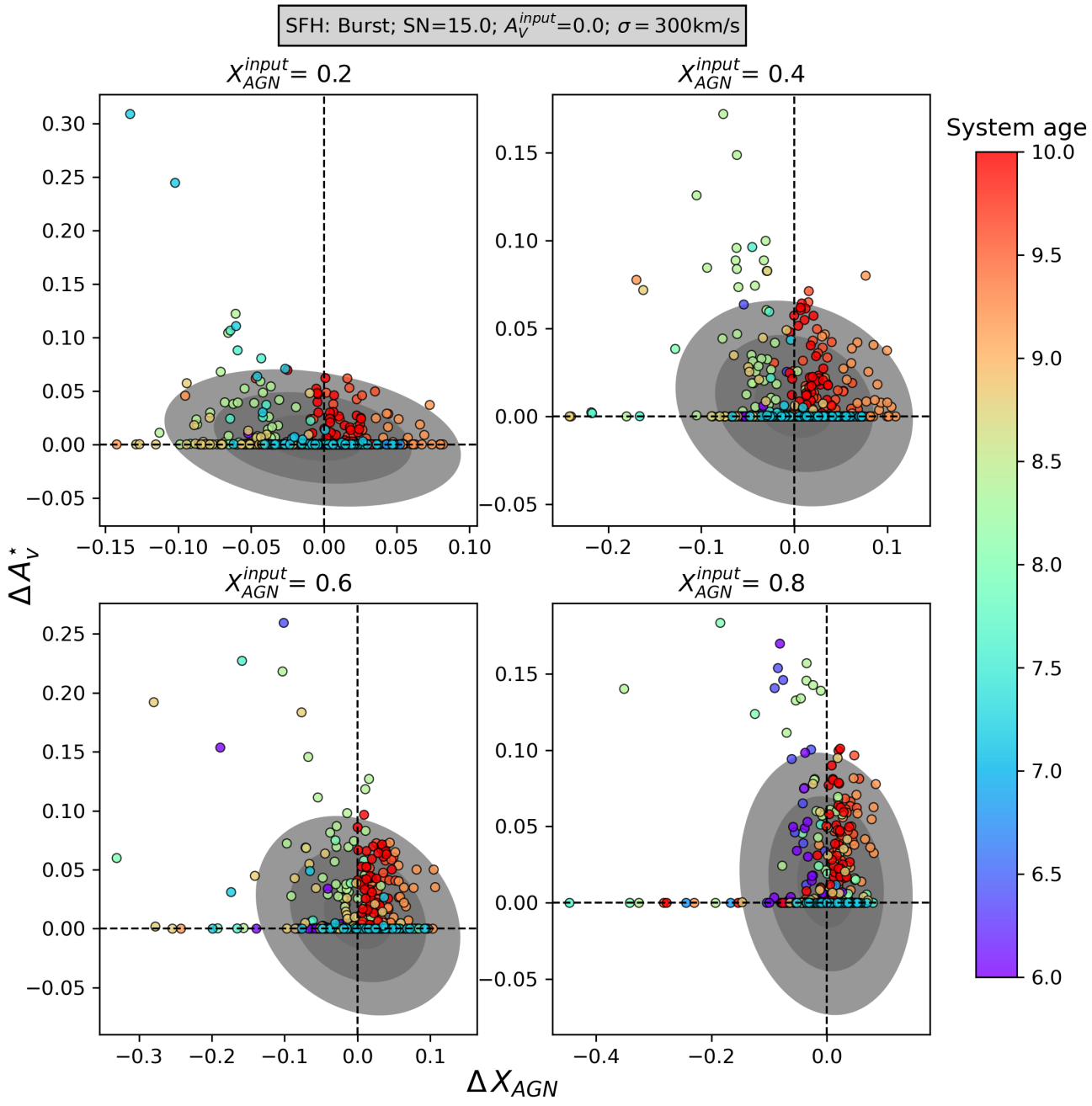

FIGURE A.8: $\Delta A_v^\star$ vs ΔX_{AGN}; SFH: Burst, SN = 15.0, base: BaseA

A.2.2 Figures: Constant SFH, Av=0.0, SN = 15.0, base: BaseA

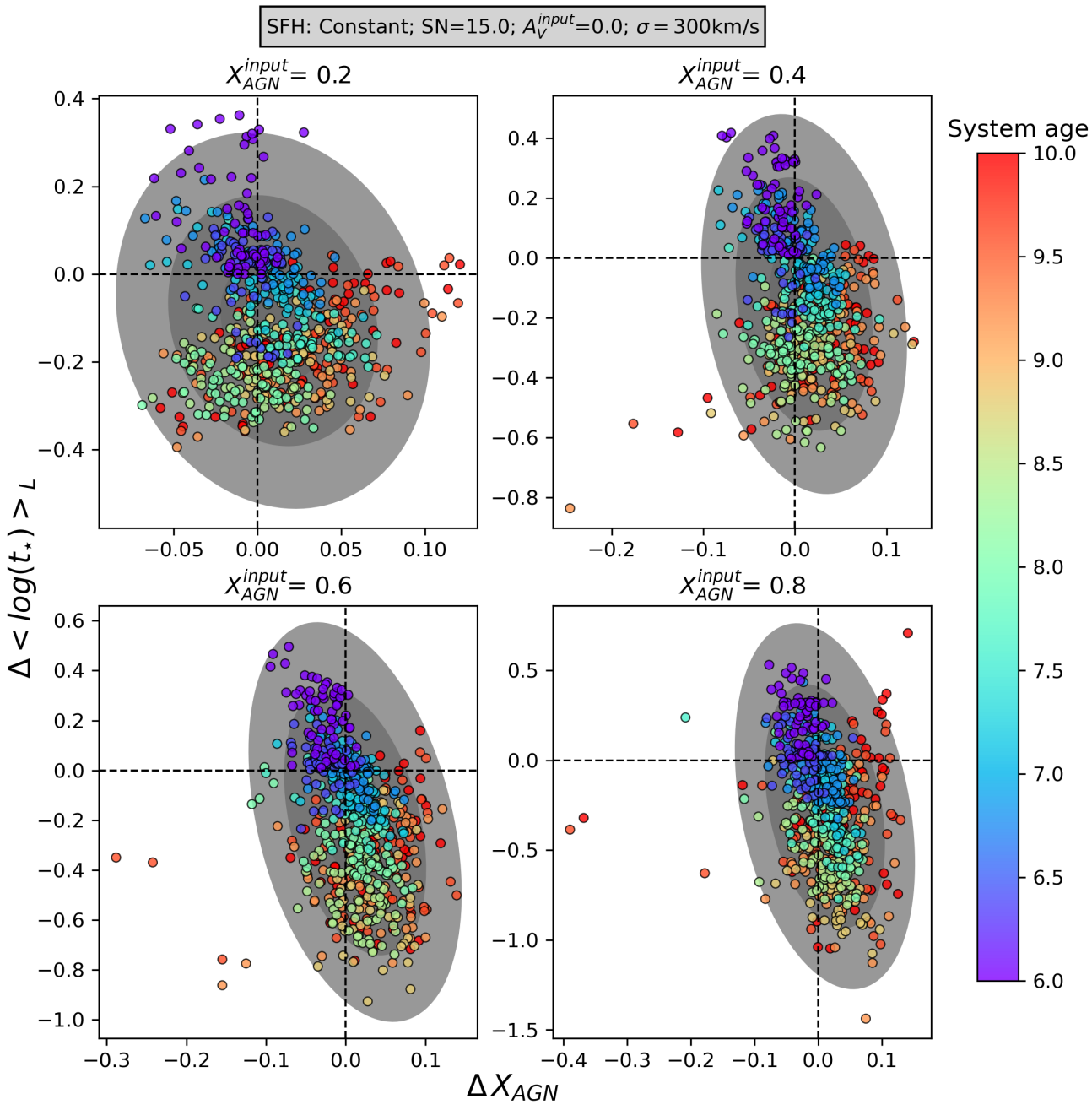

FIGURE A.9: $\Delta < log(t_\star) >_L$ vs ΔX_{AGN}; SFH: Constant, SN = 15.0, base: BaseA

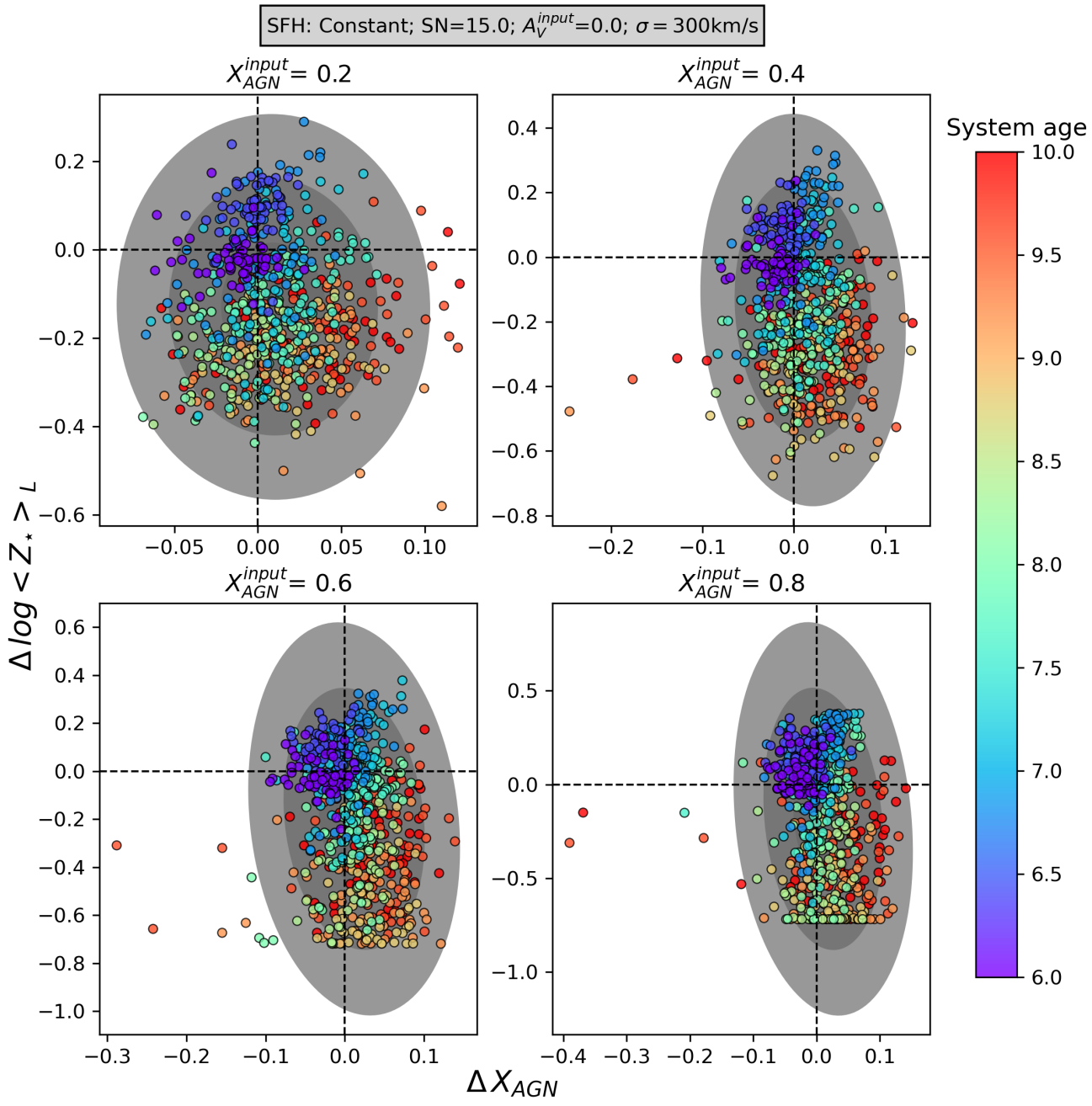

FIGURE A.10: $\Delta\, log < Z_\star >_L$ vs $\Delta\, X_{AGN}$; SFH: Constant, SN = 15.0, base: BaseA

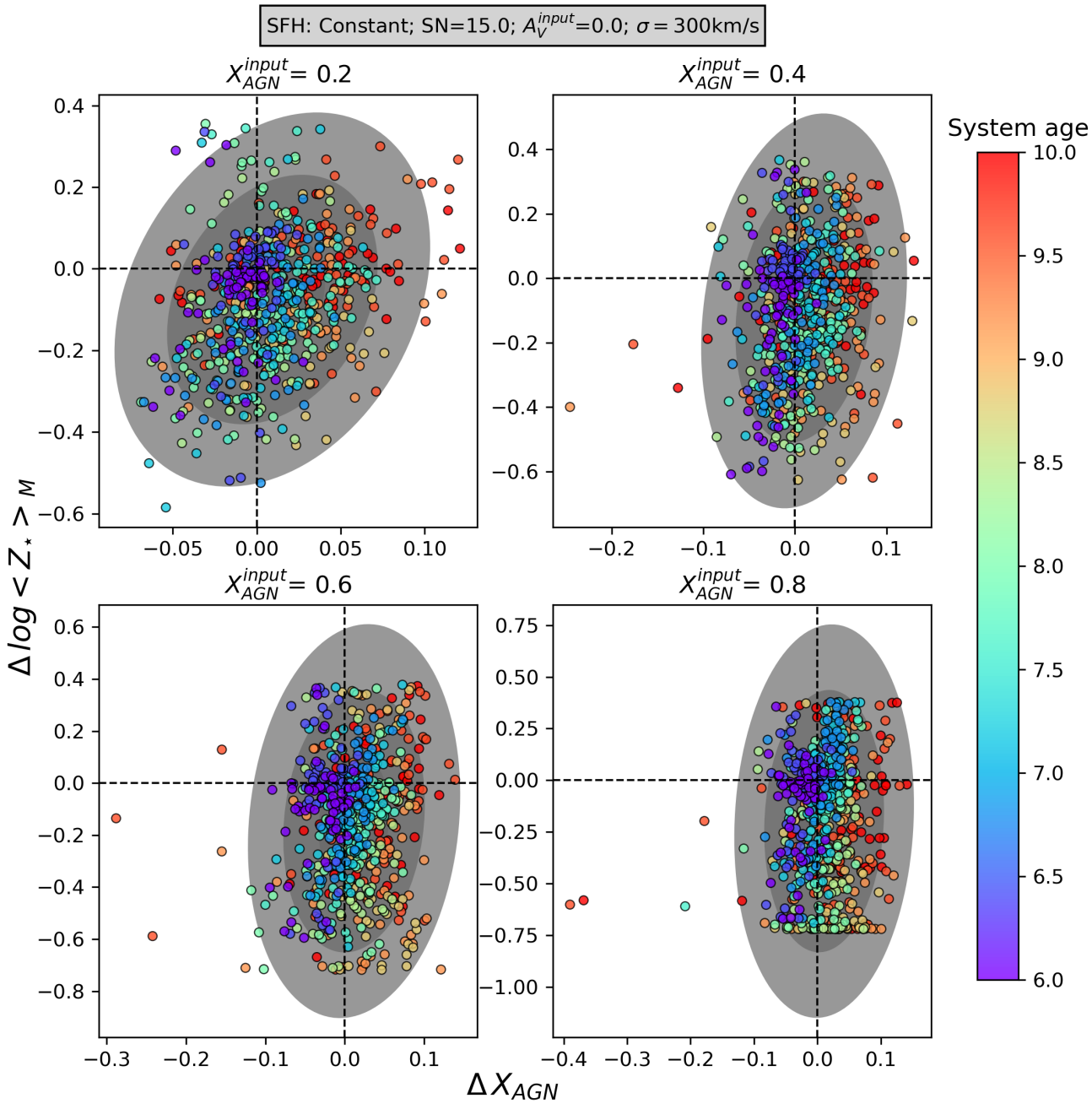

FIGURE A.11: $\Delta\, log < Z_\star >_M$ vs vs $\Delta\, X_{AGN}$; SFH: Constant, SN = 15.0, base: BaseA

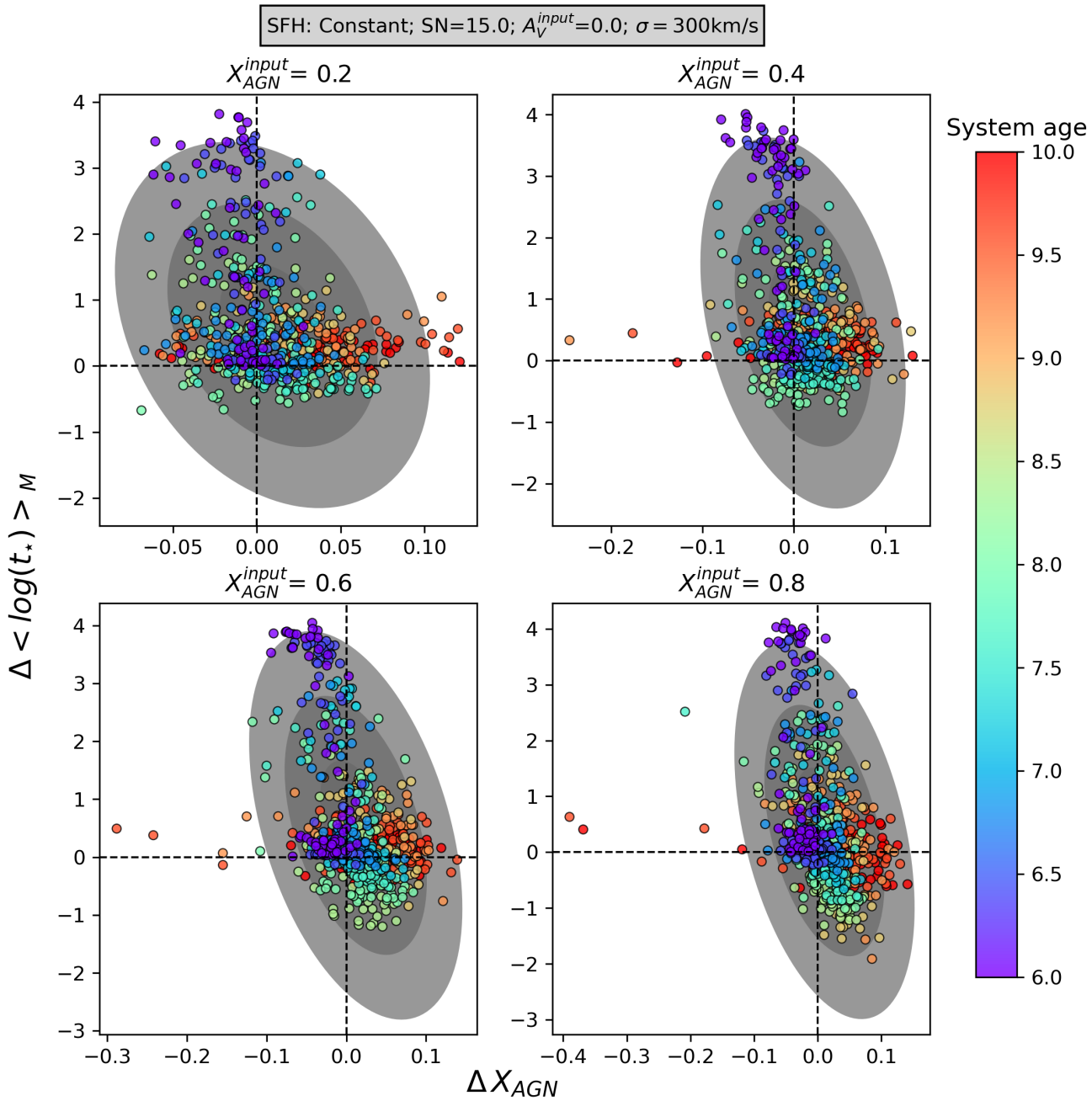

FIGURE A.12: $\Delta < log(t_\star) >_M$ vs ΔX_{AGN}; SFH: Constant, SN = 15.0, base: BaseA

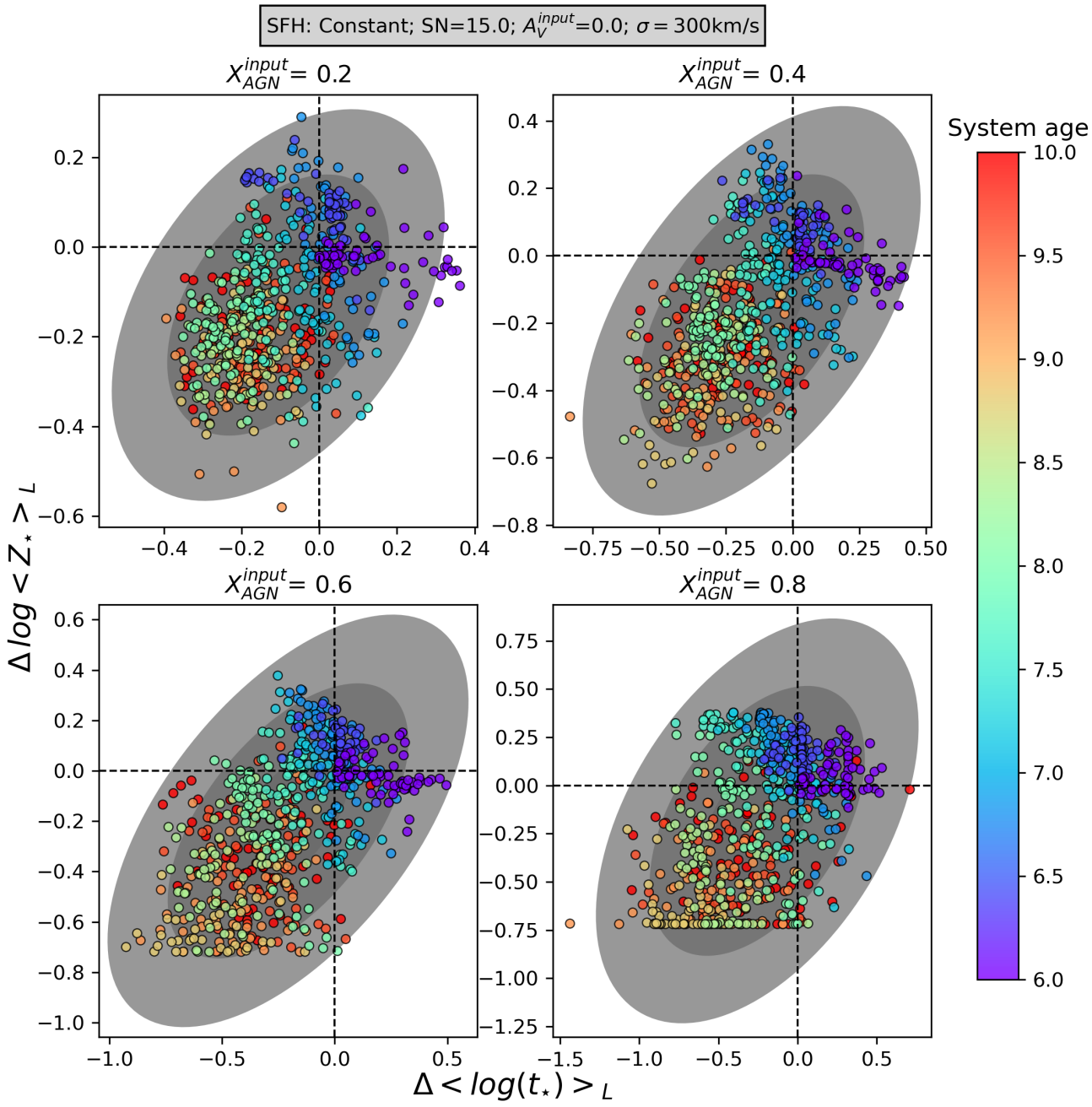

FIGURE A.13: $\Delta log < Z_\star >_L$ vs $\Delta < log(t_\star) >_L$; SFH: Constant, SN = 15.0, base: BaseA

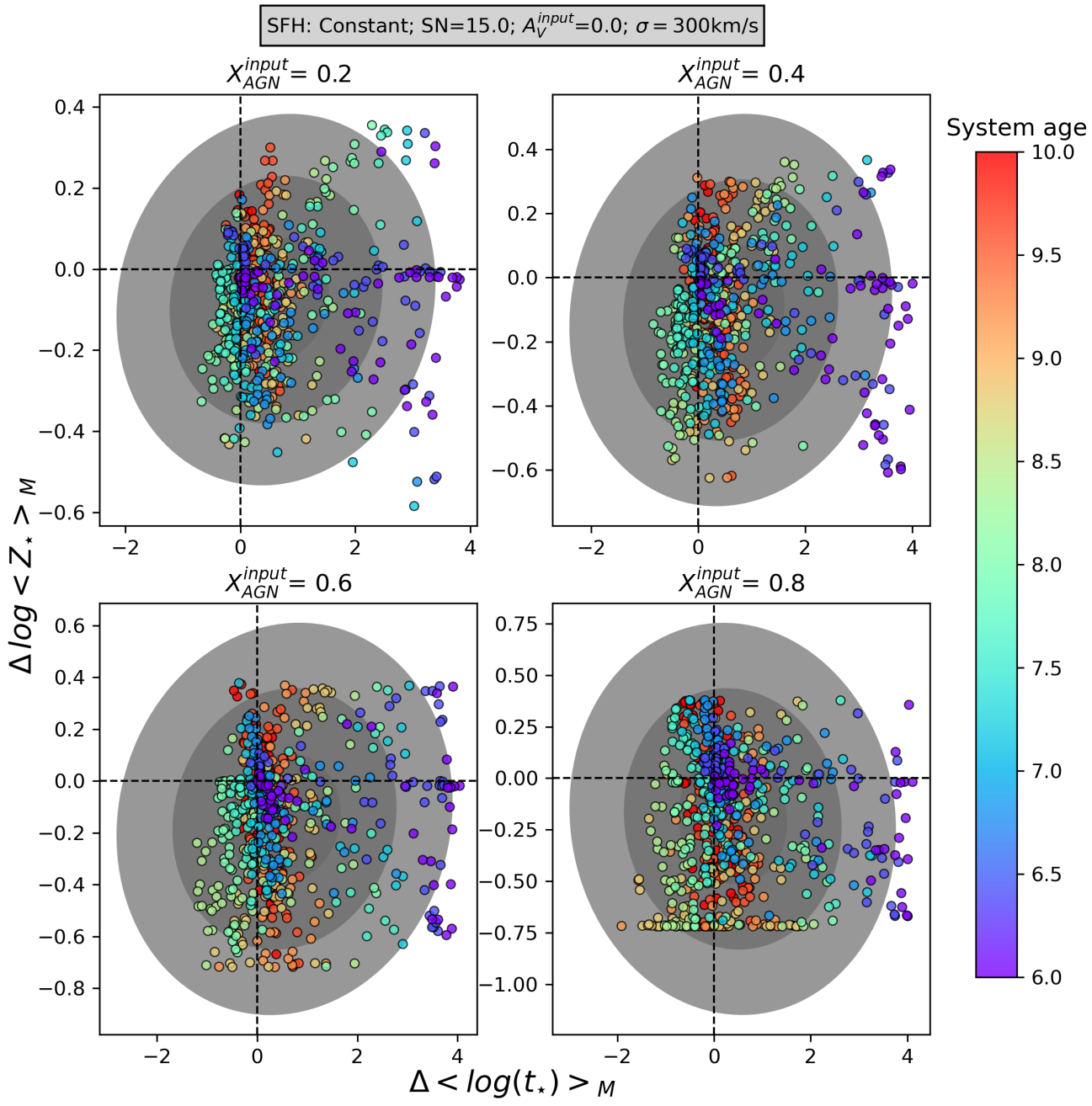

FIGURE A.14: $\Delta log < Z_\star >_M$ vs $\Delta < log(t_\star) >_M$; SFH: Constant, SN = 15.0, base: BaseA

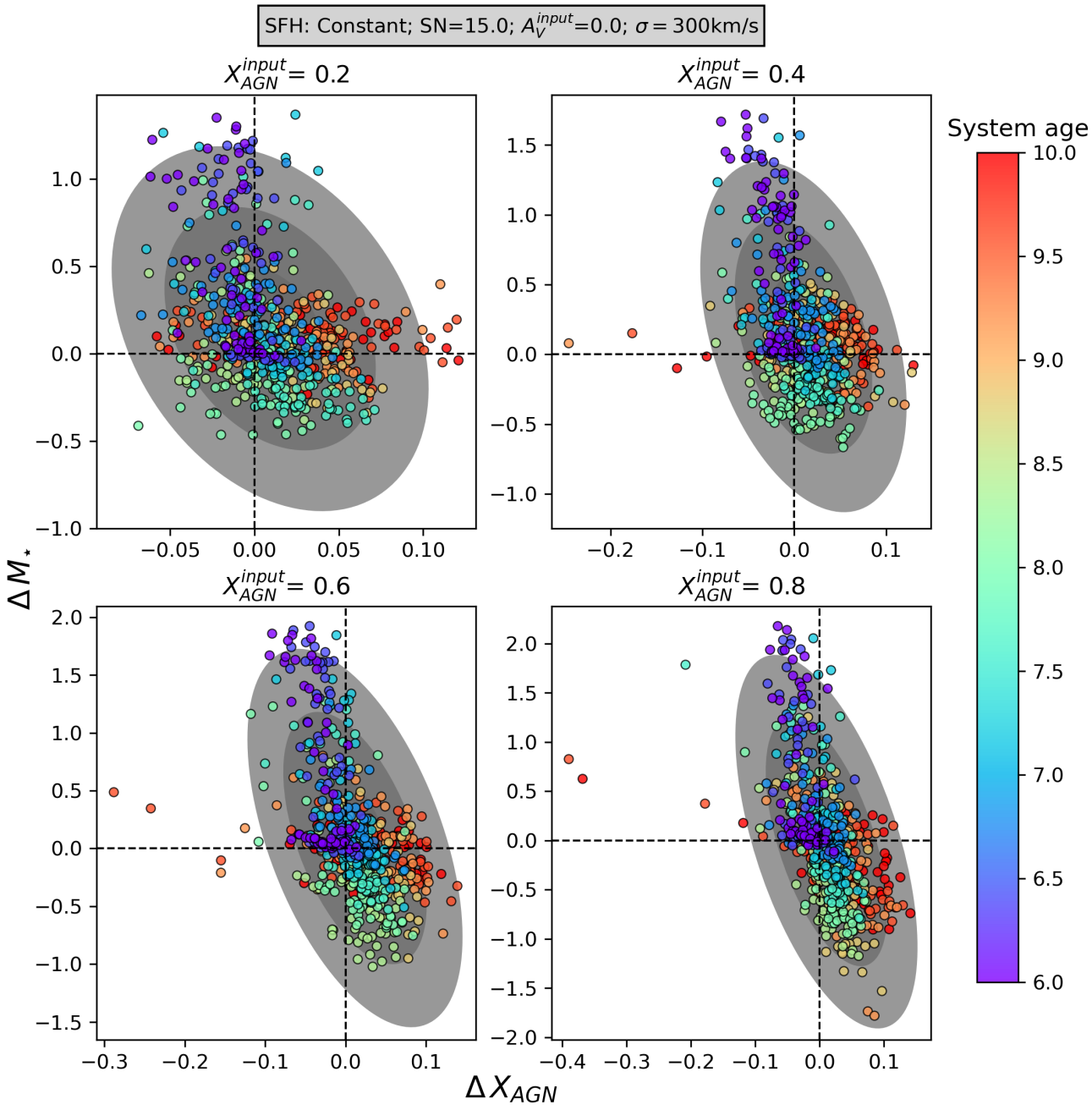

FIGURE A.15: $\Delta M_\star$ vs ΔX_{AGN}; SFH: Constant, SN = 15.0, base: BaseA

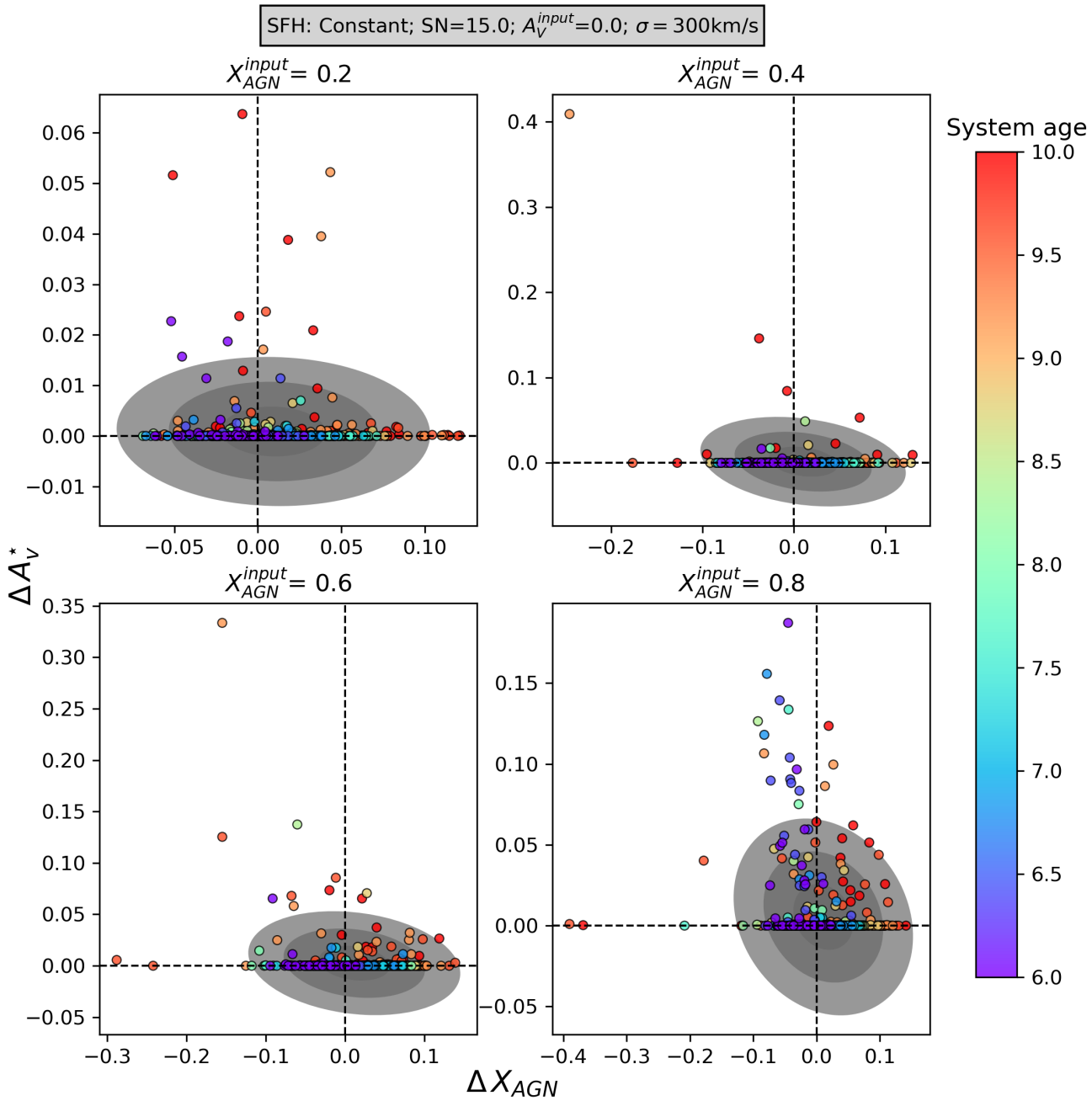

FIGURE A.16: $\Delta A_v^\star$ vs ΔX_{AGN}; SFH: Constant, SN = 15.0, base: BaseA

A.2.3 Figures: Instantaneous burst SFH, Av=1.0, SN = 15.0, base: BaseA

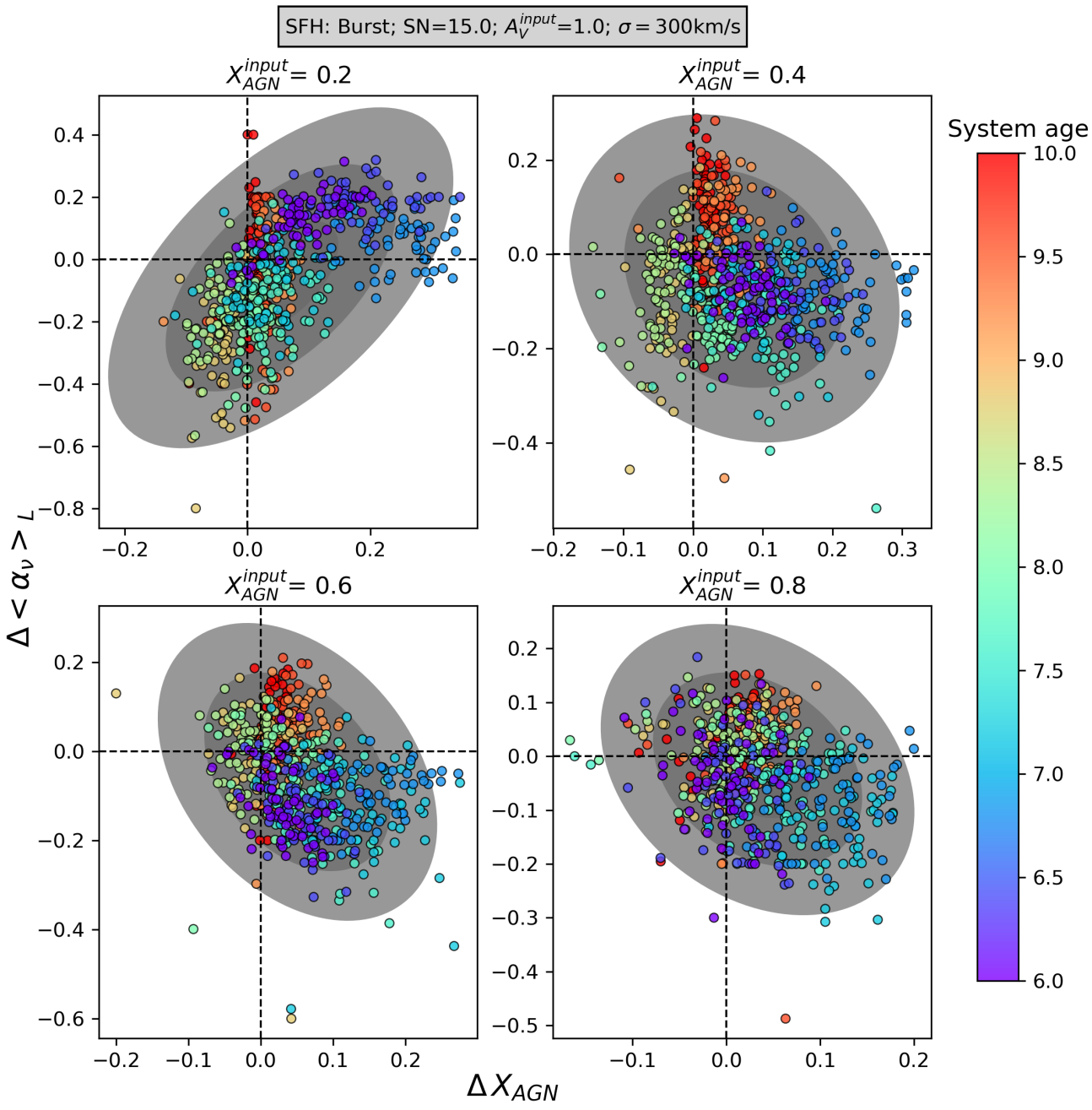

FIGURE A.17: $\Delta < \alpha_\nu >_L$ vs ΔX_{AGN}; SFH: Burst, SN = 15.0, base: BaseA

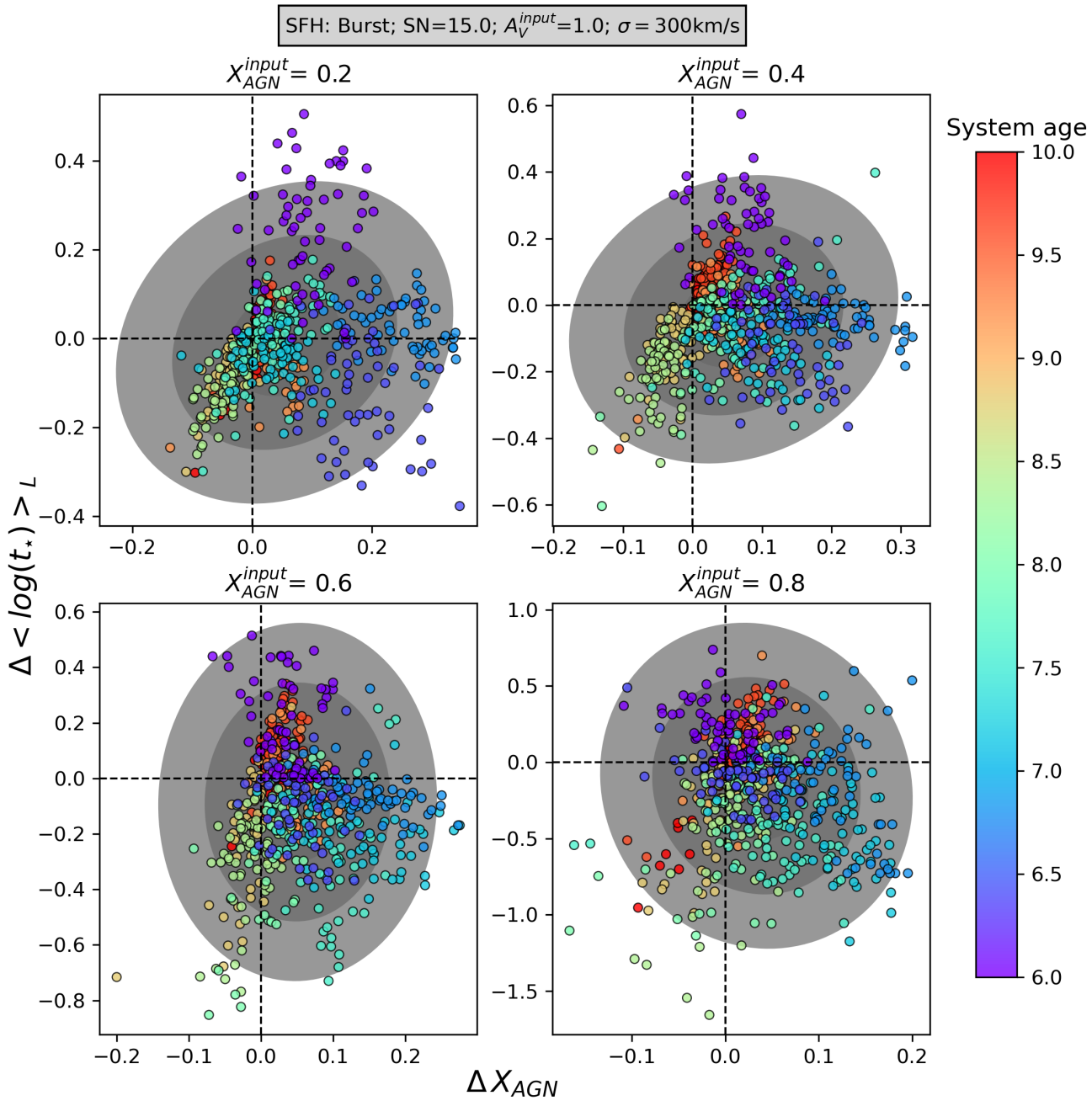

FIGURE A.18: $\Delta < log(t_\star) >_L$ vs ΔX_{AGN}; SFH: Burst, SN = 15.0, base: BaseA

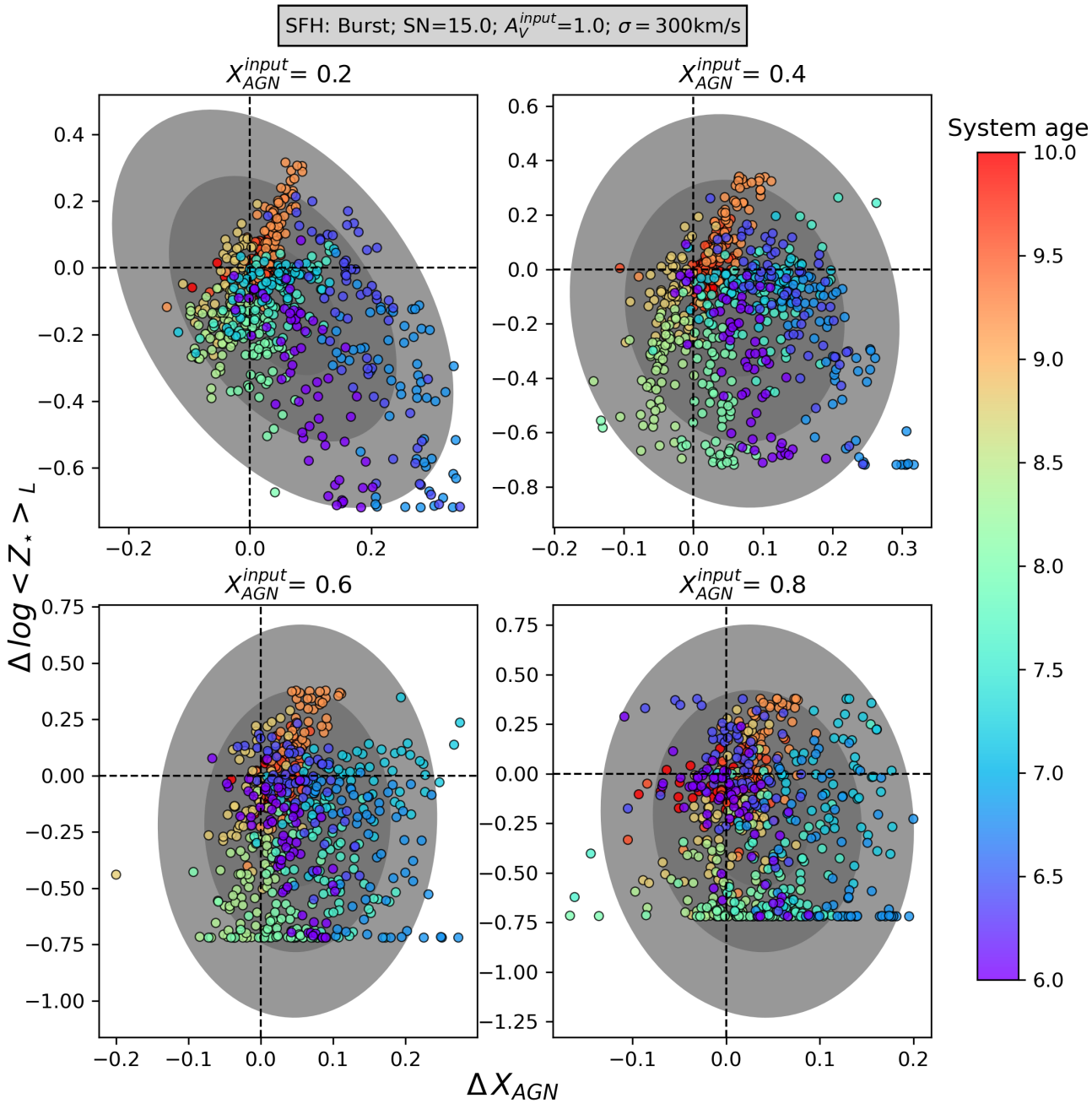

FIGURE A.19: $\Delta\, log < Z_\star >_L$ vs $\Delta\, X_{AGN}$; SFH: Burst, SN = 15.0, base: BaseA

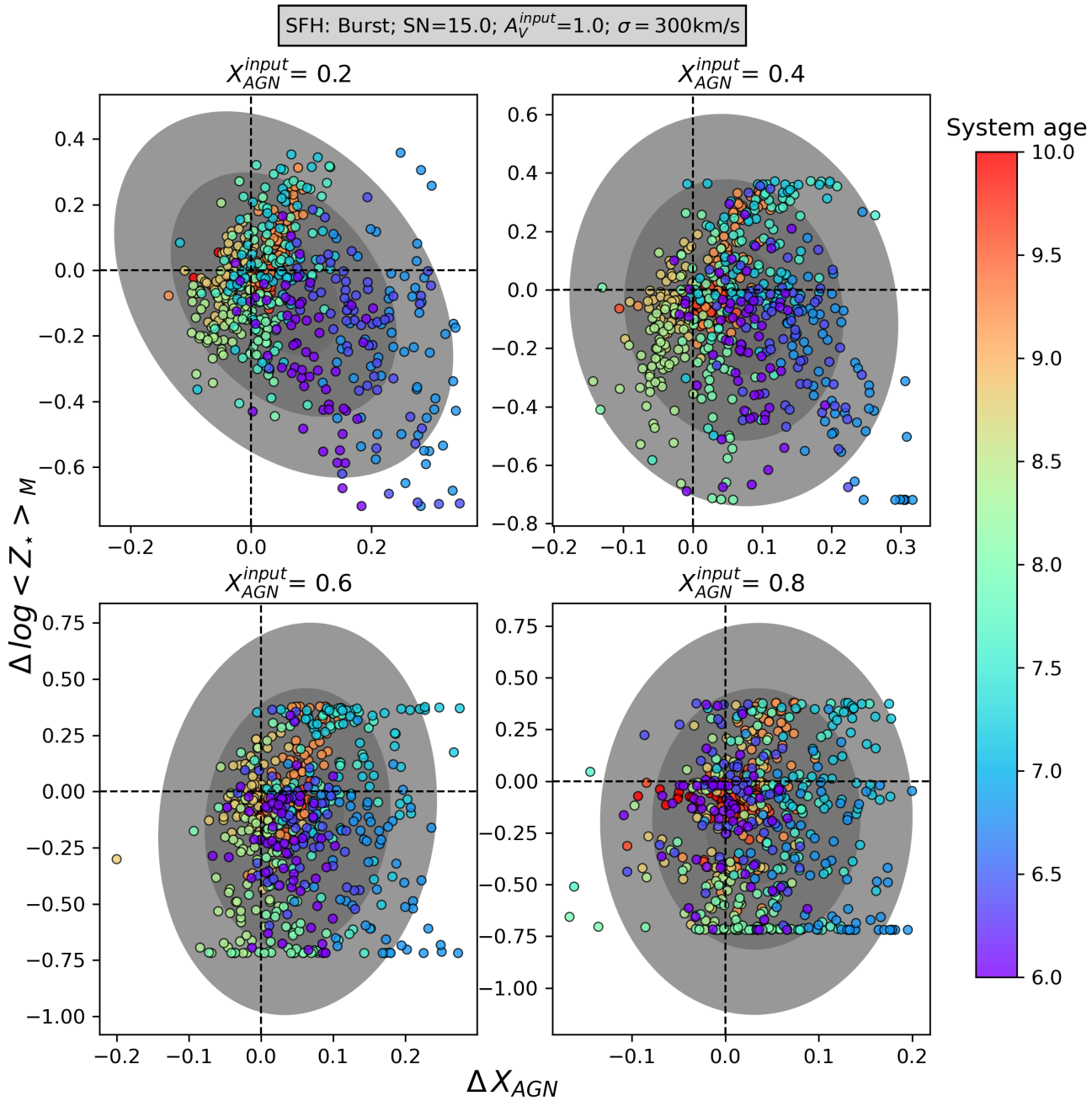

FIGURE A.20: $\Delta log < Z_\star >_M$ vs vs ΔX_{AGN}; SFH: Burst, SN = 15.0, base: BaseA

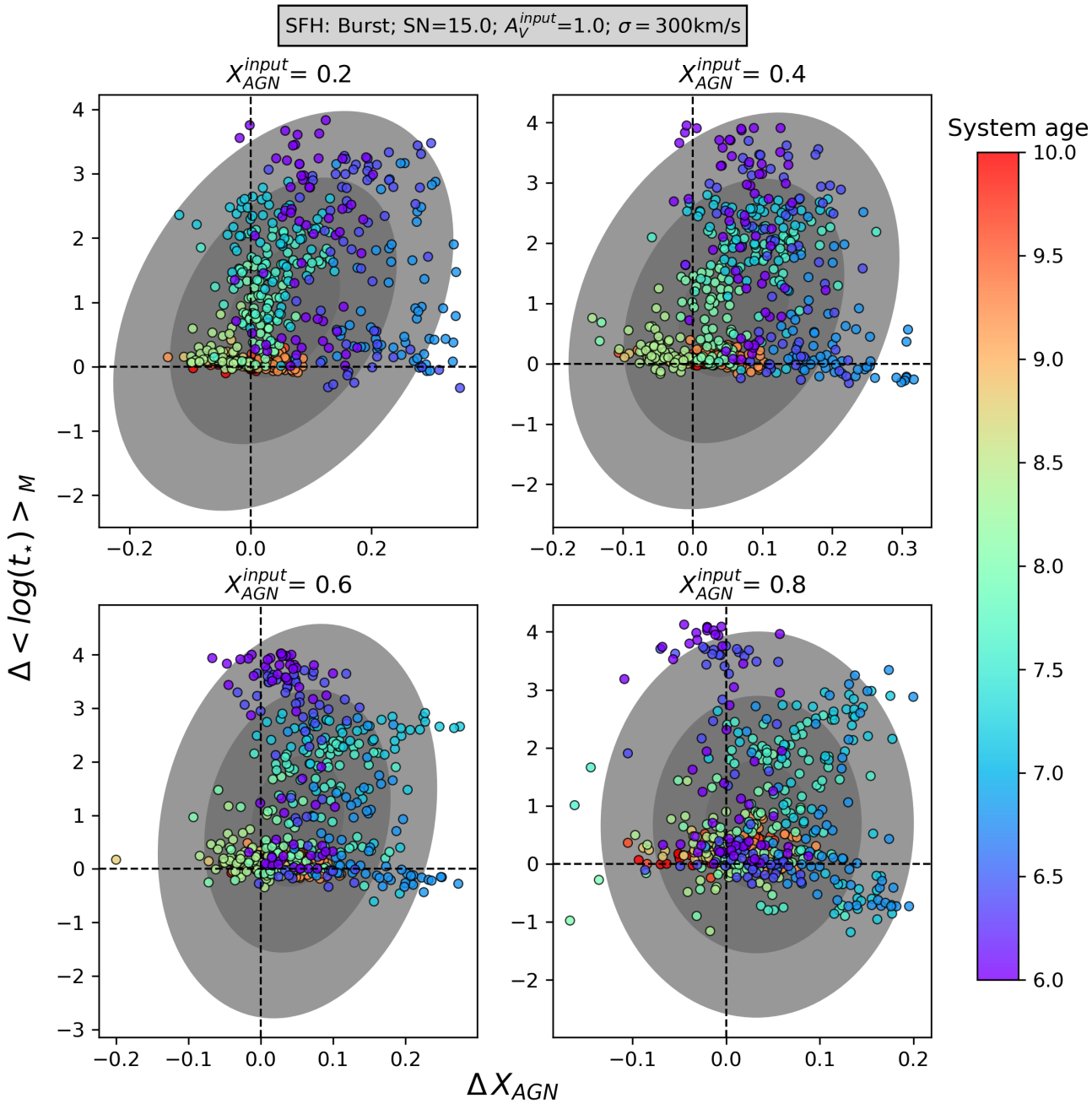

FIGURE A.21: $\Delta < log(t_\star) >_M$ vs ΔX_{AGN}; SFH: Burst, SN = 15.0, base: BaseA

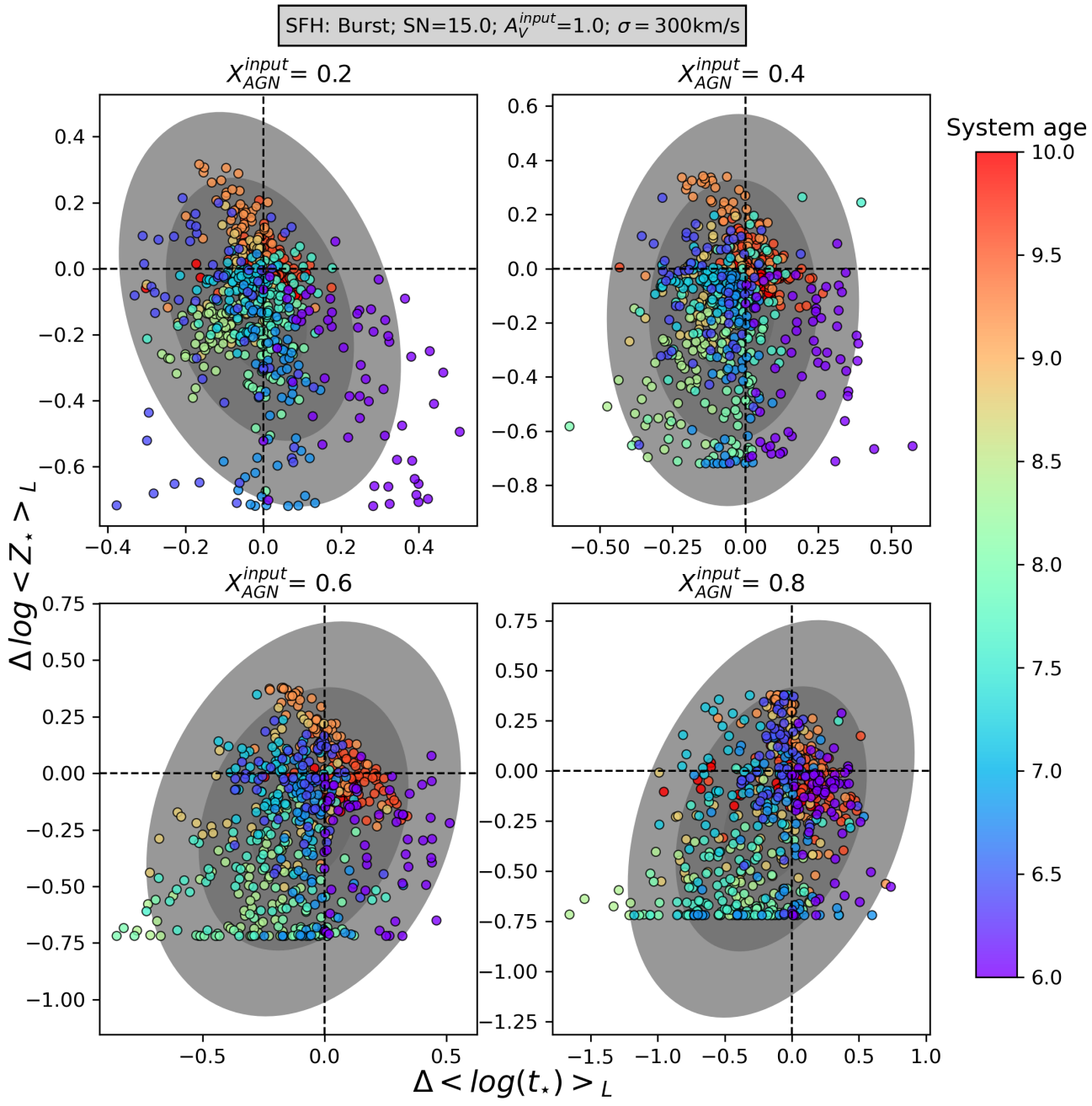

FIGURE A.22: $\Delta log < Z_\star >_L$ vs $\Delta < log(t_\star) >_L$; SFH: Burst, SN = 15.0, base: BaseA

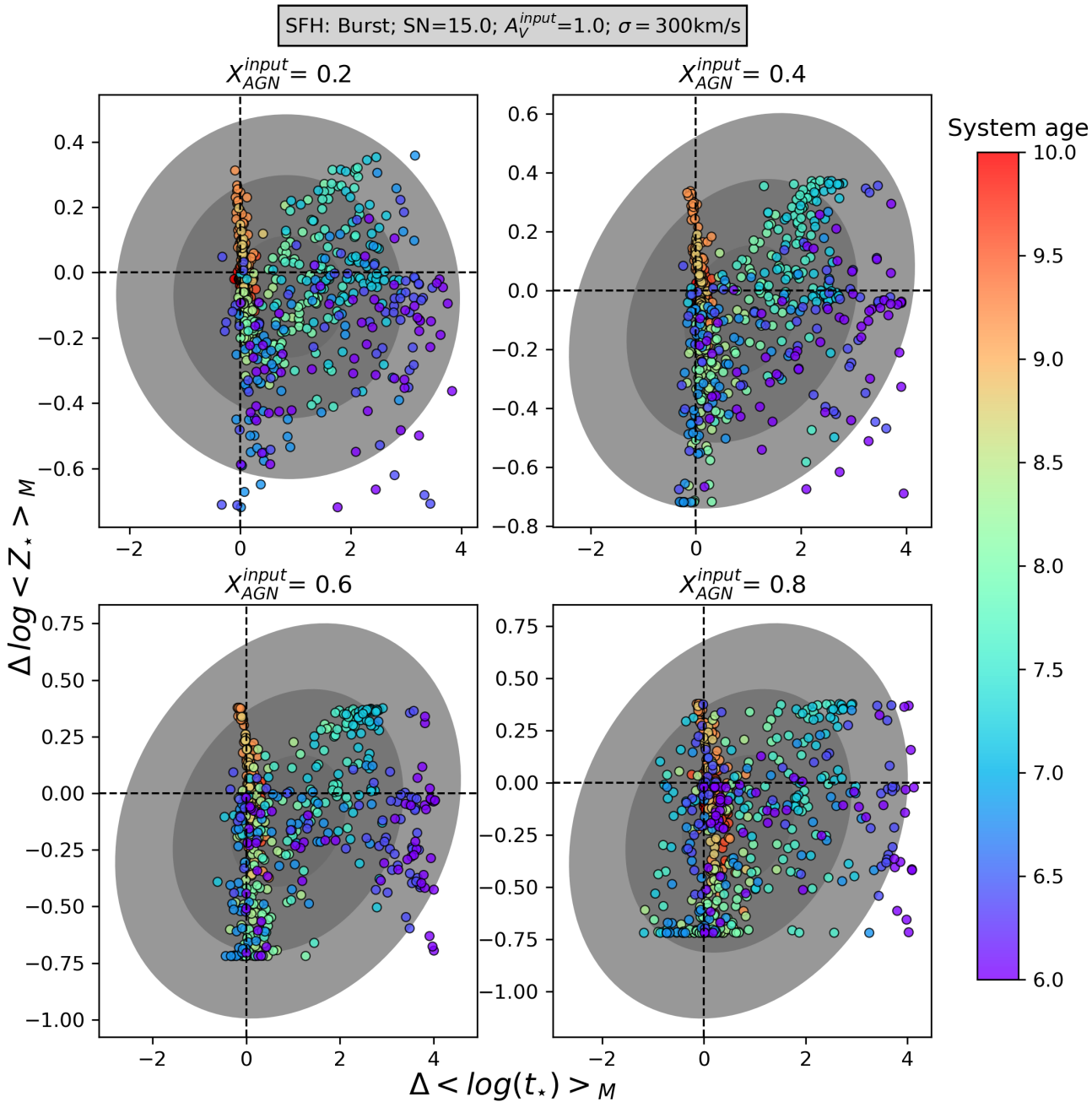

FIGURE A.23: $\Delta log < Z_\star >_M$ vs $\Delta < log(t_\star) >_M$; SFH: Burst, SN = 15.0, base: BaseA

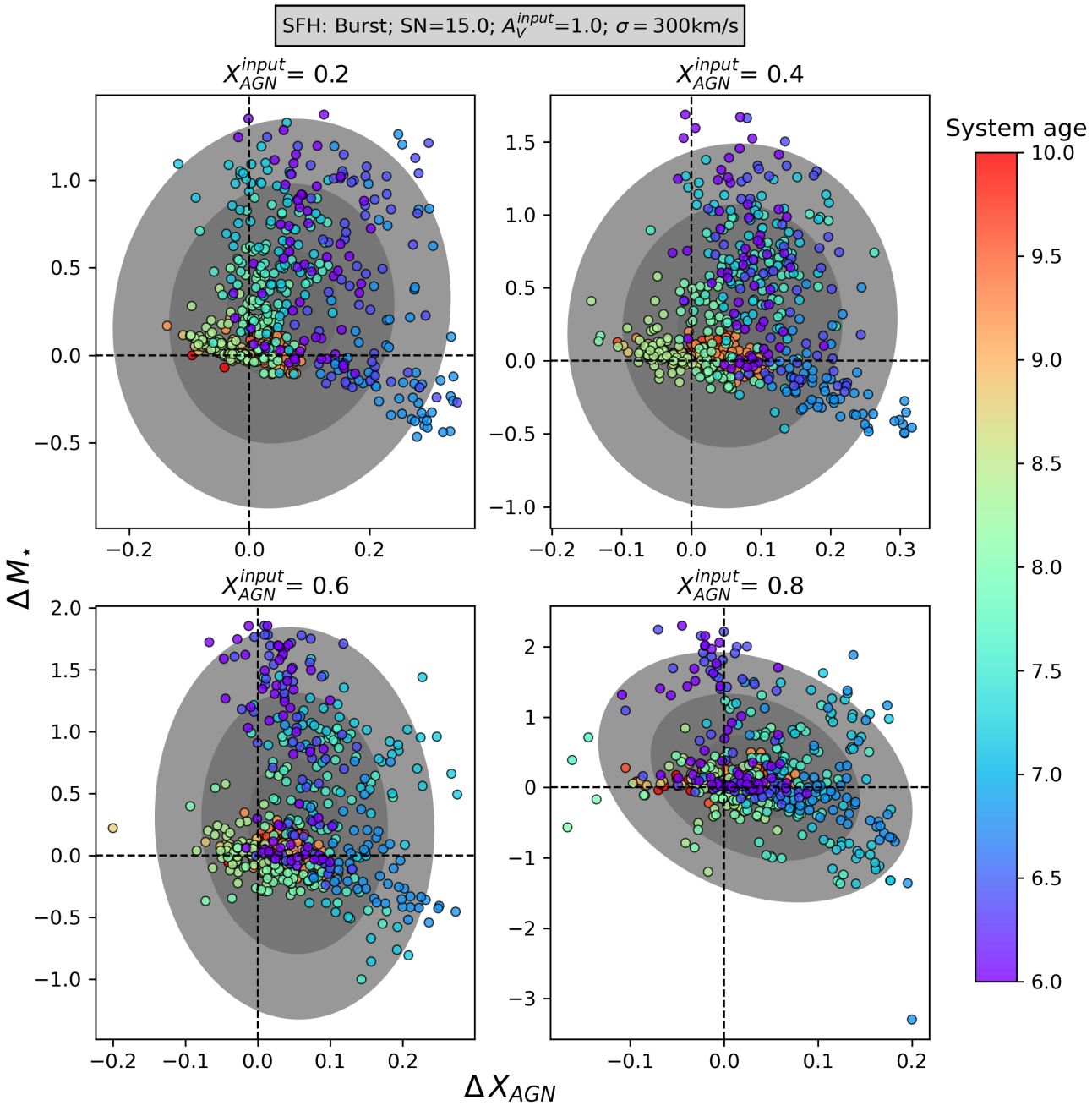

FIGURE A.24: $\Delta M_\star$ vs ΔX_{AGN}; SFH: Burst, SN = 15.0, base: BaseA

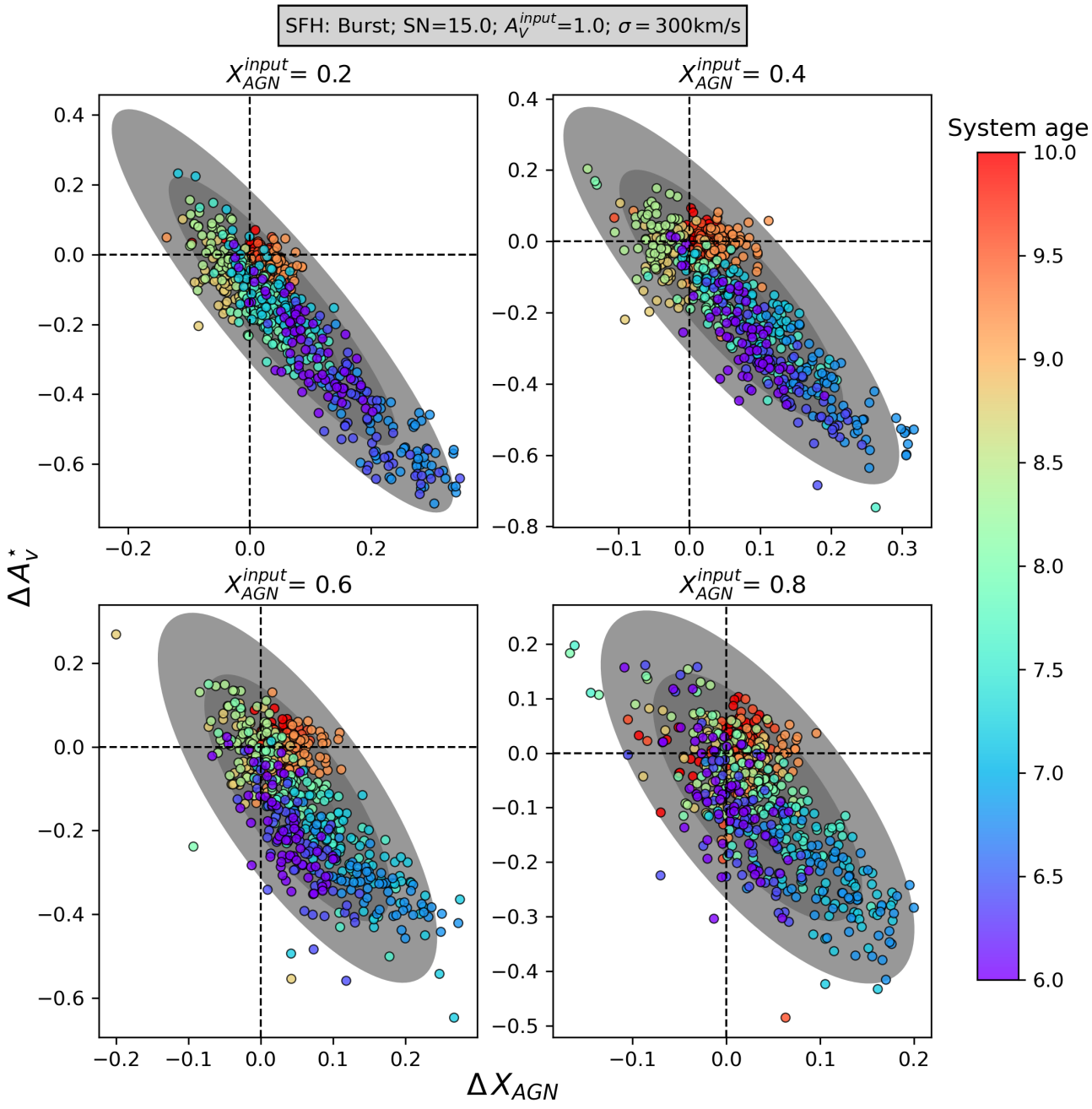

FIGURE A.25: $\Delta A_v^\star$ vs ΔX_{AGN}; SFH: Burst, SN = 15.0, base: BaseA

A.2.4 Figures: Constant SFH, Av=1.0, SN = 15, base: BaseA

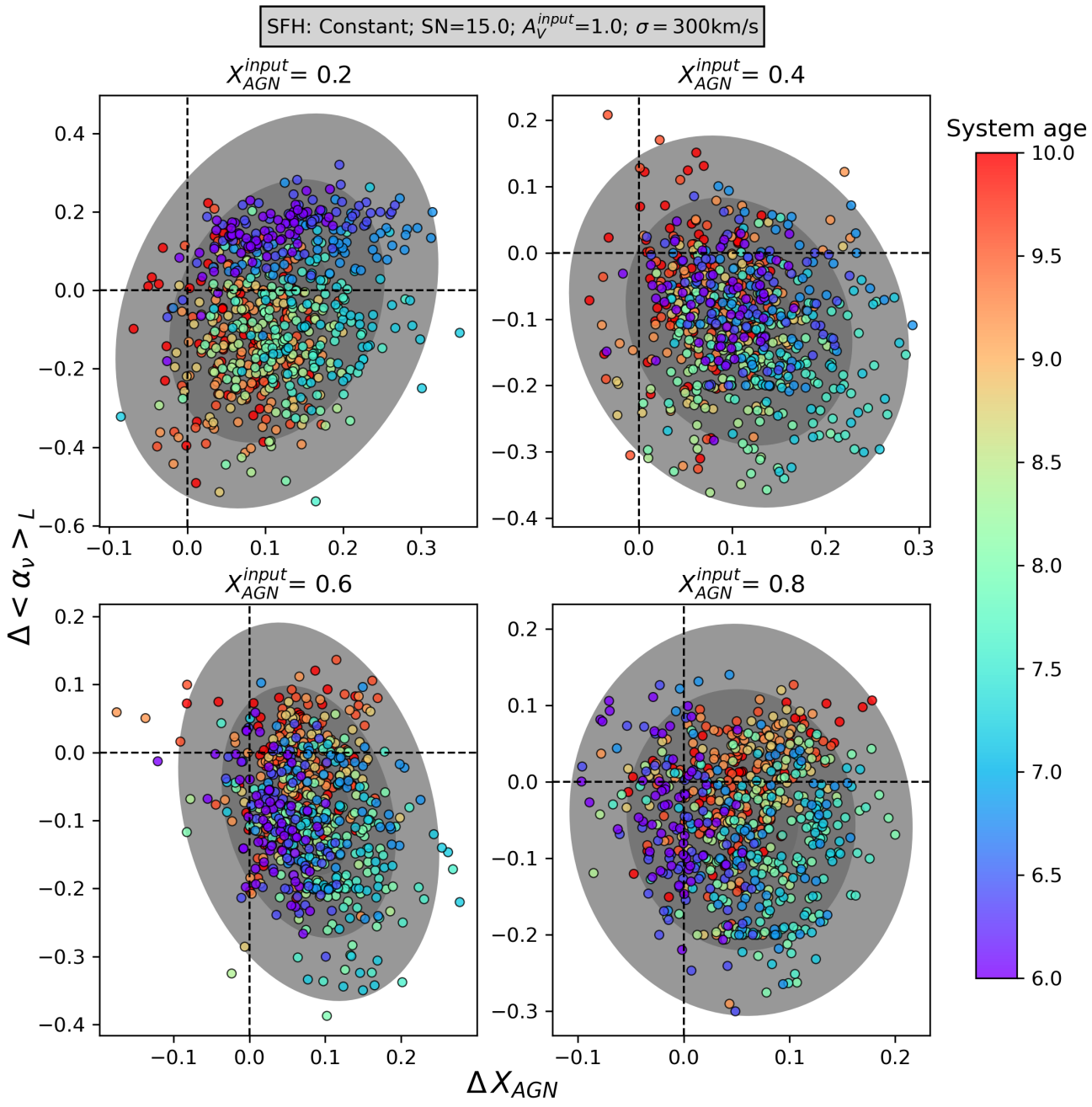

FIGURE A.26: $\Delta < \alpha_\nu >_L$ vs ΔX_{AGN}; SFH: Constant, SN = 15.0, base: BaseA

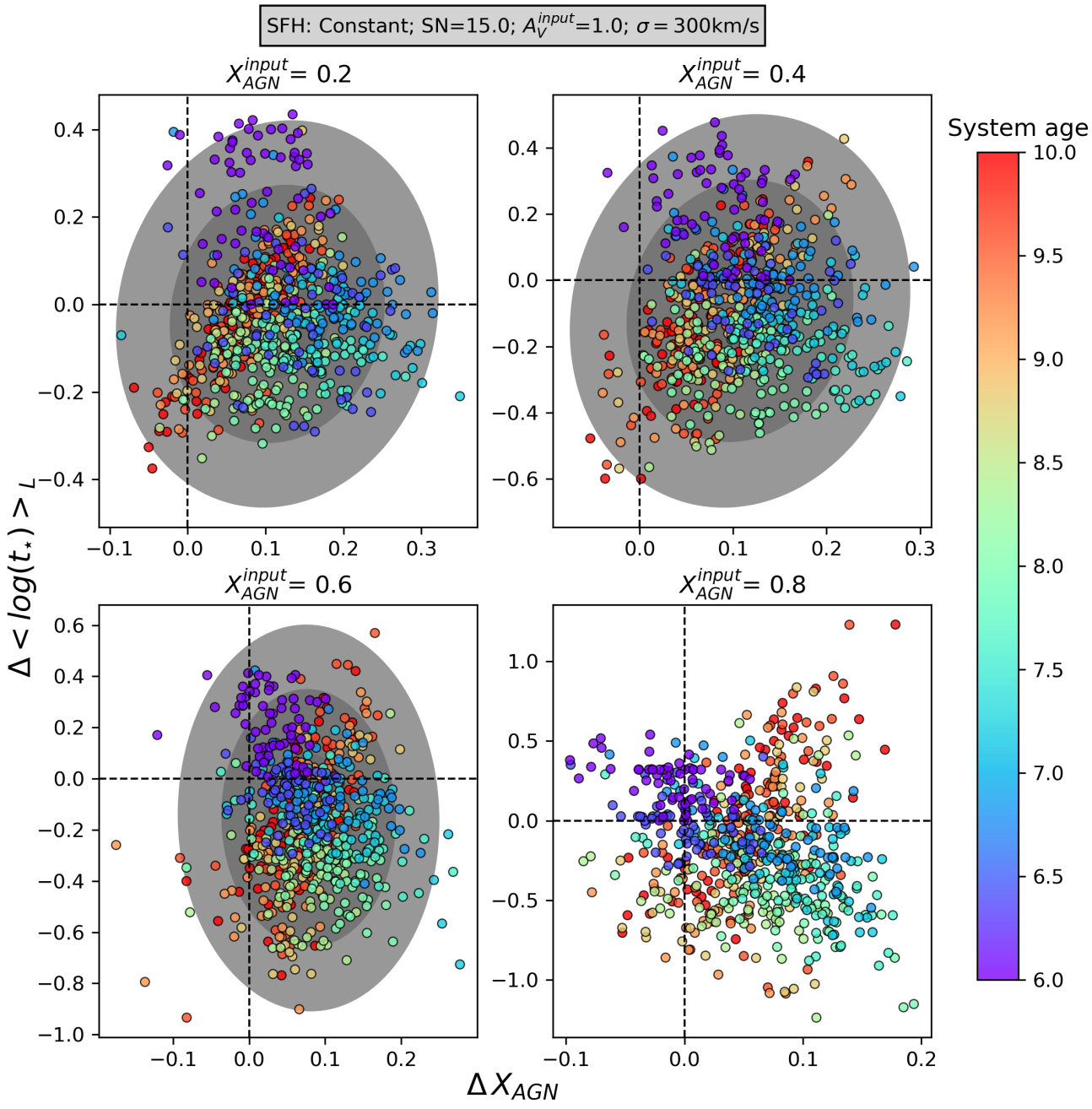

FIGURE A.27: $\Delta < log(t_\star) >_L$ vs $\Delta\, X_{AGN}$; SFH: Constant, SN = 15.0, base: BaseA

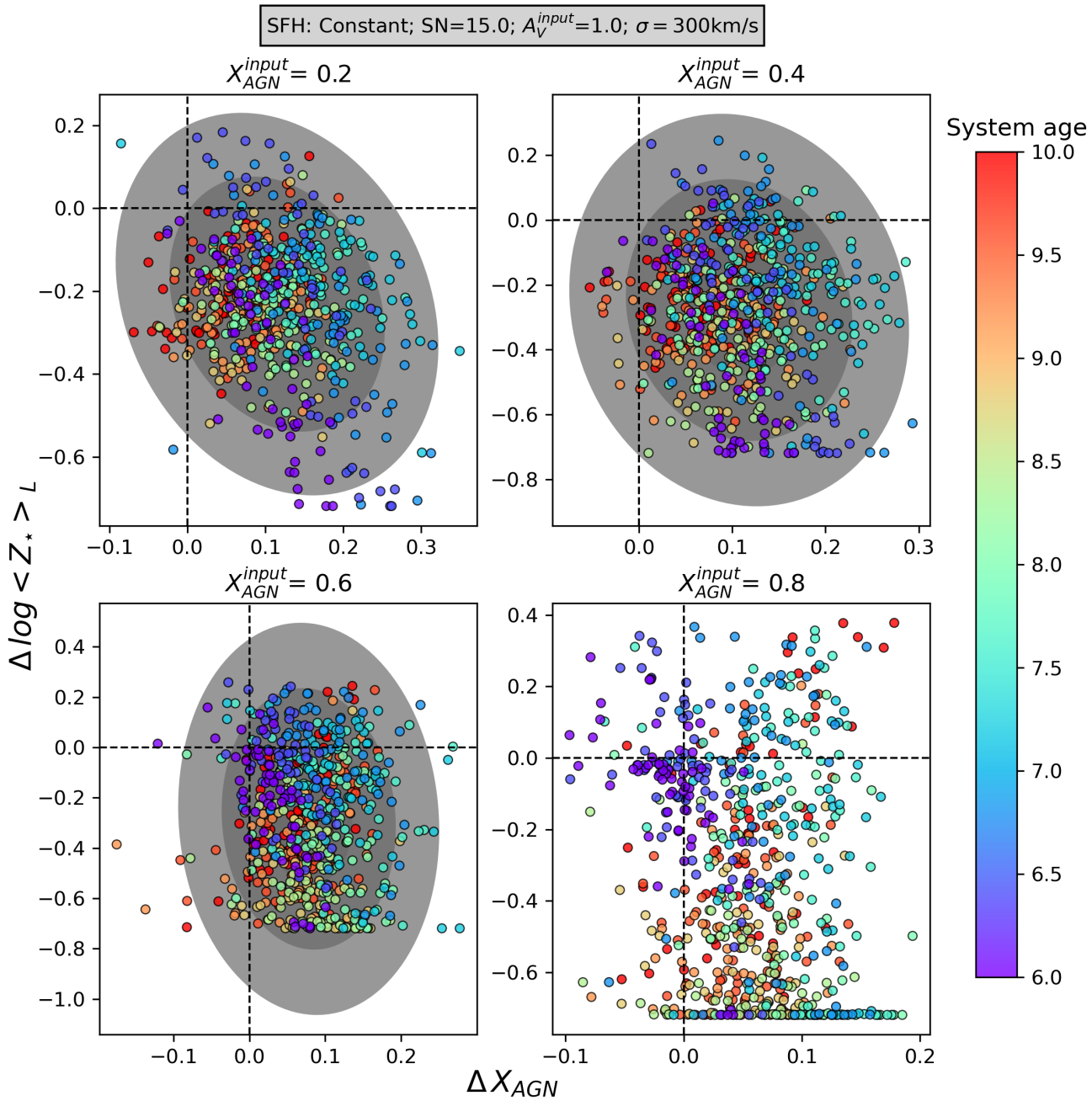

FIGURE A.28: $\Delta\, log < Z_\star >_L$ vs $\Delta\, X_{AGN}$; SFH: Constant, SN = 15.0, base: BaseA

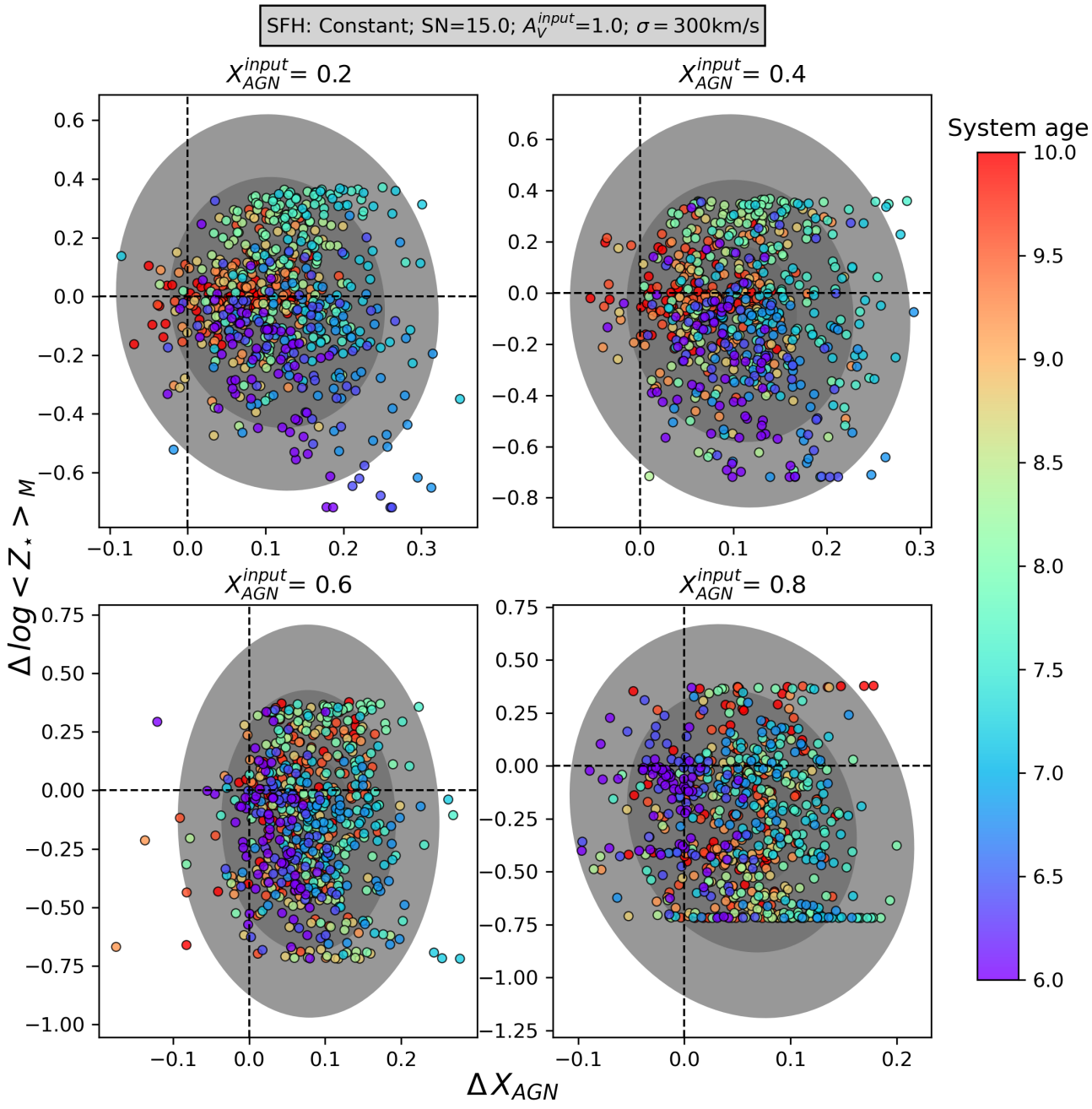

FIGURE A.29: $\Delta\, log < Z_\star >_M$ vs vs $\Delta\, X_{AGN}$; SFH: Constant, SN = 15.0, base: BaseA

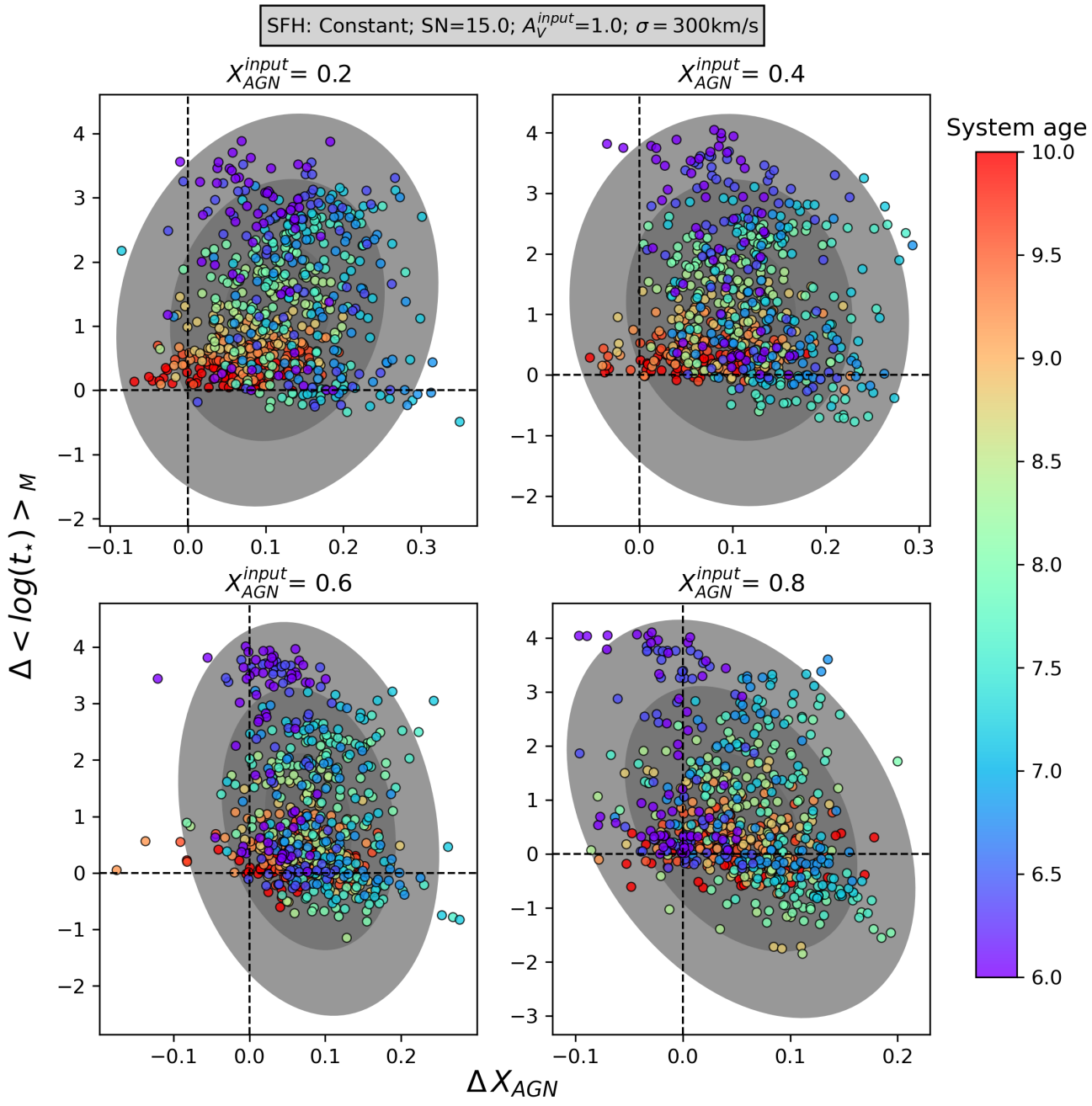

FIGURE A.30: $\Delta < log(t_\star) >_M$ vs ΔX_{AGN}; SFH: Constant, SN = 15.0, base: BaseA

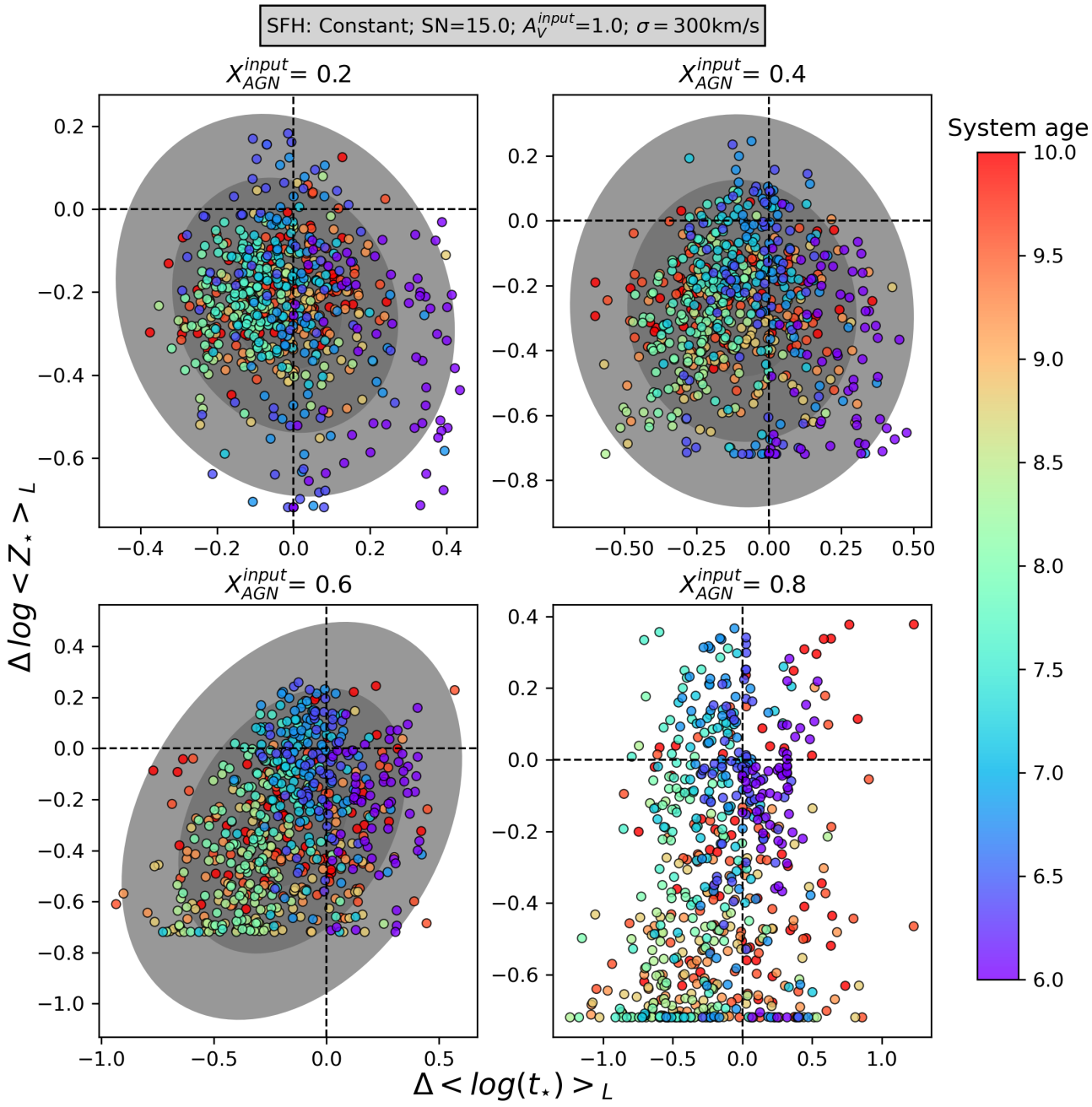

FIGURE A.31: $\Delta log < Z_\star >_L$ vs $\Delta < log(t_\star) >_L$; SFH: Constant, SN = 15.0, base: BaseA

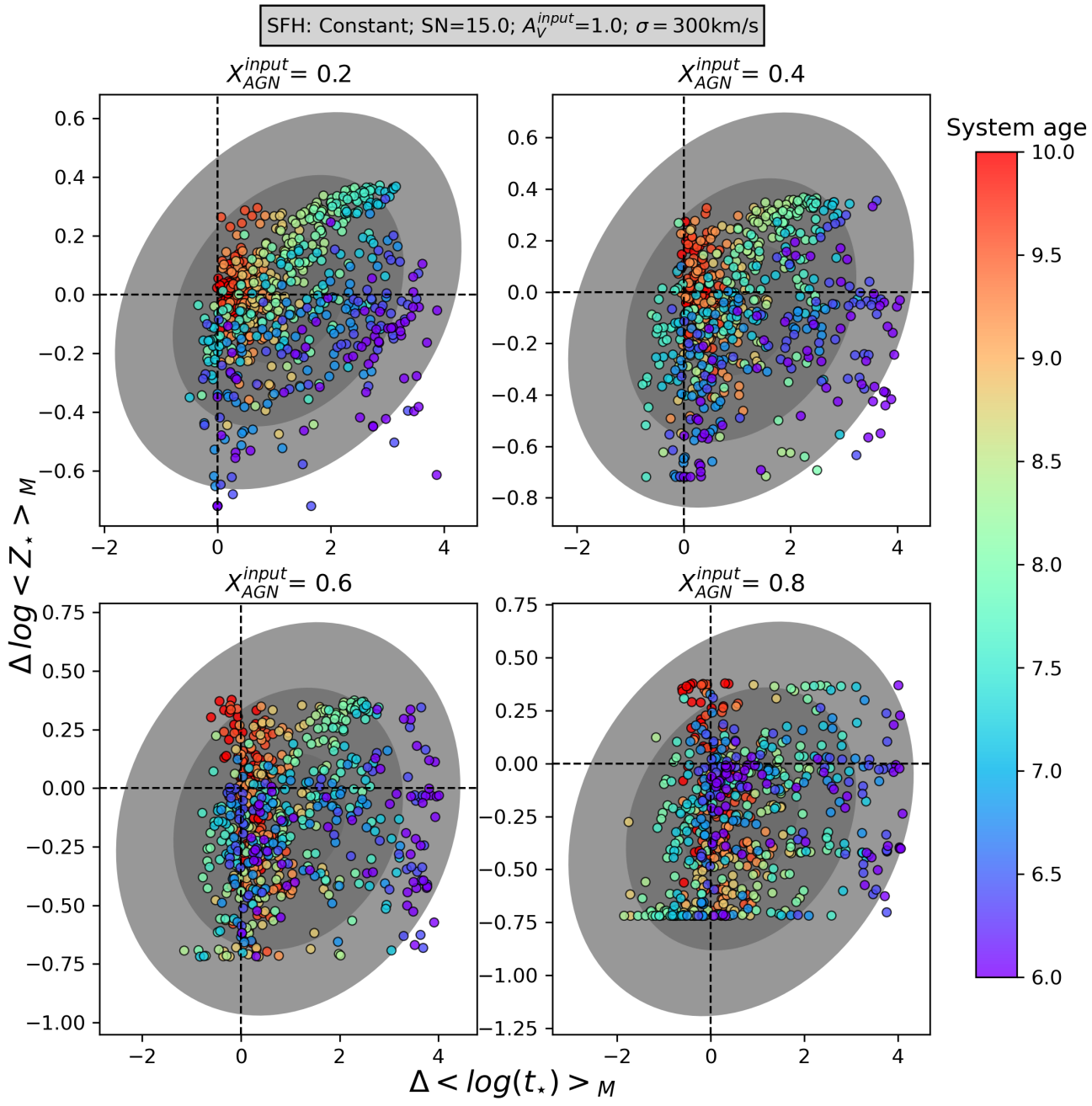

FIGURE A.32: $\Delta log < Z_\star >_M$ vs $\Delta < log(t_\star) >_M$; SFH: Constant, SN = 15.0, base: BaseA

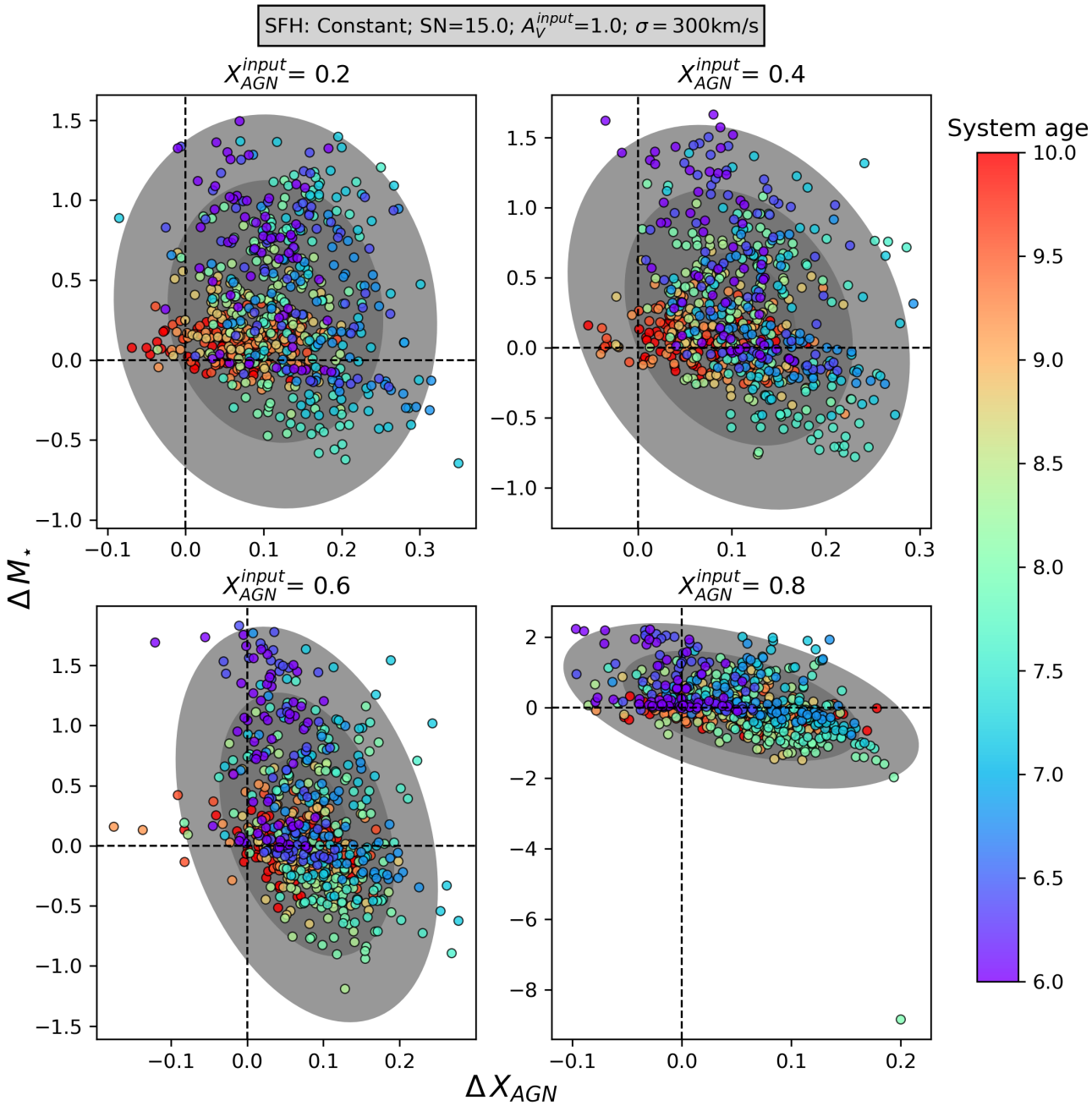

FIGURE A.33: $\Delta M_\star$ vs ΔX_{AGN}; SFH: Constant, SN = 15.0, base: BaseA

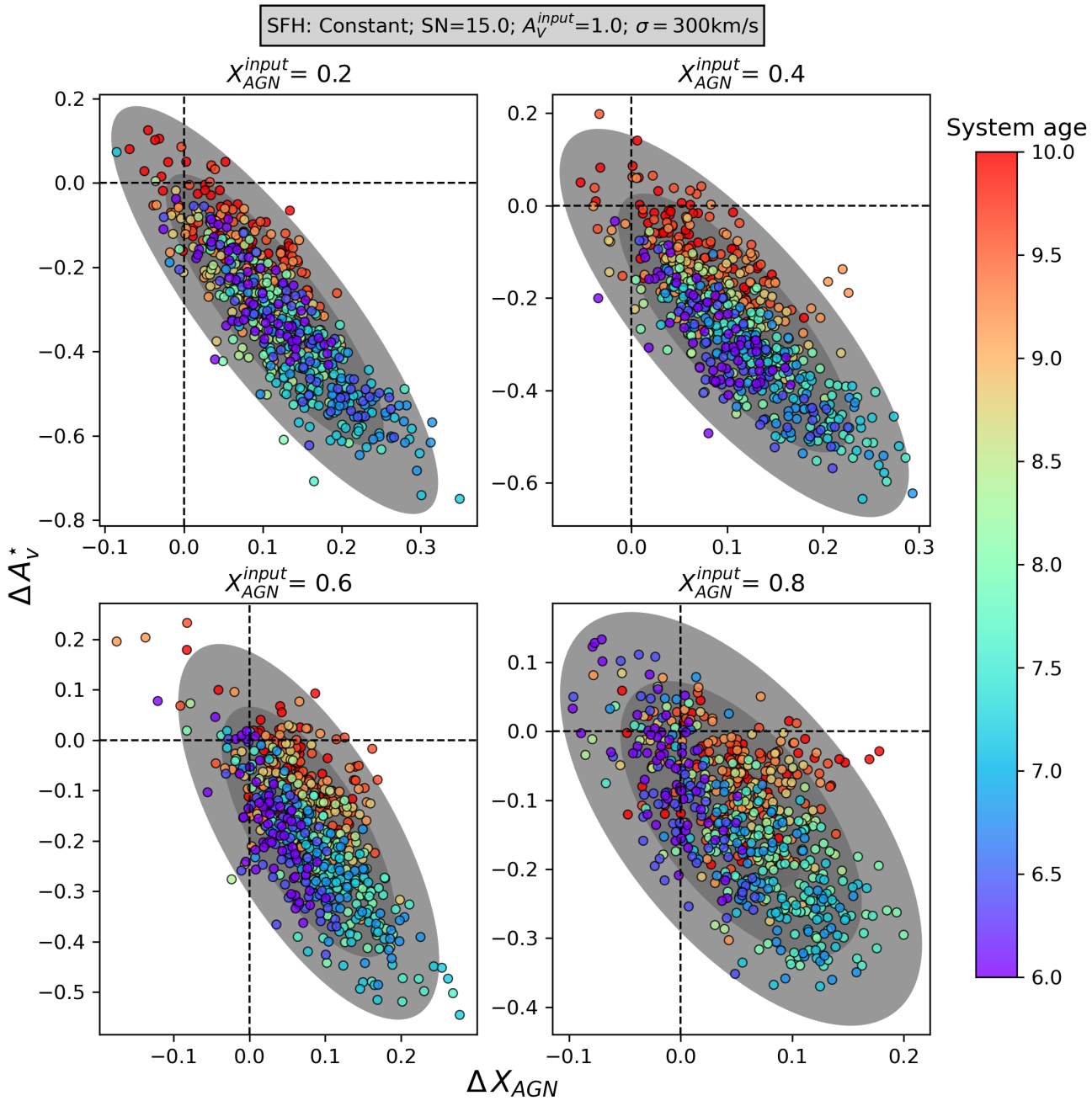

FIGURE A.34: $\Delta A_v^\star$ vs ΔX_{AGN}; SFH: Constant, SN = 15.0, base: BaseA

A.2.5 Figures: Instantaneous burst SFH, Av=2.0, SN = 15.0, base: BaseA

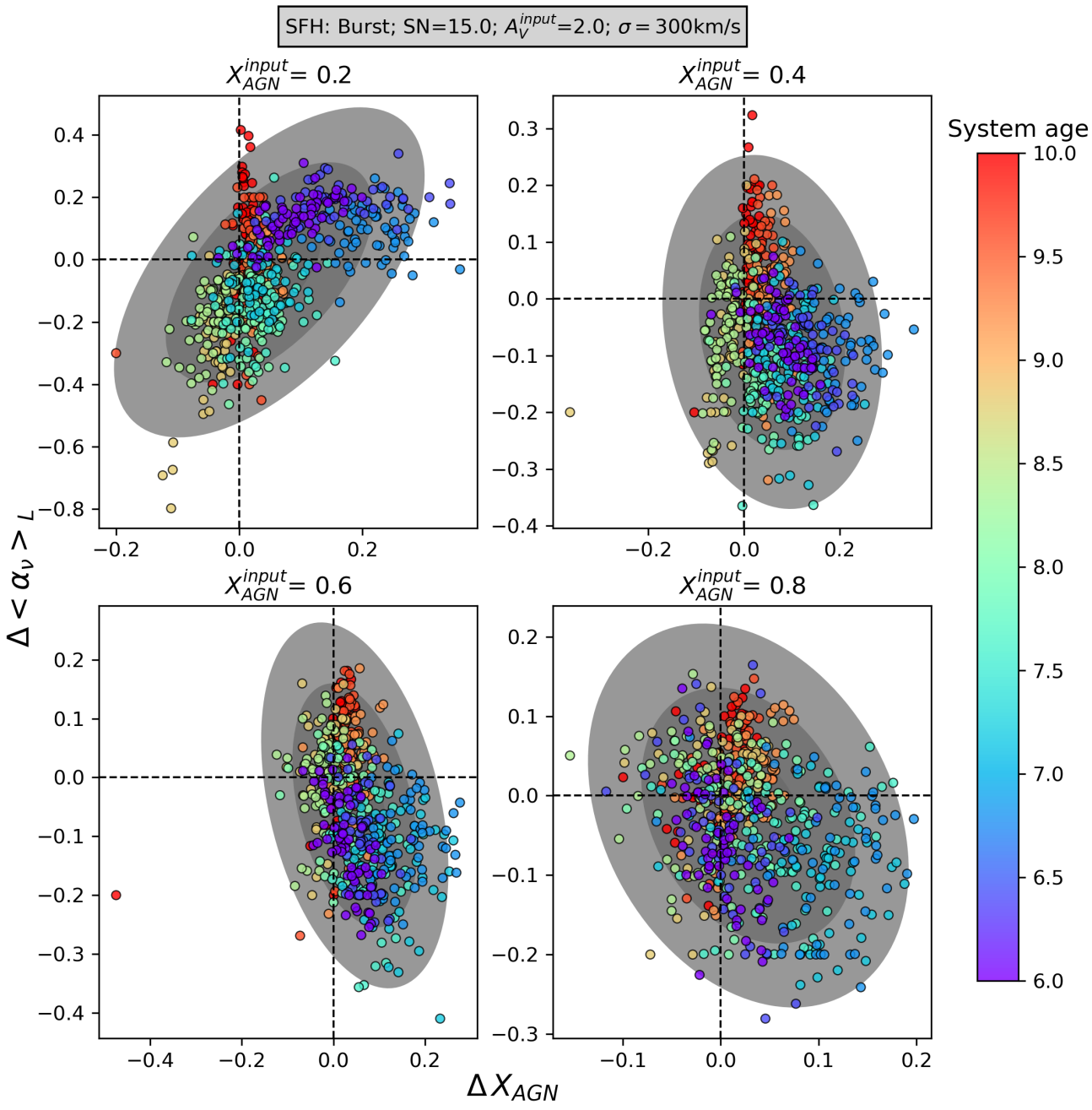

FIGURE A.35: $\Delta < \alpha_\nu >_L$ vs ΔX_{AGN}; SFH: Burst, SN = 15.0, base: BaseA

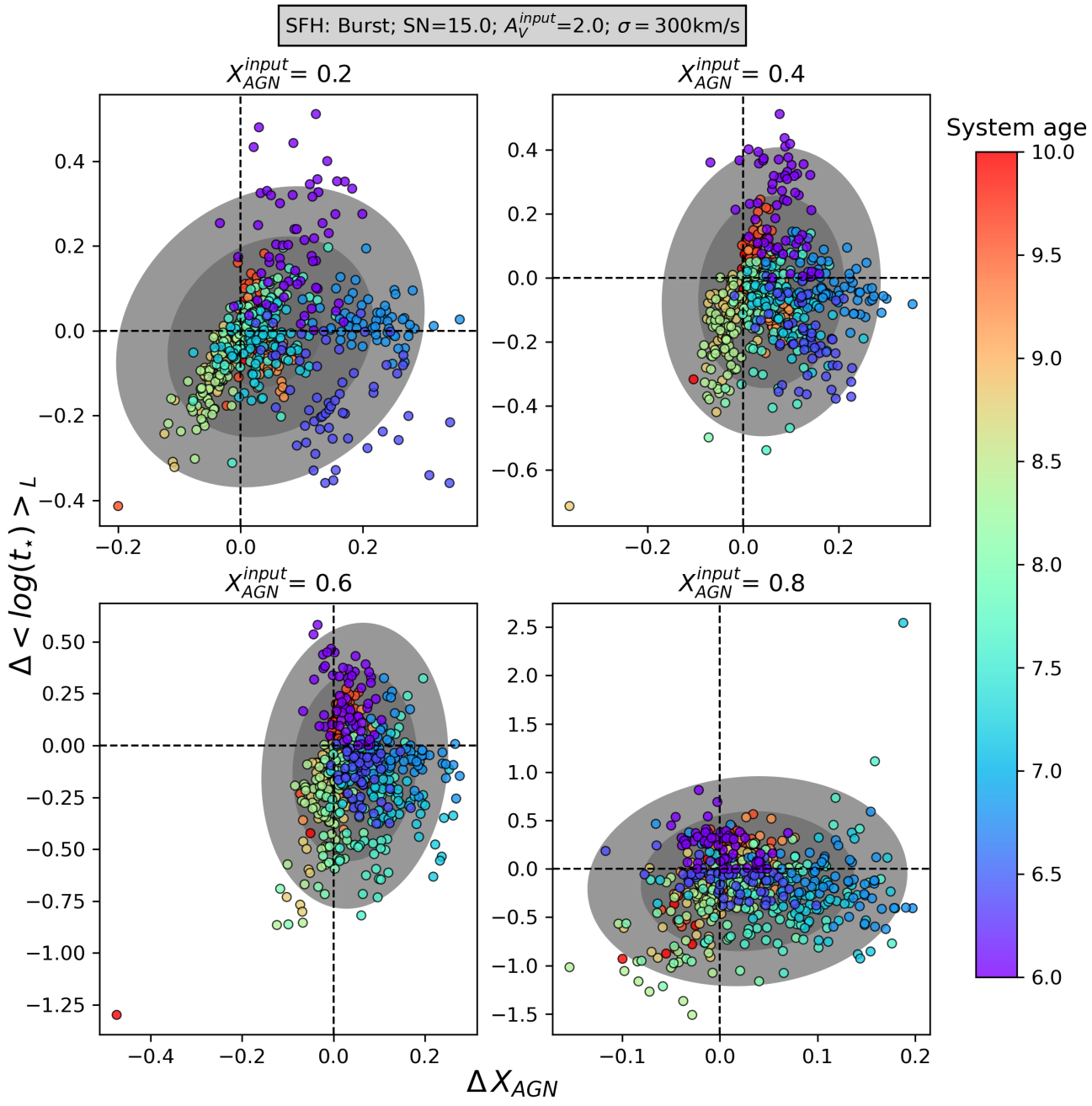

FIGURE A.36: $\Delta < log(t_\star) >_L$ vs ΔX_{AGN}; SFH: Burst, SN = 15.0, base: BaseA

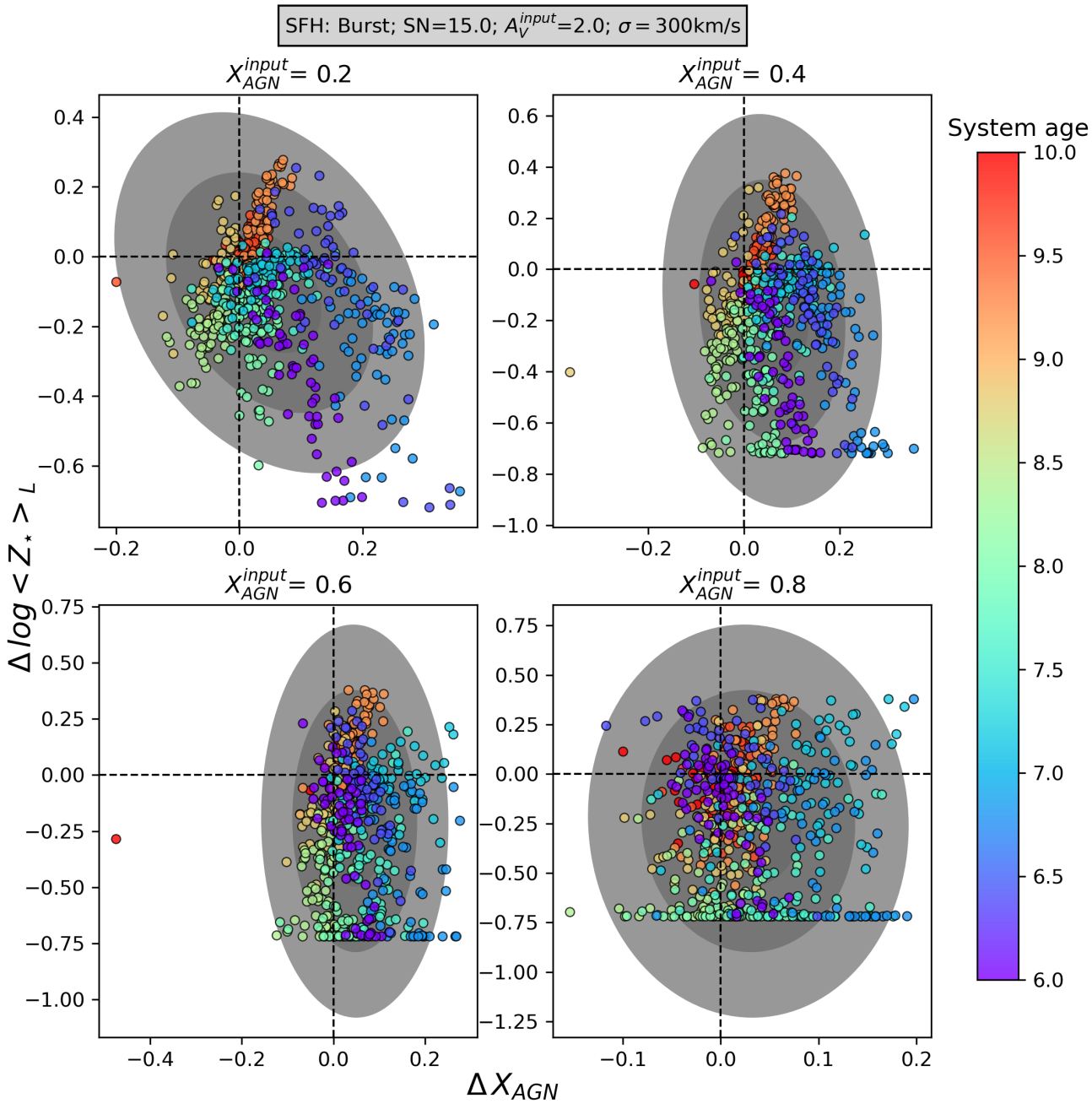

FIGURE A.37: $\Delta\, log < Z_\star >_L$ vs $\Delta\, X_{AGN}$; SFH: Burst, SN = 15.0, base: BaseA

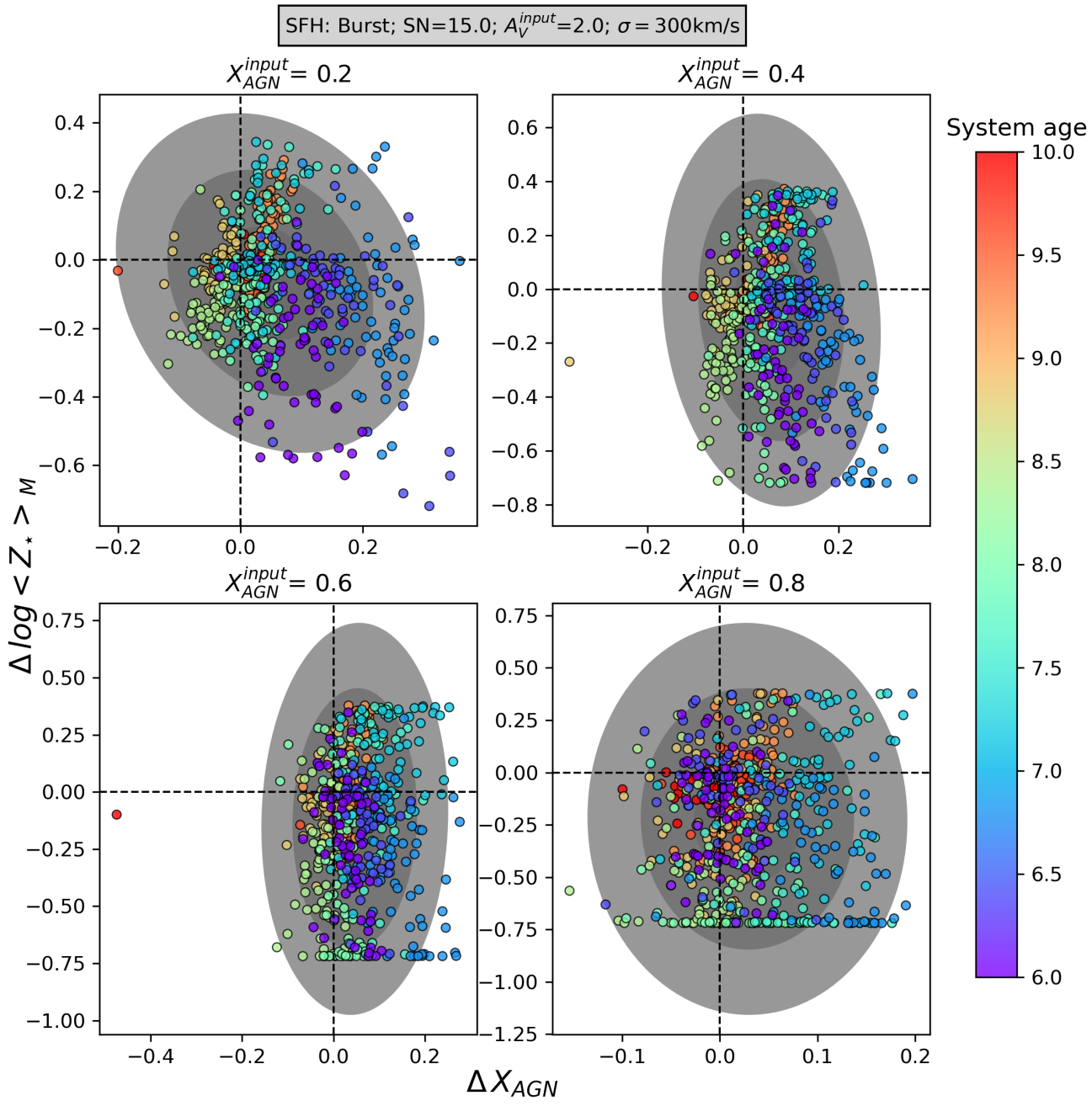

FIGURE A.38: $\Delta log < Z_\star >_M$ vs vs ΔX_{AGN}; SFH: Burst, SN = 15.0, base: BaseA

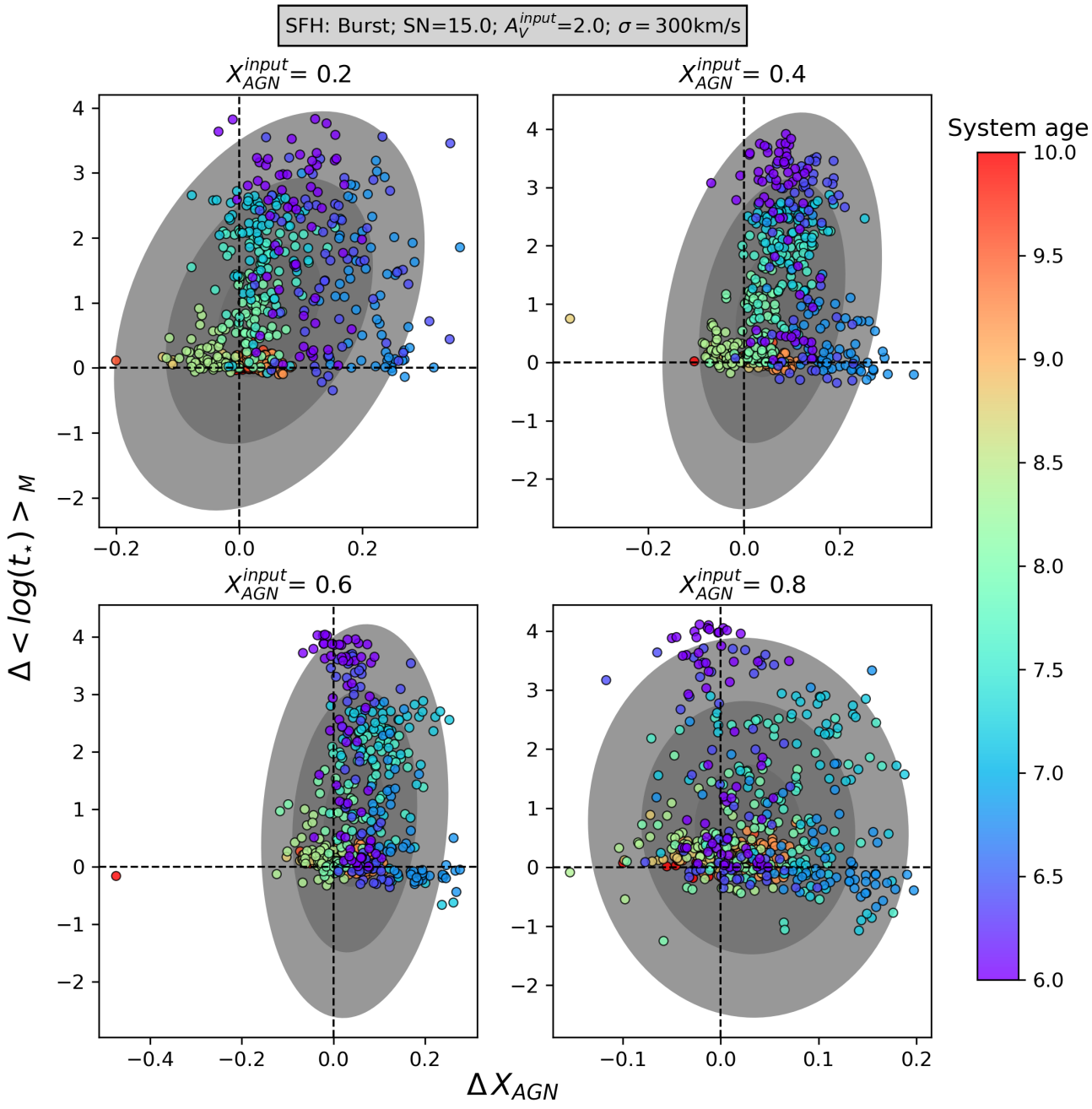

FIGURE A.39: $\Delta < log(t_\star) >_M$ vs ΔX_{AGN}; SFH: Burst, SN = 15.0, base: BaseA

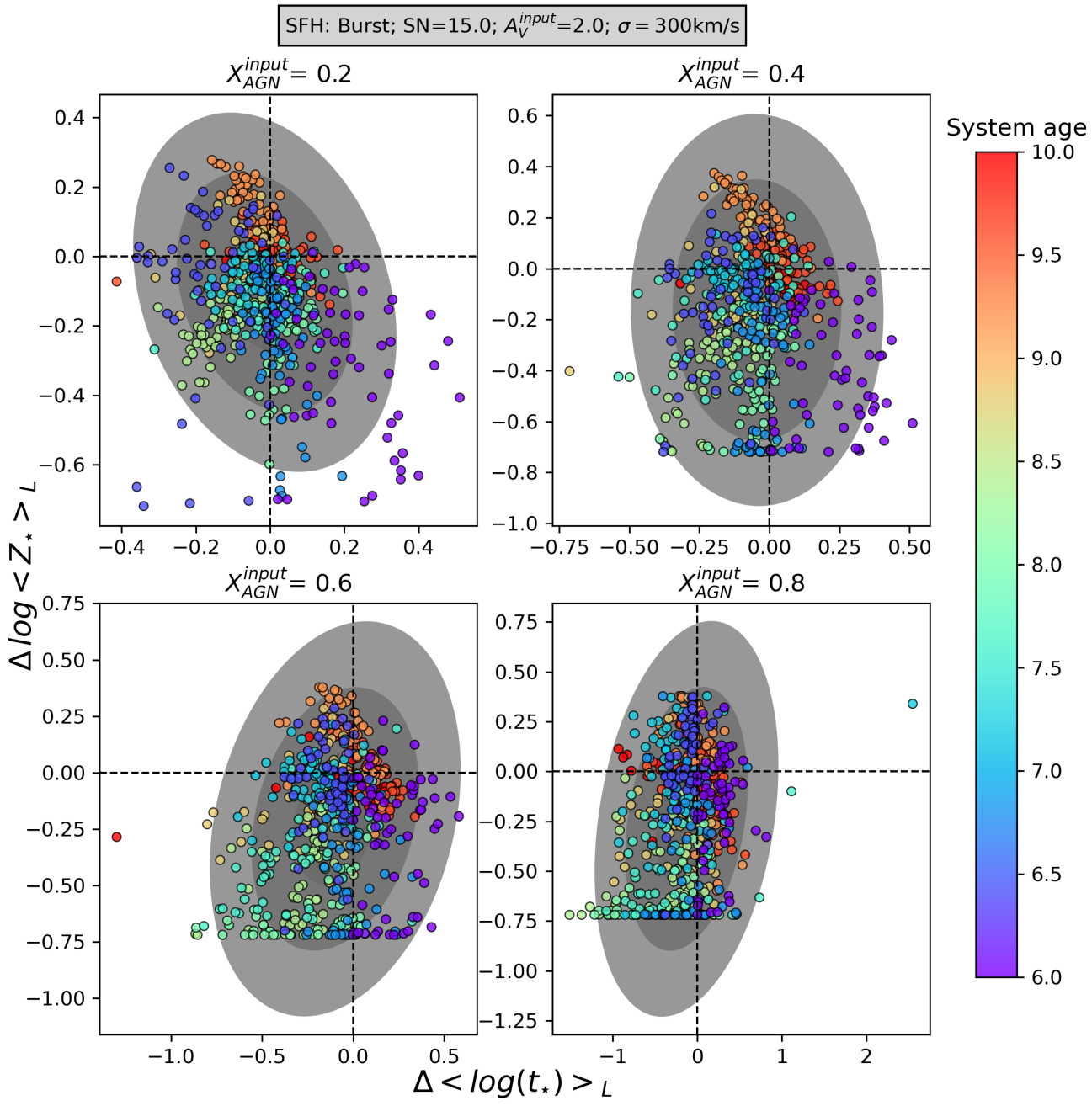

FIGURE A.40: $\Delta log < Z_\star >_L$ vs $\Delta < log(t_\star) >_L$; SFH: Burst, SN = 15.0, base: BaseA

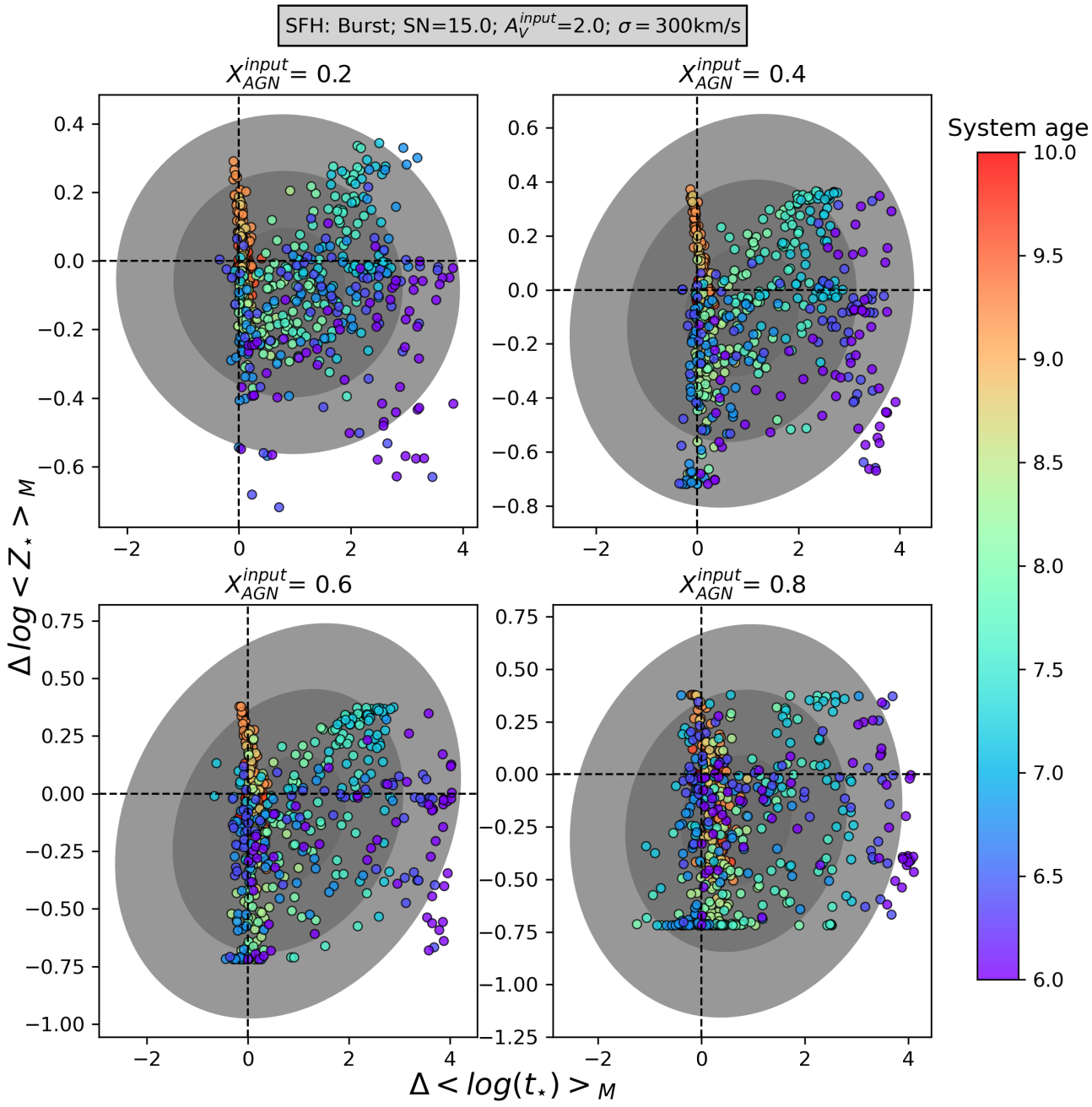

FIGURE A.41: $\Delta log < Z_\star >_M$ vs $\Delta < log(t_\star) >_M$; SFH: Burst, SN = 15.0, base: BaseA

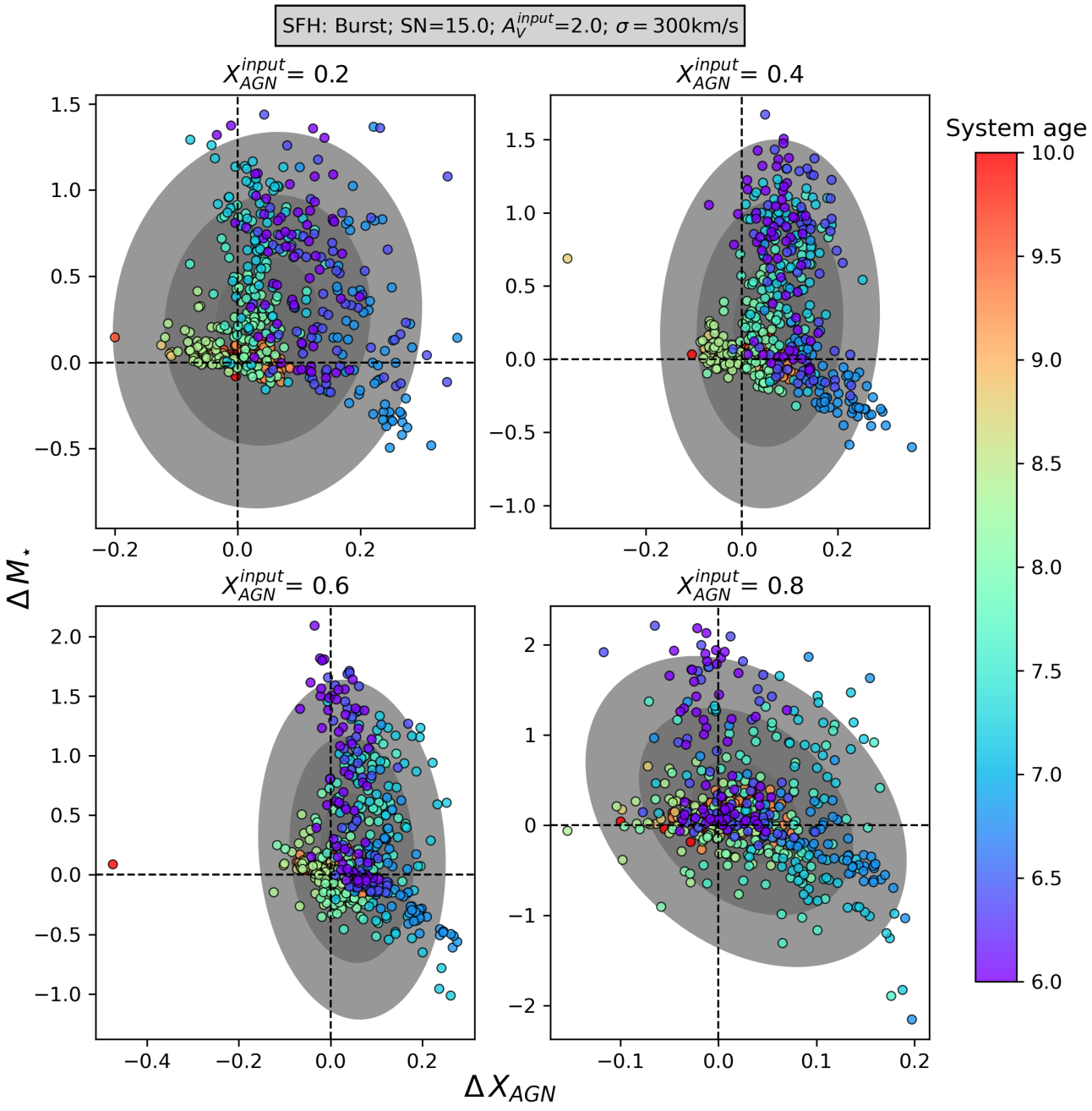

FIGURE A.42: $\Delta M_\star$ vs ΔX_{AGN}; SFH: Burst, SN = 15.0, base: BaseA

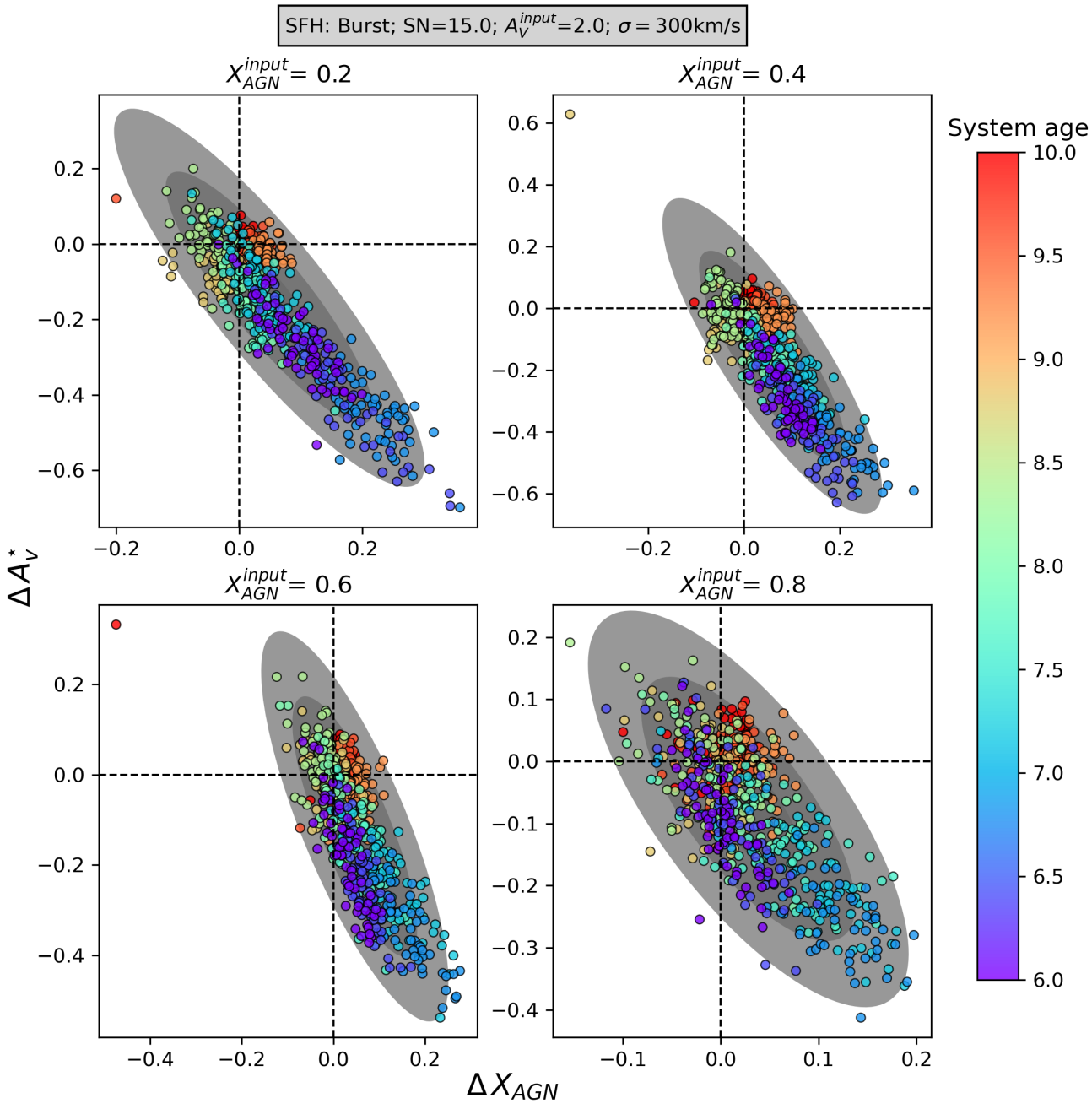

FIGURE A.43: $\Delta A_v^\star$ vs ΔX_{AGN}; SFH: Burst, SN = 15.0, base: BaseA

A.2.6 Figures: Constant SFH, Av=2.0, SN = 15, base: BaseA

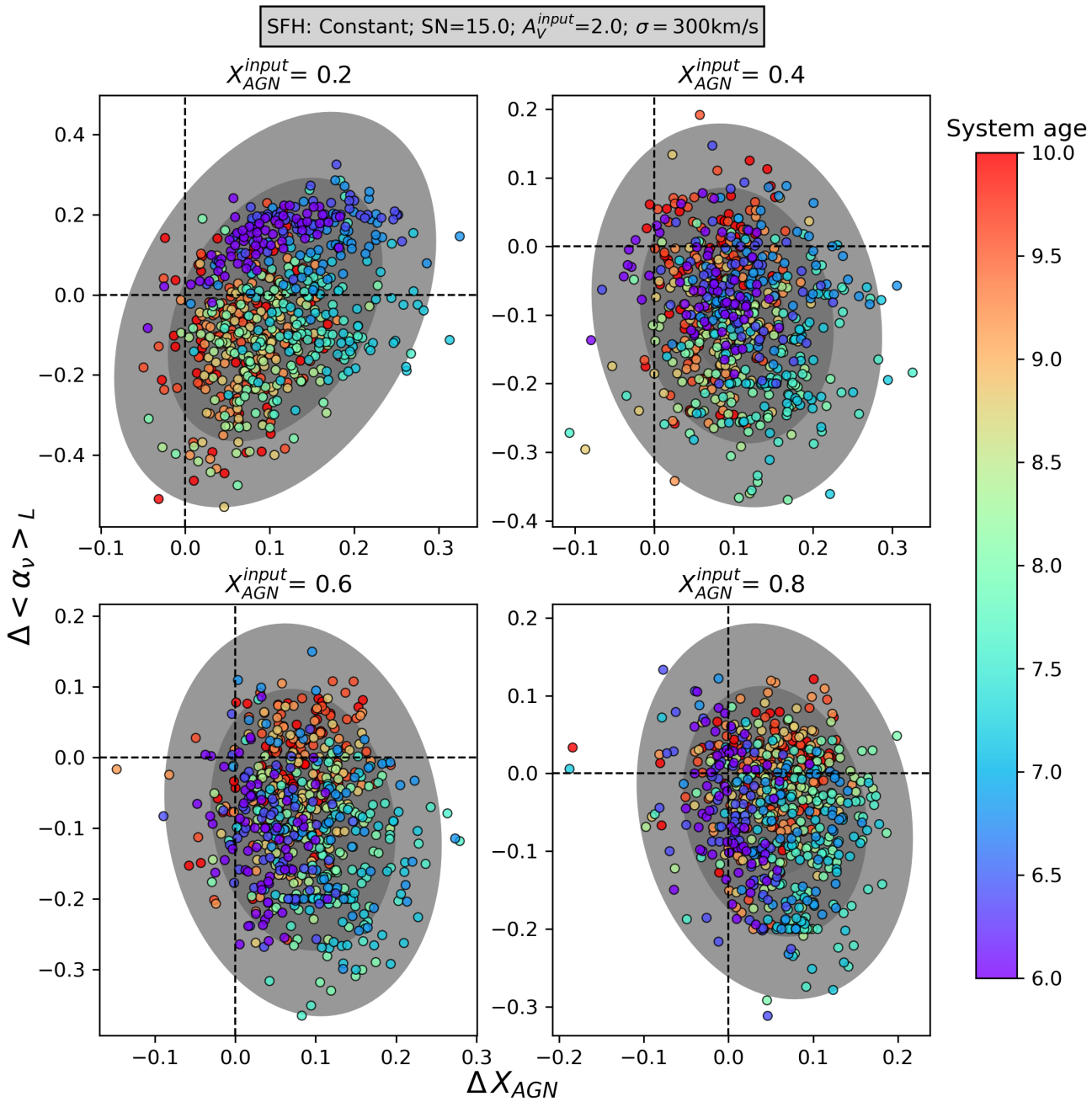

FIGURE A.44: $\Delta < \alpha_\nu >_L$ vs ΔX_{AGN}; SFH: Constant, SN = 15.0, base: BaseA

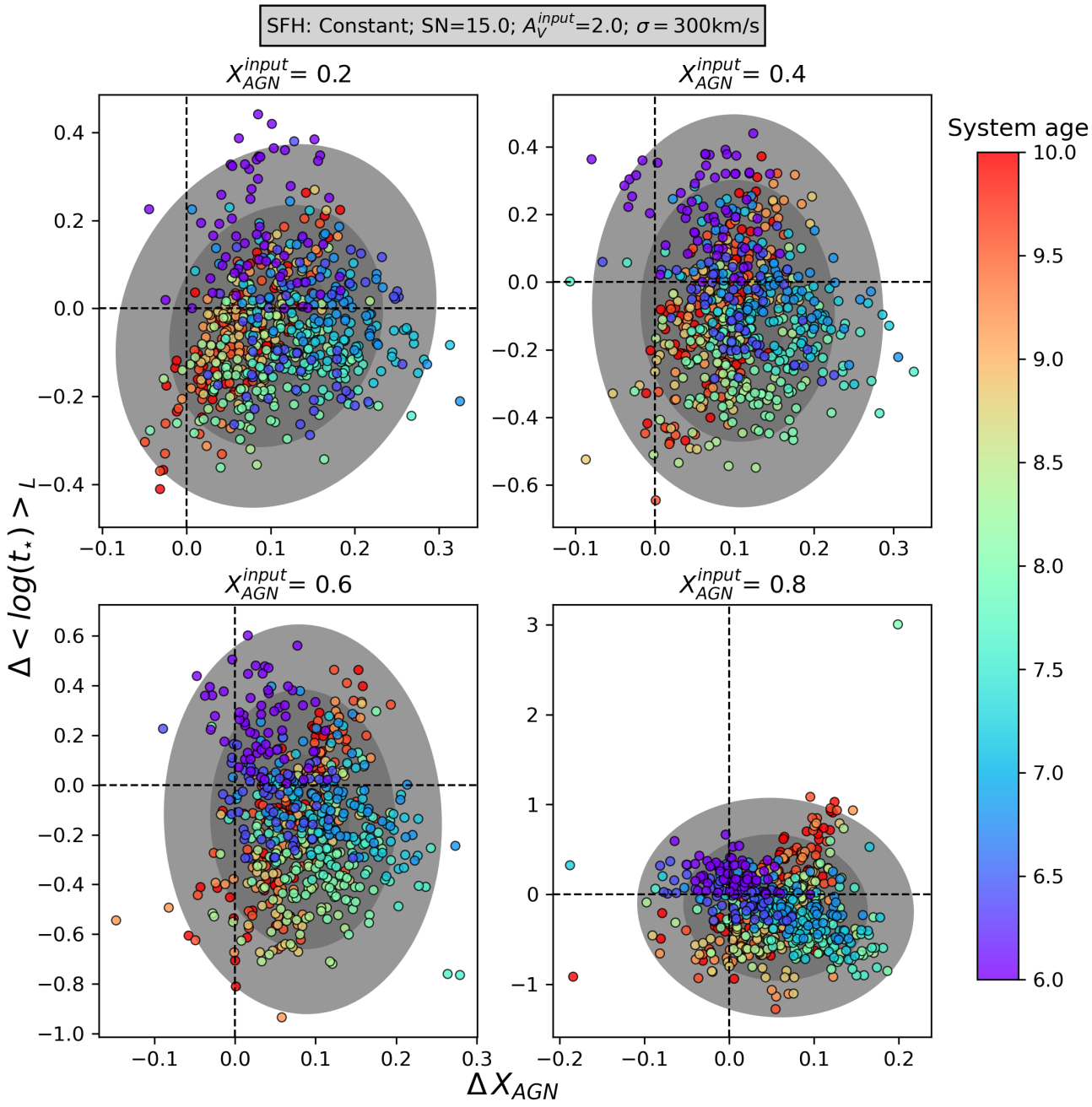

FIGURE A.45: $\Delta < log(t_\star) >_L$ vs $\Delta\, X_{AGN}$; SFH: Constant, SN = 15.0, base: BaseA

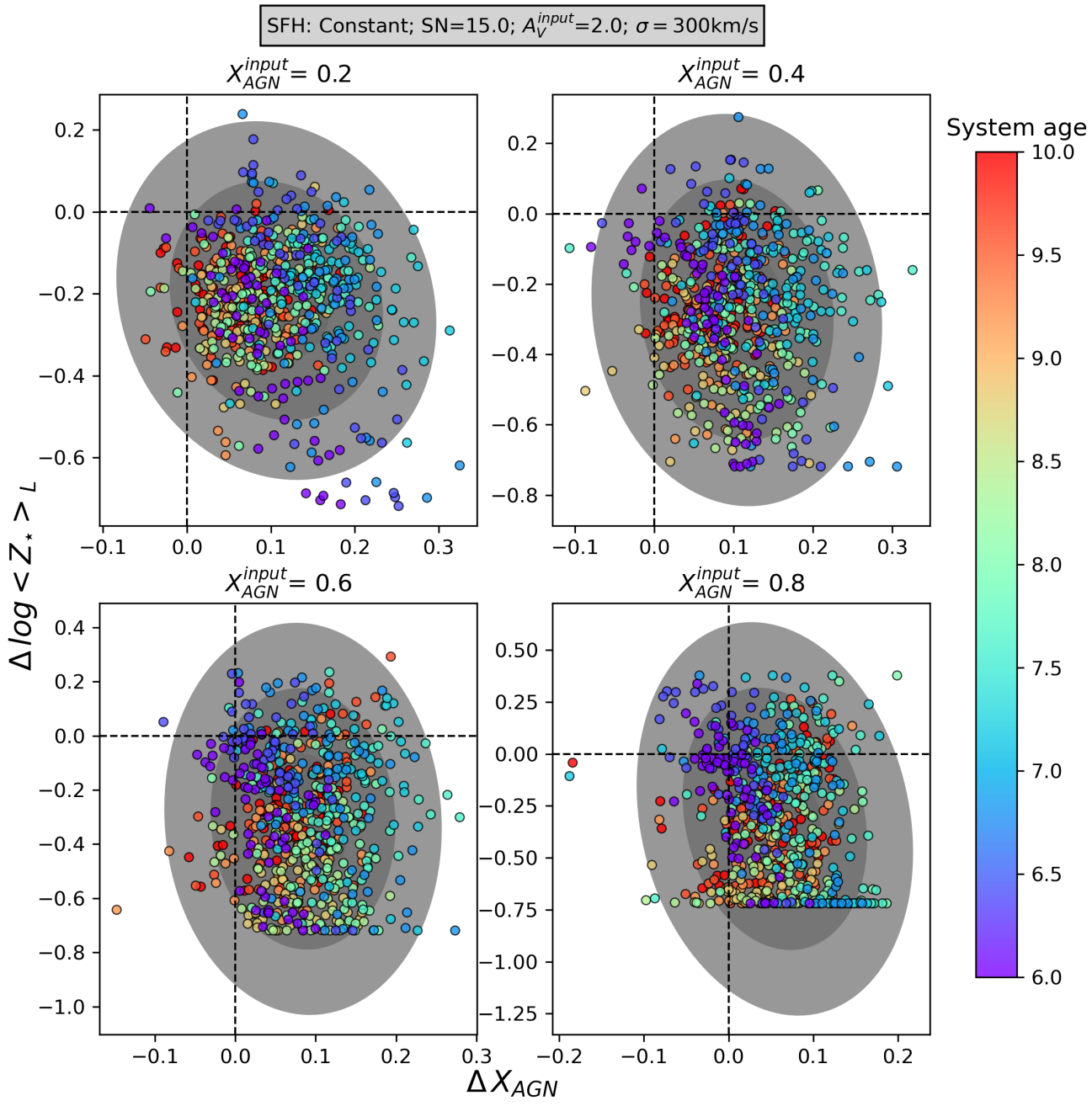

FIGURE A.46: $\Delta\, log < Z_\star >_L$ vs $\Delta\, X_{AGN}$; SFH: Constant, SN = 15.0, base: BaseA

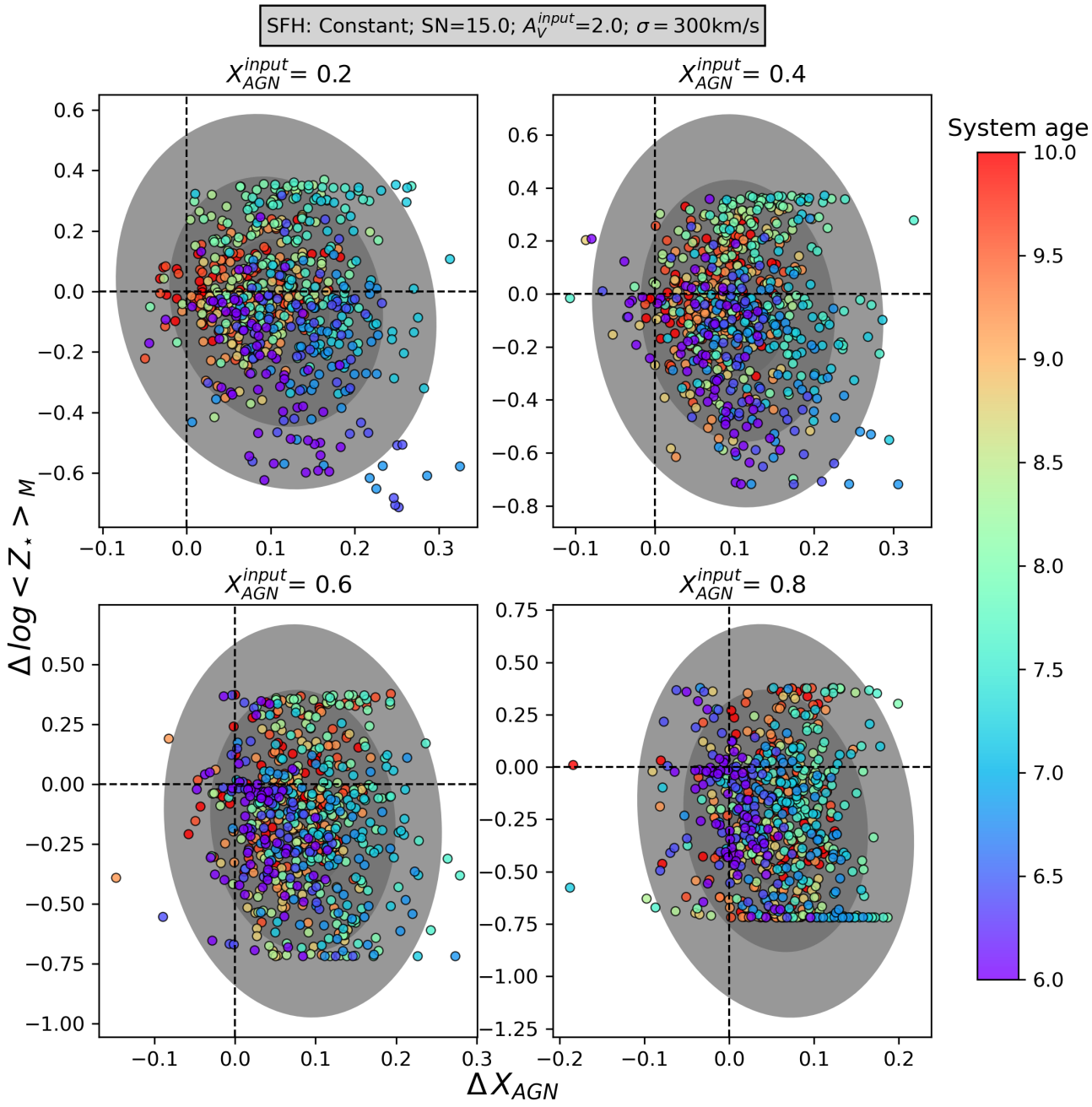

FIGURE A.47: $\Delta\, log < Z_\star >_M$ vs vs $\Delta\, X_{AGN}$; SFH: Constant, SN = 15.0, base: BaseA

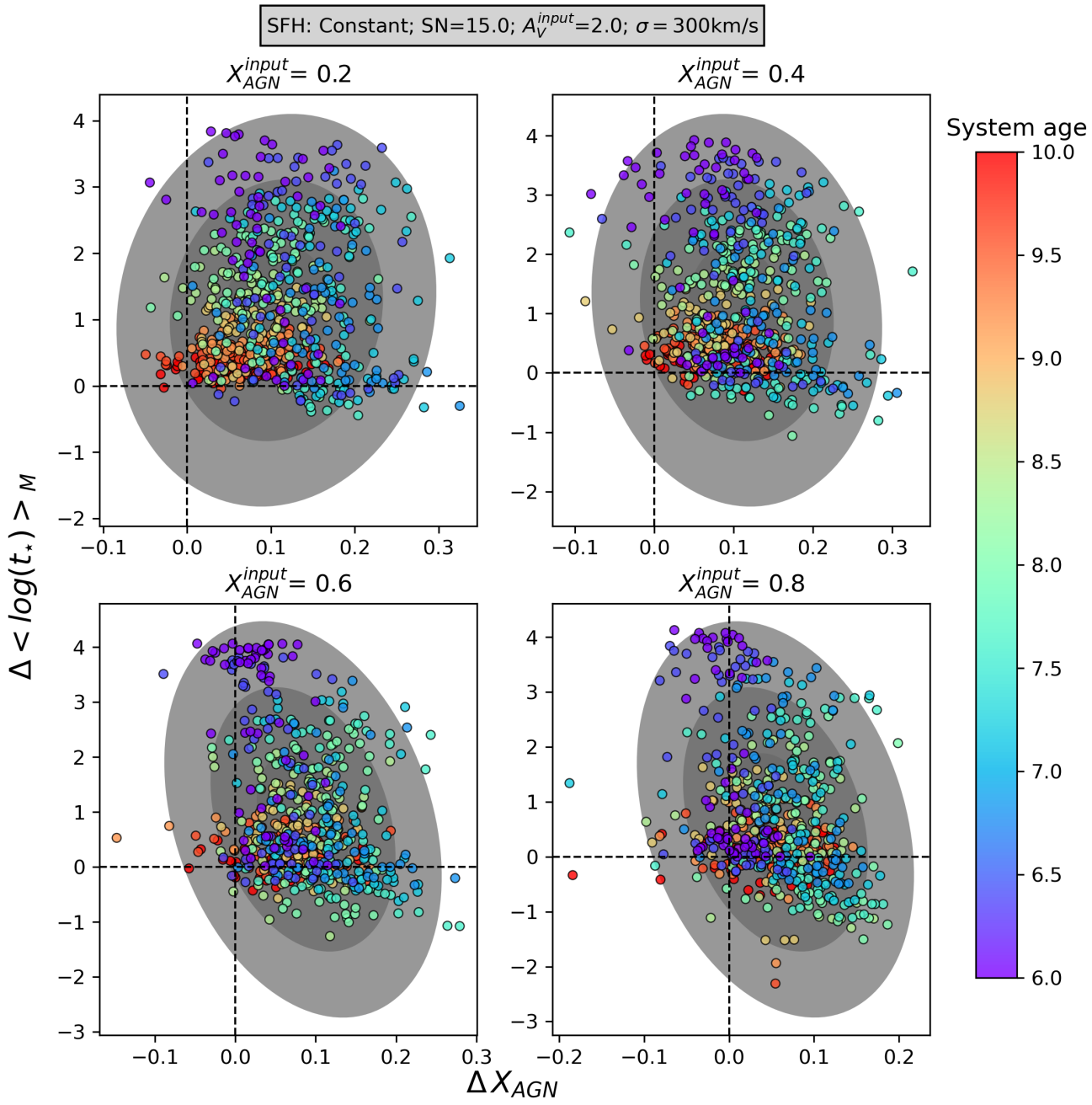

FIGURE A.48: $\Delta < log(t_\star) >_M$ vs ΔX_{AGN}; SFH: Constant, SN = 15.0, base: BaseA

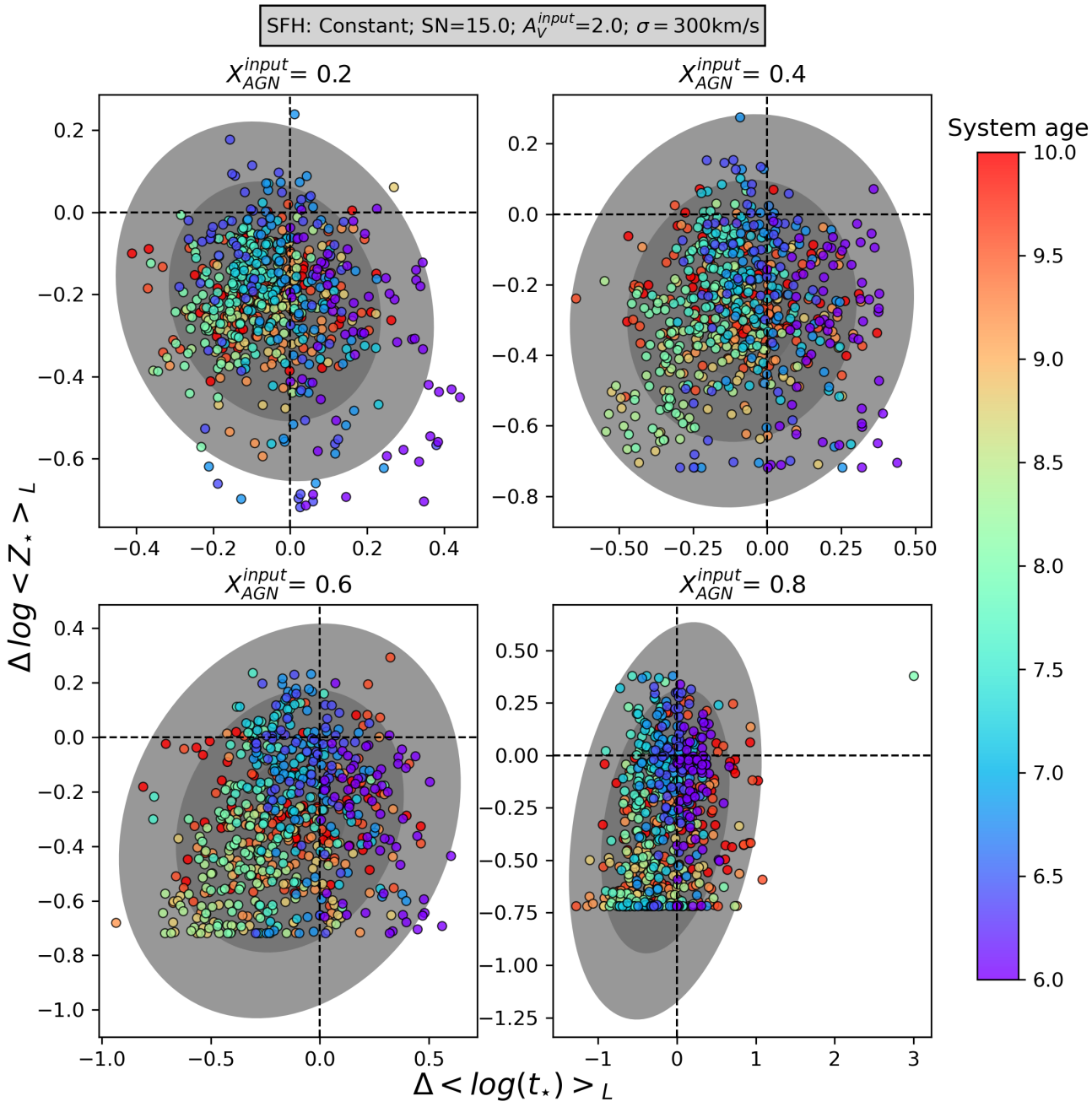

FIGURE A.49: $\Delta log < Z_\star >_L$ vs $\Delta < log(t_\star) >_L$; SFH: Constant, SN = 15.0, base: BaseA

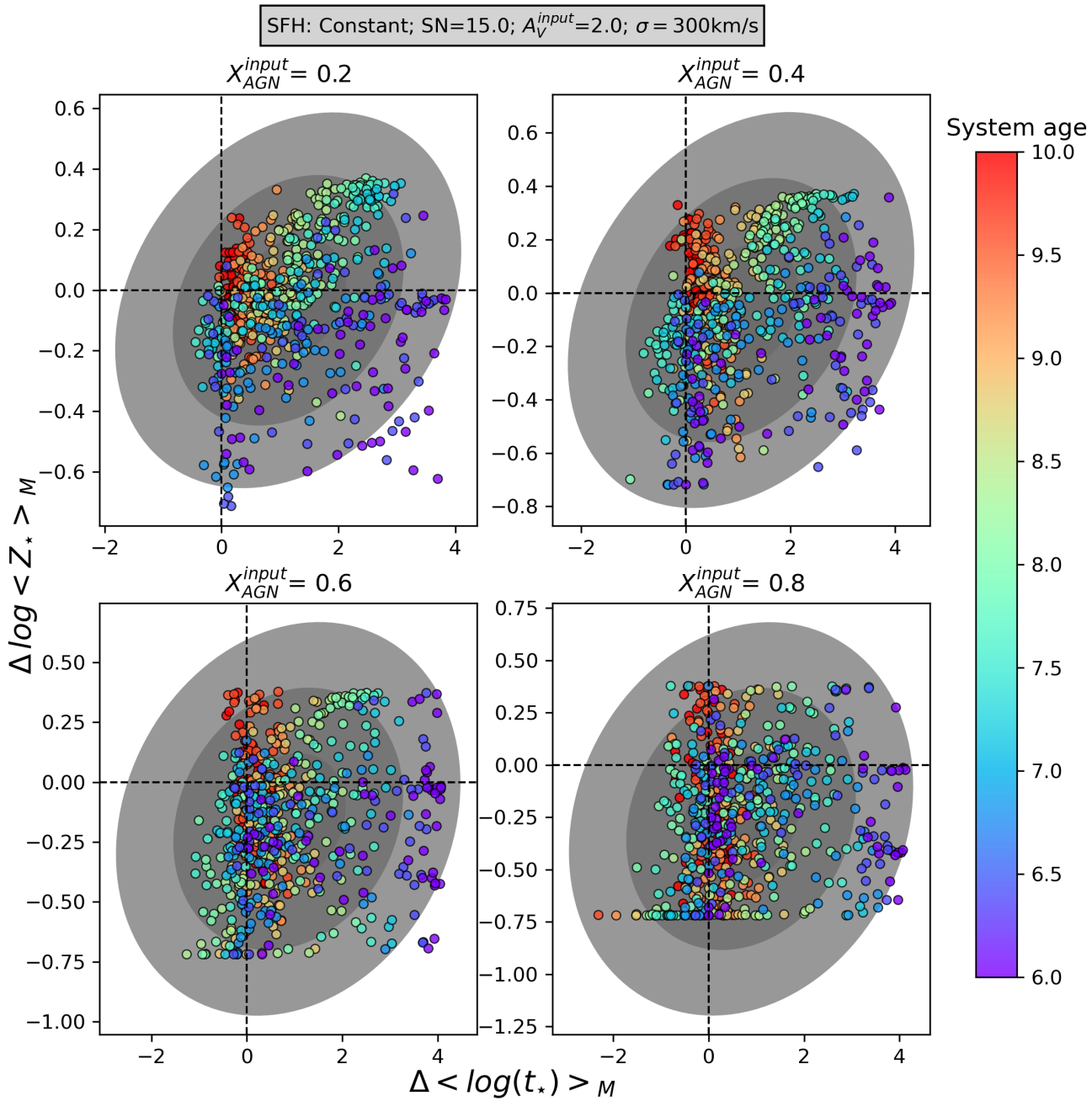

FIGURE A.50: $\Delta log < Z_\star >_M$ vs $\Delta < log(t_\star) >_M$; SFH: Constant, SN = 15.0, base: BaseA

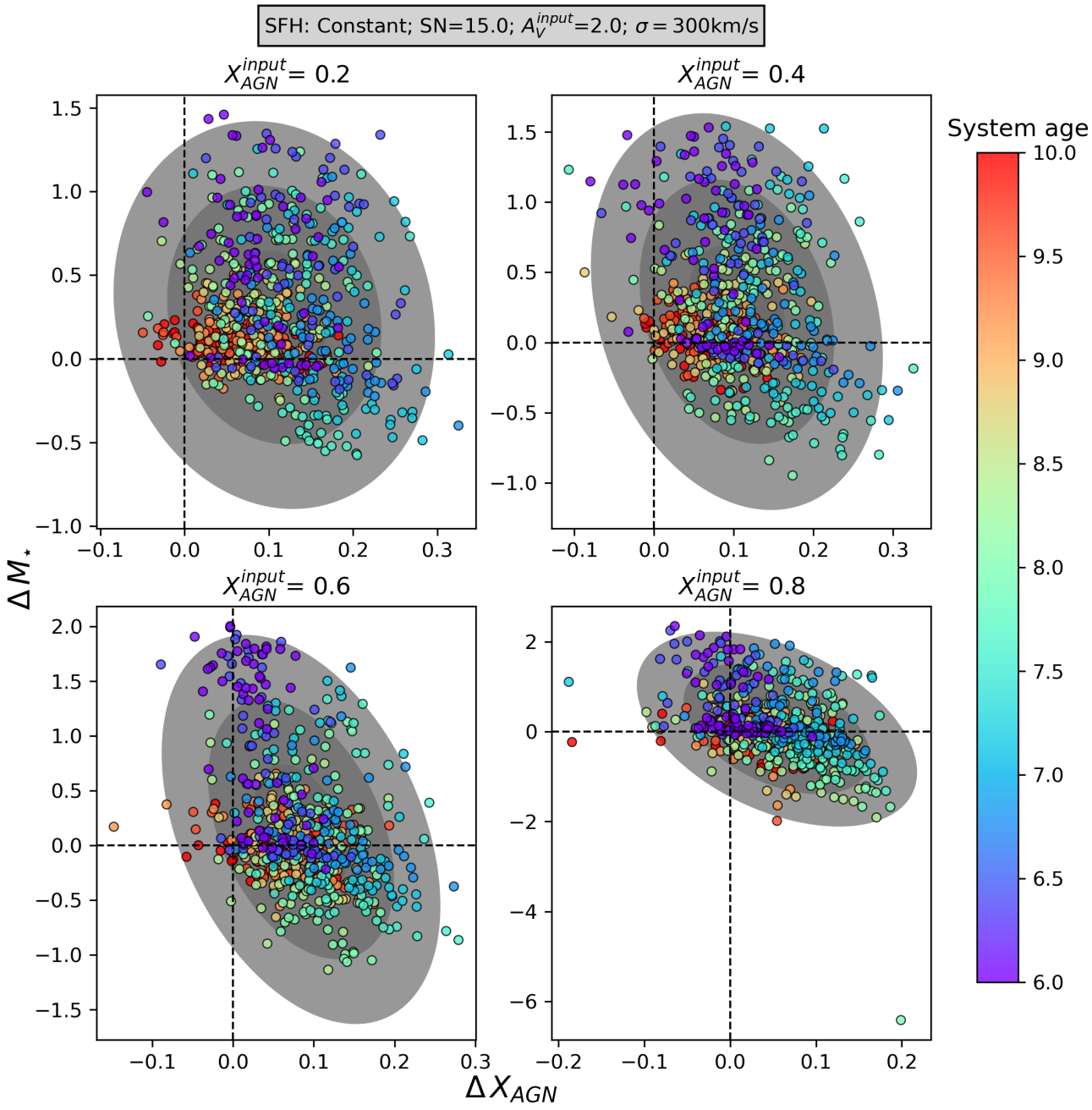

FIGURE A.51: $\Delta M_\star$ vs ΔX_{AGN}; SFH: Constant, SN = 15.0, base: BaseA

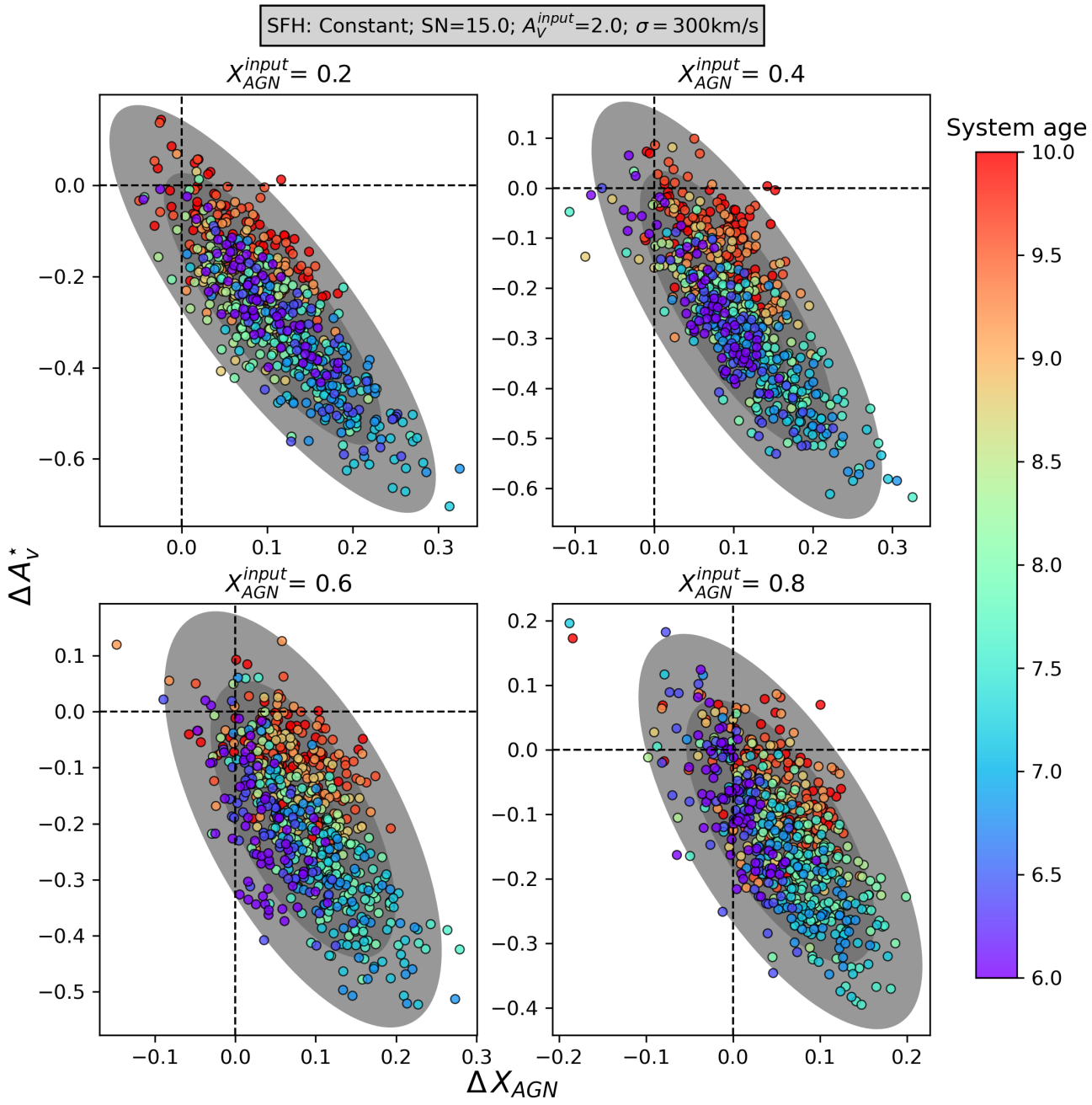

FIGURE A.52: $\Delta A_v^\star$ vs ΔX_{AGN}; SFH: Constant, SN = 15.0, base: BaseA

Bibliography

Abazajian, K. N., Adelman-McCarthy, J. K., Agüeros, M. A., Allam, S. S., Allende Prieto, C., An, D., Anderson, K. S. J., Anderson, S. F., Annis, J., Bahcall, N. A., Bailer-Jones, C. A. L., Barentine, J. C., Bassett, B. A., Becker, A. C., Beers, T. C., Bell, E. F., Belokurov, V., Berlind, A. A., Berman, E. F., Bernardi, M., Bickerton, S. J., Bizyaev, D., Blakeslee, J. P., Blanton, M. R., Bochanski, J. J., Boroski, W. N., Brewington, H. J., Brinchmann, J., Brinkmann, J., Brunner, R. J., Budavári, T., Carey, L. N., Carliles, S., Carr, M. A., Castander, F. J., Cinabro, D., Connolly, A. J., Csabai, I., Cunha, C. E., Czarapata, P. C., Davenport, J. R. A., de Haas, E., Dilday, B., Doi, M., Eisenstein, D. J., Evans, M. L., Evans, N. W., Fan, X., Friedman, S. D., Frieman, J. A., Fukugita, M., Gänsicke, B. T., Gates, E., Gillespie, B., Gilmore, G., Gonzalez, B., Gonzalez, C. F., Grebel, E. K., Gunn, J. E., György, Z., Hall, P. B., Harding, P., Harris, F. H., Harvanek, M., Hawley, S. L., Hayes, J. J. E., Heckman, T. M., Hendry, J. S., Hennessy, G. S., Hindsley, R. B., Hoblitt, J., Hogan, C. J., Hogg, D. W., Holtzman, J. A., Hyde, J. B., Ichikawa, S.-i., Ichikawa, T., Im, M., Ivezić, Ž., Jester, S., Jiang, L., Johnson, J. A., Jorgensen, A. M., Jurić, M., Kent, S. M., Kessler, R., Kleinman, S. J., Knapp, G. R., Konishi, K., Kron, R. G., Krzesinski, J., Kuropatkin, N., Lampeitl, H., Lebedeva, S., Lee, M. G., Lee, Y. S., French Leger, R., Lépine, S., Li, N., Lima, M., Lin, H., Long, D. C., Loomis, C. P., Loveday, J., Lupton, R. H., Magnier, E., Malanushenko, O., Malanushenko, V., Mandelbaum, R., Margon, B., Marriner, J. P., Martínez-Delgado, D., Matsubara, T., McGehee, P. M., McKay, T. A., Meiksin, A., Morrison, H. L., Mullally, F., Munn, J. A., Murphy, T., Nash, T., Nebot, A., Neilsen, Eric H., J., Newberg, H. J., Newman, P. R., Nichol, R. C., Nicinski, T., Nieto-Santisteban, M., Nitta, A., Okamura, S., Oravetz, D. J., Ostriker, J. P., Owen, R., Padmanabhan, N., Pan, K., Park, C., Pauls, G., Peoples, John, J., Percival, W. J., Pier, J. R., Pope, A. C., Pourbaix, D., Price, P. A., Purger, N., Quinn, T., Raddick, M. J., Re Fiorentin, P., Richards, G. T., Richmond, M. W., Riess, A. G., Rix, H.-W., Rockosi, C. M., Sako, M., Schlegel, D. J., Schneider, D. P., Scholz, R.-D., Schreiber, M. R., Schwope, A. D., Seljak, U., Sesar, B., Sheldon, E., Shimasaku, K., Sibley, V. C., Simmons, A. E., Sivarani, T., Allyn Smith, J., Smith, M. C., Smolčić, V., Snedden, S. A., Stebbins, A., Steinmetz, M., Stoughton, C., Strauss, M. A., SubbaRao, M., Suto, Y., Szalay, A. S., Szapudi, I., Szkody,

P., Tanaka, M., Tegmark, M., Teodoro, L. F. A., Thakar, A. R., Tremonti, C. A., Tucker, D. L., Uomoto, A., Vanden Berk, D. E., Vandenberg, J., Vidrih, S., Vogeley, M. S., Voges, W., Vogt, N. P., Wadadekar, Y., Watters, S., Weinberg, D. H., West, A. A., White, S. D. M., Wilhite, B. C., Wonders, A. C., Yanny, B., Yocum, D. R., York, D. G., Zehavi, I., Zibetti, S., and Zucker, D. B. (2009). The Seventh Data Release of the Sloan Digital Sky Survey. The Astrophysical Journal Supplement Series, 182(2):543–558. [Cited on pages 21 and 59.]

Anders, P. and Fritze-v. Alvensleben, U. (2003). Spectral and photometric evolution of young stellar populations: The impact of gaseous emission at various metallicities. Astronomy and Astrophysics, 401:1063–1070. [Cited on page 38.]

Antonucci, R. (1993). Unified models for active galactic nuclei and quasars. Annual Review of Astron and Astrophysis, 31:473–521. [Cited on page 6.]

Antonucci, R. R. J. (1982). Optical polarization position angle versus radio source axis in radio galaxies. Nature, 299(5884):605–606. [Cited on page 6.]

Antonucci, R. R. J. (1984). Optical spectropolarimetry of radio galaxies. The Astrophysical Journal, 278:499–520. [Cited on page 6.]

Antonucci, R. R. J. and Miller, J. S. (1985). Spectropolarimetry and the nature of NGC 1068. The Astrophysical Journal, 297:621–632. [Cited on pages 6 and 24.]

Asari, N. V., Cid Fernandes, R., Stasińska, G., Torres-Papaqui, J. P., Mateus, A., Sodré, L., Schoenell, W., and Gomes, J. M. (2007). The history of star-forming galaxies in the Sloan Digital Sky Survey. Monthly Notices of the Royal Astronomical Society, 381(1):263–279. [Cited on pages 12, 44, and 48.]

Baldwin, J. A., Phillips, M. M., and Terlevich, R. (1981). Classification parameters for the emission-line spectra of extragalactic objects. Publications of the ASP, 93:5–19. [Cited on pages 20, 22, 31, and 59.]

Baskin, A. and Laor, A. (2005). What controls the [OIII]λ5007 line strength in active galactic nuclei? Monthly Notices of the Royal Astronomical Society, 358(3):1043–1054. [Cited on page 29.]

Baumann, M., Boch, T., Pineau, F.-X., Fernique, P., Bot, C., and Allen, M. (2022). Aladin Lite v3: Behind the Scenes of a Major Overhaul. In Ruiz, J. E., Pierfedereci, F., and Teuben, P., editors, Astronomical Society of the Pacific Conference Series, volume 532 of Astronomical Society of the Pacific Conference Series, page 7. [Cited on page vi.]

Becker, R. H., White, R. L., and Helfand, D. J. (1995). The FIRST Survey: Faint Images of the Radio Sky at Twenty Centimeters. The Astrophysical Journal, 450:559. [Cited on page 68.]

Best, P. N. and Heckman, T. M. (2012). On the fundamental dichotomy in the local radio-AGN population: accretion, evolution and host galaxy properties. Monthly Notices of the Royal Astronomical Society, 421(2):1569–1582. [Cited on page 8.]

Binette, L., Wilson, A. S., and Storchi-Bergmann, T. (1996). Excitation and temperature of extended gas in active galaxies. II. Photoionization models with matter-bounded clouds. Astronomy and Astrophysics, 312:365–379. [Cited on page 20.]

Boch, T. and Fernique, P. (2014). Aladin Lite: Embed your Sky in the Browser. In Manset, N. and Forshay, P., editors, Astronomical Data Analysis Software and Systems XXIII, volume 485 of Astronomical Society of the Pacific Conference Series, page 277. [Cited on page vi.]

Boisson, C., Joly, M., Moultaka, J., Pelat, D., and Serote Roos, M. (2000). Stellar populations in active galactic nuclei. II. Population synthesis. Astronomy and Astrophysics, 357:850–870. [Cited on page 15.]

Bon, N., Popović, L. Č., and Bon, E. (2014). Efficiency tests for estimating the gas and stellar population parameters in Type 2 objects. Advances in Space Research, 54(7):1389–1400. [Cited on page 15.]

Bonnarel, F., Fernique, P., Bienaymé, O., Egret, D., Genova, F., Louys, M., Ochsenbein, F., Wenger, M., and Bartlett, J. G. (2000). The ALADIN interactive sky atlas. A reference tool for identification of astronomical sources. Astronomy and Astrophysicss, 143:33–40. [Cited on page vi.]

Boquien, M., Buat, V., and Perret, V. (2014). Impact of star formation history on the measurement of star formation rates. Astronomy and Astrophysics, 571:A72. [Cited on page 34.]

Breda, I. and Papaderos, P. (2018). The continuous rise of bulges out of galactic disks. Astronomy and Astrophysics, 614:A48. [Cited on pages 11 and 77.]

Brinchmann, J., Charlot, S., White, S. D. M., Tremonti, C., Kauffmann, G., Heckman, T., and Brinkmann, J. (2004). The physical properties of star-forming galaxies in the low-redshift Universe. Monthly Notices of the Royal Astronomical Society, 351(4):1151–1179. [Cited on pages 11 and 78.]

Brown, R. L. and Mathews, W. G. (1970). Theoretical Continuous Spectra of Gaseous Nebulae. The Astrophysical Journal, 160:939. [Cited on page 37.]

Bruzual, G. and Charlot, S. (2003). Stellar population synthesis at the resolution of 2003. Monthly Notices of the Royal Astronomical Society, 344(4):1000–1028. [Cited on pages 35, 46, and 65.]

Byrne, C. M., Stanway, E. R., Eldridge, J. J., McSwiney, L., and Townsend, O. T. (2022). The dependence of theoretical synthetic spectra on α-enhancement in young, binary stellar populations. Monthly Notices of the Royal Astronomical Society, 512(4):5329–5338. [Cited on page 65.]

Cappellari, M. and Emsellem, E. (2004). Parametric Recovery of Line-of-Sight Velocity Distributions from Absorption-Line Spectra of Galaxies via Penalized Likelihood. Publications of the ASP, 116(816):138–147. [Cited on page 12.]

Cardelli, J. A., Clayton, G. C., and Mathis, J. S. (1989). The Relationship between Infrared, Optical, and Ultraviolet Extinction. The Astrophysical Journal, 345:245. [Cited on pages 59 and 60.]

Cardoso, L. S. M. (2017). Impact of AGN and nebular emission on the estimation of stellar properties of galaxies. PhD thesis. University of Porto, Portugal. [Cited on page 34.]

Cardoso, L. S. M., Gomes, J.-M., and Papaderos, P. (2016). Semi-empirical AGN detection threshold in spectral synthesis studies of Lyman-continuum-leaking early-type galaxies. Astronomy and Astrophysics, 594:L2. [Cited on pages 16 and 64.]

Cardoso, L. S. M., Gomes, J. M., and Papaderos, P. (2017). Impact of an AGN featureless continuum on estimation of stellar population properties. Astronomy and Astrophysics, 604:A99. [Cited on pages 16, 17, and 64.]

Cardoso, L. S. M., Gomes, J. M., and Papaderos, P. (2019). Self-consistent population spectral synthesis with FADO. I. The importance of nebular emission in modelling star-forming galaxies. Astronomy and Astrophysics, 622:A56. [Cited on pages 17 and 38.]

Cardoso, L. S. M., Gomes, J. M., Papaderos, P., Pappalardo, C., Miranda, H., Paulino-Afonso, A., Afonso, J., and Lagos, P. (2022). Revisiting stellar properties of star-forming galaxies with stellar and nebular spectral modelling. Astronomy and Astrophysics, 667:A11. [Cited on page 59.]

Chabrier, G. (2003). Galactic Stellar and Substellar Initial Mass Function. Publications of the ASP, 115(809):763–795. [Cited on page 46.]

Charlot, S. and Longhetti, M. (2001). Nebular emission from star-forming galaxies. Monthly Notices of the Royal Astronomical Society, 323(4):887–903. [Cited on page 38.]

Chowdhury, R. K., Chatterjee, S., Paul, A., Sarazin, C. L., and Dai, J. L. (2022). Cosmological Simulation of Galaxy Groups and Clusters. II. Studying Different Modes of Feedback through X-Ray Observations. The Astrophysical Journal, 940. [Cited on page 11.]

Cid Fernandes, R., Gu, Q., Melnick, J., Terlevich, E., Terlevich, R., Kunth, D., Rodrigues Lacerda, R., and Joguet, B. (2004). The star formation history of Seyfert 2 nuclei. Monthly Notices of the Royal Astronomical Society, 355(1):273–296. [Cited on pages 13 and 14.]

Cid Fernandes, R., Mateus, A., Sodré, L., Stasińska, G., and Gomes, J. M. (2005). Semi-empirical analysis of Sloan Digital Sky Survey galaxies - I. Spectral synthesis method. Monthly Notices of the Royal Astronomical Society, 358(2):363–378. [Cited on pages 12 and 48.]

Cohen, M. H., Kellermann, K. I., Shaffer, D. B., Linfield, R. P., Moffet, A. T., Romney, J. D., Seielstad, G. A., Pauliny-Toth, I. I. K., Preuss, E., Witzel, A., Schilizzi, R. T., and Geldzahler, B. J. (1977). Radio sources with superluminal velocities. Nature, 268(5619):405–409. [Cited on page 5.]

Condon, J. J., Cotton, W. D., Greisen, E. W., Yin, Q. F., Perley, R. A., Taylor, G. B., and Broderick, J. J. (1998). The NRAO VLA Sky Survey. Astronomical Journal, 115(5):1693–1716. [Cited on page 70.]

Conroy, C. (2013). Modeling the Panchromatic Spectral Energy Distributions of Galaxies. Annual Review of Astron and Astrophysis, 51(1):393–455. [Cited on page 36.]

Cowie, L. L., Songaila, A., Hu, E. M., and Cohen, J. G. (1996). New Insight on Galaxy Formation and Evolution From Keck Spectroscopy of the Hawaii Deep Fields. Astronomical Journal, 112:839. [Cited on page 11.]

Cresci, G. and Maiolino, R. (2018). Triggered and quenched star formation in the outflowing gas of a QSO-SMG pair at z = 4.7. Nature Astronomy, 2:179–184. [Cited on page 10.]

Cutri, R. M., Wright, E. L., Conrow, T., Fowler, J. W., Eisenhardt, P. R. M., Grillmair, C., Kirkpatrick, J. D., Masci, F., McCallon, H. L., Wheelock, S. L., Fajardo-Acosta, S., Yan, L., Benford, D., Harbut, M., Jarrett, T., Lake, S., Leisawitz, D., Ressler, M. E., Stanford, S. A., Tsai, C. W., Liu, F., Helou, G., Mainzer, A., Gettings, D., Gonzalez, A., Hoffman, D., Marsh, K. A., Padgett, D., Skrutskie, M. F., Beck, R. P., Papin, M., and Wittman, M. (2013). Explanatory Supplement to the AllWISE Data Release Products. Explanatory Supplement to the AllWISE Data Release Products, by R. M. Cutri et al. [Cited on page 70.]

de Vaucouleurs, G. (1959). Classification and Morphology of External Galaxies. Handbuch der Physik, 53:275. [Cited on page 34.]

Di Matteo, T., Springel, V., and Hernquist, L. (2005). Energy input from quasars regulates the growth and activity of black holes and their host galaxies. Nature, 433:604–607. [Cited on page 10.]

Done, C., Davis, S. W., Jin, C., Blaes, O., and Ward, M. (2012). Intrinsic disc emission and the soft X-ray excess in active galactic nuclei. Monthly Notices of the Royal Astronomical Society, 420(3):1848–1860. [Cited on page 21.]

Dopita, M. A., Groves, B. A., Sutherland, R. S., Binette, L., and Cecil, G. (2002). Are the Narrow-Line Regions in Active Galaxies Dusty and Radiation Pressure Dominated? The Astrophysical Journal, 572(2):753–761. [Cited on pages 29, 45, and 50.]

Eldridge, J. J., Stanway, E. R., Xiao, L., McClelland, L. A. S., Taylor, G., Ng, M., Greis, S. M. L., and Bray, J. C. (2017). Binary Population and Spectral Synthesis Version 2.1: Construction, Observational Verification, and New Results. Publications of the Astron. Soc. of Australia, 34:e058. [Cited on page 65.]

Eracleous, M. and Halpern, J. P. (2001). NGC 3065: A Certified LINER with Broad, Variable Balmer Lines. The Astrophysical Journal, 554(1):240–244. [Cited on page 14.]

Faber, S. M. (1972). Quadratic programming applied to the problem of galaxy population synthesis. Astronomy and Astrophysics, 20:361. [Cited on page 11.]

Fabian, A. C. (2012). Observational Evidence of Active Galactic Nuclei Feedback. Annual Review of Astronomy and Astrophysics, 50:455–489. [Cited on page 10.]

Feain, I. J., Ekers, R. D., Murphy, D. W., and Gaensler, B. M. (2007). Triggering Star Formation with AGN Outflows. The Astrophysical Journal, 663:L1–L4. [Cited on page 10.]

Feltre, A., Charlot, S., and Gutkin, J. (2016). Nuclear activity versus star formation: emission-line diagnostics at ultraviolet and optical wavelengths. Monthly Notices of the Royal Astronomical Society, 456(3):3354–3374. [Cited on pages 20, 21, 22, and 31.]

Feltre, A., Hatziminaoglou, E., Fritz, J., and Franceschini, A. (2012). Smooth and clumpy dust distributions in AGN: a direct comparison of two commonly explored infrared emission models. Monthly Notices of the Royal Astronomical Society, 426(1):120–127. [Cited on page 28.]

Ferguson, J. W., Korista, K. T., Baldwin, J. A., and Ferland, G. J. (1997). Locally Optimally Emitting Clouds and the Narrow Emission Lines in Seyfert Galaxies. The Astrophysical Journal, 487(1):122–141. [Cited on page 20.]

Ferland, G. J. and Netzer, H. (1983). Are there any shock-heated galaxies ? The Astrophysical Journal, 264:105–113. [Cited on page 29.]

Ferland, G. J. and Osterbrock, D. E. (1986). IUE Spectra and a Resulting Model of Seyfert 2 Galaxies. The Astrophysical Journal, 300:658. [Cited on page 29.]

Ferland, G. J., Porter, R. L., van Hoof, P. A. M., Williams, R. J. R., Abel, N. P., Lykins, M. L., Shaw, G., Henney, W. J., and Stancil, P. C. (2013). The 2013 Release of Cloudy. Revista Mexicana de Astronomia y Astrofisica, 49:137–163. [Cited on pages 21, 29, and 49.]

Ferrarese, L. and Merritt, D. (2000). A Fundamental Relation between Supermassive Black Holes and Their Host Galaxies. The Astrophysical Journal, 539:L9–L12. [Cited on page 10.]

Ferreras, I. et al. (2019). The sami galaxy survey: stellar population gradients in galaxies. Monthly Notices of the Royal Astronomical Society, 489(1):608–619. [Cited on page 12.]

Fioc, M. and Rocca-Volmerange, B. (1997). PEGASE: a UV to NIR spectral evolution model of galaxies. Application to the calibration of bright galaxy counts. Astronomy and Astrophysics, 326:950–962. [Cited on pages 34 and 35.]

Fricke, K. J., Izotov, Y. I., Papaderos, P., Guseva, N. G., and Thuan, T. X. (2001). An Imaging and Spectroscopic Study of the Very Metal-deficient Blue Compact Dwarf Galaxy Tol 1214-277. Astronomical Journal, 121(1):169–181. [Cited on page 65.]

Gan, Z., Yuan, F., Ostriker, J. P., Ciotti, L., and Novak, G. S. (2014). Active Galactic Nucleus Feedback in an isolated Elliptical GalaxY: The effect of strong radiative feedback in the kinetic mode. The Astrophysical Journal, 789:150. [Cited on page 10.]

Gaspari, M., Brighenti, F., and Temi, P. (2012). Mechanical AGN feedback: controlling the thermodynamical evolution of elliptical galaxies. Monthly Notices of the Royal Astronomical Society, 424:190–209. [Cited on page 10.]

Gavazzi, G., Bonfanti, C., Sanvito, G., Boselli, A., and Scodeggio, M. (2002). Spectrophotometry of Galaxies in the Virgo Cluster. I. The Star Formation History. The Astrophysical Journal, 576(1):135–151. [Cited on page 34.]

Gebhardt, K., Bender, R., Bower, G., Dressler, A., Faber, S. M., Filippenko, A. V., Green, R., Grillmair, C., Ho, L. C., Kormendy, J., Lauer, T. R., Magorrian, J., Pinkney, J., Richstone, D., and Tremaine, S. (2000). A Relationship between Nuclear Black Hole Mass and Galaxy Velocity Dispersion. The Astrophysical Journal, 539:L13–L16. [Cited on page 10.]

Goerdt, A. and Kollatschny, W. (1998). Combined population and evolutionary synthesis of galaxy spectra. Astronomy and Astrophysics, 337:699–710. [Cited on page 14.]

Gomes, J. M. (2024). PyFluxconserving. [Cited on page 59.]

Gomes, J. M. and Papaderos, P. (2017). Fitting Analysis using Differential evolution Optimization (FADO):. Spectral population synthesis through genetic optimization under self-consistency boundary conditions. Astronomy and Astrophysics, 603:A63. [Cited on pages 17 and 35.]

Gomes, J. M., Papaderos, P., Kehrig, C., Vílchez, J. M., Lehnert, M. D., Sánchez, S. F., Ziegler, B., Breda, I., Dos Reis, S. N., Iglesias-Páramo, J., Bland-Hawthorn, J., Galbany, L., Bomans, D. J., Rosales-Ortega, F. F., Cid Fernandes, R., Walcher, C. J., Falcón-Barroso, J., García-Benito, R., Márquez, I., Del Olmo, A., Masegosa, J., Mollá, M., Marino, R. A., González Delgado, R. M., López-Sánchez, Á. R., and CALIFA Collaboration (2016a). Warm ionized gas in CALIFA early-type galaxies. 2D emission-line patterns and kinematics for 32 galaxies. Astronomy and Astrophysics, 588:A68. [Cited on page 64.]

Gomes, J. M., Papaderos, P., Vílchez, J. M., Kehrig, C., Iglesias-Páramo, J., Breda, I., Lehnert, M. D., Sánchez, S. F., Ziegler, B., Dos Reis, S. N., Bland-Hawthorn, J., Galbany, L., Bomans, D. J., Rosales-Ortega, F. F., Walcher, C. J., García-Benito, R., Márquez, I., Del Olmo, A., Mollá, M., Marino, R. A., Catalán-Torrecilla, C., González Delgado, R. M., López-Sánchez, Á. R., and CALIFA Collaboration (2016b). Spectroscopic aperture biases in inside-out evolving early-type galaxies from CALIFA. Astronomy and Astrophysics, 586:A22. [Cited on pages 11 and 78.]

Gonzáez-Delgado, R. M., García-Benito, R., Pérez, E., Cid Fernandes, R., de Amorim, A. L., Cortijo-Ferrero, C., Lacerda, E. A. D., López-Fernández, R., Vale-Asari, R. L., Sánchez, S., and Califa Collaboration (2016). The CALIFA Survey Across the Hubble Sequence: How Galaxies Grow their Bulges and Disks. In Skillen, I., Balcells, M., and Trager, S., editors, Multi-Object Spectroscopy in the Next Decade: Big Questions, Large Surveys, and Wide Fields, volume 507 of Astronomical Society of the Pacific Conference Series, page 251. [Cited on page 11.]

González Delgado, R. M., Cid Fernandes, R., García-Benito, R., Pérez, E., de Amorim, A. L., Cortijo-Ferrero, C., Lacerda, E. A. D., López Fernández, R., Sánchez, S. F., Vale Asari, N., Alves,

J., Bland-Hawthorn, J., Galbany, L., Gallazzi, A., Husemann, B., Bekeraite, S., Jungwiert, B., López-Sánchez, A. R., de Lorenzo-Cáceres, A., Marino, R. A., Mast, D., Mollá, M., del Olmo, A., Sánchez-Blázquez, P., van de Ven, G., Vílchez, J. M., Walcher, C. J., Wisotzki, L., Ziegler, B., and CALIFA Collaboration (2014). Insights on the Stellar Mass-Metallicity Relation from the CALIFA Survey. The Astrophysical Journal l, 791(1):L16. [Cited on page 11.]

Goto, T. (2006). Post-starburst-active galactic nucleus connection: spatially resolved spectroscopy of Hδ-strong active galactic nuclei. Monthly Notices of the Royal Astronomical Society, 369(4):1765–1772. [Cited on page 68.]

Grevesse, N. and Anders, E. (1989). Solar-system abundances of the elements: A new table. In Waddington, C. J., editor, Cosmic Abundances of Matter, volume 183 of American Institute of Physics Conference Series, pages 1–8. [Cited on page 31.]

Groves, B., Dopita, M. A., Sutherland, R. S., Kewley, L. J., Fischera, J., Leitherer, C., Brandl, B., and van Breugel, W. (2008). Modeling the Pan-Spectral Energy Distribution of Starburst Galaxies. IV. The Controlling Parameters of the Starburst SED. The Astrophysical Journal Supplement Series, 176(2):438–456. [Cited on page 38.]

Groves, B. A., Dopita, M. A., and Sutherland, R. S. (2004). Dusty, Radiation Pressure-Dominated Photoionization. II. Multiwavelength Emission Line Diagnostics for Narrow-Line Regions. The Astrophysical Journal Supplement Series, 153(1):75–91. [Cited on pages 20, 29, and 31.]

Gutkin, J., Charlot, S., and Bruzual, G. (2016). Modelling the nebular emission from primeval to present-day star-forming galaxies. Monthly Notices of the Royal Astronomical Society, 462(2):1757–1774. [Cited on page 44.]

Halpern, J. P. and Steiner, J. E. (1983). Low ionization active galactic nuclei : X-ray or shock heated ? The Astrophysical Journal l, 269:L37–L41. [Cited on page 29.]

Häring, N. and Rix, H.-W. (2004). On the Black Hole Mass-Bulge Mass Relation. The Astrophysical Journal, 604:L89–L92. [Cited on page 10.]

Heavens, A., Panter, B., Jimenez, R., and Dunlop, J. (2004). The star-formation history of the Universe from the stellar populations of nearby galaxies. Nature, 428(6983):625–627. [Cited on page 11.]

Heavens, A. F., Jimenez, R., and Lahav, O. (2000). Massive lossless data compression and multiple parameter estimation from galaxy spectra. Monthly Notices of the Royal Astronomical Society, 317(4):965–972. [Cited on page 12.]

Heckman, T. M. (1980). An Optical and Radio Survey of the Nuclei of Bright Galaxies - Activity in the Normal Galactic Nuclei. Astronomy and Astrophysics, 87:152. [Cited on page 13.]

Heckman, T. M. and Best, P. N. (2014). The Coevolution of Galaxies and Supermassive Black Holes: Insights from Surveys of the Contemporary Universe. Annual Review of Astron and Astrophysis, 52:589–660. [Cited on pages 8 and 9.]

Hickox, R. C., Mullaney, J. R., Alexander, D. M., Chen, C.-T. J., Civano, F. M., Goulding, A. D., and Hainline, K. N. (2014). Black Hole Variability and the Star Formation-Active Galactic Nucleus Connection: Do All Star-forming Galaxies Host an Active Galactic Nucleus? The Astrophysical Journal, 782(1):9. [Cited on page 8.]

Ho, L. C. (2008). Nuclear activity in nearby galaxies. Annual Review of Astron and Astrophysis, 46:475–539. [Cited on page 13.]

Hubble, E. P. (1926). Extragalactic nebulae. The Astrophysical Journal, 64:321–369. [Cited on page 34.]

Hummer, D. G. and Storey, P. J. (1987). Recombination-line intensities for hydrogenic ions - I. Case B calculations for H I and He II. Monthly Notices of the Royal Astronomical Society, 224:801–820. [Cited on page 38.]

Ichikawa, K., Ueda, Y., Terashima, Y., Oyabu, S., Gandhi, P., Matsuta, K., and Nakagawa, T. (2012). Mid- and Far-infrared Properties of a Complete Sample of Local Active Galactic Nuclei. The Astrophysical Journal, 754(1):45. [Cited on page 25.]

Iglesias-Páramo, J., Vílchez, J. M., Galbany, L., Sánchez, S. F., Rosales-Ortega, F. F., Mast, D., García-Benito, R., Husemann, B., Aguerri, J. A. L., Alves, J., Bekeraité, S., Bland-Hawthorn, J., Catalán-Torrecilla, C., de Amorim, A. L., de Lorenzo-Cáceres, A., Ellis, S., Falcón-Barroso, J., Flores, H., Florido, E., Gallazzi, A., Gomes, J. M., González Delgado, R. M., Haines, T., Hernández-Fernández, J. D., Kehrig, C., López-Sánchez, A. R., Lyubenova, M., Marino, R. A., Mollá, M., Monreal-Ibero, A., Mourão, A., Papaderos, P., Rodrigues, M., Sánchez-Blázquez, P., Spekkens, K., Stanishev, V., van de Ven, G., Walcher, C. J., Wisotzki, L., Zibetti, S., and Ziegler, B. (2013). Aperture corrections for disk galaxy properties derived from the CALIFA survey. Balmer emission lines in spiral galaxies. Astronomy and Astrophysics, 553:L7. [Cited on page 78.]

Izotov, Y. I., Guseva, N. G., and Thuan, T. X. (2011). Green Pea Galaxies and Cohorts: Luminous Compact Emission-line Galaxies in the Sloan Digital Sky Survey. The Astrophysical Journal, 728(2):161. [Cited on page 17.]

Izotov, Y. I., Noeske, K. G., Guseva, N. G., Papaderos, P., Thuan, T. X., and Fricke, K. J. (2004). Discovery of the high-ionization emission line [Ne V] λ3426 in the blue compact dwarf galaxy Tol 1214-277. Astronomy and Astrophysics, 415:L27–L30. [Cited on page 65.]

Izotov, Y. I., Thuan, T. X., and Guseva, N. G. (2021). Large binocular telescope observations of new six compact star-forming galaxies with [Ne V] λ3426 Å emission. Monthly Notices of the Royal Astronomical Society, 508(2):2556–2574. [Cited on page 65.]

Jackson, N., Tadhunter, C., and Sparks, W. B. (1998). Cygnus A: stars, dust and cones. Monthly Notices of the Royal Astronomical Society, 301(1):131–141. [Cited on page 6.]

Jarrett, T. H., Cohen, M., Masci, F., Wright, E., Stern, D., Benford, D., Blain, A., Carey, S., Cutri, R. M., Eisenhardt, P., Lonsdale, C., Mainzer, A., Marsh, K., Padgett, D., Petty, S., Ressler, M., Skrutskie, M., Stanford, S., Surace, J., Tsai, C. W., Wheelock, S., and Yan, D. L. (2011). The Spitzer-WISE Survey of the Ecliptic Poles. The Astrophysical Journal, 735(2):112. [Cited on pages 70 and 71.]

Kakkad, D., Stalevski, M., Kishimoto, M., Knežević, S., Asmus, D., and Vogt, F. P. A. (2023). Dissecting the active galactic nucleus in Circinus - IV. MUSE-NFM observations unveil a tuning-fork ionized outflow morphology. Monthly Notices of the Royal Astronomical Society, 519(4):5324–5332. [Cited on page 78.]

Kauffmann, G., Heckman, T. M., Tremonti, C., Brinchmann, J., Charlot, S., White, S. D. M., Ridgway, S. E., Brinkmann, J., Fukugita, M., Hall, P. B., Ivezić, Ž., Richards, G. T., and Schneider, D. P. (2003). The host galaxies of active galactic nuclei. Monthly Notices of the Royal Astronomical Society, 346(4):1055–1077. [Cited on pages 13 and 22.]

Kellermann, K. I., Sramek, R. A., Schmidt, M., Green, R. F., and Shaffer, D. B. (1994). The Radio Structure of Radio Loud and Quiet Quasars in the Palomar Bright Quasar Survey. Astronomical Journal, 108:1163. [Cited on page 7.]

Kennicutt, Robert C., J. (1989). The Star Formation Law in Galactic Disks. The Astrophysical Journal, 344:685. [Cited on page 35.]

Kewley, L. J., Dopita, M. A., Sutherland, R. S., Heisler, C. A., and Trevena, J. (2001). Theoretical Modeling of Starburst Galaxies. The Astrophysical Journal, 556(1):121–140. [Cited on page 22.]

Koleva, M., de Rijcke, S., Prugniel, P., Zeilinger, W. W., and Michielsen, D. (2009). Formation and evolution of dwarf elliptical galaxies - II. Spatially resolved star formation histories. Monthly Notices of the Royal Astronomical Society, 396(4):2133–2151. [Cited on page 12.]

Komossa, S. and Schulz, H. (1997). Interpretation of the emission line spectra of Seyfert 2 galaxies by multi-component photoionization models. Astronomy and Astrophysics, 323:31–46. [Cited on page 20.]

Koski, A. T. (1978). Spectrophotometry of Seyfert 2 galaxies and narrow-line radio galaxies. The Astrophysical Journal, 223:56–73. [Cited on pages 13 and 29.]

Kotulla, R., Fritze, U., Weilbacher, P., and Anders, P. (2009). GALEV evolutionary synthesis models - I. Code, input physics and web interface. Monthly Notices of the Royal Astronomical Society, 396(1):462–484. [Cited on pages 34 and 35.]

Lal, D. V. (2015). Study of Milli-Jansky Seyfert Galaxies with Strong Forbidden High-Ionization Lines Using the Very Large Array Survey Images. Journal of Korean Astronomical Society, 48(6):399–412. [Cited on page 68.]

LaMassa, S. M., Cales, S., Moran, E. C., Myers, A. D., Richards, G. T., Eracleous, M., Heckman, T. M., Gallo, L., and Urry, C. M. (2015). The Discovery of the First "Changing Look" Quasar: New Insights Into the Physics and Phenomenology of Active Galactic Nucleus. The Astrophysical Journal, 800(2):144. [Cited on page 8.]

Lara-López, M. A., Bongiovanni, A., Cepa, J., Pérez García, A. M., Sánchez-Portal, M., Castañeda, H. O., Fernández Lorenzo, M., and Pović, M. (2010). Study of star-forming galaxies in SDSS up to redshift 0.4. II. Evolution from the fundamental parameters: mass, metallicity and star formation rate. Astronomy and Astrophysics, 519:A31. [Cited on page 12.]

Leitherer, C., Schaerer, D., Goldader, J. D., Delgado, R. M. G., Robert, C., Kune, D. F., de Mello, D. F., Devost, D., and Heckman, T. M. (1999). Starburst99: Synthesis Models for Galaxies with Active Star Formation. The Astrophysical Journal Supplement Series, 123(1):3–40. [Cited on page 38.]

Lequeux, J., Peimbert, M., Rayo, J. F., Serrano, A., and Torres-Peimbert, S. (1979). Chemical Composition and Evolution of Irregular and Blue Compact Galaxies. Astronomy and Astrophysics, 80:155. [Cited on page 11.]

López Fernández, R., Cid Fernandes, R., González Delgado, R. M., Vale Asari, N., Pérez, E., García-Benito, R., de Amorim, A. L., Lacerda, E. A. D., Cortijo-Ferrero, C., and Sánchez, S. F. (2016). Simultaneous spectroscopic and photometric analysis of galaxies with STARLIGHT: CALIFA+GALEX. Monthly Notices of the Royal Astronomical Society, 458(1):184–199. [Cited on page 12.]

MacLeod, C. L., Ross, N. P., Lawrence, A., Goad, M., Horne, K., Burgett, W., Chambers, K. C., Flewelling, H., Hodapp, K., Kaiser, N., Magnier, E., Wainscoat, R., and Waters, C. (2016). A systematic search for changing-look quasars in SDSS. Monthly Notices of the Royal Astronomical Society, 457(1):389–404. [Cited on page 8.]

Maiolino, R., Marconi, A., and Oliva, E. (2001). Dust in active nuclei. II. Powder or gravel? Astronomy and Astrophysics, 365:37–48. [Cited on page 29.]

Maiolino, R., Russell, H. R., Fabian, A. C., Carniani, S., Gallagher, R., Cazzoli, S., Arribas, S., Belfiore, F., Colina, L., Cresci, G., Ishibashi, W., Marconi, A., Oliva, E., and Salvato, M. (2017). Positive feedback in the extragalactic gas component triggered by AGN jets: Evidence from a z = 2.6 galaxy. Monthly Notices of the Royal Astronomical Society, 466:892–905. [Cited on page 10.]

Malkan, M. A. and Filippenko, A. V. (1983). The stellar and nonstellar continua of Seyfert galaxies : nonthermal emission in the near-infrared. The Astrophysical Journal, 275:477–492. [Cited on page 14.]

Marconi, A. and Hunt, L. K. (2003). The Relation between Black Hole Mass, Bulge Mass, and Near-Infrared Luminosity. The Astrophysical Journal, 589:L21–L24. [Cited on page 10.]

Mathews, W. G. and Ferland, G. J. (1987). What Heats the Hot Phase in Active Nuclei? The Astrophysical Journal, 323:456. [Cited on page 13.]

Mingo, B., Hardcastle, M. J., Croston, J. H., Dicken, D., Evans, D. A., Morganti, R., and Tadhunter, C. (2014). An X-ray survey of the 2 Jy sample - I. Is there an accretion mode dichotomy in radio-loud AGN? Monthly Notices of the Royal Astronomical Society, 440(1):269–297. [Cited on page 8.]

Mollá, M., García-Vargas, M. L., and Bressan, A. (2009). PopStar I: evolutionary synthesis model description. Monthly Notices of the Royal Astronomical Society, 398(1):451–470. [Cited on page 38.]

Moultaka, J. (2005). A new inverse method for stellar population synthesis and error analysis. Astronomy and Astrophysics, 430:95–106. [Cited on page 15.]

Netzer, H. (1987). Quasar discs. II - A composite model for the broad-line region. Monthly Notices of the Royal Astronomical Society, 225:55–72. [Cited on page 25.]

Nikutta, R., Elitzur, M., and Lacy, M. (2009). On the 10 μm Silicate Feature in Active Galactic Nuclei. The Astrophysical Journal, 707(2):1550–1559. [Cited on page 25.]

Norman, C. (2009). Positive Feedback in Galactic Centers. Proceedings of the International Astronomical Union, 4:305–312. [Cited on page 10.]

Nussbaumer, H. and Schmutz, W. (1984). The hydrogenic 2s-1s two-photon emission. Astronomy and Astrophysics, 138(2):495. [Cited on page 37.]

Ocvirk, P., Pichon, C., Lançon, A., and Thiébaut, E. (2006). STECKMAP: STEllar Content and Kinematics from high resolution galactic spectra via Maximum A Posteriori. Monthly Notices of the Royal Astronomical Society, 365(1):74–84. [Cited on page 12.]

Osterbrock, D. E. (1989). Book-Review - Astrophysics of Gaseous Nebulae and Active Galactic Nuclei. Sky and Telescope, 78:491. [Cited on page 37.]

Osterbrock, D. E. and Ferland, G. J. (2006). Astrophysics of gaseous nebulae and active galactic nuclei. [Cited on pages 37 and 38.]

Panuzzo, P., Bressan, A., Granato, G. L., Silva, L., and Danese, L. (2003). Dust and nebular emission. I. Models for normal galaxies. Astronomy and Astrophysics, 409:99–114. [Cited on page 38.]

Papaderos, P., Gomes, J. M., Vílchez, J. M., Kehrig, C., Lehnert, M. D., Ziegler, B., Sánchez, S. F., Husemann, B., Monreal-Ibero, A., García-Benito, R., Bland-Hawthorn, J., Cortijo-Ferrero, C., de Lorenzo-Cáceres, A., del Olmo, A., Falcón-Barroso, J., Galbany, L., Iglesias-Páramo, J., López-Sánchez, Á. R., Marquez, I., Mollá, M., Mast, D., van de Ven, G., and Wisotzki, L. (2013). Nebular emission and the Lyman continuum photon escape fraction in CALIFA early-type galaxies. Astronomy and Astrophysics, 555:L1. [Cited on page 64.]

Pérez, E., Cid Fernandes, R., González Delgado, R. M., García-Benito, R., Sánchez, S. F., Husemann, B., Mast, D., Rodón, J. R., Kupko, D., Backsmann, N., de Amorim, A. L., van de Ven, G., Walcher, J., Wisotzki, L., Cortijo-Ferrero, C., and CALIFA Collaboration (2013). The Evolution of Galaxies Resolved in Space and Time: A View of Inside-out Growth from the CALIFA Survey. The Astrophysical Journal l, 764(1):L1. [Cited on page 11.]

Plat, A., Charlot, S., Bruzual, G., Feltre, A., Vidal-García, A., Morisset, C., Chevallard, J., and Todt, H. (2019). Constraints on the production and escape of ionizing radiation from the emission-line spectra of metal-poor star-forming galaxies. Monthly Notices of the Royal Astronomical Society, 490(1):978–1009. [Cited on page 44.]

Pogge, R. W. (1988). An Extended Ionizing Radiation Cone from the Nucleus of the Seyfert 2 Galaxy NGC 1068. The Astrophysical Journal, 328:519. [Cited on page 6.]

Pucha, R. (2021). Joint spectroscopic and photometric analysis of low-redshift galaxies. AAS 237 Special Session: The Data Lab Science Platform and Open-Data Ecosystem at NSF's NOIRLab. Virtual. [Cited on page 20.]

Quillen, A. C. and Bland-Hawthorn, J. (2008). When is star formation episodic? A delay differential equation 'negative feedback' model. Monthly Notices of the Royal Astronomical Society, 386(4):2227–2234. [Cited on page 34.]

Richardson, C. T., Allen, J. T., Baldwin, J. A., Hewett, P. C., and Ferland, G. J. (2014). Interpreting the ionization sequence in AGN emission-line spectra. Monthly Notices of the Royal Astronomical Society, 437(3):2376–2403. [Cited on page 20.]

Riffel, R., Pastoriza, M. G., Rodríguez-Ardila, A., and Bonatto, C. (2010). Probing the stellar population of seyfert galaxies: a near infrared perspective. In Bruzual, G. R. and Charlot, S., editors, Stellar Populations - Planning for the Next Decade, volume 262, pages 164–167. [Cited on page 15.]

Sánchez, S. F., Barrera-Ballesteros, J. K., Sánchez-Menguiano, L., Walcher, C. J., Marino, R. A., Galbany, L., Bland-Hawthorn, J., Cano-Díaz, M., García-Benito, R., López-Cobá, C., Zibetti, S., Vilchez, J. M., Iglésias-Páramo, J., Kehrig, C., López Sánchez, A. R., Duarte Puertas, S., and Ziegler, B. (2017). The mass-metallicity relation revisited with CALIFA. Monthly Notices of the Royal Astronomical Society, 469(2):2121–2140. [Cited on page 11.]

Sánchez, S. F., Kennicutt, R. C., Gil de Paz, A., van de Ven, G., Vílchez, J. M., Wisotzki, L., Walcher, C. J., Mast, D., Aguerri, J. A. L., Albiol-Pérez, S., Alonso-Herrero, A., Alves, J., Bakos, J., Bartáková, T., Bland-Hawthorn, J., Boselli, A., Bomans, D. J., Castillo-Morales, A., Cortijo-Ferrero, C., de Lorenzo-Cáceres, A., Del Olmo, A., Dettmar, R. J., Díaz, A., Ellis, S., Falcón-Barroso, J., Flores, H., Gallazzi, A., García-Lorenzo, B., González Delgado, R., Gruel, N., Haines, T., Hao, C., Husemann, B., Iglésias-Páramo, J., Jahnke, K., Johnson, B., Jungwiert, B., Kalinova, V., Kehrig, C., Kupko, D., López-Sánchez, Á. R., Lyubenova, M., Marino, R. A., Mármol-Queraltó, E., Márquez, I., Masegosa, J., Meidt, S., Mendez-Abreu, J., Monreal-Ibero, A., Montijo, C., Mourão, A. M., Palacios-Navarro, G., Papaderos, P., Pasquali, A., Peletier, R., Pérez, E., Pérez, I., Quirrenbach, A., Relaño, M., Rosales-Ortega, F. F., Roth, M. M., Ruiz-Lara, T., Sánchez-Blázquez, P., Sengupta, C., Singh, R., Stanishev, V., Trager, S. C., Vazdekis, A., Viironen, K., Wild, V., Zibetti, S., and Ziegler, B. (2012). CALIFA, the Calar Alto Legacy Integral Field Area survey. I. Survey presentation. Astronomy and Astrophysics, 538:A8. [Cited on page 11.]

Sánchez, S. F., Pérez, E., Sánchez-Blázquez, P., González, J. J., Rosáles-Ortega, F. F., Cano-Díaz, M., López-Cobá, C., Marino, R. A., Gil de Paz, A., Mollá, M., López-Sánchez, A. R., Ascasibar, Y., and Barrera-Ballesteros, J. (2016). Pipe3D, a pipeline to analyze Integral Field Spectroscopy Data: I. New fitting philosophy of FIT3D. Revista Mexicana de Astronomia y Astrofisica, 52:21–53. [Cited on page 12.]

Schaerer, D. and de Barros, S. (2010). On the physical properties of z $\approx$ 6-8 galaxies. Astronomy and Astrophysics, 515:A73. [Cited on page 38.]

Schaerer, D. and de Koter, A. (1997). Combined stellar structure and atmosphere models for massive stars. III. Spectral evolution and revised ionizing fluxes of O3-B0 stars. Astronomy and Astrophysics, 322:598–614. [Cited on page 65.]

Schaerer, D., Fragos, T., and Izotov, Y. I. (2019). X-ray binaries as the origin of nebular He II emission in low-metallicity star-forming galaxies. Astronomy and Astrophysics, 622:L10. [Cited on page 65.]

Schlafly, E. F. and Finkbeiner, D. P. (2011). Measuring Reddening with Sloan Digital Sky Survey Stellar Spectra and Recalibrating SFD. The Astrophysical Journal, 737(2):103. [Cited on page 59.]

Schmidt, M. (1959). The Rate of Star Formation. The Astrophysical Journal, 129:243. [Cited on page 35.]

Schmitt, H. R., Storchi-Bergmann, T., and Cid Fernandes, R. (1999). Spectral synthesis of the nuclear regions of Seyfert 2 and radio galaxies. Monthly Notices of the Royal Astronomical Society, 303(1):173–178. [Cited on pages 13 and 14.]

Schneider, P. (2015). Extragalactic Astronomy and Cosmology: An Introduction. [Cited on pages 2, 4, 5, and 7.]

Scott, N. et al. (2017). The sami galaxy survey: the global stellar populations of galaxies. Monthly Notices of the Royal Astronomical Society, 472(3):2833–2855. [Cited on page 12.]

Serra, P., Amblard, A., Temi, P., Burgarella, D., Giovannoli, E., Buat, V., Noll, S., and Im, S. (2011). CIGALEMC: Galaxy Parameter Estimation Using a Markov Chain Monte Carlo Approach with CIGALE. The Astrophysical Journal, 740(1):22. [Cited on page 35.]

Shirazi, M. and Brinchmann, J. (2012). Strongly star forming galaxies in the local Universe with nebular He IIλ4686 emission. Monthly Notices of the Royal Astronomical Society, 421(2):1043–1063. [Cited on page 65.]

Silk, J. (2013). Unleashing Positive Feedback: Linking the Rates of Star Formation, Supermassive Black Hole Accretion, and Outflows in Distant Galaxies. The Astrophysical Journal, 772:112. [Cited on page 10.]

Smith, K. L., Koss, M., Mushotzky, R., Wong, O. I., Shimizu, T. T., Ricci, F., and Ricci, C. (2020). Significant Suppression of Star Formation in Radio-quiet AGN Host Galaxies with Kiloparsec-scale Radio Structures. The Astrophysical Journal, 904. [Cited on page 11.]

Springel, V., Di Matteo, T., and Hernquist, L. (2005). Modelling feedback from stars and black holes in galaxy mergers. Monthly Notices of the Royal Astronomical Society, 361:776–794. [Cited on page 10.]

Stalevski, M., Fritz, J., Baes, M., Nakos, T., and Popović, L. Č. (2012). 3D radiative transfer modelling of the dusty tori around active galactic nuclei as a clumpy two-phase medium. Monthly Notices of the Royal Astronomical Society, 420(4):2756–2772. [Cited on page 25.]

Stalevski, M., Ricci, C., Ueda, Y., Lira, P., Fritz, J., and Baes, M. (2016). The dust covering factor in active galactic nuclei. Monthly Notices of the Royal Astronomical Society, 458(3):2288–2302. [Cited on page 25.]

Stasińska, G. (1984a). A grid of model nebulae photoionized by a power-law continuum. Astronomy and Astrophysicss, 55:15–32. [Cited on page 29.]

Stasińska, G. (1984b). Confrontation of a sample of Seyfert 2 galaxies with photoionized models. Astronomy and Astrophysics, 135:341–355. [Cited on page 29.]

Storchi-Bergmann, T., Baldwin, J. A., and Wilson, A. S. (1993). Double-peaked Broad Line Emission from the LINER Nucleus of NGC 1097. The Astrophysical Journal l, 410:L11. [Cited on page 13.]

Struck-Marcell, C. and Tinsley, B. M. (1978). Star formation rates and infrared radiation. The Astrophysical Journal, 221:562–566. [Cited on page 11.]

Sutherland, R., Dopita, M., Binette, L., and Groves, B. (2018). MAPPINGS V: Astrophysical plasma modeling code. Astrophysics Source Code Library, record ascl:1807.005. [Cited on page 21.]

Tadhunter, C. and Tsvetanov, Z. (1989). Anisotropic ionizing radiation in NGC5252. Nature, 341(6241):422–424. [Cited on page 6.]

Tanimoto, A., Ueda, Y., Odaka, H., Kawaguchi, T., Fukazawa, Y., and Kawamuro, T. (2019). XCLUMPY: X-Ray Spectral Model from Clumpy Torus and Its Application to the Circinus Galaxy. The Astrophysical Journal, 877(2):95. [Cited on page 25.]

Terlevich, R. and Melnick, J. (1985). Warmers : the missing link between Starburst and Seyfert galaxies. Monthly Notices of the Royal Astronomical Society, 213:841–856. [Cited on page 29.]

Thomas, A. D., Groves, B. A., Sutherland, R. S., Dopita, M. A., Kewley, L. J., and Jin, C. (2016). A Physically based Model of the Ionizing Radiation from Active Galaxies for Photoionization Modeling. The Astrophysical Journal, 833(2):266. [Cited on pages 21 and 23.]

Trager, S. C., Faber, S. M., Worthey, G., and González, J. J. (2000). The Stellar Population Histories of Early-Type Galaxies. II. Controlling Parameters of the Stellar Populations. Astronomical Journal, 120(1):165–188. [Cited on page 11.]

Tran, H. D. (1995a). The Nature of Seyfert 2 Galaxies with Obscured Broad-Line Regions. I. Observations. The Astrophysical Journal, 440:565. [Cited on page 24.]

Tran, H. D. (1995b). The Nature of Seyfert 2 Galaxies with Obscured Broad-Line Regions. II. Individual Objects. The Astrophysical Journal, 440:578. [Cited on page 24.]

Vazdekis, A., Sánchez-Blázquez, P., Falcón-Barroso, J., Cenarro, A. J., Beasley, M. A., Cardiel, N., Gorgas, J., and Peletier, R. F. (2010). Evolutionary stellar population synthesis with MILES - I. The base models and a new line index system. Monthly Notices of the Royal Astronomical Society, 404(4):1639–1671. [Cited on page 65.]

Vega, L. R., Asari, N. V., Cid Fernandes, R., Garcia-Rissmann, A., Storchi-Bergmann, T., González Delgado, R. M., and Schmitt, H. (2009). The CaT strength in Seyfert nuclei revisited: analysing young stars and non-stellar light contributions to the spectra. Monthly Notices of the Royal Astronomical Society, 393(3):846–857. [Cited on page 14.]

Veilleux, S. and Osterbrock, D. E. (1987). Spectral Classification of Emission-Line Galaxies. The Astrophysical Journal Supplement Series, 63:295. [Cited on page 13.]

Wilkinson, D. M., Maraston, C., Goddard, D., Thomas, D., and Parikh, T. (2017). FIREFLY (Fitting IteRativEly For Likelihood analYsis): a full spectral fitting code. Monthly Notices of the Royal Astronomical Society, 472(4):4297–4326. [Cited on page 12.]

Wilkinson, D. M., Maraston, C., Thomas, D., et al. (2015). p-manga: full spectral fitting and stellar population maps from prototype observations with the manga ifu survey. Monthly Notices of the Royal Astronomical Society, 449(4):328–350. [Cited on page 12.]

Yang, G., Boquien, M., Buat, V., Burgarella, D., Ciesla, L., Duras, F., Stalevski, M., Brandt, W. N., and Papovich, C. (2020). X-CIGALE: Fitting AGN/galaxy SEDs from X-ray to infrared. Monthly Notices of the Royal Astronomical Society, 491(1):740–757. [Cited on page 24.]

York, D. G., Adelman, J., Anderson, John E., J., Anderson, S. F., Annis, J., Bahcall, N. A., Bakken, J. A., Barkhouser, R., Bastian, S., Berman, E., Boroski, W. N., Bracker, S., Briegel, C., Briggs, J. W., Brinkmann, J., Brunner, R., Burles, S., Carey, L., Carr, M. A., Castander, F. J., Chen, B., Colestock, P. L., Connolly, A. J., Crocker, J. H., Csabai, I., Czarapata, P. C., Davis, J. E., Doi, M., Dombeck, T., Eisenstein, D., Ellman, N., Elms, B. R., Evans, M. L., Fan, X., Federwitz, G. R., Fiscelli, L., Friedman, S., Frieman, J. A., Fukugita, M., Gillespie, B., Gunn, J. E., Gurbani, V. K., de Haas, E., Haldeman, M., Harris, F. H., Hayes, J., Heckman, T. M., Hennessy, G. S., Hindsley, R. B., Holm, S., Holmgren, D. J., Huang, C.-h., Hull, C., Husby, D., Ichikawa, S.-I., Ichikawa, T., Ivezić, Ž., Kent, S., Kim, R. S. J., Kinney, E., Klaene, M., Kleinman, A. N., Kleinman, S., Knapp, G. R., Korienek, J., Kron, R. G., Kunszt, P. Z., Lamb, D. Q., Lee, B., Leger, R. F., Limmongkol, S., Lindenmeyer, C., Long, D. C., Loomis, C., Loveday, J., Lucinio, R., Lupton, R. H., MacKinnon, B., Mannery, E. J., Mantsch, P. M., Margon, B., McGehee, P., McKay, T. A., Meiksin, A., Merelli, A., Monet, D. G., Munn, J. A., Narayanan, V. K., Nash, T., Neilsen, E., Neswold, R., Newberg, H. J., Nichol, R. C., Nicinski, T., Nonino, M., Okada, N., Okamura, S., Ostriker, J. P., Owen, R., Pauls, A. G., Peoples, J., Peterson, R. L., Petravick, D., Pier, J. R., Pope, A., Pordes, R., Prosapio, A., Rechenmacher, R., Quinn, T. R., Richards, G. T., Richmond, M. W., Rivetta, C. H., Rockosi,

C. M., Ruthmansdorfer, K., Sandford, D., Schlegel, D. J., Schneider, D. P., Sekiguchi, M., Sergey, G., Shimasaku, K., Siegmund, W. A., Smee, S., Smith, J. A., Snedden, S., Stone, R., Stoughton, C., Strauss, M. A., Stubbs, C., SubbaRao, M., Szalay, A. S., Szapudi, I., Szokoly, G. P., Thakar, A. R., Tremonti, C., Tucker, D. L., Uomoto, A., Vanden Berk, D., Vogeley, M. S., Waddell, P., Wang, S.-i., Watanabe, M., Weinberg, D. H., Yanny, B., Yasuda, N., and SDSS Collaboration (2000). The Sloan Digital Sky Survey: Technical Summary. Astronomical Journal, 120(3):1579–1587. [Cited on page 12.]

Zanstra, H. (1961). The Gaseous Nebula as a Quantum Counter (George Darwin Lecture). Quarterly Journal of the RAS, 2:137. [Cited on page 38.]

Zhou, S., Mo, H. J., Li, C., Boquien, M., and Rossi, G. (2020). Sdss-iv manga: Bayesian analysis of the star formation history of low-mass galaxies in the local universe. Monthly Notices of the Royal Astronomical Society, 497:4753–4772. [Cited on page 12.]

Zinn, P.-C., Norris, R. P., Middelberg, E., and Hales, C. A. (2013). Triggering Star Formation with AGN-driven Shocks: Evidence from the Radio Spectral Ages of Compact Steep Spectrum Sources. The Astrophysical Journal, 774:66. [Cited on page 10.]